The thesis committee for Nawaf Khaled Alotaibi
Certifies that this is the approved version of the following thesis:

Shear Strengthening of Reinforced Concrete Beams with Bi-directional Carbon Fiber Reinforced Polymer (CFRP) Strips and CFRP Anchors

APPROVED BY
SUPERVISING COMMITTEE:

James O. Jirsa, Supervisor

Wassim Ghannoum, Co-Supervisor

Shear Strengthening of Reinforced Concrete Beams with Bi-directional Carbon Fiber Reinforced Polymer (CFRP) Strips and CFRP Anchors

by

Nawaf Khaled Alotaibi, B.C.E.

Thesis

Presented to the Faculty of the Graduate School of

The University of Texas at Austin

in Partial Fulfillment

of the Requirements

for the Degree of

Master of Science in Engineering

The University of Texas at Austin

August 2014

Dedication

To the memory of my beloved grandmother,

Damjah Bint Matar,

who passed away when I started my Master's studies.

Her love I always carry with me

Acknowledgements

I would first like to thank my family: my beloved mother, who made me who I am today, my beloved father, who always believed in me, my beloved wife, whose support was constant, my lovely daughter, for her patience with the long hours of my absence during the work on this research.

I am deeply grateful to my advisor, Dr. James Jirsa. His experience, constant guidance, and support throughout the course of this research are highly appreciated. It has been an honor working under his supervision. I would also like to thank my co-advisor, Dr. Wassim Ghannoum, for his valuable advice and his dedication to this project.

I would also like to acknowledge the technical and administrative staff of the Ferguson Structural Engineering Laboratory (FSEL), especially Blake Staseny, Dennis Fillip, and David Braley; their assistance is truly appreciated.

I am deeply indebted to my research partner, William Shekarchi; his friendship is very much appreciated. Will, thanks for all the help and hard work. Special thanks to my fellow students: Hossein Yousefpour, Chang Hyuk Kim, David Garber, Amir Ghiami, and Jun Zhang for their help with my research work. My appreciation also goes out to all other students in FSEL for their friendship and support.

I wish to express my appreciation to Kuwait University for the scholarship that supported my studies at The University of Texas at Austin. I also gratefully acknowledge the Texas Department of Transportation for providing financial support for this research and Fyfe Co. LLC for donating the CFRP material.

August, 2014

Abstract

Shear Strengthening of Reinforced Concrete Beams with Bi-directional Carbon Fiber Reinforced Polymer (CFRP) Strips and CFRP Anchors

Nawaf Khaled Alotaibi, M.S.E

The University of Texas at Austin, 2014

Supervisor: James O. Jirsa

Co-Supervisor: Wassim Ghannoum

The use of externally bounded Carbon Fiber Reinforced Polymer (CFRP) for strengthening existing RC structures has shown promising results. Although CFRP materials have high tensile strength, the ability to utilize that strength is limited by debonding of the CFRP laminates from the concrete surface. In order to prevent or delay debonding, CFRP anchors were used to provide an alternative means of transferring forces from CFRP strips to the concrete.

Previous tests on prestressed I-girders strengthened with uni-directional and bi-directional CFRP strips showed that bi-directional CFRP application resulted in significant shear strength gain in comparison to a uni-directional application. The objective of this thesis is to evaluate the behavior of reinforced concrete beams strengthened in shear with bi-directional CFRP strips and CFRP

anchors so that the findings from the previous work can be understood and implemented.

Four 24 in. deep T-beams were fabricated at the Phil M. Ferguson Structural Engineering Laboratory at The University of Texas at Austin. Eight tests were conducted on these specimens to examine the effect of the bi-directional layout of CFRP on the shear strength. Specimens with 14-in. web width were selected as a part of the experimental program to allow for direct comparison with test results from the previous project. Additional beams with a web width of 8 in. were included to evaluate thinner webs similar to those in the I-girders.

Test results indicate a significant increase in shear strength due to the bi-directional application of CFRP strips with CFRP anchors installed on beams with a shear span-to-depth ratio (a/d) of 3. Substantial shear strength gain up to 62% was achieved in beams with 14-in. webs. and up to 43% for beams with 8-in. webs. However, negligible shear strength gain was observed in beams with a/d of 1.5 (deep beams). Experimental test results demonstrate an interaction between the contribution of concrete, transverse steel and CFRP to the shear resistance of a reinforced concrete beam.

The findings of this research contribute to a better understanding of the shear behavior of reinforced concrete members strengthened with externally bonded CFRP applied bi-directionally. Experimental results from this research project provide data needed in the field of CFRP shear strengthening since limited data are available on large-scale tests.

Table of Contents

CHAPTER 1 INTRODUCTION 1

1.1 Research significance 1

1.2 Research Significance 1

1.3 Research Objectives 2

1.4 Thesis Organization 3

CHAPTER 2 BACKGROUND 4

2.1 Overview 4

2.1.1 FRP material 5

2.1.2 Shear strengthening of reinforced concrete beams 5

2.2 Failure Modes of Strengthening System 6

2.2.1 CFRP configuration 6

2.2.2 FRP debonding 8

2.2.3 FRP rapture 9

2.3 Current Design Models for Shear Strengthening by CFRP 11

2.3.1 Traditional 45° truss model 11

2.3.2 Shear resistance of RC beam strengthened with CFRP 12

2.4 Interaction between Transverse Steel and CFRP Strips 14

2.4.1 Effect of the transverse steel on the shear strength gain 14

2.4.2 Strains in transverse steel and CFRP 16

2.5 Shear Strength Gain 17
2.6 Anchorage Systems to Enhance Shear Strength Gain 19
2.7 CFRP Anchors 22
2.8 Use of CFRP Anchors in Shear Strengthening Applications 23
2.9 Bi-directional Application of CFRP Strips with CFRP Anchors 27
2.9.1 Tx-DOT Project No. 0-6306 (Kim, Quinn et al. 2012) 28
CHAPTER 3 EXPERIMENTAL PROGRAM 31
3.1 overview 31
3.2 Test specimen construction 33
3.2.1 Test Specimen Design 33
3.2.2 Formwork 37
3.2.3 Steel Reinforcement 43
3.2.4 Concrete 49
3.2.5 CFRP Installation 55
3.2.5.1 Surface preparation 56
3.2.5.2 Anchor hole preparation: 57
3.2.5.3 Bi-directional CFRP strip installation (Wet lay-up procedure): 60
3.3 Experimental test setup 78
3.3.1 Loading and reaction 82
3.3.2 External clamps 83
3.4 Instrumentation 87
3.4.1 Steel strain gauges 87
3.4.2 CFRP strain gauges 90
3.4.3 Linear Variable Differential Transformers (LVDTs) 93

3.5 UT Vision System 94
3.5.1 Setup of the UT Vision System 94
3.5.2 Monitoring Shear Deformation 100
3.5.3 Monitoring CFRP Strains 101

CHAPTER 4 EXPERIMENTAL RESULTS 104

4.1 Overview 104
4.2 Test Specimen Details 104
4.3 Shear Contribution of Steel, CFRP, and Concrete 106
4.4 Test results 109
4.4.1 Results of 14-in. web specimen with a/d of 1.5 110
4.4.1.1 14–1.5–Bi–S (Bi-directional with single layer of CFRP) 110
4.4.1.2 14–1.5–Bi–D (Bi-directional with single layer of CFRP) 118
4.4.2 Results of 14-in. web specimens with a/d of 3 125
4.4.2.1 14–3–Bi–S (Bi-directional with single layer of CFRP) 125
4.4.2.2 14–3–Bi–D (Bi-directional with double layer of CFRP) 135
4.4.3 Results of 8-in. web specimens with a/d of 3 144
4.4.3.1 8–3–Control 144
4.4.3.2 8–3–Uni (Unidirectional with single layer of CFRP) 151
4.4.3.3 8–3–B–S (Bi-directional with single layer of CFRP) 160
4.4.3.4 8–3–Bi–D (Bi-directional with double layer of CFRP) 169

CHAPTER 5 ANALYSIS OF RESULTS 179

5.1 Overview 179
5.2 Shear Force-Displacement Relationships 181
5.2.1 Specimens with 14-in. webs and a/d of 1.5 (deep beams) 181
5.2.2 Specimens with 14-in. webs and a/d of 3 185
5.2.3 Specimens with 8-in. webs and a/d of 3 188

5.3 Strain Analysis in bi-directional applications 190
5.3.1 Strains in transverse steel for bi-directional application of CFRP . 190
5.3.2 Strains in vertical CFRP strips for bi-directional application 194
5.4 Shear Contribution Analysis of Concrete, Steel, and CFRP 200
5.4.1 Components of shear for 14-in. webs specimens with a/d of 3..... 200
5.4.2 Components of shear for 8-in. web specimens with a/d of 3 203
5.5 Observations of the Cracking Patterns 209
CHAPTER 6 SUMMARY AND CONCLUSIONS 213
6.1 Summary 213
6.2 Conclusions 214
REFERENCES 217
VITA 223

List of Tables

Table 3-1: Mechanical properties of of Tyfo© SCH -11UP composite..... 55
Table 4-1: Test matrix for 24-in deep T-beams 105
Table 5-1: Test Matrix for T-beams..... 179
Table 5-2: Relation between current program and project 0-6306 180
Table 5-3: Test results of 14-in. web specimens with a/d of 1.5..... 182
Table 5-4: Test results of 14-in. web specimens with a/d of 3..... 186
Table 5-5: Test results of 8-in. web specimens with a/d of 3..... 188
Table 5-6: Shear contributions and strength gain for 14-in. web specimens 200
Table 5-7: Shear contributions and strength gain for 8-in. web specimens 204
Table 5-8: Summary of test results 208

List of Figures

Figure 2-1: Stress-strain relationship of FRP composite 5
Figure 2-2: Shear Strengthening Scheme Using CFRP sheets or strips..... 7
Figure 2-3: Type of FRP reinforcement applied on the critical shear span 7
Figure 2-4: Debonding in FRP due to concrete crack (adopted from Quinn 2009) 9
Figure 2-5: Tensile properties of CFRP and steel 10
Figure 2-6: U-anchorage system (Khalifa and Nanni 2000) 20
Figure 2-7: Using steel threaded rods to form mechanical anchorage (Deifalla and Ghobarah 2010)..... 21
Figure 2-8: Anchorage systems tested by Belarbi, Bae et al. (2012) 22
Figure 2-9: CFRP Anchor (Pham 2009) 23
Figure 2-10: Anchor rupture observed when using the first detail (Quinn 2009) 24
Figure 2-11: Detailed description of the anchorage system (Quinn 2009, Kim 2011) 24
Figure 2-12: CFRP anchorage system used in (Quinn 2009, Kim 2011) 25
Figure 2-13: CFRP strip rupture observed when using the modified anchorage (Quinn 2009, Kim 2011)..... 26
Figure 2-14: Addition of horizontal strip (Hutchinson and Rizkalla 1999)..... 27
Figure 2-15: I-girders test matrix in Tx-DOT Project No. 0-6306..... 28
Figure 2-16: Amount of CFRP material used in strengthening (Tx-DOT 0-6306) 29
Figure 2-17: Shear strength gain exhibited by each test (Tx-DOT 0-6306) 29
Figure 2-18: Shear deformation curves for I-girder tests (Tx-DOT 0-6306)..... 30
Figure 3-1: Test Matrix for 24-in. Deep T-beams..... 31

Figure 3-2: Transvers reinforcement 34
Figure 3-3: Cross section of 14-in. web T-beam 36
Figure 3-4: Cross section of 8-in. web T-beam 37
Figure 3-5: Formwork cross section for 14-in. web specimen 38
Figure 3-6: 4x4 Lumber at 2-ft 38
Figure 3-7: Formwork's strong base 39
Figure 3-8: As-built formwork for 14-in. specimen 39
Figure 3-9: Formwork for specimens with different span-to-depth ratios 40
Figure 3-10: Form divider allowing for casting two specimens at the same time 41
Figure 3-11: 2x4 kickers for lateral support 41
Figure 3-12: Formwork for 8-in. web specimen by shifting one side 42
Figure 3-13: Caulk used to seal gaps and chamfer used to round bottom edge of the specimen 43
Figure 3-14: Steel reinforcement for beams A and B 44
Figure 3-15: Steel reinforcement for beams C and D 44
Figure 3-16: Transverse reinforcement for deep specimen with a/d of 1.5 45
Figure 3-17: Transverse reinforcement for slender specimens with a/d of 3 46
Figure 3-18: Flange reinforcement 47
Figure 3-19: Steel lifting insert to lift the cage 47
Figure 3-20: Steel cages and formwork before placement for 14-in. specimen 48
Figure 3-21: Placement of steel cages in the formwork for 14-in. specimens 48
Figure 3-22: Placement of steel cage in the formwork for 8-in. specimen 49
Figure 3-23: Concrete placement using one cubic yard concrete bucket 50
Figure 3-24: Vibrating the concrete by electrical vibrators 51
Figure 3-25: Concrete placement in three layers from left to right 52

Figure 3-26: Finishing the specimen's top surface 53
Figure 3-27: Concrete cylinders stored next to the specimen 53
Figure 3-28: 28-day concrete compressive strength 54
Figure 3-29: Adding water to maintain a 6-in. slump 54
Figure 3-30: Grinding the concrete surface to apply CFRP laminates 56
Figure 3-31: Rounded edge to relieve stress concentrations on the CFRP strip 57
Figure 3-32: Drilling the anchor hole 58
Figure 3-33: Typical anchor hole 58
Figure 3-34: Anchor holes after rounded (double layer application of CFRP) 59
Figure 3-35: Anchor holes layout for specimen with a/d of 1.5 (deep) 59
Figure 3-36: Vertical CFRP strips application (a) for beam A and (b) for the rest of the specimens 61
Figure 3-37: Middle-anchor holes for horizontal strips (single layer application) 62
Figure 3-38: Splitting the middle-anchor to form two opposite anchors 62
Figure 3-39: (a) Horizontal strip (b) Vertical strip (c)&(d) Middle-anchor patches 63
Figure 3-40: Typical CFRP anchor with 4-in. long insertion tool 64
Figure 3-41: End-anchorage for vertical strip left (single anchor), right (double anchor) 65
Figure 3-42: Marking CFRP strip locations 66
Figure 3-43: Preparation for CFRP installation 67
Figure 3-44: The two components of the epoxy 68
Figure 3-45: Proportioning the epoxy components 68
Figure 3-46: Mixing epoxy components 69
Figure 3-47: Pouring the epoxy in small trays 69

Figure 3-48: Saturating anchor holes using bundled CFRP strip 70
Figure 3-49: Saturating the concrete surface before CFRP application 70
Figure 3-50: Impregnating both sides of CFRP strip before attaching it to the surface 71
Figure 3-51: Attaching horizontal CFRP strip 72
Figure 3-52: Removing excessive epoxy from the strip using plastic putty knife 72
Figure 3-53: First 5x5-in patch placed on top of the hole location 73
Figure 3-54 Making an opening for the anchor using a knife 73
Figure 3-55: Removing excessive epoxy from CFRP anchor 74
Figure 3-56: Second 5x5-in. patch placed over CFRP anchors 75
Figure 3-57: (1) Middle-anchors suspended after insertion (2) Overlap of anchor fan and vertical strips 76
Figure 3-58: 5/8-in. middle-anchor spread in both directions 76
Figure 3-59: Bi-directional application layout for double layers configuration 77
Figure 3-60: Side view of the test setup 78
Figure 3-61: Test setup for a/d of 3 specimens (16-ft. long) 79
Figure 3-62: Test setup for a/d of 1.5 specimens (12-ft. long) 80
Figure 3-63: (A) regular position, (B) rotated 25-degrees. 81
Figure 3-64: As-built test setup with 25-degrees rotation 81
Figure 3-65: Loading system 82
Figure 3-66: Components of a typical reaction 83
Figure 3-67: External clamps for specimens of a/d =3 84
Figure 3-68: 3-in bearing pads to protect the web of the specimen 85
Figure 3-69: Two hydraulic rams pre-stressing not tested region 85
Figure 3-70: External pre-stressing system 86

Figure 3-71: Protected strain gauge: (1) in transverse reinforcement, (2) in longitudinal reinforcement 88
Figure 3-72: Steel strain gauges grid system for specimens with an a/d of 1.5 (deep) 88
Figure 3-73: Steel strain gauges grid system for specimens with a/d of 3 (slender) 89
Figure 3-74: Notation for steel strain gauges 89
Figure 3-75: Typical strain gauge for composite material 90
Figure 3-76: The two components adhesive used to provide smooth surface 90
Figure 3-77: Process of installing CFRP stain gauges: (1) apply the gauges (2) separate the wires (3) cover it with electrical tape 91
Figure 3-78: CFRP strain gauges grid system for specimens with a/d of 1.5 91
Figure 3-79: CFRP strain gauges grid system for specimens with a/d of 3 92
Figure 3-80: Notation for CFRP strain gauges 92
Figure 3-81: LVDT's to measure mid-span displacement 93
Figure 3-82: Identifying the test span 94
Figure 3-83: Grid lines drawn on the test span 95
Figure 3-84: Placing paper targets in their location using spray adhesive 96
Figure 3-85: No target was located over the boundaries between different material 96
Figure 3-86: Two high resolution cameras stand on tripod 97
Figure 3-87: Left camera (master) straight, right (slave) rotated 98
Figure 3-88: Computer system associated with the Vision System 99
Figure 3-89: Lights for better images 99
Figure 3-90: Shear deformation triangular 100
Figure 3-91: Dimensions of shear deformation triangle 101

Figure 3-92: Vertical strips in bi-directional with targets associated with UTVS 101
Figure 3-93: Three targets selected across the width to measure strains CFRP strips 102
Figure 3-94: Strains across the width of a vertical strip 102
Figure 4-1: Test specimen notation 105
Figure 4-2: Internal forces in a cracked strengthened beam 106
Figure 4-3: Applied load and shear force 110
Figure 4-4: CFRP configuration of 14-1.5-Bi-S 111
Figure 4-5: left (before) and right (after) loading of 14-1.5-Bi-S 111
Figure 4-6: Load-displacement curve of 14-1.5-Bi-S 112
Figure 4-7: Cracking pattern of west face 14-1.5-Bi-S 113
Figure 4-8: Crushing of concrete at nodal zone (left) and crushing of strut (right) 113
Figure 4-9: Cracks at the edges of the strips 114
Figure 4-10: Strains in vertical strips at different loading stages of 14-1.5-Bi-S 115
Figure 4-11: Load versus maximum recorded strain in steel stirrups (14-1.5-Bi-S) 116
Figure 4-12: Strains in steel stirrups at different loading stages of 14-3-Bi-S 116
Figure 4-13: Strains in steel stirrups and CFRP strips during loading of 14-1.5-Bi-S 117
Figure 4-14: CFRP configuration of 14-1.5-Bi-D 118
Figure 4-15: left (before) and right (after) loading of 14-1.5-Bi-D 119
Figure 4-16: Load-displacement curve of 14-1.5-Bi-D 120
Figure 4-17: Cracking pattern of west face 14-3-Bi-D 120
Figure 4-18: Crushing of concrete strut and node 121

Figure 4-19: Separation of CFRP strip and anchor as one unit 121
Figure 4-20: Strains in vertical strips at different loading stages of 14-1.5-Bi-D 122
Figure 4-21: Load versus maximum measured strain in stirrups for 14-1.5-Bi-D 123
Figure 4-22: Strains in steel stirrups at different loading stages of 14-1.5-Bi-D 123
Figure 4-23: Strains in steel stirrups and CFRP strips during loading of 14-1.5-Bi-D 124
Figure 4-24: CFRP configuration of 14-3-Bi-S 125
Figure 4-25: left (before), right (after) loading of 14-3-Bi-S 126
Figure 4-26: Load-displacement curve of 14-3-Bi-S 127
Figure 4-27: Shear deformation curve of 14-3-Bi-S 127
Figure 4-28: Cracking pattern of east face of 14-3-Bi-S 128
Figure 4-29: Cracking pattern of west face of 14-3-Bi-S 128
Figure 4-30: Cracking at the boundaries between concrete and CFRP 129
Figure 4-31: Critical crack at web-flange interface 129
Figure 4-32: Strains in vertical strips at different loading stages of 14-3-Bi-S 130
Figure 4-33: Load versus maximum measured strain in stirrups for 14-3-Bi-S 131
Figure 4-34: Strains in steel stirrups at different loading stages of 14-3-Bi-S 132
Figure 4-35: Strains in steel stirrups and CFRP strips during loading of 14-3-Bi-S 133
Figure 4-36: Estimated shear contribution of concrete, steel, and CFRP(14-3-Bi-S) 134
Figure 4-37: CFRP configuration of 14-3-Bi-D 135

Figure 4-38: left (before), right (after) loading of 14-3-Bi-D 135
Figure 4-39: Load-displacement curve of 14-3-Bi-D 136
Figure 4-40: Shear deformation curve of 14-3-Bi-D 136
Figure 4-41: Cracking pattern of east face of 14-3-Bi-D 137
Figure 4-42: Cracking pattern of west face of 14-3-Bi-D 137
Figure 4-43: Development of cracks at CFRP edges for 14-3-Bi-D 138
Figure 4-44: Critical crack in 14-3-Bi-D: left (east), right (west) 138
Figure 4-45: Separation of CFRP strips 139
Figure 4-46: Strains in vertical strips at different loading stages of 14-3-Bi-D 140
Figure 4-47: Load versus maximum measured strain in stirrups for 14-3-Bi-D 141
Figure 4-48: Strains in steel stirrups at different loading stages of 14-3-Bi-D ... 141
Figure 4-49: Strains in steel stirrups and CFRP strips during loading of 14-3-Bi-D 142
Figure 4-50: Estimated shear contribution of concrete, steel, and CFRP (14-3-Bi-D) 143
Figure 4-51: Typical cross-section of 8-in. web specimen 144
Figure 4-52: Test 8-3-Control (non-strengthened specimen) 145
Figure 4-53: left (before), right (after) loading of 8-3-Control 145
Figure 4-54: Load-displacement curve of 8-3-Control 146
Figure 4-55: Shear deformation curve of 14-8-Control 146
Figure 4-56: Cracking pattern of east face 8-3-Control 147
Figure 4-57: Cracking pattern of west face 8-3-Control 147
Figure 4-58: Diagonal cracks at 50-kips applied load 148
Figure 4-59: Cracking pattern at applied load of 144-kips. 148
Figure 4-60: Applied load vs strain in stirrups of 8-3-Control 149

Figure 4-61: Strains in steel stirrups at different applied loading stages of 8-3-Control 150
Figure 4-62: Estimated shear contribution of concrete and steel (8-3-Control) 151
Figure 4-63: CFRP configuration of 8-3-Uni 152
Figure 4-64: left (before), right (after) loading of 8-3-Uni 152
Figure 4-65: Load-displacement curve of 8-3-Uni 153
Figure 4-66: Shear deformation curve of 8-3-Uni 153
Figure 4-67: Cracking pattern of east face 8-3-Uni 154
Figure 4-68: Cracking pattern of west face 8-3-Uni 154
Figure 4-69: Cracking at different load stages of 8-3-Uni 155
Figure 4-70: failure mode of 8-3-Uni 155
Figure 4-71: Failure of web behind CFRP anchor 155
Figure 4-72: Strains in vertical strips at different loading stages of 8-3-Uni 156
Figure 4-73: Applied load versus maximum measured strain in stirrups for 8-3-Uni 157
Figure 4-74: Strains in steel stirrups at different loading stages of 8-3-Uni 158
Figure 4-75: Strains in steel stirrups and CFRP strips during loading of 8-3-Uni 159
Figure 4-76: Estimated shear contribution of concrete, steel and CFRP (8-3-Uni) 160
Figure 4-77: CFRP configuration of 8-3-Bi-S 161
Figure 4-78: left (before), right (after) loading of 8-3-Bi-S 161
Figure 4-79: Load-displacement curve of 8-3-Bi-S 162
Figure 4-80: Shear deformation cure of 8-3-Bi-S 162
Figure 4-81: Cracking pattern of east face 8-3-Bi-S 163
Figure 4-82: Cracking pattern of west face 8-3-Bi-S 163

Figure 4-83: Development of cracks in 8-3-Bi-S 164
Figure 4-84: Failure mode of 8-3-Bi-S 164
Figure 4-85: Applied load vs maximum strain in vertical strips for 8-3-Bi-S 165
Figure 4-86: Strains in vertical strips at different loading stages of 8-3-Bi-S 166
Figure 4-87: Applied load versus maximum strain in stirrups for 8-3-Bi-S 167
Figure 4-88: Strains in steel stirrups at different loading stages of 8-3-Bi-S..... 167
Figure 4-89: Strains in steel stirrups and CFRP strips during loading of 8-3-Bi-S 168
Figure 4-90: Estimated Contribution of concrete, steel, and CFRP (8-3-Bi-S) 169
Figure 4-91: CFRP configuration of 8-3-Bi-D..... 170
Figure 4-92: left (before), right (after) loading of 8-3-Bi-D 170
Figure 4-93: Load-displacement curve of 8-3-Bi-D..... 171
Figure 4-94: Shear deformation of 8-3-Bi-D 171
Figure 4-95: Cracking pattern of east face of 8-3-Bi-D 172
Figure 4-96: Cracking pattern of west face of 8-3-Bi-D..... 172
Figure 4-97: Cracking at initial loading (up to100-kips.) of 8-3-Bi-D 173
Figure 4-98: Failure mode of 8-3-Bi-D due to extreme loading 173
Figure 4-99: Applied load versus maximum strain in vertical strips of 8-3-Bi-D..... 174
Figure 4-100: Strains in vertical strips at different loading stages of 8-3-Bi-S 175
Figure 4-101: Applied load versus maximum measured strain in stirrups for 8-3-Bi-D..... 176
Figure 4-102: Strains in steel stirrups at different loading stages of 8-3-Bi-D ... 176
Figure 4-103: Strains in steel stirrups and CFRP strips during loading of 8-3-Bi-D 177

Figure 4-104: Estimated Contribution of concrete, steel, and CFRP (8-3-Bi-D) 178
Figure 5-1: Normalized shear versus displacement curve for 14-in. web beams with a/d of 1.5 182
Figure 5-2: Failure of 14-1.5-Bi-S 183
Figure 5-3: Failure of 14-1.5-Bi-D 184
Figure 5-4: Normalized shear versus displacement curve for 14-in. web beams with a/d of 1.5 185
Figure 5-5: Normalized shear versus displacement curve for 14-in. web beams with a/d of 3 187
Figure 5-6: Normalized shear versus displacement curve for 8-in. web beams with a/d of 3 189
Figure 5-7: Strain variations in steel stirrups between 14-3-Uni and 14-3-Bi-S 191
Figure 5-8: Strain variations in transverse steel of 8-3-Control, 8-3-Uni, and 8-3-Bi-S 192
Figure 5-9: Strain variations in transverse steel of 8-3-Bi-S, and 8-3-Bi-D 193
Figure 5-10: Three targets selected across the width to measure strains in vertical CFRP strips 194
Figure 5-11: Strain variations in vertical strips of 14-3-Uni and 14-3-Bi-S 195
Figure 5-12: Strain variations in vertical strips of 8-3-Uni and 8-3-Bi-S 196
Figure 5-13: Strain variations in vertical strips of 8-3-Bi-S and 8-3-Bi-D 197
Figure 5-14: Strain in steel and CFRP of 8-3-Uni (left) and 8-3-Bi-S (right)..... 199
Figure 5-15: Shear contribution of each component in 14-in. web specimens ... 201
Figure 5-16: Shear contribution component of 14-3-Bi-S and 14-3-Bi-D 202
Figure 5-17: Estimated shear contributions for specimens with 14-in. webs 203
Figure 5-18: Shear contribution of each component in 8-in. web specimens 204

Figure 5-19: Shear contribution component of 8-3-Bi-S and 8-3-Bi-D..... 206
Figure 5-20: Estimated shear contributions for specimens with 8-in. webs 207
Figure 5-21: Transverse steel contribution in 8-in. web specimens..... 208
Figure 5-22: Cracking of control and uni-directionally strengthened..... 209
Figure 5-23: Principal crack of 8-3-Uni: west face (top), east face (bottom) 210
Figure 5-24: Distribution of cracks in 8-3-Uni 210
Figure 5-25: Cracking pattern of 8-3-Bi-S (west face) 211
Figure 5-26: Cracking pattern of 14-in. web specimens 212

CHAPTER 1
Introduction

1.1 RESEARCH SIGNIFICANCE

Reinforced concrete structures (RC) may deteriorate due to excessive permit loads, inadequate design, or exposure to extreme environmental conditions. Carbon Fiber Reinforced Polymer (CFRP) materials offer an effective technique for repairing, upgrading or strengthening existing RC members. Externally bonded CFRP materials have proven to be reliable and efficient for strengthening applications because of their high strength-to-weight ratio, resistance to corrosion, formability, high tensile strength, and ease of installation (Deniaud and Cheng 2001). Many RC members are deficient in shear as a result of insufficient shear reinforcement, corrosion of shear reinforcement, or increase in permit loads (Khalifa and Nanni 2000).

1.2 RESEARCH SIGNIFICANCE

A considerable amount of research has been conducted in the last decade to evaluate the use of externally bonded CFRP material in strengthening RC members in shear. The use of externally bonded CFRP material in laboratory tests has demonstrated the value of strengthening with CFRP (Triantafillou 1998, Khalifa, Tumialan et al. 1999, Adhikary, Mutsuyoshi et al. 2004, Zhang and Hsu 2005, Pellegrino and Modena 2006). However, the majority of these studies mainly focused on small scale, rectangular cross sections with no or little transverse reinforcement and are not representative of actual in-service members (Bousselham and Chaallal 2006). A significant increase in shear strength was observed when externally bonded CFRP material is fully wrapped around the RC beams. Yet, when CFRP laminates were U-wrapped or side-bonded, debonding between CFRP laminates and concrete surface prevented the full utilization of the tensile

capacity of CFRP material (Khalifa and Nanni 2000, Chen and Teng 2003, Zhang and Hsu 2005) .

The effectiveness of CFRP anchors was found to provide an excellent option for flexural strengthening applications (Orton, Jirsa et al. 2008, Kim, Jirsa et al. 2013). Also, the effectiveness of CFRP anchors was confirmed in shear strengthening applications (Quinn 2009, Kim 2011). The use of CFRP anchors was found to prevent premature debonding; therefore, enabling CFRP laminates to reach their full tensile capacity and increase the CFRP contribution to shear strength.

Consequently, the use of CFRP systems consisting of uni-directional CFRP strips anchored with CFRP anchors for shear strengthening of RC beams can result in a significant shear strength gain. However, the use of uni-directional CFRP laminates with CFRP anchors for shear strengthening of prestressed concrete I-girders resulted in only a slight increase in shear strength while the application of bi-directional CFRP laminates with CFRP anchorage provided a shear strength gain up to 40%. This behavior, however, has not yet been fully explained.

For this reason, the performance of the bi-directional application of CFRP laminates with CFRP anchors needs to be investigated to understand the shear mechanism that caused this difference between uni-directional and bi-directional applications of CFRP.

1.3 RESEARCH OBJECTIVES

The objectives of this research project were 1) to evaluate the feasibility of using bi-directional CFRP laminates with CFRP anchors in shear strengthening of reinforced concrete beams, and 2) to determine the difference between the uni-directional and bi-directional applications of CFRP in shear strengthening of RC beams. In order to meet these objectives, an experimental program consisting of eight tests was carried out on four 24-in. deep RC T-beams. The experimental testing program was designed to evaluate the effect of three parameters on the shear behavior of a RC beam strengthened with bi-directional application of CFRP strips and CFRP anchors: 1) shear span-to-depth

ratio (a/d), 2) number of CFRP layers applied to strengthen the beam, and 3) web width of the beam.

1.4 THESIS ORGANIZATION

A brief introduction to the research project including overview, significance, and objectives is presented in Chapter 1. In Chapter 2, background information on the use of externally bonded CFRP in shear strengthening applications is discussed. Details related to the specimens; their design and fabrication, the test setup, and the instrumentation used in the experimental program are presented in Chapter 3. The test results are presented in Chapter 4 and the findings from those results are analyzed and discussed in Chapter 5. The summary and conclusions are covered in Chapter 6.

CHAPTER 2
Background

2.1 OVERVIEW

Many existing structures suffer from deficiencies relative to current usage or expectations. Thousands of bridges throughout the world are in need of urgent strengthening or upgrading due to poor design, increase in service loads, or corrosion of steel reinforcement. The use of Fiber Reinforced Polymers (FRP) as a strengthening technique provides an economically efficient solution to extend the structural life of these bridges. In the past, a deteriorated bridge was typically upgraded by replacing the deficient part of that bridge. This was a costly process that usually required closing of the bridge. Another upgrading and strengthening technique was to add external transverse steel stirrups which usually required the removal of the bridge deck which could accelerate the risk of corrosion. These options always required at least partial closing of the bridge and, in many situations, created additional labor and cost.

FRP materials, with thier high strength-to-weight ratio, non-corrosive nature, excellent mechanical and stiffness properties, ease of installation, and speed of application became an attractive choice for rehabilitation. These unique properties resulted in the use of FRP materials in the rehabilitation and strengthening of reinforced concrete structures. FRP sheets can be adhered to the tension side of flexural members to increase their moment capacities. It can also be used in axial members to enhance the strength and ductility of reinforced concrete columns.

This chapter presents a brief background on the use of Carbon Fiber Reinforced Polymers (CFRP) in the shear strengthening of reinforced concrete beams.

2.1.1 FRP material

FRP composites used in strengthening applications consist of fibers (carbon, glass, or aramid) and resin. The fibers provide the strength and the stiffness of the composite. Epoxy is usually used as a resin to bind the fibers, allowing for stress transfer and providing some sort of protection against damage. The fibers have a higher tensile modulus of elasticity and a lower ultimate strain than the epoxy. As a result, the composite has an average of the properties of the fibers and the epoxy, as shown in Figure 2-1.

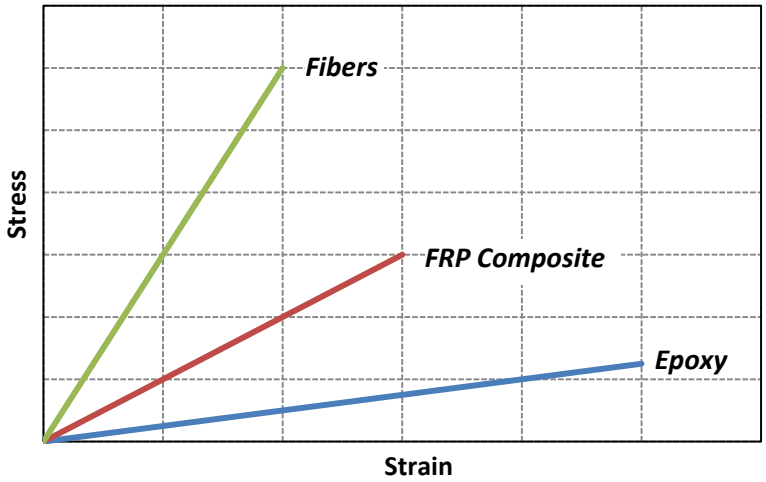

Figure 2-1: Stress-strain relationship of FRP composite

2.1.2 Shear strengthening of reinforced concrete beams

A significant amount of research has been conducted on the use of FRP materials in strengthening existing reinforced concrete members. However, most of these investigations focused on enhancing the load-carrying capacity of flexural members and/or increasing the strength and ductility of compression members by providing additional confinement.

Shear failures are considered catastrophic because they usually occur with no advance warning. The brittle failure of reinforced concrete members in shear increased the need for strengthening to avoid sudden failure.

Recently, numerous research studies have been conducted on the shear strengthening of reinforced concrete members; however, most of these investigations do not represent the typical in-service reinforced concrete beams. The majority of these studies were conducted on reduced size specimens with rectangular cross sections, while beams are usually part of a bridge deck or floor slab (Al-Sulaimani, Sharif et al. 1994, Triantafillou 1998, Khalifa, Tumialan et al. 1999, Pellegrino and Modena 2002, Carolin and Täljsten 2005, Pellegrino and Modena 2006, Grande, Imbimbo et al. 2009).

2.2 FAILURE MODES OF STRENGTHENING SYSTEM

2.2.1 CFRP configuration

CFRP materials are often used for shear strengthening applications. CFRP continuous sheets or CFRP strips are applied in different layouts on the webs of the reinforced concrete members in order to enhance shear capacity. The three main schemes are complete wrapping of the member, the U-wrapping, and side-bonded. The three configurations are shown in Figure 2-2. For cases where the four sides of the beam needing strengthening can be reached, the full wrapping of the CFRP materials is most likely the best choice since it eliminates the possibility of premature debonding failures. If the beam is part of a monolithic floor, the complete wrap of the section is impractical; the U-wrap configuration is more appropriate for these cases. Studies showed that in most cases, a full wrap of FRP materials results in a higher shear strength gain than the U-wrap configuration (Adhikary, Mutsuyoshi et al. 2004). In special circumstances, CFRP sheets or CFRP strips are applied only to the sides of the beam to form side-bonded configurations.. The shear strength gain obtained by the U-wrap configuration is greater than that obtained when the CFRP sheets are bonded to the sides of the specimen (Sato, Ueda et al. 1996, Khalifa and Nanni 2000).

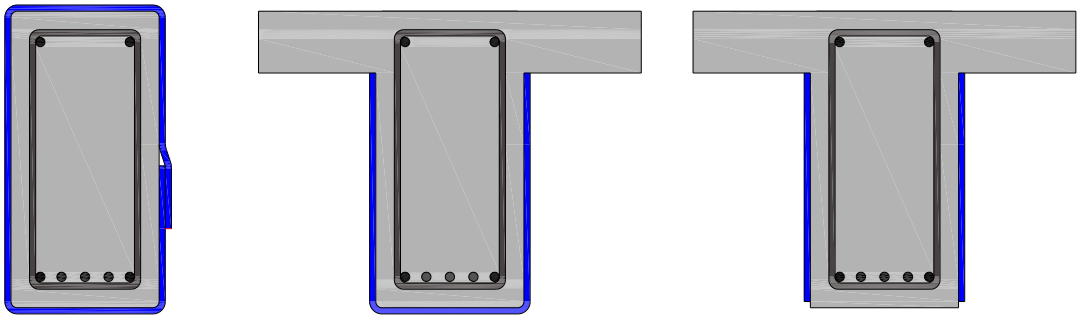

(a) Complete wrap (b) U-wrap (C) Side-bounded

Figure 2-2: Shear Strengthening Scheme Using CFRP sheets or strips

CFRP materials are applied in the form of continuous sheets or discrete strips, as shown in Figure 2-3. Applying the CFRP materials in the form of discrete strips provides the ability to inspect the critical shear span after strengthening. To achieve the optimum performance of the material, the fiber should be oriented perpendicular to the principal tensile stress (fibers oriented at 45°) (Deniaud and Cheng 2003). This diagonal application of CFRP strips was found to result in higher shear strength than the vertical application since it better controls crack propagation (Hsu, Punurai et al. 2003, Zhang, Hsu et al. 2004). However, applying the strips perpendicular to the longitudinal axis (θ = 90°) is more practical than diagonal application (Kim 2011).

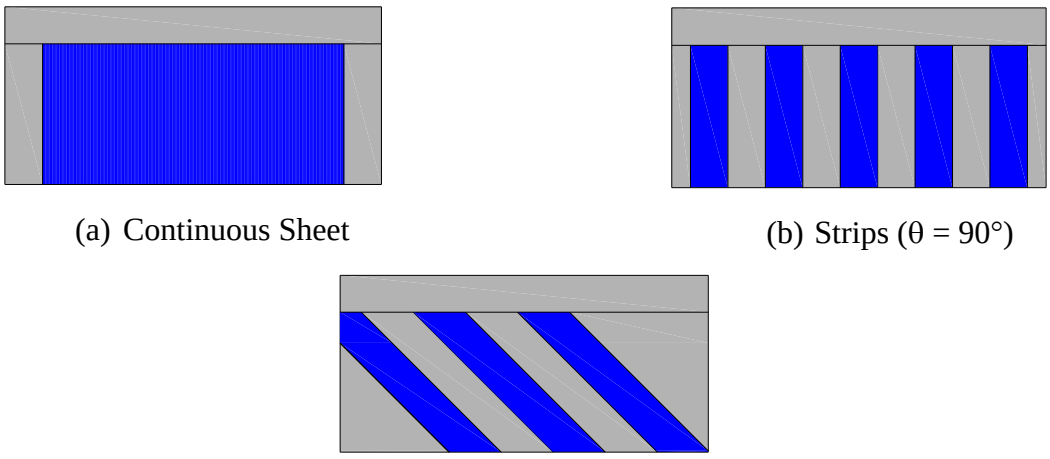

(a) Continuous Sheet (b) Strips (θ = 90°)

(c) Strips (θ = 45°)

Figure 2-3: Type of FRP reinforcement applied on the critical shear span

Early research studies on the shear strengthening of reinforced concrete beams with FRP materials have shown that FRP debonding and FRP rupture are the two main possible failure modes. Several studies were conducted to investigate these failure modes and to account for these failures in their proposed models (Khalifa, Gold et al. 1998, Triantafillou 1998, Triantafillou and Antonopoulos 2000). Current codes and design guidelines evaluate the FRP contribution to the shear strength of the strengthened member based on its failure mode (FRP debonding or FRP rupture).

2.2.2 FRP debonding

Debonding is the predominant mode of failure in shear strengthened members and causes a significant reduction in the shear strength gain. At debounding, failure is initiated when the interfacial shear transfer mechanism between the concrete and the FRP is lost. Debonding was observed to occur at strains that much lower than the fracture strain of the CFRP, thereby preventing the utilization of the material strength. Several research studies were conducted to model the debonding failure mechanism and to examine the factors that affect this particular mode of failure (Khalifa, Gold et al. 1998, Triantafillou 1998, Pellegrino and Modena 2002, Chen and Teng 2003, Cao, Chen et al. 2005).

Debonding can occur along the FRP/adhesive interface or the adhesive/concrete interface. However, it often occurs within the concrete substrate resulting in some of the concrete remaining on the debonded FRP laminates (delamination of concrete surface). Therefore, the concrete tensile strength or, in other words the compressive strength of the concrete, is an important factor in this mode of failure. Moreover, improper surface preparation may result in the delamination of the FRP material before achieving the designed load. To avoid premature debonding failure of strengthened members, guidelines for shear strengthening of reinforced concrete members with FRP material limit the maximum strain in the FRP laminates to 0.004. Experimental investigations have shown that debonding was the main failure mode of most of the beams strengthened

with the U-wrap configuration and almost all the beams strengthened with the side-bonded configuration (Chen and Teng 2003).

The debonding mechanism starts when a critical shear crack forms and leads to local debonding, as shown in Figure 2-4. As the applied load increases, debonding continues to extend until a full debonding is observed at the edges of the sheet. Chen and Teng (2003) stated that in most cases, debonding is essential before rupture of the FRP laminate occurs.

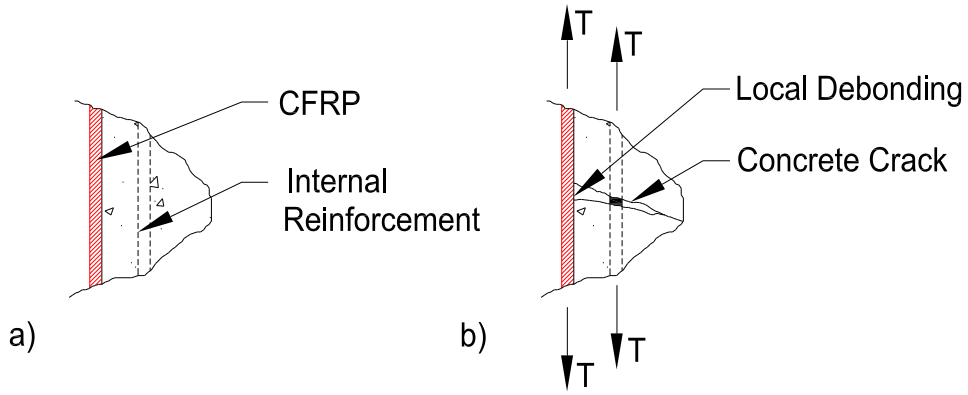

Figure 2-4: Debonding in FRP due to concrete crack (adopted from Quinn 2009)

2.2.3 FRP rapture

CFRP material is a brittle material that has a linear stress-strain relationship up to fracture. Unlike steel reinforcement, a CFRP strip does not exhibit any yielding plateau (plastic behavior), as shown in Figure 2-5.

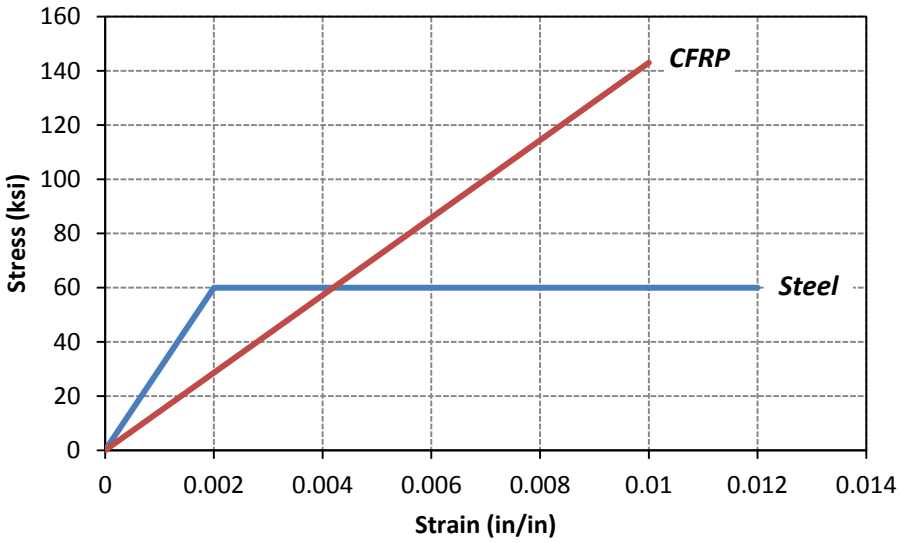

Figure 2-5: Tensile properties of CFRP and steel

When CFRP material is fully wrapped around the entire cross-section, FRP rupture is the likely mode of failure. Rupture of CFRP occurs when the main fibers reach their ultimate strain. The full tensile capacity of the CFRP material will not be utilized without some local debonding. First, a critical shear crack develops and propagates from the support to the load point. As the load increases, the width of this crack increases, causing high strains in the CFRP strips that cross this crack. When one of the CFRP strips reaches its ultimate strength, it will rupture and lose its load-carrying capacity. At that time, adjacent strips will start taking over the forces released by the ruptured strip. The remaining strips will continue carrying the load until one of the strips reaches its ultimate tensile strength and then ruptures. The propagation of CFRP strip rupture usually occurs almost instantaneously. Making this kind of failure catastrophic (Chen and Teng 2003).

CFRP strips may rupture at strains lower than their ultimate strain due to the stress concentration that occurs at rounded corners or debonded areas (Triantafillou 1998).

2.3 CURRENT DESIGN MODELS FOR SHEAR STRENGTHENING BY CFRP

Numerous research investigations were conducted to understand the shear behavior of reinforced concrete members strengthened in shear with CFRP strips or continuous sheets. From these research studies, various analytical models that evaluate the shear contribution of FRP were proposed. Several were implemented in codes and design guidelines. However, due to the complexity of the shear mechanism of the members strengthened with FRP, predictions of the shear capacity of strengthened members obtained from existing codes and guidelines are still considered unsatisfactory (Pellegrino and Modena 2006, Bousselham and Chaallal 2009, Mofidi and Chaallal 2011).

2.3.1 Traditional 45° truss model

The shear strength of a conventional reinforced concrete beam can be estimated by the simple truss model which is the basis of several current guidelines. The truss consists of tensile forces in the chords representing transverse steel and inclined compressive forces representing the compression in the concrete strut. This method ignores the tensile stress in cracked concrete and assumes concrete struts to form diagonally at 45° even though in reality this angle may differ. Assuming all steel stirrups crossing the critical crack yield before the concrete crushes, the truss then becomes statically determinate.

Based on this approach, the shear contribution of each material can be evaluated individually, which assumes no interaction between these components. Therefore, the nominal shear resistance is then evaluated by adding the shear contribution of the concrete (V_c) to the shear contribution of the transverse steel (V_s).

$$V_n = V_c + V_s \qquad \textit{Equation 2-1}$$

The concrete contribution is expressed as a function of the concrete tensile strength where several other influencing factors such as longitudinal reinforcement, transverse reinforcement, shear span to depth ratio, and beams size are ignored. The steel contribution is evaluated from the equilibrium. The complexity of the shear mechanism of a reinforced concrete member is the result of 1) the various possible failure modes that can dominate the shear capacity of those members, and 2) the influence of several factors related to the concrete contribution to the shear strength.

2.3.2 Shear resistance of RC beam strengthened with CFRP

In retrofitted members, the addition of a new component (CFRP) to the shear resistance adds more complexity to the shear mechanism. The CFRP material, unlike the transverse steel, is a perfect elastic material up to rupture with no yielding plateau. The brittle behavior of this material makes it difficult to predict the effective strain attained by the CFRP at failure (Bousselham and Chaallal 2009).

Several analytical models were proposed to predict the shear strength of a reinforced concrete beam strengthened in shear with CFRP material (Chajes, Januszka et al. 1995, Khalifa, Gold et al. 1998, Triantafillou 1998, Khalifa and Nanni 2000, Triantafillou and Antonopoulos 2000, Deniaud and Cheng 2001, Pellegrino and Modena 2002, Chen and Teng 2003, Chen and Teng 2003, Hsu, Punurai et al. 2003, Carolin and Täljsten 2005, Pellegrino and Modena 2006, Mofidi and Chaallal 2011). Some of these models were implemented in code format with or without some modifications (Khalifa, Gold et al. 1998, Triantafillou and Antonopoulos 2000, Chen and Teng 2003).

Most guidelines and codes in North America use the simple additive approach to evaluate the nominal shear resistance of a reinforced concrete member strengthened in shear with CFRP material.

$$V_n = V_c + V_s + V_f \qquad \textbf{\textit{Equation 2-2}}$$

Based on this approach, the contribution of the CFRP material to the shear resistance (V_f) is added to the shear contribution of the concrete and the transverse steel. The shear contribution of the concrete (V_c) and the shear contribution of the transverse steel (V_s) are evaluated, as in guidelines for conventional reinforced concrete members. Consequently, the main difference between existing codes and guidelines is in the way the CFRP contribution (V_f) is evaluated. Using the same expressions in evaluating (V_c) and (V_s) for conventional and strengthened members means that the CFRP shear strengthening has no effect on the shear contributions of the concrete (V_c) and the steel (V_s). This is in reality not true, as will be shown in the following section (Chen, Teng et al. 2010, Kim 2011, Mofidi and Chaallal 2011).

The CFRP contribution to the shear resistance is evaluated using the same truss analogy as that used for the transverse steel. Therefore, the CFRP contribution (V_f) provided by the number of vertical discrete CFRP strips is obtained by multiplying the axial stress in the CFRP strips by the cross-sectional area of the strips that cross the critical shear crack. It is also important to note that the above equation assumed that all steel stirrups that cross the critical shear crack have reached yield strain, and all CFRP strips that cross the same critical shear crack have reached the assumed effective strain. Most codes and guidelines use this simple truss analogy with different definitions of the effective strain.

This basic additive approach is based on several assumptions to simplify the complex shear behavior of reinforced concrete member retrofitted with CFRP. These assumptions are as follows: 1) the contribution of CFRP to the shear resistance can be simply added to the contributions of the concrete and the steel, and therefore, the shear capacity of a strengthened member is the sum of these three contributions, 2) the CFRP contribution to the shear resistance is evaluated using the same truss mechanism used for transverse steel. 3) The angle of the critical shear crack is assumed conservatively to be 45° with respect to the horizontal axis; however, observations from research studies showed the critical crack angle usually forms at an angle less than 45° (Pellegrino and

Modena 2002, Carolin and Täljsten 2005, Bousselham and Chaallal 2008). The critical shear crack may form at an angle greater than 45° if the member is highly reinforced, as the crack prefers to pass through a lesser amount of transverse steel resulting in a steep angle. Kim (2011), in his comprehensive experimental investigation, conducted 24 tests on full-scale specimens. He observed that the critical crack angle became shallower (less than 45°) as the applied load increased, which means that additional steel stirrups and CFRP strips were engaged as the load increased.

2.4 INTERACTION BETWEEN TRANSVERSE STEEL AND CFRP STRIPS

Recent research studies have confirmed the interaction between the transverse steel and the CFRP. This interaction was found to have a direct effect on the effectiveness of the strengthening system (Pellegrino and Modena 2002). However, current design equations for shear strengthening evaluate the shear contributions of the concrete and the steel as in conventional non-strengthened members, assuming that the concrete and the steel contributions are not affected by the addition of the CFRP. Consequently, this interaction between the steel and CFRP is neglected in current guidelines.

2.4.1 Effect of the transverse steel on the shear strength gain

One of the earliest studies on the interaction between the transverse steel and the CFRP was done by Pellegrino and Modena (2002). All test specimens were strengthened with FRP sheets bonded to the sides of the web. They conducted eleven tests on specimens with and without transverse steel. They observed that specimens without transverse steel tended to fail by a single critical shear crack while specimens with transverse steel experienced a multi-crack pattern. This failure mechanism accelerates the possibility of debonding and reduces the efficiency of the strengthening system. They concluded that the presence of the transverse steel results in a reduction in the shear contribution of the FRP.

An extensive experimental program was conducted by Chaallal et al. (2002). They investigated the effect of the stirrup spacing and the amount of CFRP material on the shear capacity of a retrofitted beam. Results showed that the shear capacity increased as the amount of CFRP material increased; however, this increase depends on the transverse steel ratio. As the transverse steel ratio increased, the contribution of the CFRP to the shear capacity became insignificant

Deniaud and Chen (2003) performed eight tests with various stirrup spacing. They observed that the amount of the transverse steel directly affects the gain in the shear strength. A shear strength gain up to approximately 40% was obtained in beams with stirrup spacing of 400-mm while only 20% increase was obtained in beams with stirrup spacing of 200-mm. Test results indicate that the net increase in the shear strength in lightly reinforced concrete is higher (twice in their case) than the net increase in heavily reinforced concrete.

Bousselham and Chaallal (2006) conducted 22 tests on full-scale reinforced concrete beams strengthened in shear with CFRP. One of the main objectives of their study was to investigate the effect of the transverse steel ratio on the performance of a retrofitted reinforced concrete girder. Three series of specimens were tested: 1) specimens without transverse steel, 2) specimens with transverse steel spaced at d/2, and 3) specimens with transverse steel spaced at d/4. Test results showed that the contribution of the CFRP to the shear resistance is greater for specimens without transverse steel (up to 50% gain) than for specimens with transverse steel spaced at d/2 (7% gain). Specimens with transverse steel spaced at d/4 experienced flexural failure. This substantial reduction in the shear strength gain is due to increasing the transverse steel ratio.

Pellegrino and Modena (2006) conducted 12 tests on full-scale rectangular beams strengthened with CFRP. All specimens were strengthened with CFRP applied in a U-wrapped configuratiom. Steel stirrups were spaced at 200-mm and 170-mm. Test results have shown that the CFRP contribution to the shear strength (V_f) dropped from 50-kN to 30-kN due to increaseing the amount of transverse resinforcement. They also observed

that the increase in the transverse steel ratio results in a reduction in the strengthening efficiency. Baesd on their test results, they found that the simplification of superimposing the contributions of each material without accounting for any interaction between those materials causes an overestimation of the FRP contribution to the shear capacity.

2.4.2 Strains in transverse steel and CFRP

The aforementioned studies on the interaction between the transverse steel and the CFRP in strengthened members confirmed the fact that the contribution of CFRP to the shear strength is reduced when the strengthened members are heavily reinforced (Pellegrino and Modena 2002, Deniaud and Cheng 2003).

According to the test results obtained by Bousselham and Chaallal (2006), the strains in the transverse steel of control specimens were greater than in retrofitted specimens. The difference in the strains of the transverse steel between the strengthened and non-strengthened were as high as 1000 microstrains. They also observed that the yielding of the transverse steel was delayed in retrofitted specimens when compared to control specimens. However, yielding of transverse steel was observed in most cases.

Bousselham and Chaallal (2008) observed that all stirrups within the test region were highly strained, and most of them reached yielding strain, which is in agreement with the assumptions made in current guidelines. Yielding of stirrups were observed at 85% to 95% of the ultimate load. Conversely, CFRP strips were not as highly stressesd as the steel stirrups. In fact, the reported CFRP strains were relatively small. For double layer CFRP, reported strains were as low as 10% of the ultimate strain. This minimal CFRP strain is due to the lack of anchorage. The transverse steel contribution in retrofitted beams was found to be less than its contribution in non-strengthened beams.

Grande, Imbimbo et al. (2009) conducted tests on 15 full-scale beams strengthened in shear with CFRP. The CFRP strips were applied in three configurations (side-bonded, modified U-jacketing, and complete wrapping). The transverse steel stirrups were placed at different spacings: 400, 300, and 200-mm. They observed, for beams strengthened with a U-wrapped configuration, that transverse steel yielded only

for beams with 400-mm and 300-mm spacing, while the transverse steel in beams with 200-mm did not yield. Since the shear capacities of these beams were dominated by premature debonding, cracks could not open widely enough to cause the yielding of the transverse steel. Therefore, for this case, the full steel contribution assumed by code provisions and guidelines is no longer valid.

Chen, Teng et al. (2010) suggested that beams retrofitted with U-wrap or side-bonded CFRP material usually failed by premature debonding. This type of brittle failure limits the critical crack width such that not all steel stirrups intersected by this crack reach yielding strain. Consequently, the stirrups in this case contribute less than what was predicted by guidelines and codes. Based on their proposed model, they assume that not all steel stirrups yielded; hence, the full contribution of steel stirrups can not be obtained.

Mofidi and Chaallal (2014) conducted a series of tests on beams with and without transverse steel. Specimens with transverse steel consisted of heavily reinforced beams (stirrups at d/2) and moderately reinforced beams (stirrups at 3d/4). They observed that all transverse steel yielded before failure, and the addition of the CFRP did not affect the strain in the transverse steel. This observation was in contrast to what had been proposed in Chen, Teng et al. (2010). In that study, they concluded that the full contribution of transverse steel cannot be utilized.

2.5 SHEAR STRENGTH GAIN

The effectiveness of using FRP material in enhancing the shear capacity of reinforced concrete beams was demonstrated by earlier studies in the field of shear strengthening (Al-Sulaimani, Sharif et al. 1994, Chajes, Januszka et al. 1995, Khalifa, Gold et al. 1998, Triantafillou 1998, Deniaud and Cheng 2001, Pellegrino and Modena 2002). Most of these studies were conducted on specimens of reduced size. Existing analytical models in current guidelines are based on this small-scale testing (Khalifa, Gold et al. 1998, Triantafillou and Antonopoulos 2000, Chen and Teng 2003, Monti, Renzelli et al. 2003).

Substantial shear strength gains were observed in several research studies; however, these studies were conducted on specimens that do not represent the actual in-service members. The significant shear strength gain (60% to 150%) observed in tests conducted by Chajes, Januszka et al. (1995) was due to the fact that no transverse steel was used in tested specimens, which allowed the FRP to contribute significantly to the shear capacity of the control specimen. Pellegrino and Modena (2002) reported shear strength gains between 51% and 88% for specimens without transverse steel; however, strength gain was approximately 30% for specimens with steel stirrups spaced at 0.9d. This 30% increase in shear capacity was expected in reduced-size specimens with three layers of CFRP as an external reinforcement.

Adhikary and Mutsuyoshi (2004) reported a shear strength gain up to 120%. As in previous studies, thier study was based on reduced-size specimens without transverse reinforcement. Bousselham and Chaallal (2006) reported shear strength gains of up to 50% for specimens without transverse steel, and only a 7% increase in shear capacity for the same specimens with transverse steel spaced at d/2.

According to Mofidi and Chaallal (2011), an up to 85% increase in shear capacity was obtained in beams without transverse steel, while only a 9% increase in shear capacity was achieved in beams with transverse steel spaced at d/2.

Dirar, Lees et al. (2012) conducted seven tests on moderate-sized beams strengthened with three layers of CFRP sheets. All tested beams had transverse steel spaced at 0.85d. Reported shear strength gains ranged from 9% to 26%.

As shown in the above literature, most of the substantial shear strength gains were achieved in beams without transverse steel. However, in existing structures, minimum transverse steel nearly always exists to enhance shear capacity or, in other cases, to satisfy crack width limitations set by building codes (Carolin and Täljsten 2005). For beams designed with transverse steel mimicking real conditions in the field, reported shear strength gains were negligible as confirmed by several studies (Adhikary and Mutsuyoshi 2004, Bousselham and Chaallal 2006, Mofidi and Chaallal 2011, Dirar, Lees et al. 2012).

The minimal shear contribution of CFRP in these cases was mainly due to premature failure by debonding of CFRP strips from the concrete surface (Pellegrino and Modena 2002).

2.6 ANCHORAGE SYSTEMS TO ENHANCE SHEAR STRENGTH GAIN

Numerous research studies have shown that members retrofitted with CFRP material can exhibit premature failure due to debonding (Khalifa, Gold et al. 1998, Triantafillou 1998, Deniaud and Cheng 2001, Zhang and Hsu 2005, Higgins, Williams et al. 2012). As a result, a number of studies were conducted to provide some sort of anchorage for the CFRP material to prevent or delay debonding failure and to improve the structural performance of the retrofitted members. When sufficient anchorage to prevent premature debonding is provided, the capacity of the member will be controlled by a more predictable mode of failure such as CFRP rupture (Kim and Smith 2009).

Various anchorage systems were investigated in the literature, most commonly: adding horizontal CFRP strips, using CFRP anchors, using near surface mounted (NSM) strips, and various types of mechanical anchorage systems that use steel bolts and plates. A detailed description of various types of anchorage is provided in (Quinn 2009).

Khalifa and Nanni (2000) evaluated the use of NSM techniques in enhancing the shear cpacities of concrete beams. The anchorage was provided by making grooves in the bottom side of the flange along the web-flange interface as shown in Figure 2-6. This technique, however, requires much more labor than other techniques. An increase in shear capacity up to 145% was achieved by using this anchorage system. However, this substantial shear strength gain was for member with no shear reinforcement.

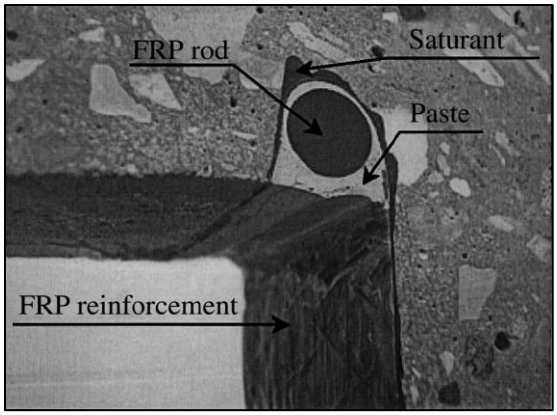

Figure 2-6: U-anchorage system (Khalifa and Nanni 2000)

Hutchinson and Rizkalla (1999) examined the use of horizontal strips on top of diagonal CFRP strips to provide anchorage for the main strengthening strips. There was an increase of 16% in shear capacity due to the addition of the horizontal strips. This is compared to a 10% increase in shear cpacity when no anchorage is provided.

The use of mechanical devices to provide anchorage for reinforced concrete members was investigated by several researchers. The premature failure of the anchorage system before the CFRP sheet reaches its full tensile capacity was still observed in this type of anchorage. This is mainly due to high stress concentrations that these steel fasteners generate on the CFRP sheets. The use of CFRP straps as an anchorage system was evaluated by Hoult and Lees (2009). However, the difficulty associated with installing this type of anchorage sytem diminishes its attractiveness.

The use of steel threaded rods along with steel plates to form an anchorage system was investigated by Deifalla and Ghobarah (2010). This technique was found to be costly and in many cases impractical for field conditions, especially for cases when access to the slab surface is impossible.

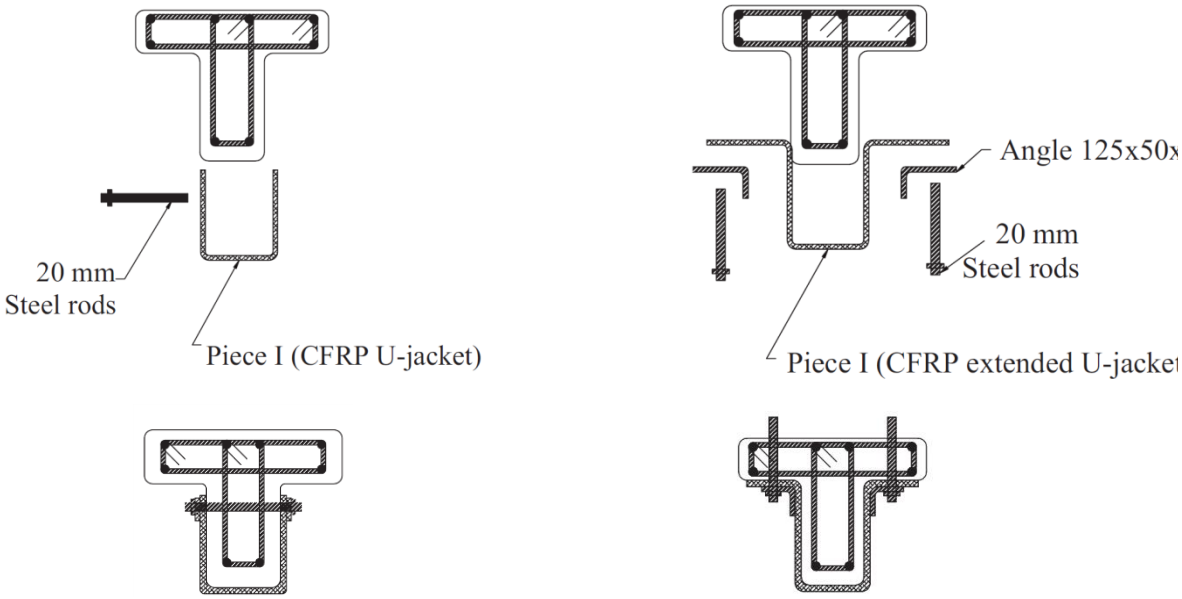

(a)U-Jacket (b)Extended U-Jacket

Figure 2-7: Using steel threaded rods to form mechanical anchorage (Deifalla and Ghobarah 2010)

Belarbi, Bae et al. (2012) studied the effectiveness of various mechanical anchorage systems. Tests were conducted on full-scale T-beams strengthened wirh CFRP strips that were anchored with 1) additional horizontal strip, 2) discountinous mechanical anchorage (DMA), or 3) sandwish panel mechnical anchorage (SDMA), as shown in Figure 2-8. All three systems provided anchorage that resulted in enhancing the shear strength gain. However, specimens anchored with horizontal strips or DMA failed due to delayed debonding. The SDMA anchorage system was found to perform the best among the systems.

(1)

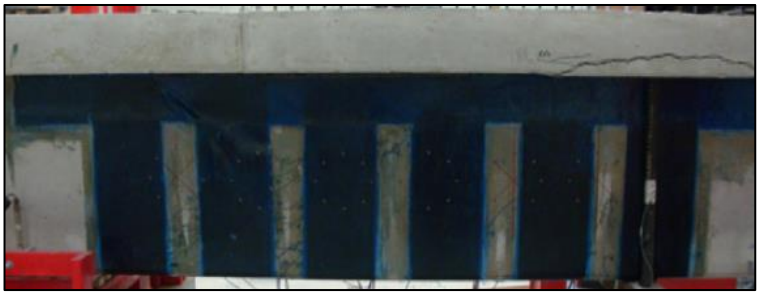

(2)

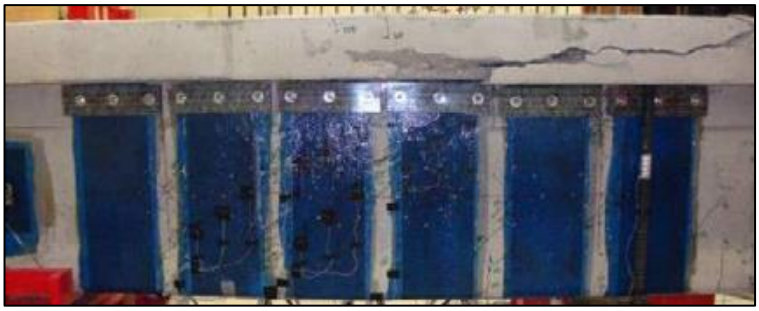

(3)

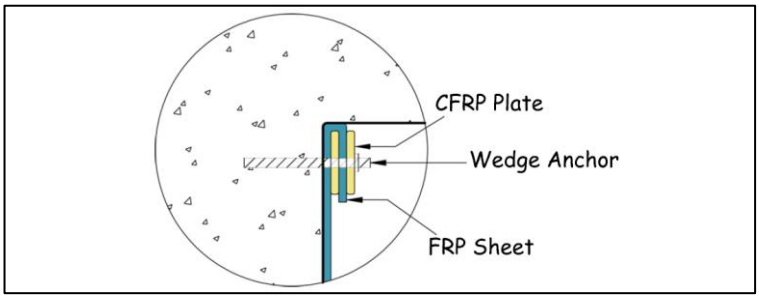

Figure 2-8: Anchorage systems tested by Belarbi, Bae et al. (2012)

2.7 CFRP ANCHORS

Debonding can severely limit the efficiency of the strengthening system. When debonding dominated the shear capacity of a strengthened beam, only 40-50% of the tensile capacity of the CFRP sheets was utilized (Orton, Jirsa et al. 2008). Using CFRP anchors to provide anchorage for CFRP sheets is a relatively new technique.

A CFRP anchor (also known as a spike anchor) can be easily made by bundling carbon fibers or by rolling a CFRP sheet, inserting it in a pre-drilled hole saturated with epoxy, and then fanning out the remaining free part on the CFRP sheet, as shown in Figure 2-9. This allows forming an anchorage system that is made up of a continuous

composite unit. Studies have shown that using CFRP anchors can successfully utilize the full tensile capacity of CFRP sheets, leading to the fracture of the sheet (Kim, Jirsa et al. 2013).

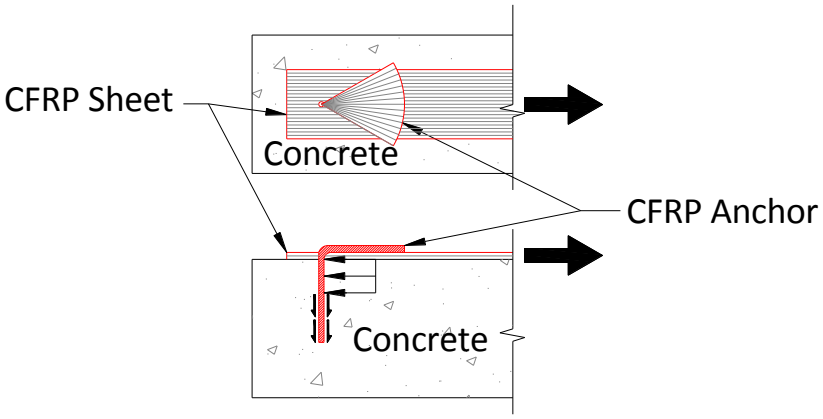

Figure 2-9: CFRP Anchor (Pham 2009)

Although using CFRP anchors to provide anchorage for CFRP strengthening systems have been successfully studied by several researchers and its efficiency has been proven in various structural applications (Eshwar, Nanni et al. 2008, Orton, Jirsa et al. 2008, Kim and Smith 2009, Ozbakkaloglu and Saatcioglu 2009, Kim, Jirsa et al. 2011, Kalfat, Al-Mahaidi et al. 2013, Kim, Jirsa et al. 2013), more research studies are needed to fully understand the behavior of this anchorage system.

2.8 USE OF CFRP ANCHORS IN SHEAR STRENGTHENING APPLICATIONS

The use of CFRP anchors in strengthening reinforced concrete beams in shear has been studied by Quinn (2009) and Kim (2011). A total of 24 tests were conducted on reinforced concrete beams that were strengthened in shear with CFRP material.

Two different anchorage details were used in the experimental investigations carried out by Quinn (2009) and Kim (2011). The first detail used was originally developed by Kim (2008) for flexural applications. This anchorage system involves using a CFRP anchor containing 1.5 times the amount of material that the CFRP strip contains. It also involves an anchorage hole with a bend radius of 0.25-in. Although this detail

performed well in enhancing the shear capacity of the tested beams, anchor rupture was observed in several cases, as shown in Figure 2-10. This was attributed to the large amount of stress that generated at the base of the fanned portion of the anchor.

Figure 2-10: Anchor rupture observed when using the first detail (Quinn 2009)

This premature failure prevented the CFRP sheet from developing its full tensile strength. To overcome this unpredictable failure in the strengthening system, a newly detailed CFRP anchorage system was developed by Kim (2011), as shown in Figure 2-11 and Figure 2-12.

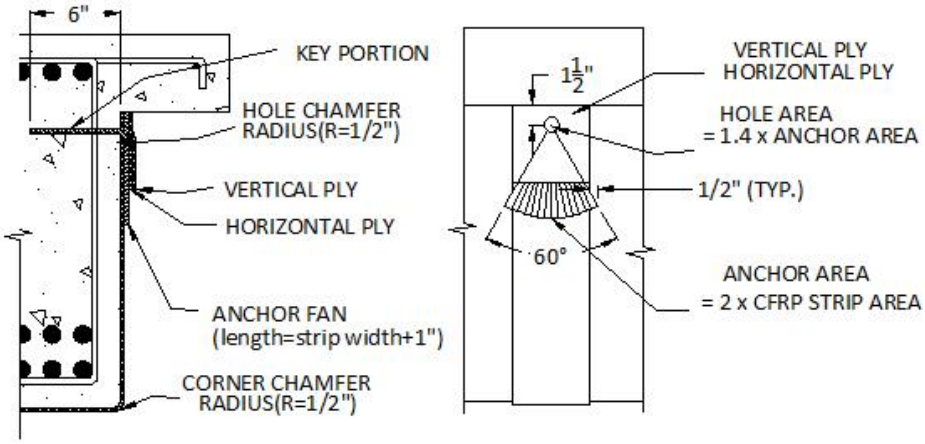

Figure 2-11: Detailed description of the anchorage system (Quinn 2009, Kim 2011)

The newly developed anchorage system involves some modificatons to prevent the CFRP anchor from rupturing. To reduce the high stress concentrations that develop on the anchors at the opening of the anchor holes: 1) the amount of material used to form the anchor was increased from 1.5 to 2 times the amount of material of the sheet, and 2) the bend radius of the anchor hole was increased from 0.25-in. to 0.5-in., as shown in Figure 2-11

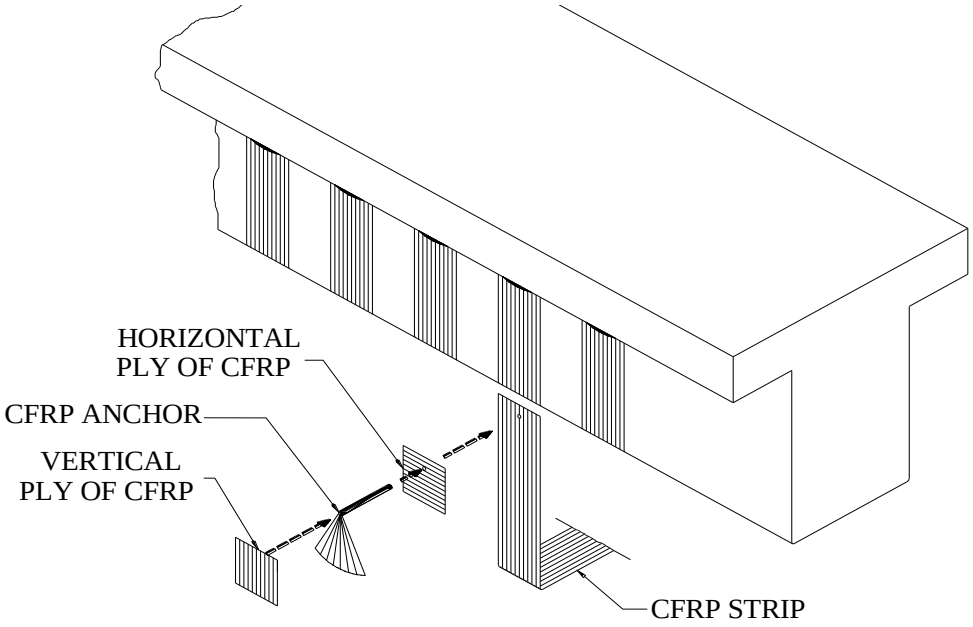

Figure 2-12: CFRP anchorage system used in (Quinn 2009, Kim 2011)

Additionally, as shown in Figure 2-12, the new details included two 5x5-in. patches to improve the performance of the anchorage system. The first patch is placed above the main strip, before inserting the anchor, with fibers oriented transversely with respect to the strip. The second patch is placed above the anchor with fibers parallel to those of the main strip. The modified detail performed very well since it allowed the CFRP strips to reach their rupture strain. As a result, beams strengthened with CFRP strips and anchored with CFRP anchors according to the newly developed system failed by strip rupture, not by anchor fracture.

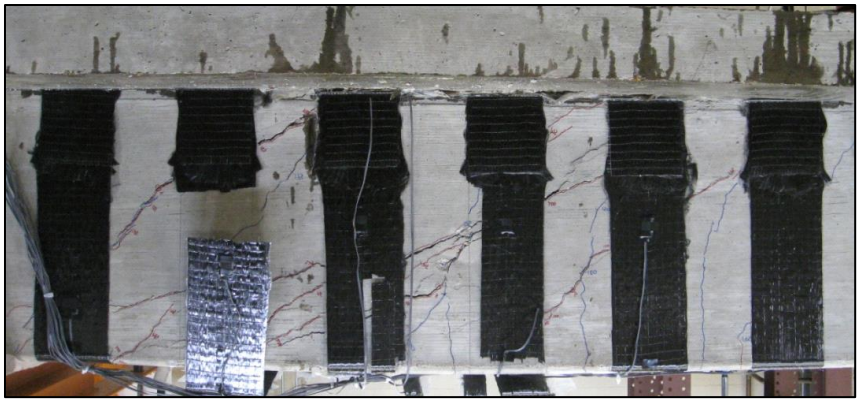

Figure 2-13: CFRP strip rupture observed when using the modified anchorage (Quinn 2009, Kim 2011)

Test results confirmed the effectiveness of CFRP anchors in preventing premature debonding failure. A substantial increase in shear capacity of up to 45% was reported for strengthened beams with CFRP anchors, while strengthened beams without CFRP anchors exhibited less than a 5% increase in shear capacity. The newly detailed anchorage system developed in these studies enabled CFRP strips to reach their rupture strain.

They also conducted a shear test on a beams strengthened with CFRP strips and CFRP anchors where the bond between the CFRP strips and the concrete surface was eliminated by plastic sheets. The beam failed by CFRP strip fracture with a significant shear strength gain of up to 44% confirming the efficiency of this anchorage system. They concluded that the strength of the CFRP system depends on the strength of the anchor and not on the bond between the CFRP strips and the concrete surface.

2.9 BI-DIRECTIONAL APPLICATION OF CFRP STRIPS WITH CFRP ANCHORS

The effect of applying CFRP material bi-directionally in shear strengthening applications has not yet been investigated (Higgins, Williams et al. 2012). The first attempt to examine the effect of using horizontal strips in addition to the main vertical strips in shear strengthening applications was carried out by Hutchinson and Rizkalla (1999). The main objective of their study was to examine the effect of different CFRP schemes on the shear capacity of I-girders. Fourteen tests were conducted on a reduced-size model of pretensioned AASHTO I-girder strengthened with different configurations.

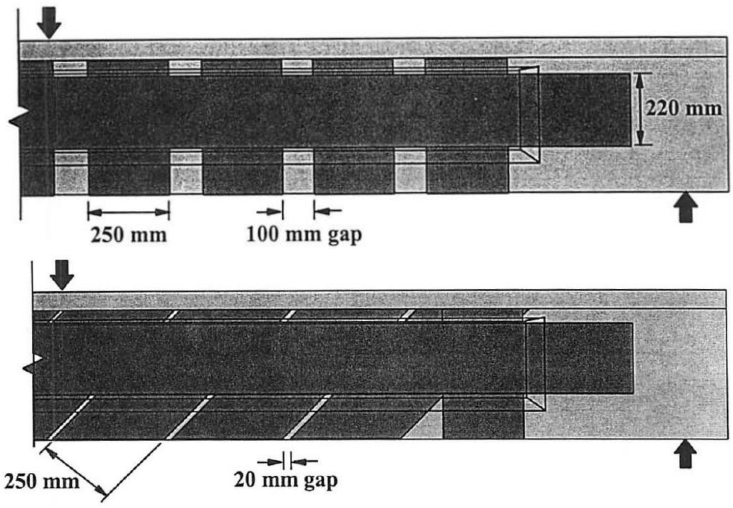

Figure 2-14: Addition of horizontal strip (Hutchinson and Rizkalla 1999)

Two beam series were investigated: series B with bent-legged stirrups and series S with stright-legged stirrups. The spacing was identical for both series. It is important to note that no anchorage was provided for the strengthening system.

For beams with bent-legged stirrups (series B), beams strengthened with horizontal vertical strips exhibited a 6% increase in the shear capacity when compared to the clamped control beam. This negligible gain in shear strength was attributed to the premature debonding of vertical strips. Due to the shape of the web, the straightening of the vertical CFRP sheet at the bottom of the web was observed prior to failure.

For beams with stright-legged stirrups (series S), beams strengthened with horizontal and diagonal strips exhibited a 16% increase in shear capacity. The increase in shear capacities was limited by premature debonding failure.

2.9.1 Tx-DOT Project No. 0-6306 (Kim, Quinn et al. 2012)

The use of the bi-directional application of CFRP with CFRP anchors for shear strengthening was carried out by Kim, Quinn et al. (2012). As part of Tx-DOT Project No. 0-6306, they investigated the effectiveness of using CFRP strips with CFRP anchors in enhancing the shear strength of AASHTO Type IV I-beams. The test matrix consisted of four 54-in. deep I-beams as follows: I-1 (control beam), I-2 (uni-directionally strengthened beam), I-3 (completely wrapped beam in both directions), and I-4 (bi-directionally strengthened beam using strips). CFRP anchors were used in all the strengthened beams to avoid premature debonding failure.

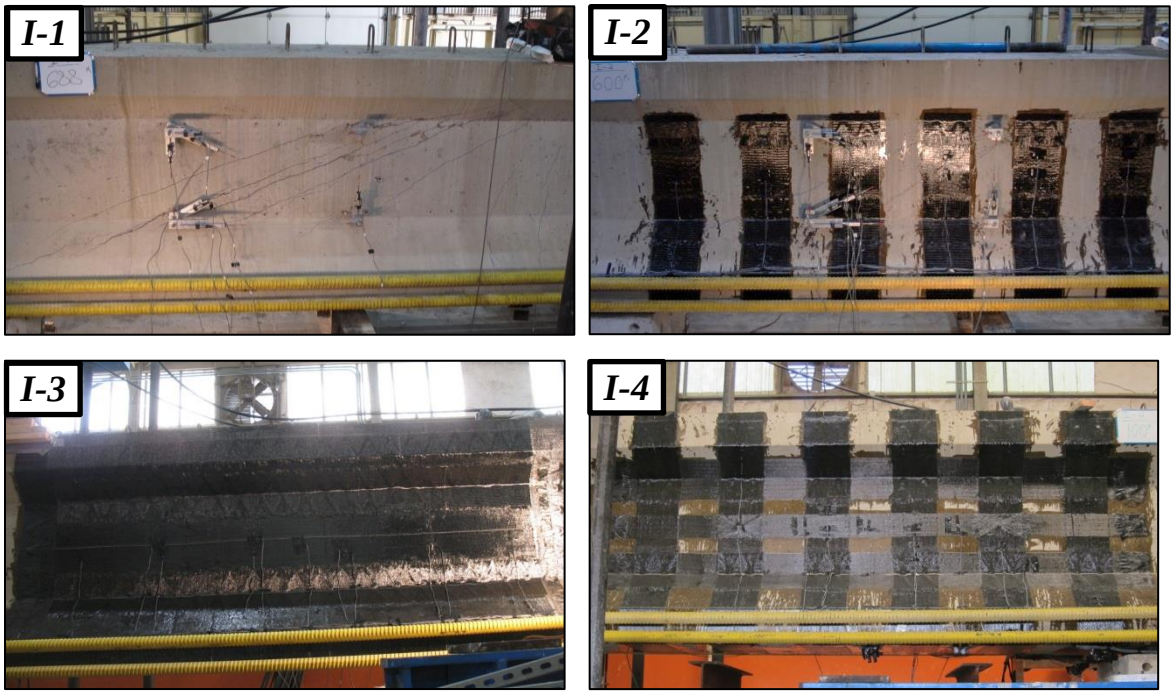

Figure 2-15: I-girders test matrix in Tx-DOT Project No. 0-6306

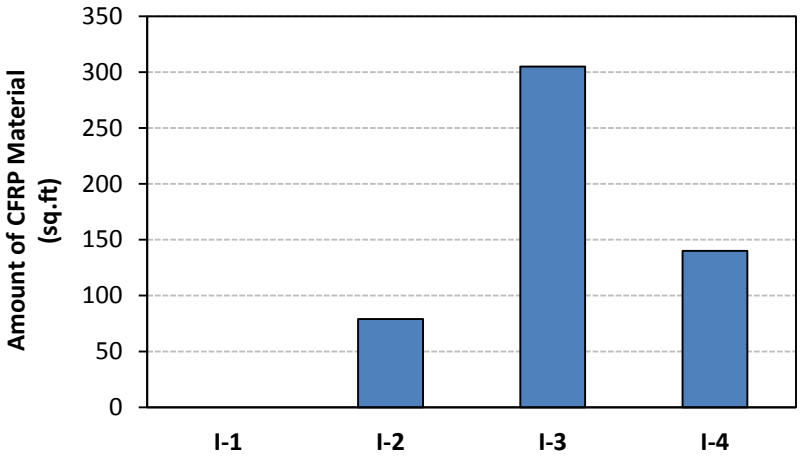

Figure 2-16: Amount of CFRP material used in strengthening (Tx-DOT 0-6306)

As shown in Figure 2-16, the amount of CFRP material used in strengthening the tested beams varies where the fully-wrapped beam consumed the largest amount of CFRP material.

Test results showed that using vertical strips with CFRP anchors did not enhance the shear capacity (only a 2% increase), while significant increases in shear capacity were observed in I-3 and I-4 (38% and 36%, respectively). Results indicated that the performance of the bi-directional application of CFRP is superior and equivalent to the performance of completely wrapped application, even though the amount of material that was used in the bi-directional application was less than half that of the fully wrapped.

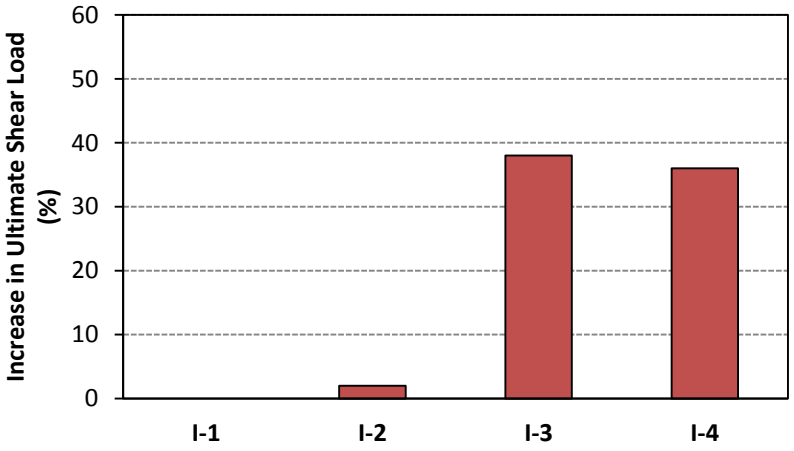

Figure 2-17: Shear strength gain exhibited by each test (Tx-DOT 0-6306)

As shown in Figure 2-18, the responses of I-3 and I-4 were identical in terms of strength, stiffness and shear deformation.

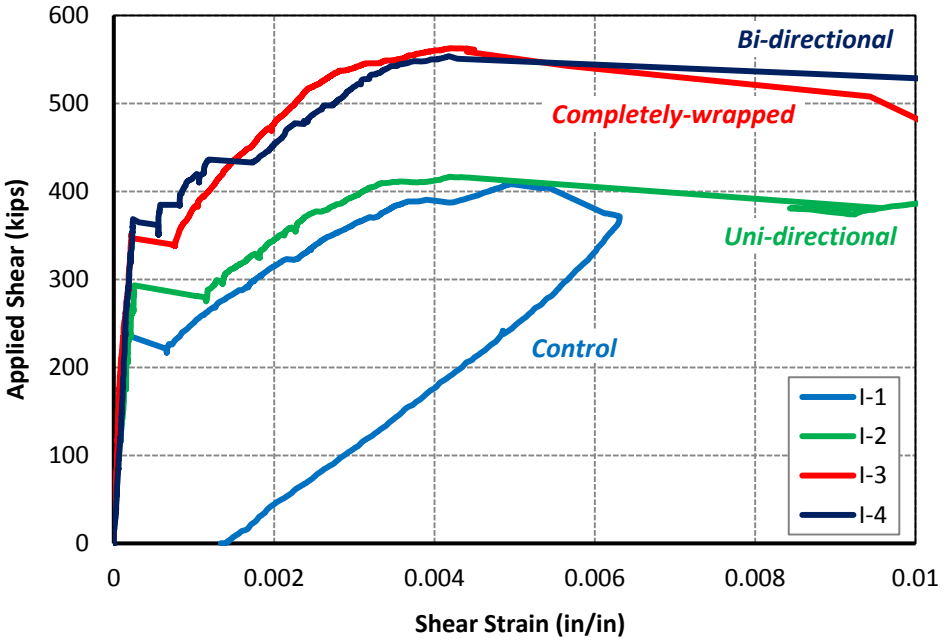

Figure 2-18: Shear deformation curves for I-girder tests (Tx-DOT 0-6306)

The superior behavior of the bi-directional application in shear strengthening this type of I-girder is not fully understood due to limited test data. Further experimental investigations are needed to verify and explained the improved performance of the bi-directional application of CFRP.

The research study presented in this thesis builds on the findings of Tx-DOT Project No. 0-6306. The main objective of this thesis is to evaluate the use of bi-directional application of CFRP strips and CFRP anchors in strengthening reinforced concrete T-beams in shear. Thereby extending the tests conducted by (Quinn 2009, Kim 2011).

CHAPTER 3
Experimental Program

3.1 OVERVIEW

The experimental program consisted of eight tests performed on four full-scale reinforced concrete (RC) T-beams designed to allow for direct comparison with previous experimental testing conducted by Quinn (2009) and Kim (2011).

A T-beam section was selected to reflect a typical bridge where the beam is part of a monolithic bridge deck. In this case, a complete wrapping of the cross-section is an inconvenient approach. The U-wrap of CFRP laminates around the web of the cross section is more suitable. However, as discussed earlier, the failure mode of the U-wrap approach is likely to involve premature debonding. Therefore, CFRP anchors were provided to prevent this type of failure. The test matrix is shown in Figure 3-1.

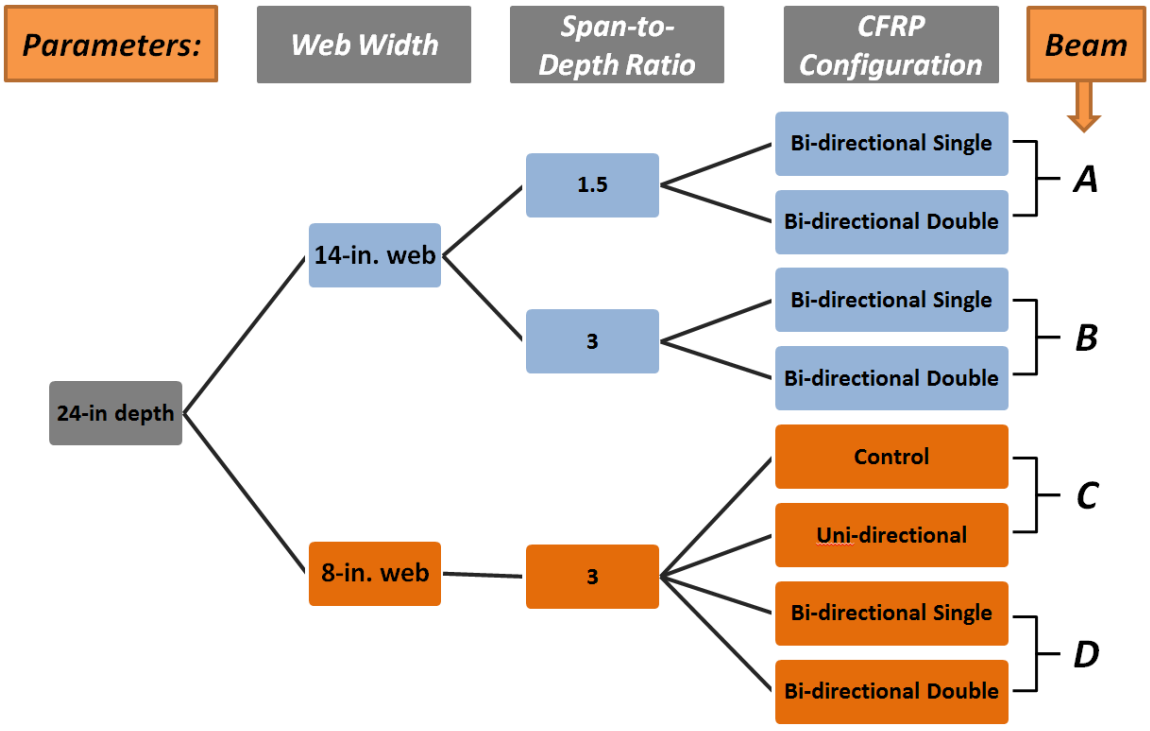

Figure 3-1: Test Matrix for 24-in. Deep T-beams

All test specimens were designed to provide two distinct test regions on each beam. CFRP strips were applied on the web of the specimen vertically and horizontally to form a bi-directional configuration in order to meet the experimental program objectives. CFRP anchors were applied to provide anchorage for CFRP strips. Tests were conducted on strengthened specimens to investigate the shear performance of RC T-beams with bi-directional application of CFRP strips and CFRP anchors.

3.2 TEST SPECIMEN CONSTRUCTION

The Test specimens were constructed and cast at the Ferguson Structural Engineering Laboratory (FSEL) at The University of Texas at Austin. Detailed description of the design and construction the test specimen is provided in this section as follows:

- Design of the specimens
- Formwork
- Steel reinforcement cages
- Concrete mix and placement
- Installation of CFRP material

3.2.1 Test Specimen Design

Test specimens were designed according to American Concrete Institute (ACI 318-11) and American Association of State Highway and Transportation Officials (AASHTO) guidelines related to minimum requirements for shear. Since the main objective of the experimental testing was to examine the shear behavior of RC beams, specimens where purposely designed with a flexural capacity that considerably exceeded the expected shear capacity to ensure a shear failure.

Internal transverse steel shear reinforcement has a significant impact on the contribution of CFRP to the shear resistance of strengthened RC beams, and hence on the shear behavior of these beams. Consequently, internal transverse shear reinforcement was included in the design of the specimens to provide specimens that will reflect field conditions.

The amount of internal transverse shear reinforcement greatly affects the shear resistance of RC members. Furthermore, numerous in-service RC beams were found to be deficient in shear due to insufficient shear reinforcement (Khalifa and Nanni 2000). As

a result, maximum allowable spacing for transverse reinforcement was used based on current code provisions (AASHTO and ACI-318-11) to match actual in-service members. Figure 3-2 shows the transverse reinforcement used in this experimental program.

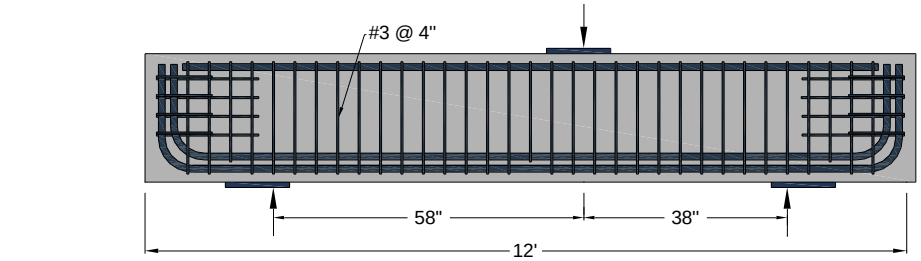

(a) a/d = 1.5

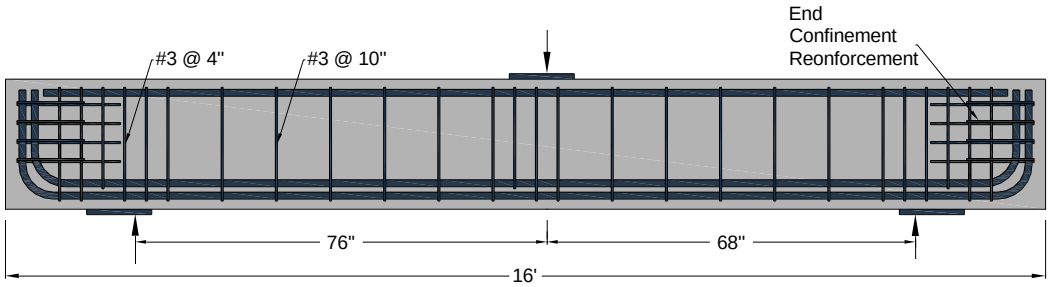

(b) a/d = 3

Figure 3-2: Transvers reinforcement

The shear failure of RC beams with a span-to-depth-ratio less than two (deep beam) is usually due to the crushing of the concrete compression strut in the web of the beam between the applied load and support reaction. The strength of this strut is directly related to the 28-day concrete compressive strength.

The shear failure of RC beams is usually initiated by the formation of web-cracks. These cracks are assumed to form a 45 degree with the longitudinal axis of the beam. The formation of this shear cracking mainly depends on the maximum tensile strength of concrete. It has been proven that tensile strength of concrete is related to a multiple of the square root of the maximum compressive strength of concrete at 28-days.

Consequently, high compressive strength concrete increases the concrete contribution to the shear resistance. Therefore, a low concrete compressive strength is

desirable to minimize the concrete contribution to the beams' shear resistance to allow for a higher shear contribution from external reinforcement (CFRP strips). In this experimental program a concrete with a 28-day compressive strength of 3000 psi was used.

An important point to mention here is that even though it is common in practice for the concrete supplier to supply a concrete with a compressive strength higher than the designed concrete strength, beam (D), which corresponds to tests #7 and #8, had a 28-day compressive strength of 2500 psi.

CFRP material also contributes directly to the shear strength of strengthened RC beams. The contribution of CFRP to the shear resistance is calculated according to the design guidelines provided by ACI 440.2R-08. Since ACI provisions for strengthened RC members assume that the CFRP laminates will be attached to the concrete surface by means of epoxy only without any anchorage, these provisions assume that the shear failure of these strengthened members will occur due to the debonding of CFRP laminates from the concrete surface. Therefore, the maximum tensile strain was limited to 40% of the ultimate tensile capacity of the material.

However, all test specimens in this experimental program were attachede with CFRP anchors to provide additional anchorage. Consequently, this limit was not considered in design calculations since the use of CFRP anchors will permit utilizing the full tensile capacity of the CFRP material. As a result, CFRP strains were assumed to be able to achieve their fracture strain.

The shear resistance of strengthened RC beams is obtained by summing the contributions of concrete, internal transverse steel, and external CFRP reinforcement to the shear resistance. ACI 318-11 code requirements and design guidelines for non-strengthened RC structures was used to calculate the contribution of concrete and transverse steel. The CFRP shear contribution was calculated using modified ACI 440.2R-08 equations. The three contributions were added together to determine the total shear resistance of the strengthened RC beam.

After calculating shear capacities for each cross section, the ultimate flexural capacity was calculated. Although the design shear equations are considered quite conservative, shear failure is still possible due to the uncertainty of shear contributions and the complexity of shear behavior. To enforce shear failure, a margin of safety was implemented to increase ultimate flexural capacity. This margin of safety was intended to prevent flexural failure and ensure the shear failure of the test specimens. Therefore, preventing the flexural failure was simply attained by using a large amount of longitudinal steel reinforcement to provide additional flexural capacity to the specimen.

As mentioned earlier, the T-beam geometry was selected to reflect typical bridge girders. As shown in the test matrix, one of the investigated parameters is the web width of the T-beam. This resulted in two distinct cross sections that were tested in this experimental program. The cross sections of 14-in. web specimen and 8-in. web specimen are presented in Figure 3-3 and Figure 3-4.

‘-

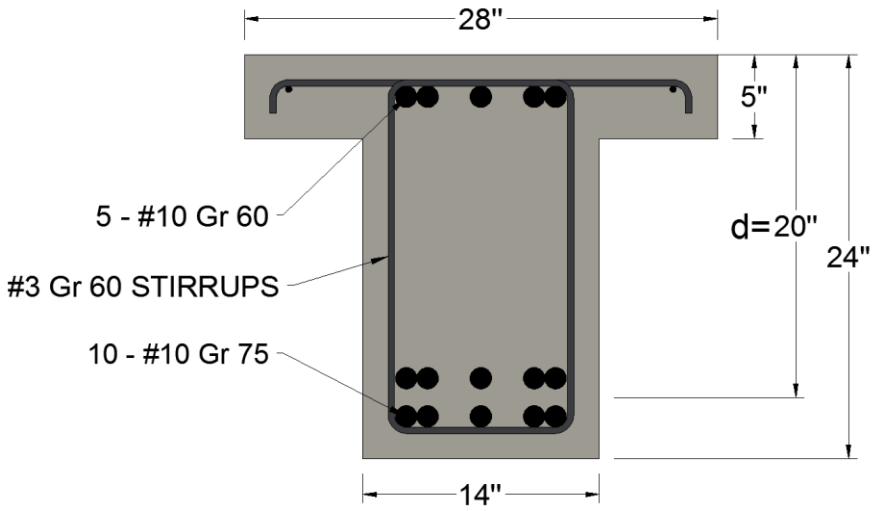

Figure 3-3: Cross section of 14-in. web T-beam

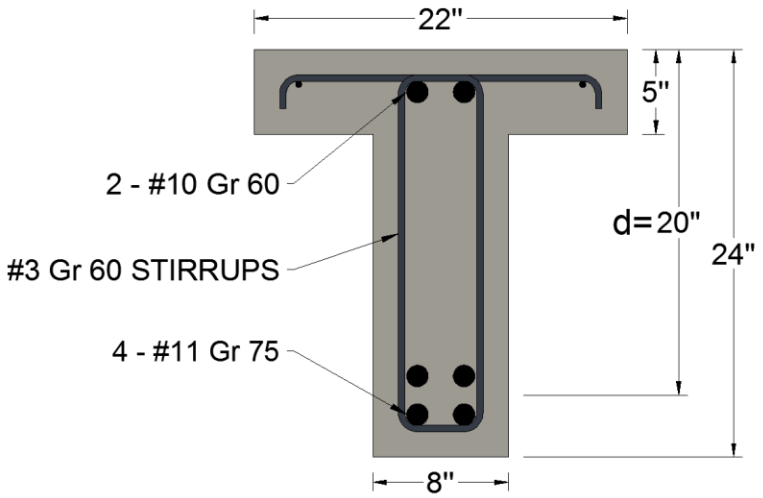

Figure 3-4: Cross section of 8-in. web T-beam

3.2.2 Formwork

All test specimens were fabricated in the lab using formwork built by the project team. Since the test matrix consists of two cross sections that differ only in web width: 14-in. and 8-in., all forms were attached by screws to ease the process of disassembling and reassembling, and to ease the process of adjusting the formwork for cross sections with 8-in. web width. The formwork used in fabricating the four beams is shown in Figure 3-5

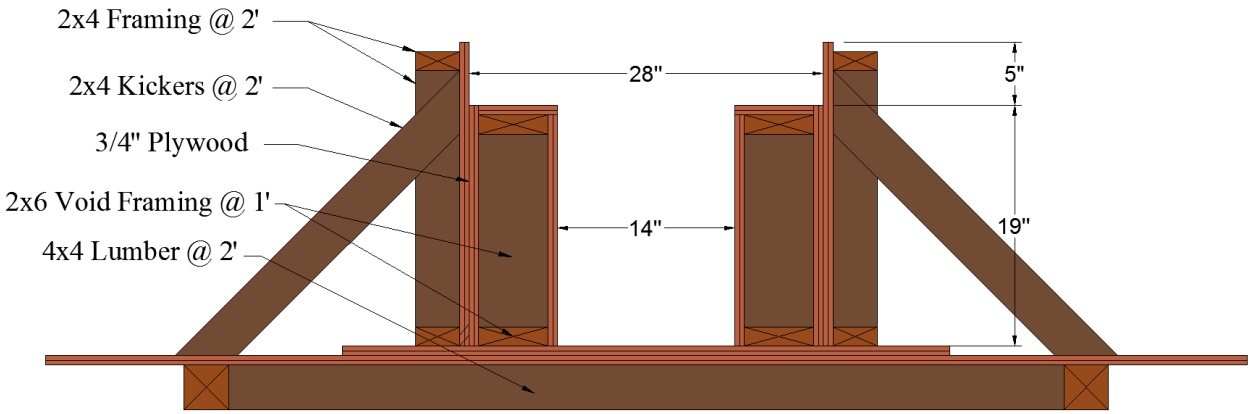

Figure 3-5: Formwork cross section for 14-in. web specimen

A strong base was built to carry the weight of the concrete and the steel cage. The base was constructed by placing ¾-in. plywood sheets on top of 5 ½-ft sections of 4x4 lumber spaces at 24-in. on center. For simplicity and ease of construction, the bas was built in three parts that were assembled later as shown in Figure 3-6 shows. Plywood sheets (4-ft wide ¾-in thick). were placed on top of the base to create the bottom layer of the specimens as can be seen in Figure 3-7.

Figure 3-6: 4x4 Lumber at 2-ft

Figure 3-7: Formwork's strong base

Multiple modules of 2x4 framing were constructed and attached on one side to ¾-in. plywood sheets to form a 28-in. by 24-in. rectangular section. The modules of 2x6 framing were constructed and attached to ¾-in. plywood sheets on all faces to form the void framing required to form the T-shape of the cross section. Figure 3-8 shows the formwork in as built cross-section for 14-in. web specimens.

Figure 3-8: As-built formwork for 14-in. specimen

At the beginning of the experimental program the focus was on testing specimens with a 14-in. web width. The formwork was constructed to allow for casting two specimens at the same time with shear span-to-depth ratios (a/d) of 1.5 and 3 and lengths of 12-ft. and 16-ft., respectively as shown in Figure 3-9.

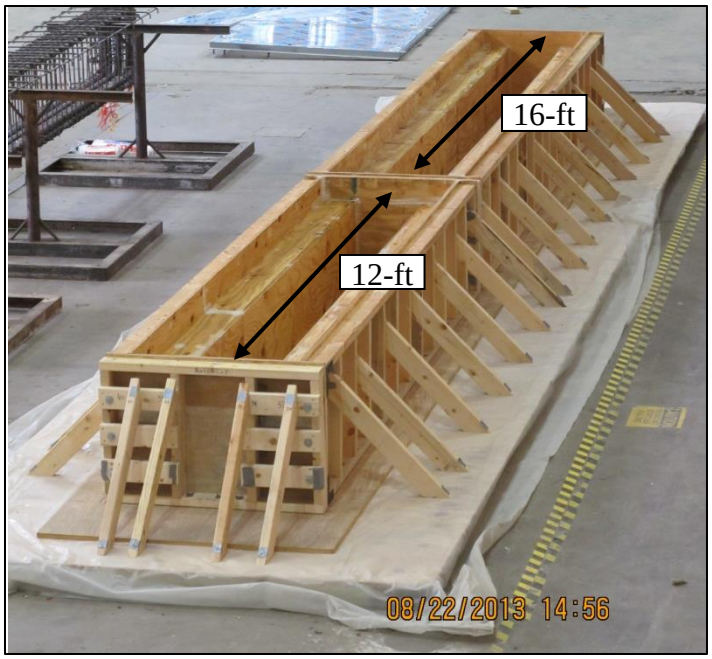

Figure 3-9: Formwork for specimens with different span-to-depth ratios

The 2x4 framing was attached to ¾-in. plywood sheets from both sides to function as a 5-in. wide internal divider and was used to serve as a partition between the two specimens (Figure 3-10). Concrete placement will generate a hydrostatic pressure applied to the sides of the form and inclined kickers spaced 2-ft. on center were used to brace the sides of the form as seen in Figure 3-11.

Figure 3-10: Form divider allowing for casting two specimens at the same time

Figure 3-11: 2x4 kickers for lateral support

After the test results of the deep beam (a/d of 1.5), the research team decided to consider a slender beam (a/d of 3) only, and excluded the deep beam from the next set of tests. Therefore, only one beam with a/d of 3 (16-ft. long) was allowed per cast. The formwork for 8-in. web beams was easily constructed by shifting one side of the form 6-

in. closer to the other side which results in a T-section with 8-in. web and 22-in. flange (Figure 3-12).

Figure 3-12: Formwork for 8-in. web specimen by shifting one side

Caulking was used to seal gaps between formwork parts, and to protect screws from concrete during the casting process. Chamfer strips were attached to the inner bottom edges of the formwork to help develop a desired round edge with a radius of 0.5-in. as displayed in Figure 3-13. According to ACI 440.2R-08, this rounding is necessary to avoid stress concentration on the CFRP laminates that develops at sharp edges of the web causing premature fracture of CFRP laminates.

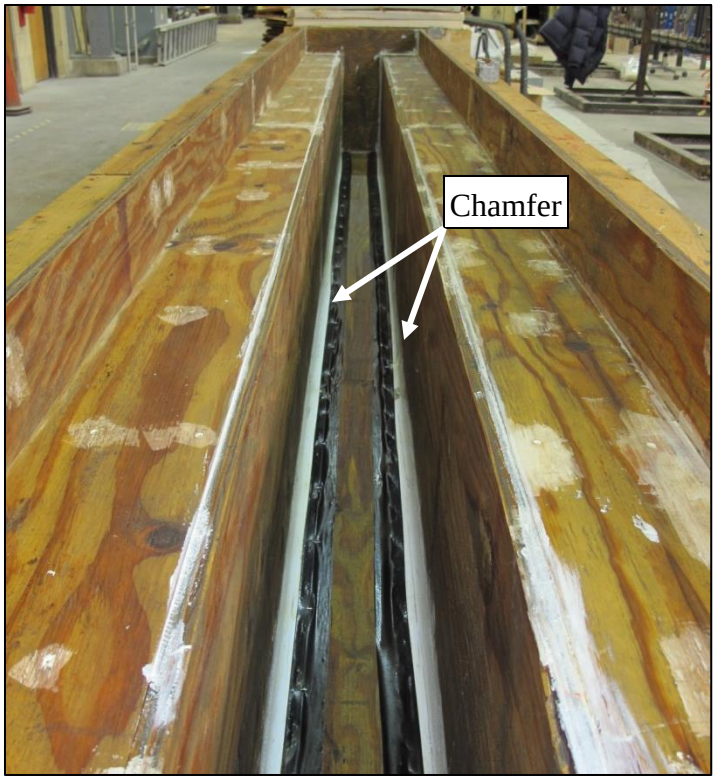

Figure 3-13: Caulk used to seal gaps and chamfer used to round bottom edge of the specimen

3.2.3 Steel Reinforcement

The first two specimens were constructed with a 14-in. web width. Both specimens had identical steel reinforcement layouts. The longitudinal reinforcement for each specimen consisted of ten #10 Grade 75 bars placed in two rows of five bars for each row. All these bars had standard hooks in accordance to ACI 318-11 design guidelines to provide sufficient anchorage to allow for the full flexural strength of the longitudinal reinforcement. In addition to the tensile longitudinal reinforcement, five # 10 Grade 60 steel bars were placed at the top of the beam to increase the compression capacity of the specimen and alleviating concerns regarding crushing of the concrete in

the compression zone. The longitudinal steel reinforcement layout of the first two beams (A and B) can be seen in Figure 3-14

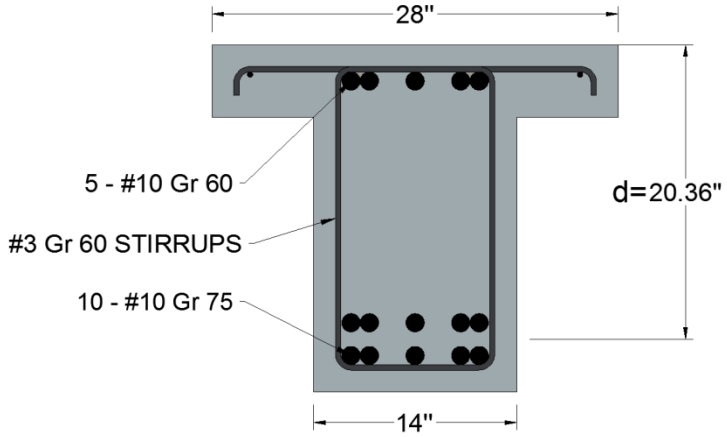

Figure 3-14: Steel reinforcement for beams A and B

However, the longitudinal reinforcement of the second two specimens (8-in. web) consisted of four #11 grade 75 bars placed in two rows of two bars for each row instead of ten #10 used in 14-in. web specimens. For compression reinforcement, two #10 grade 60 steel bars were placed within the compression region instead of five # 10 used in 14-in. web specimens. The longitudinal steel reinforcement layout of the second two beams (C and D) can be seen in Figure 3-15.

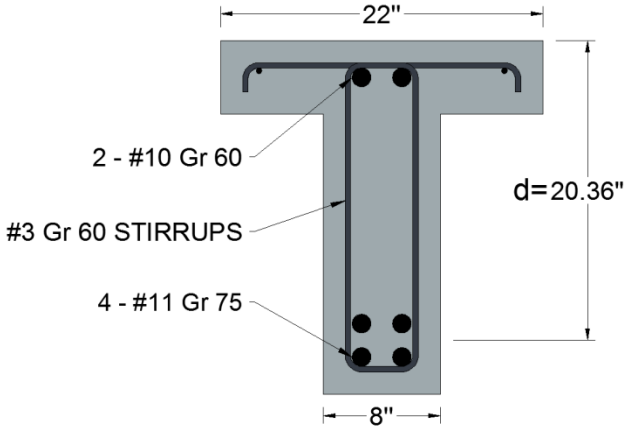

Figure 3-15: Steel reinforcement for beams C and D

The test matrix consisted of one beam (A) that was classified as a deep beam (shear span-to-depth ratio < 2), whereas the other three specimens were classified as slender beams (shear span-to-depth ratio of > 2). Deep beams have a higher concrete contribution to the shear strength than regular (slender) beams due to the greater development of arch action in deep beams. For that reason, ACI 318-11 design guidelines distinguish between these beams for the minimum required transverse reinforcement.

Since internal transverse reinforcement is unable to resist shear unless it is crossed by a crack, ACI 318-11 limits the maximum spacing of vertical stirrups placed in RC members. For deep beams, ACI 318-11 specifies a maximum spacing of transverse reinforcement equal to one-fifth of the beam's effective depth (d/5). On the other hand, ACI 318-11 specifies a maximum spacing of transverse reinforcement equal to one-half of the beam's effective depth (d/2).

Therefore, for beam A (with a/d = 1.5) stirrups were placed 4-in. on center as shown in Figure 3-16, whereas for the remaining specimens (with a/d= 3) stirrups were placed 10-in. on center (Figure 3-17)**.** Additional transverse reinforcement was placed in the loading region to preclude the failure of that region. Additional transverse reinforcement was placed in the end regions to provide confinement to the hooked longitudinal bars.

Figure 3-16: Transverse reinforcement for deep specimen with a/d of 1.5

Figure 3-17: Transverse reinforcement for slender specimens with a/d of 3

Flange reinforcement consisted of #3 Grade 60 bars transverse bars were placed on top of the steel cage at each rectangular stirrup. Two #3 Grade 60 longitudinal bars were placed along the length of the specimen at the edges of the flange. Figure 3-18 shows the flange reinforcement.

Steel lifting inserts were placed at the ends of each test specimen since all specimens had to be transported at various stages of construction and preparation for testing. Figure 3-19 shows the steel lifting inserts used in the steel cages.

Figure 3-18: Flange reinforcement

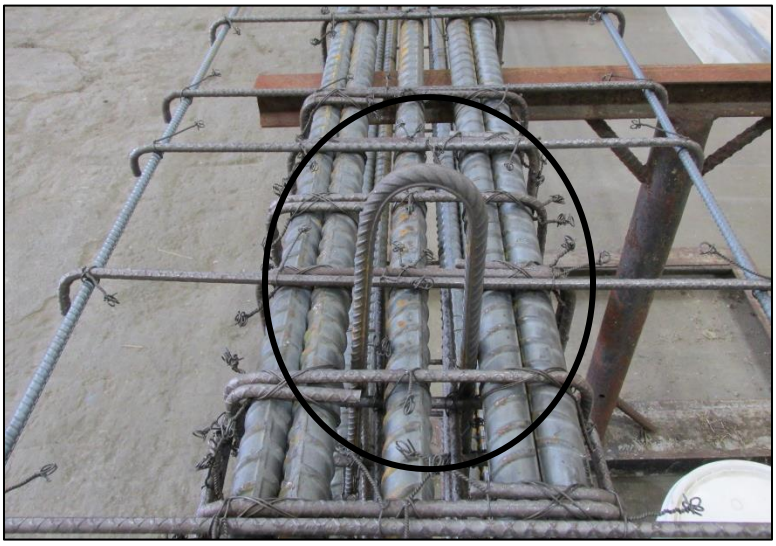

Figure 3-19: Steel lifting insert to lift the cage

An overhead crane was used to place the steel cages in the formwork. Small concrete spacers were used to maintain a concrete cover of 1.5-in. between the bottom of the steel cage and the forms, whereas circular plastic chairs were used between the sides of the steel cage and the forms. Figure 3-20, Figure 3-21, and Figure 3-22 display the final placement of the steel cage inside the formwork.

Figure 3-20: Steel cages and formwork before placement for 14-in. specimen

Figure 3-21: Placement of steel cages in the formwork for 14-in. specimens

Figure 3-22: Placement of steel cage in the formwork for 8-in. specimen

3.2.4 Concrete

Since the aim of the project was to take the advantage of available results from previously tested specimens (Kim 2011), the same concrete mix design was used in this experimental program. The concrete mix design was as follows: 4-1/4 sacks of cement, 25% Fly Ash, ¾-in. maximum aggregate size, and slump of 6-in.

To investigate the shear behavior of a reinforced concrete beam strengthened with CFRP materials, concrete with a relatively low 28-day compressive strength was desirable. A low strength concrete will reduce the concrete contribution to the total shear resistance and allow for a larger contribution from internal transverse reinforcement and external CFRP reinforcement.

Concrete placement occurred through three separate casts over the course of several months. The first two specimens with a/d ratios of 1.5 and 3 (14-in web) were cast simultaneously in one cast, whereas the third and fourth specimens (8-in. web) and a/d of 3 were cast individually.

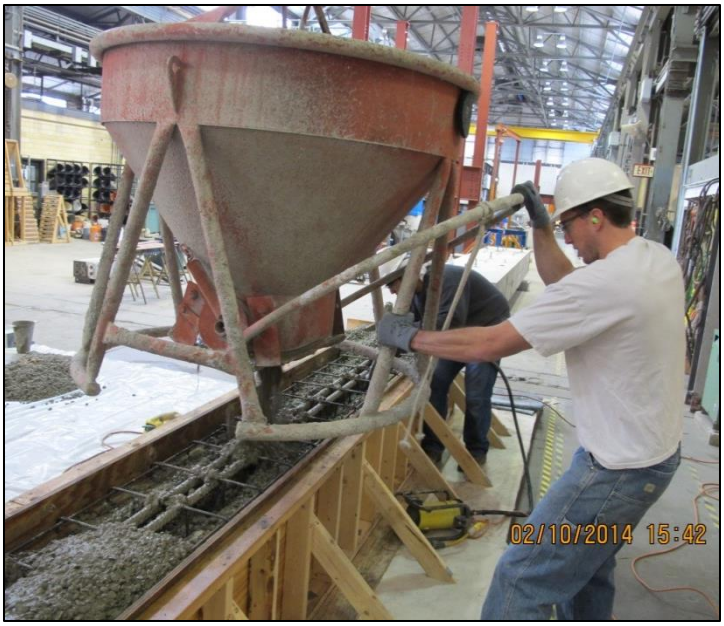

Figure 3-23: Concrete placement using one cubic yard concrete bucket

The concrete placement was accomplished using a one cubic yard concrete bucket attached to an overhead crane to transport the concrete from the truck to the formwork as seen in Figure 3-23. The concrete was placed in three layers, and each layer was vibrated before placing the following layer to ensure that the concrete was well consolidated. Figure 3-24 illustrates the vibration process during the concrete placement. After the concrete was vibrated, the top surface of the specimen was screeded using a 2x4 to remove excess concrete.

Figure 3-24: Vibrating the concrete by electrical vibrators

The first layer covered the bottom layers of longitudinal reinforcement. The second covered the web of the T-beam. The third layer completed the flanges. Figure 3-25 shows the process of casting concrete in the formwork.

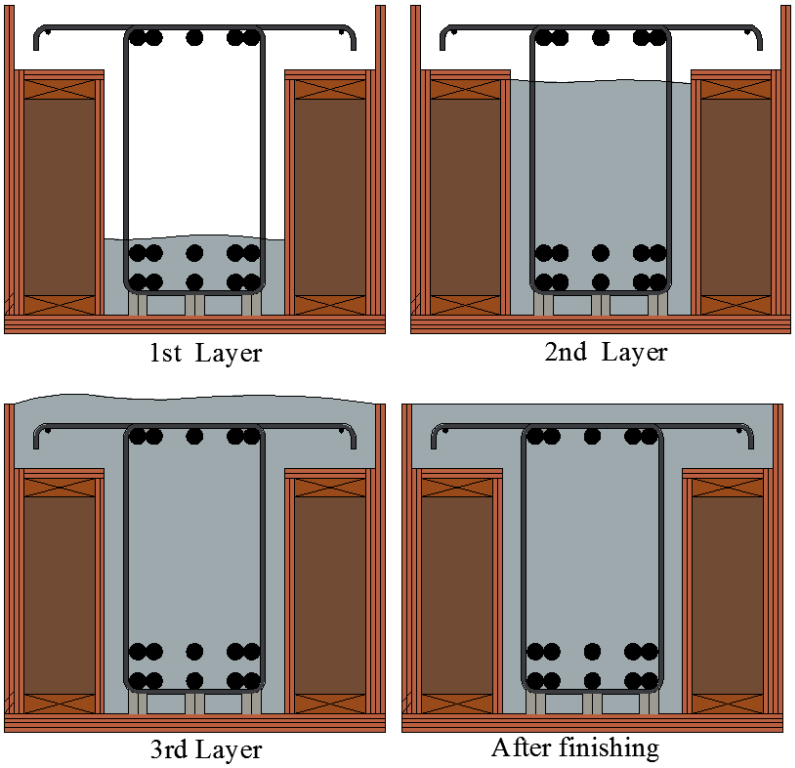

Figure 3-25: Concrete placement in three layers from left to right

The top surface finished with trowels as seen in Figure 3-26 .The specimen was then covered with a plastic sheet and left to cure for a minimum of three days. After three days, the plastic sheet was removed and the specimen was left to cure in the lab environment.

Figure 3-26: Finishing the specimen's top surface

Fifteen 4-in. by 8-in. concrete compressive cylinders were cast during each course of concrete placement and left to cure under same environmental conditions as that of the test specimens (Figure 3-27).

Figure 3-27: Concrete cylinders stored next to the specimen

These compressive cylinders were tested at ages of 3, 7, 14, 21 , and 28 days. The concrete compressive strength for each cast is shown in Figure 3-28.The 28-day compressive strength was 3200, 2500 and 3500 psi, respectively

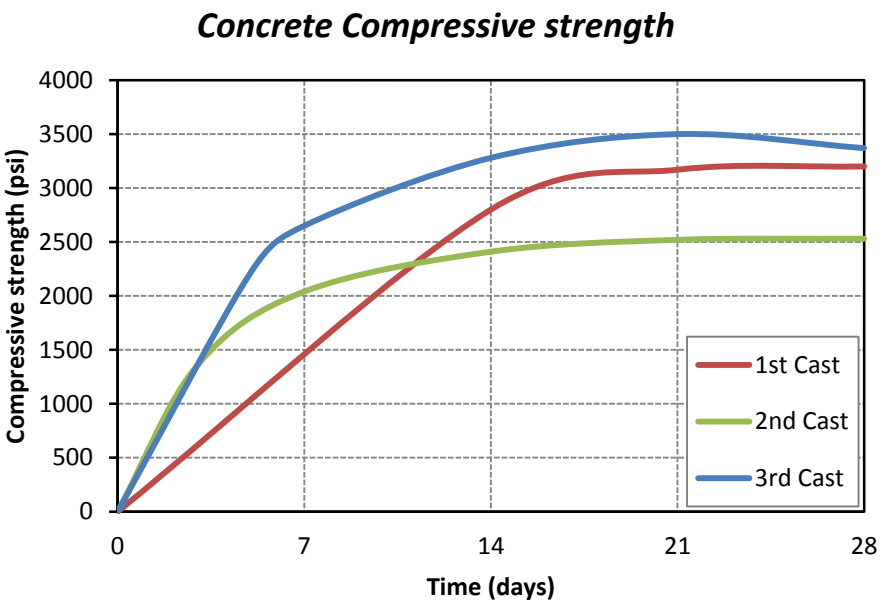

Figure 3-28: 28-day concrete compressive strength

The low strength concrete in the second cast was probably due to adding nine gallons of water to maintain an acceptable slump (6-in or higher) as seen in Figure 3-29.

(a) (b)

Figure 3-29: Adding water to maintain a 6-in. slump

3.2.5 CFRP Installation

The quality of application of FRP material is of importance to the performance of CFRP strengthening system. A poor quality application of CFRP laminates or sheets may result in an undesirable failure mode that reduces the strength gain.

The CFRP material used in this study was Tyfo© SCH -11UP composite. Tyfo® SCH Composite Anchors were used to anchor the CFRP strips. Tyfo© S Epoxy was used to bond CFRP material to the surface of the test specimen. The mechanical properties of the CFRP material were measured according to ASTM D 3039 procedures. Both the dry fiber and laminate properties are presented in Table 3-1.

Table 3-1: Mechanical properties of of Tyfo© SCH -11UP composite

Typical Dry Fiber Properties		Composite Laminate Properties	
Tensile Strength (ksi)	550	*Ultimate Tensile Strength (ksi)*	143
Tensile Modulus (ksi)	33400	*Tensile Modulus (ksi)*	13900
Ultimate Elongation (in/in)	0.0017	*Eleongation at break (in/in)*	0.001
		Thickness (in)	0.02

Care was taken in applying CFRP laminates and anchors to the test specimens. The following sections provide detailed description of the CFRP strengthening system installation process which includes the following:

- Surface preparation
- Anchor hole preparation
- CFRP strip installation (Wet lay-up procedure)
- CFRP anchor installation

3.2.5.1 Surface preparation

As discussed earlier, previous studies have demonstrated the importance of bond strength between the concrete surface and the CFRP laminates (De Lorenzis, Miller et al. 2001, Nakaba, Kanakubo et al. 2001, Cao, Chen et al. 2005, Orton, Jirsa et al. 2008). Bond strength is directly affected by the surface preparation of the test specimen. To prepare the test specimens for CFRP installation, concrete grinder with a rotating disk was used to remove laitance and slightly roughen the surface of the specimen in the regions where the CFRP material will be applied. A heavy duty vacuum was attached to the concrete grinder to minimize the amount of harmful dust produced. Figure 3-30 shows the concrete grinder used in cleaning and roughening the surface.

Figure 3-30: Grinding the concrete surface to apply CFRP laminates

Sharp corners that form at the bottom edges of the specimens' web were rounded to a radius of approximately ¾-in to prevent premature fracture of CFRP laminates due to stress concentration at these sharp edges. A rounded bottom edge is shown in Figure 3-31.

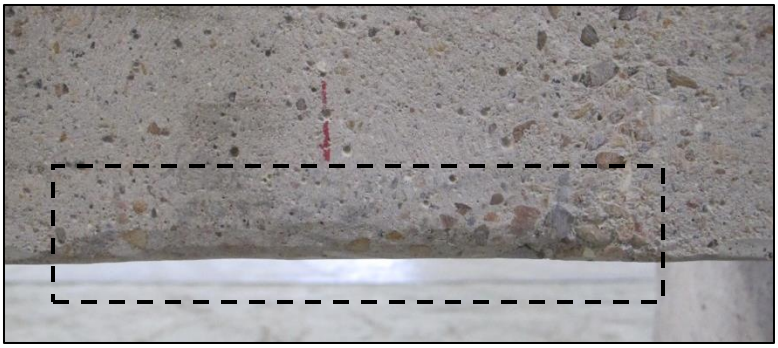

Figure 3-31: Rounded edge to relieve stress concentrations on the CFRP strip

3.2.5.2 Anchor hole preparation:

Preparation of anchor holes is no less important than surface preparation. Improper anchor hole preparation may cause premature failure of the anchors. Thus, after surface preparation and removal of any sharp corners were completed, the exact locations of anchors were marked. A concrete hammer drill was used to drill the anchor holes. A 4-in. deep hole was drilled for all anchors in the test program. End-anchor holes were drilled to form 5/8-in. in diameter where middle-anchor holes were drilled to form 3/4-in in diameter. A vacuum was attached to the drill while boring the concrete to minimize the amount of harmful dust produced throughout the drilling process (Figure 3-32).

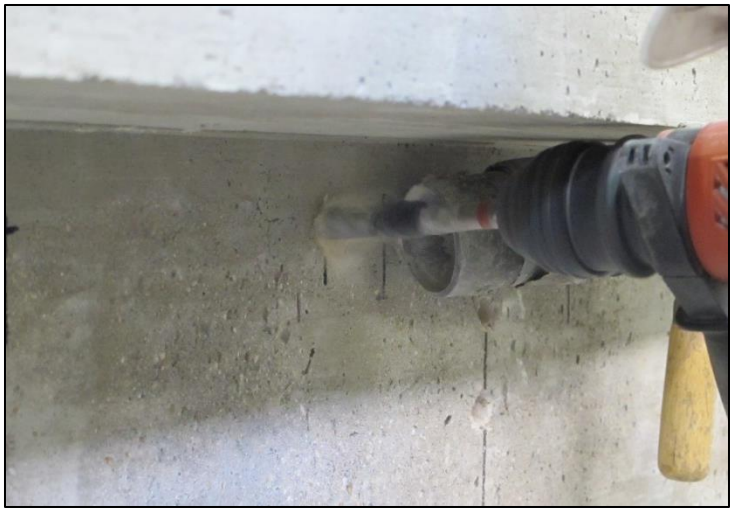

Figure 3-32: Drilling the anchor hole

After drilling the anchor holes, a large amount of debris produced in the course of drilling was removed by directly vacuuming the holes using the vacuum cleaner. However, a small amount of debris still remained in these holes. This would affect the bond strength between the inside surface of the anchor hole and the anchor itself which will result in a huge reduction in the performance of the anchorage system. Therefore, an air pressure gun was inserted into the hole to remove the remaining debris and dust. An anchor hole before and after drilling the hole and grinding the surface is shown in Figure 3-33.

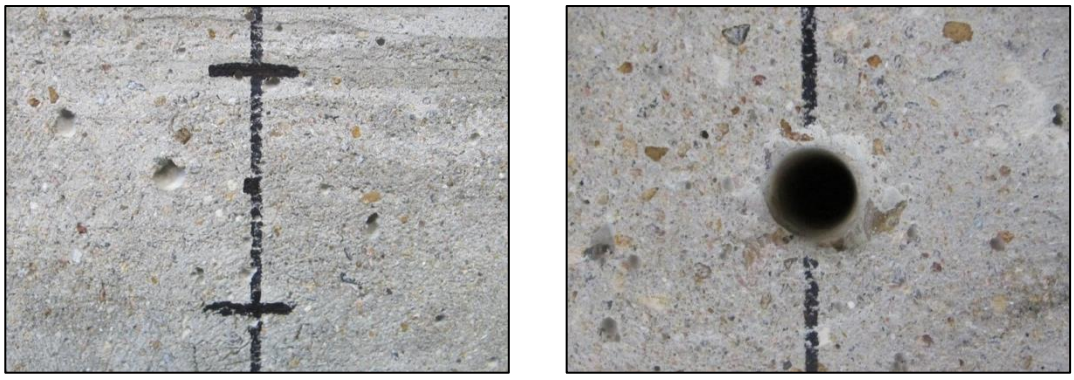

Before After

Figure 3-33: Typical anchor hole

As stated earlier, a premature anchor failure can occur due to stress concentrations at the edge of the anchor hole. To prevent this brittle mode of failure, areas of high stress concentration must be removed. For that reason, an abrasively concrete bit was used to round the sharp edges of the hole to a radius of 0.5-in. Figure 3-34 shows an anchor hole with rounded edge. It is important to mention that for end anchors where the anchor fan is spread in one direction, only one side of the hole must be rounded. Therefore, only the side where the anchor fan is in contact with concrete was rounded. However, for middle anchors where the anchor fan is spread in two directions, only the two sides in contact with the anchor were rounded. Figure 3-35 displays a test specimen after finishing surface preparation and anchor holes.

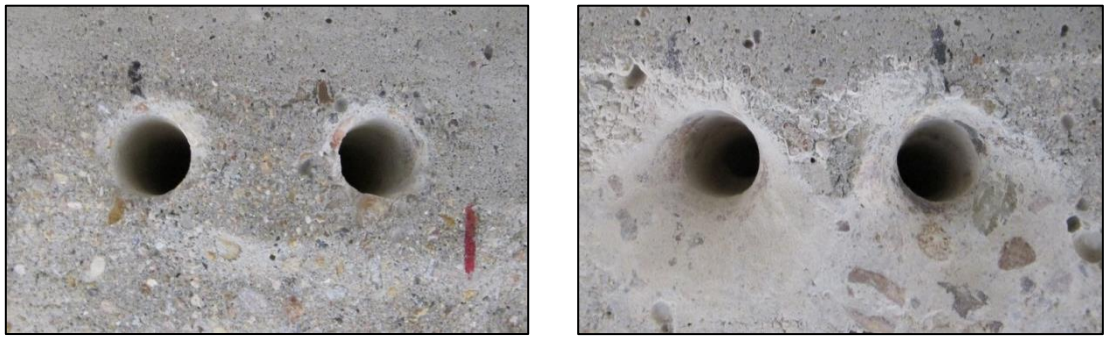

Before After

Figure 3-34: Anchor holes after rounded (double layer application of CFRP)

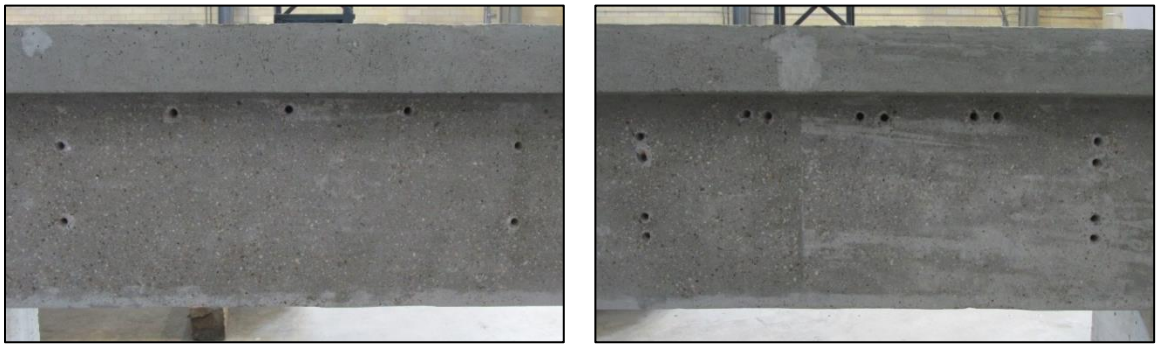

Single layer Double layer

Figure 3-35: Anchor holes layout for specimen with a/d of 1.5 (deep)

3.2.5.3 Bi-directional CFRP strip installation (Wet lay-up procedure):

There are two different procedures for Fiber Reinforced Polymer (FRP) material installation known as dry lay-up procedure and wet lay-up procedure. The dry lay-up is a common procedure used to install FRP materials, especially in large size applications. A detailed description of the dry lay-up installation procedure for uni-directional CFRP application can be found in Quinn (2009).

The wet lay-up procedure is a more common installation method to install CFRP materials. The main difference between these two installation methods is that for the dry lay-up procedure, workers place a dry CFRP strip on the epoxy saturated surface, whereas in the wet lay-up procedure, the CFRP material is impregnated with epoxy before it is applied to the surface. This makes the CFRP material heavier and more difficult to handle. For that reason, dry lay-up installation may be better for very large applications. For this experimental program, wet lay-up procedure was used for all test specimens.

It is important to note that in this experimental program, the test specimens were kept in the normal position during the course of constructing, preparing, and installing the CFRP material. Specimens were not inverted to simplify the process of applying the CFRP material as in previous project (TxDOT 0-6306). By keeping the specimens in the normal position, researchers were better able to evaluate the process of applying the bi-directional CFRP strips and CFRP anchors in the field.

3.2.5.3.1 CFRP strips:

A 24-in. wide roll of Tyfo© SCH -11UP composite provided by FYFE Co. LLC. was used as the source of CFRP strips in this experimental program.

The application process of bi-directional CFRP is more challenging than uni-directional CFRP for two reasons: 1) bi-directional application of CFRP strips involves handling horizontal strips in addition to vertical strips, and 2) test specimens, in this experimental program, are not inverted to properly mimic actual cases in the field. For

the application of bi-directional CFRP in the first test specimen, the vertical strips consisted of a single strip that was cut and installed first. Researchers attached the end of the strip to the top of the web on one side and then aligned it under the soffit and all the way to the other top side of the web. The installation of a single strip around the web of the beam within the bi-directional CFRP strip was found to make the overall process more difficult. Consequently, for the remaining three specimens, two strips were spliced over the soffit of the web. Figure 3-36 illustrates the two methods used in applying vertical CFRP strips.

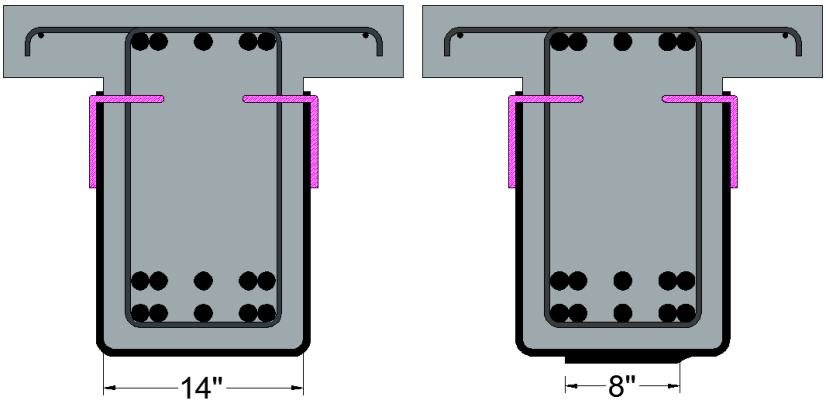

Figure 3-36: Vertical CFRP strips application (a) for beam A and (b) for the rest of the specimens

The splicing of vertical strips considerably eased the installation process of bi-directional CFRP application. The splicing of vertical strips was very effective, as will be seen in the results section.

As mentioned in the background section, for shear strengthening of RC beams with uni-directional application, CFRP strips are bonded vertically to the web of the beam. For bi-directional application of CFRP, however, horizontal strips are bonded to the web of the beam in addition to the vertically bonded strips.

To develop the full tensile capacity of the horizontal strips, CFRP end-anchors were used. However, for specimens with a shear span-to-depth ratio of 3, these horizontal

strips are long enough so that using end-anchors alone may not allow then to reach their full tensile capacity. Therefore, an additional middle-anchor was implemented to provide effective anchorage to the horizontal strips, as seen in Figure 3-37.

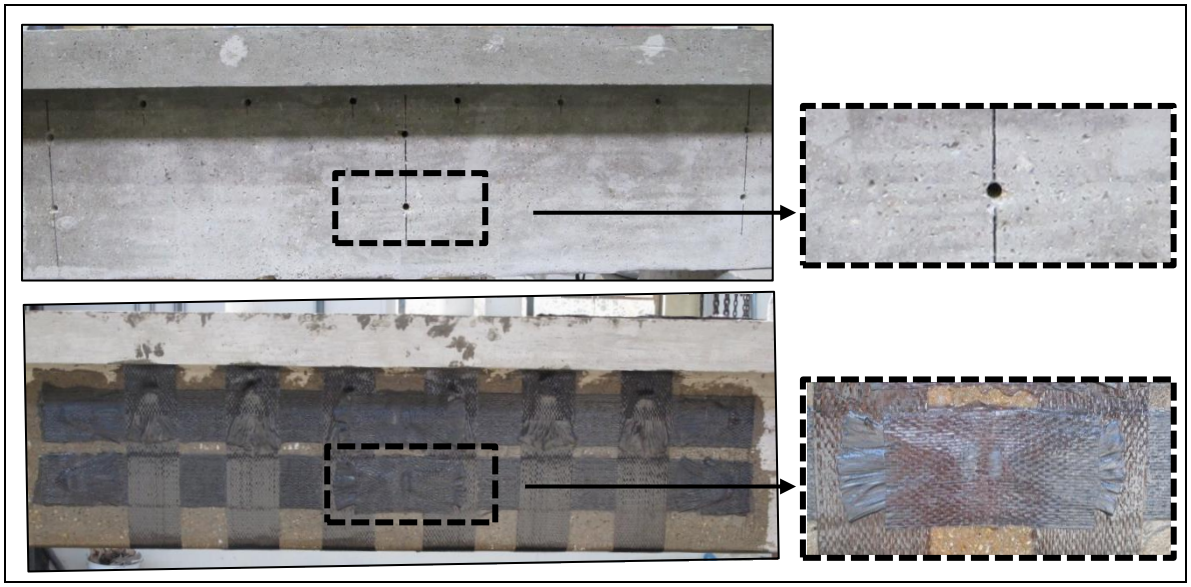

Figure 3-37: Middle-anchor holes for horizontal strips (single layer application)

The middle-anchor consisted of single anchor with a cross-sectional area greater than the end-anchor. In this study, CFRP anchors with 1/2-in diameter were used as end-anchors; while CFRP anchors with 5/8-in. diameter were used as middle-anchors. The fan portion of middle-anchor was split in two parts and fanned out in two opposite directions, as shown in Figure 3-38

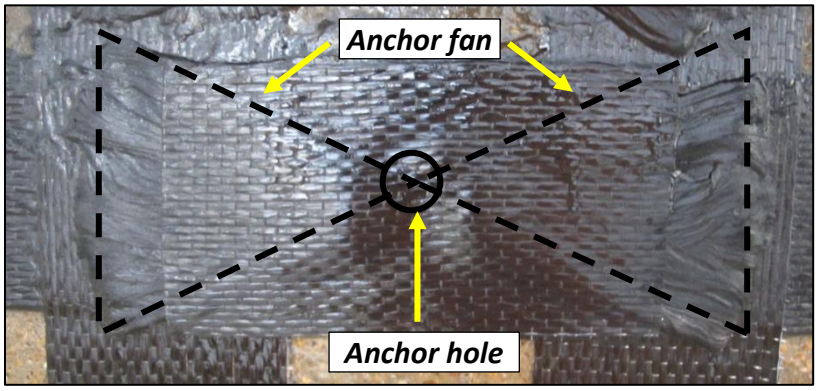

Figure 3-38: Splitting the middle-anchor to form two opposite anchors

In order to distribute anchor stresses, two 5x5-in. patches were applied below and above the CFRP end-anchors. For bi-directional application where horizontal strips exist requiring not only end-anchors but also middle-anchors, a new detail was implemented for middle-anchors. Two 10x5-in. patches were applied to reduce stress concentration on both sides of the middle-anchors. Both horizontal and vertical strips were cut to specific dimensions (Figure 3-39).

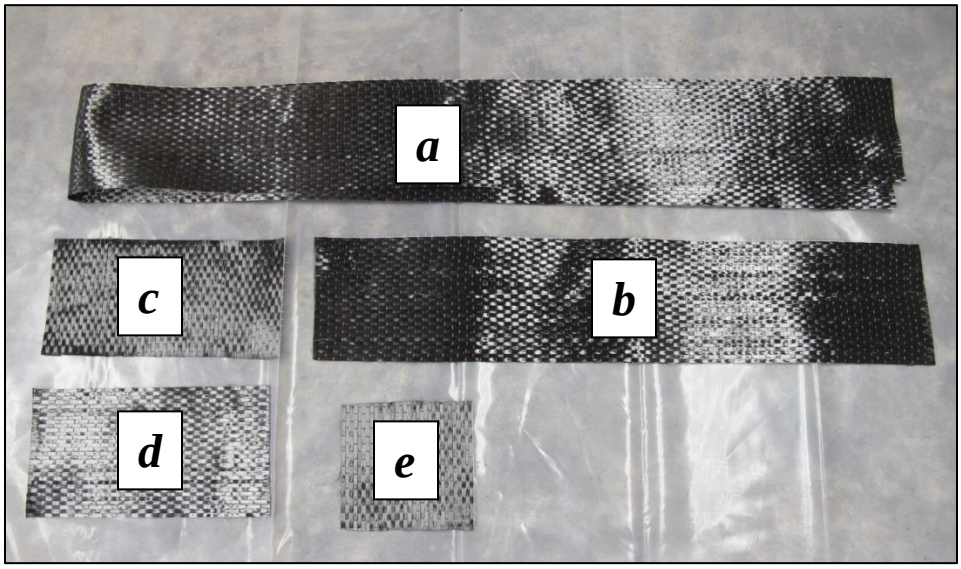

Figure 3-39: (a) Horizontal strip (b) Vertical strip (c)&(d) Middle-anchor patches (e) End-anchor patch

3.2.5.3.2 CFRP anchors

A typical CFRP anchor used in this experimental program is shown in Figure 3-40. Two types of CFRP anchors were used in strengthening the test specimens: an end-anchor that was installed at the end of each CFRP strip, and a middle-anchor that was applied in the middle of the horizontal CFRP strip. The only difference between these two anchors is the amount of carbon fiber fabric, which results in a change in the diameter of the anchor. In this experimental study, end-anchors with a 1/2-in. diameter and middle-anchors with a 5/8-in. diameter were used.

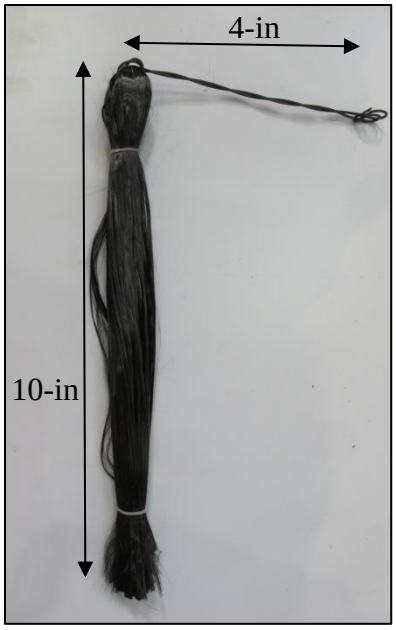

Figure 3-40: Typical CFRP anchor with 4-in. long insertion tool

As can be seen in Figure 3-40, the standard 10-in long anchor consists of bundled uni-directional fibers. The portion of the anchor that will be embedded in the concrete is known as the key portion while the remaining portion is known as the anchorage fan. The anchor at this stage is extremely difficult to insert it into the hole and some device is necessary to insert the anchor. Consequently, two rebar ties were cut in half and twisted together to insert the anchor.

The effect of the amount of CFRP material on the shear contribution of CFRP in bi-directionally strengthened RC beams was investigated as a main parameter in this experimental study. Thus, single layer bi-directional CFRP strips were tested in one span whereas double layer bi-directional CFRP strips were installed in the other span.

As discussed earlier in the background section, an anchor with a total cross-sectional area equaling twice the area of CFRP strip or greater is recommended (Orton, Jirsa et al. 2008) to develop the full tensile capacity of that CFRP strip. Therefore, for the double layer case where the area of CFRP strip was doubled, two anchors were installed instead of the area of the anchor being increased to satisfy this cross-sectional area

requirement as seen in Figure 3-41 . It was reported that multiple anchors provide better force transfer than a few large anchors (Orton, Jirsa et al. 2008).

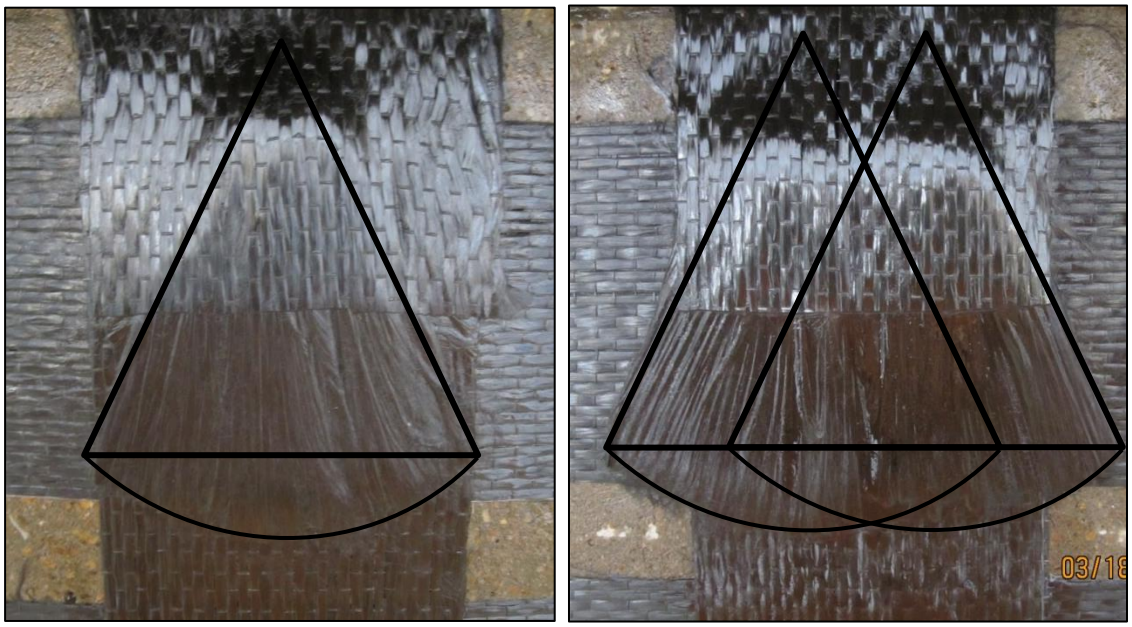

Single layer Double layer

Figure 3-41: End-anchorage for vertical strip left (single anchor), right (double anchor)

Prior to the bi-directional installation of CFRP, the exact locations of the CFRP sheets are marked on the surface of the specimen (Figure 3-42). This step simplifies the installation process, especially for the long horizontal strips associated with the bi-directional application of CFRP material.

(1)

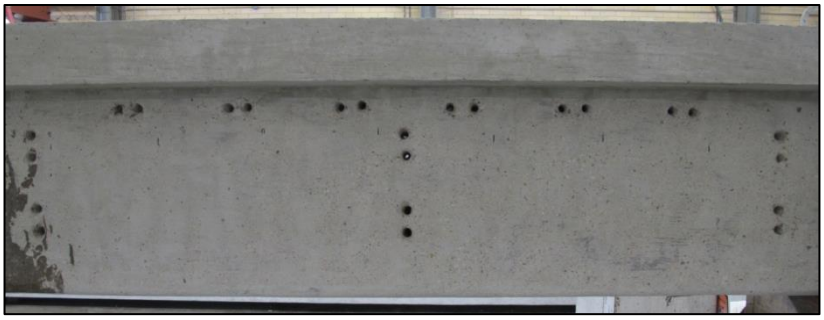

(2)

(3)

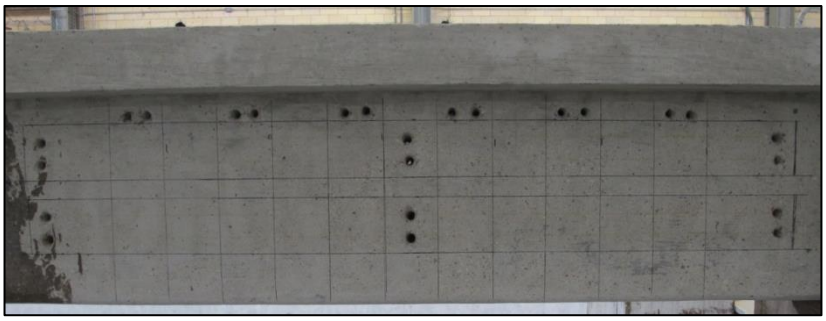

Figure 3-42: Marking CFRP strip locations

3.2.5.3.3 Installation

In this section, a brief description of the installation process of bi-directional application of CFRP is given for the double layer configuration. Before starting the installation process, the area and required equipment for CFRP applications was prepared as shown in Figure 3-43

Figure 3-43: Preparation for CFRP installation

The epoxy was prepared at the beginning of the installation process. The epoxy was a two-component matrix material (Component A and B). Component A is a high strength resin with a clear to pale yellow color, while component B is a chemical hardener with a clear color. Figure 3-44 shows the two components of the epoxy.

Figure 3-44: The two components of the epoxy

The two components were proportioned using a ratio of 100 parts of component A to 42 parts of component B by volume (Figure 3-45).

Figure 3-45: Proportioning the epoxy components

A heavy duty drill with a mixing paddle was used to combine the two components at 400-600 RPM for five minutes until both components were uniformly blended, as shown in Figure 3-46.

Figure 3-46: Mixing epoxy components

The epoxy was then poured into a plastic paint tray, as shown in Figure 3-47.

Figure 3-47: Pouring the epoxy in small trays

As it was difficult to reach the inner portion of the anchor holes, a small swab made of CFRP sheet bundled together with two rebar ties was used to saturate the inside of the holes (Figure 3-48).

Figure 3-48: Saturating anchor holes using bundled CFRP strip

A small paint roller was used to saturate the concrete surface with the epoxy, as seen in Figure 3-49. This is an essential process in CFRP installation as it allows the epoxy to fill voids in the concrete surface. Any large voids are generally filled with a material compatible with the epoxy. No large voids were encountered.

Figure 3-49: Saturating the concrete surface before CFRP application

After the concrete surface was saturated, CFRP strips were impregnated with epoxy on both sides using a small paint roller (Figure 3-50). This part of the process is the key difference between the dry lay-up and the wet lay-up procedures.

Figure 3-50: Impregnating both sides of CFRP strip before attaching it to the surface

Once the anchor hole, the concrete surface, and the CFRP strip were all saturated with epoxy, the horizontal CFRP strip could be applied to the surface of concrete, as shown in Figure 3-51. After attaching the horizontal CFRP strip, a plastic putty knife was used to remove all air bubbles that exist between the CFRP strip and concrete surface, as seen in Figure 3-52. Excessive epoxy can also be removed by firmly pushing the edge of knife along the CFRP strip. This step resulted in high quality bond between the CFRP strip and the concrete surface.

Figure 3-51: Attaching horizontal CFRP strip

Figure 3-52: Removing excessive epoxy from the strip using plastic putty knife

The end-anchor and middle-anchor holes are invisible after the horizontal strip is applied. A knife or screwdriver can be used to separate the fibers of the CFRP strip to facilitate the insertion of the CFRP anchor. A 5x5-in. patch was then applied at the location of the anchor hole with fibers oriented transversely to the fibers of the CFRP strips (Figure 3-53).

Figure 3-53: First 5x5-in patch placed on top of the hole location

The plastic putty knife was used again to remove additional air between the two CFRP layers (strip and patch) and to ensure the quality of the bond. A knife or screwdriver was used again to separate the fibers of the patch. After these last two steps, a clear opening in the CFRP over the anchor hole was produced, as seen in Figure 3-54.

Figure 3-54 Making an opening for the anchor using a knife

Once the fibers of the strip and the patch were separated appropriately, the CFRP end-anchors were saturated with epoxy. The anchor then was squeezed to remove excess epoxy in order to ease insertion into the hole. Then, the anchors were gently inserted by holding the pre-made insertion tool and pushing it gradually inside the anchor hole.

Once the key portion of the anchor was inserted, the remaining portion formed the anchorage fan. The remaining fibers of the anchor were then uniformly distributed over the width of the strip to form the anchorage fan. A putty plastic knife was used to distribute the fibers over the width of the strip and also to remove any excessive epoxy that still existed in the anchor, as shown in Figure 3-55. After that, a second 5x5-in. patch of CFRP was applied over the anchor with fibers parallel to the fibers of the CFRP strip (Figure 3-56). Once end-anchors were applied on both ends of the horizontal CFRP strip, the second horizontal strip and its end-anchors were applied following the same steps.

Figure 3-55: Removing excessive epoxy from CFRP anchor

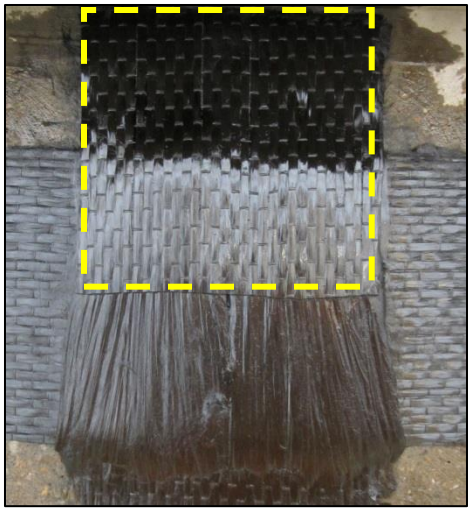

Figure 3-56: Second 5x5-in. patch placed over CFRP anchors

After the horizontal strips and their end-anchors were placed, a 10x5-in. patch with fiber oriented transversely to the horizontal strip's fibers was applied above the middle-anchors holes. Middle-anchors then were saturated and inserted in the middle holes following the same procedures followed with end-anchors but with 10x5-in patches instead of 5x5-in patches used for end-anchors.

As can be seen in Figure 3-57, middle-anchors of horizontal strips overlap the vertical strips. Vertical strips in shear strengthening applications are the main contributing component to the shear strength of the member. Therefore, a strong bond between the concrete surface and the vertical strips is desirable in order to effectively utilize the tensile capacity of the vertical strips. Consequently, after middle-anchors of horizontal strips were inserted in their holes, they were left suspended in order to apply the nearest vertical strips (middle strips in this case) to prevent weakening the bond between the vertical strips and the concrete. The vertical strips next to the middle anchors were applied following the same steps used in applying horizontal strips. When that step was completed, the middle anchors were then distributed in two opposite directions (Figure 3-58).

(1) (2)

Figure 3-57: (1) Middle-anchors suspended after insertion (2) Overlap of anchor fan and vertical strips

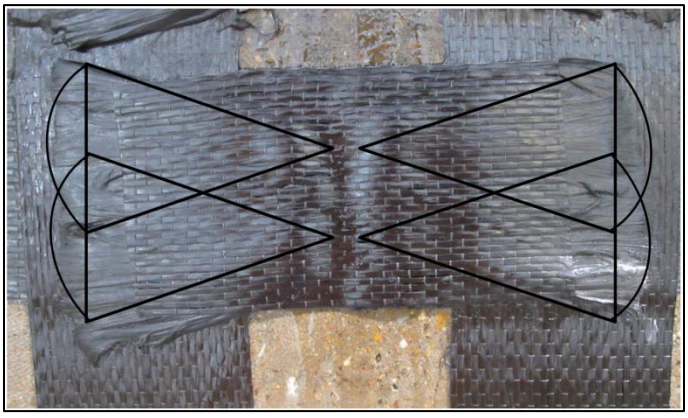

Figure 3-58: 5/8-in. middle-anchor spread in both directions

After that, a 10x5-in. patch with fibers parallel to the strip's fibers was applied to cover the middle-anchors. Then, the remaining vertical strips were applied consecutively following the previously stated procedures. After finishing all work associated with applying the CFRP material, the CFRP application should be inspected to ensure the quality of the application and to ensure that no CFRP strips, anchors, or patches move before the epoxy st. The final bi-directional double layer CFRP configuration can be seen in Figure 3-59.

Figure 3-59: Bi-directional application layout for double layers configuration

3.3 EXPERIMENTAL TEST SETUP

A test setup consisting of three point loading system was used to test all specimens. Four steel columns were erected and bolted to the laboratory strong floor with high strength bolts. Each of these columns can carry a 200-kips. in tension resulting in a total tension capacity of 800-kips for the entire setup, more than required for testing the specimens.

Each pair of columns was connected by a steel C-section. A large steel W-section was bolted to the bottom of the two steel C-sections. This large W-section supported a hydraulic loading ram with a 600-kips capacity. Figure 3-60 shows the side view of the test setup. A front view for specimens with a/d of 3 and 1.5 is shown in Figure 3-61 and Figure 3-62, respectively.

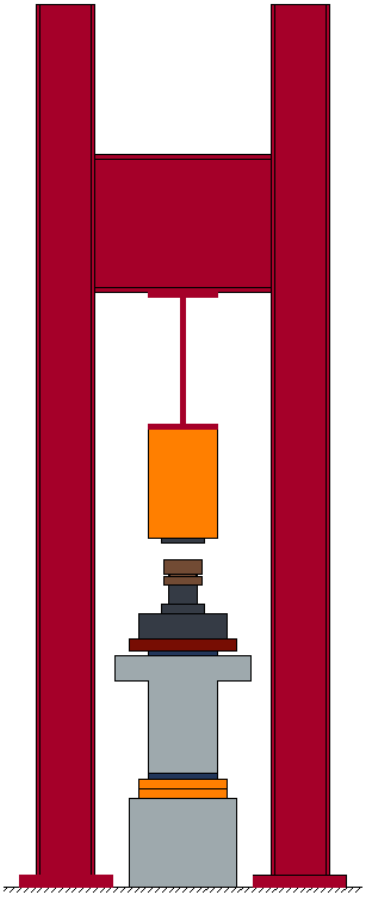

Figure 3-60: Side view of the test setup

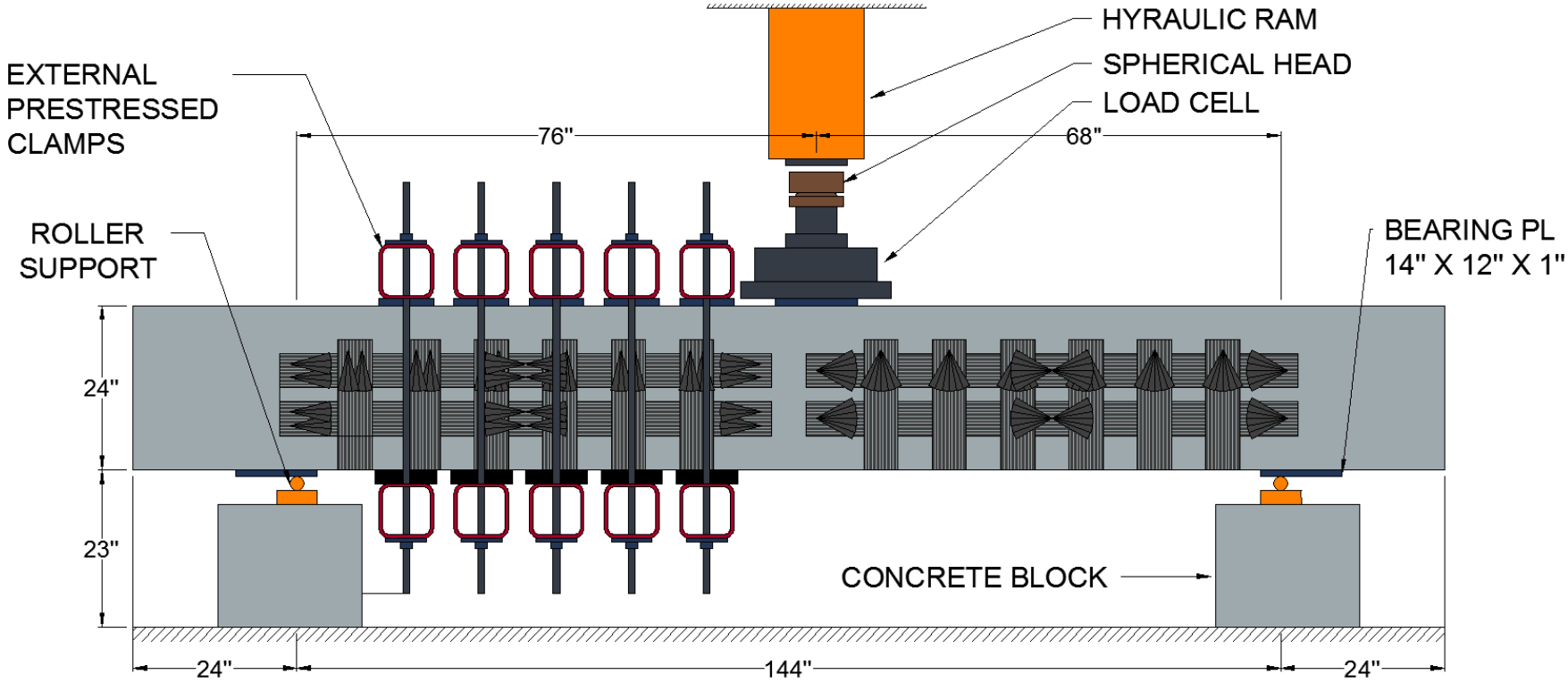

Figure 3-61: Test setup for a/d of 3 specimens (16-ft. long)

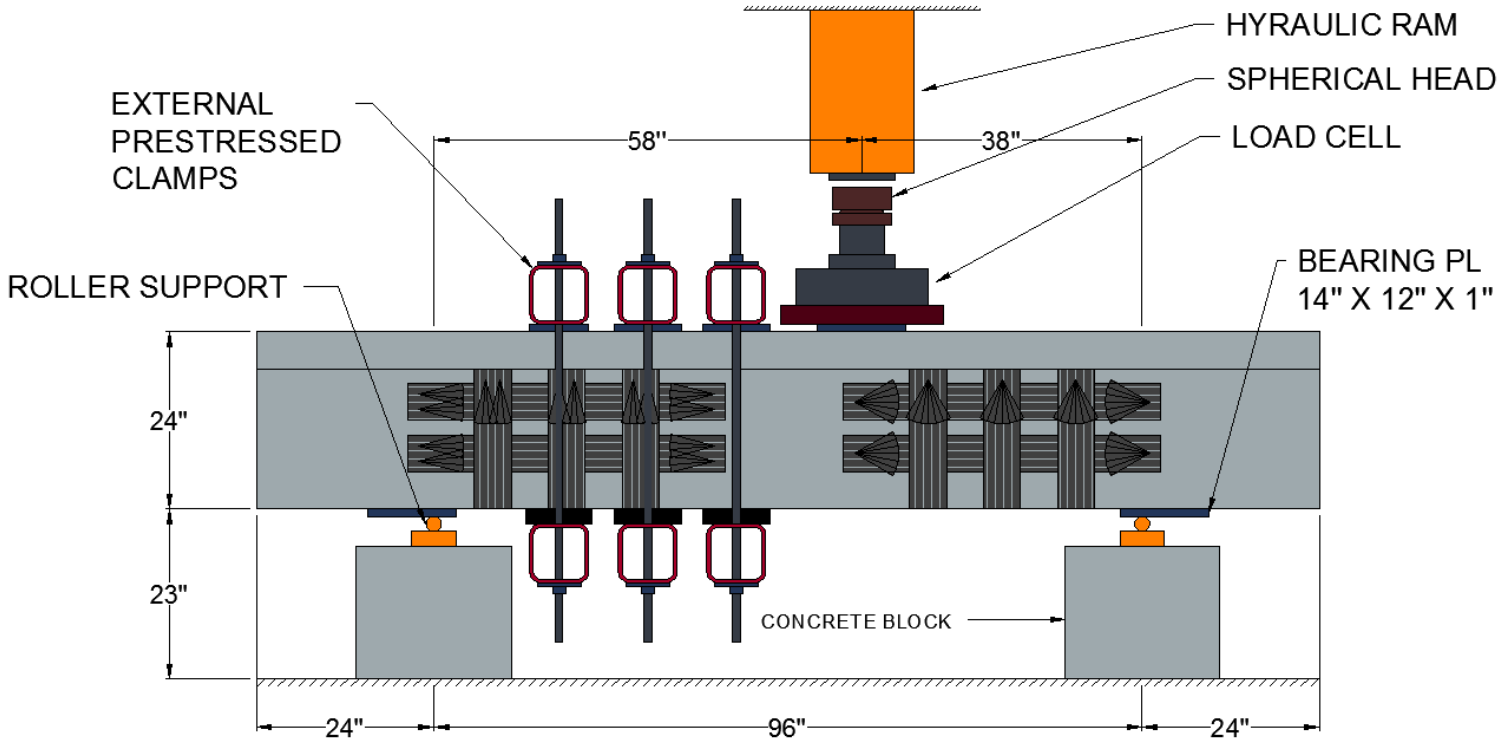

Figure 3-62: Test setup for a/d of 1.5 specimens (12-ft. long)

As will be discussed later in 3.5.1, cameras were used to record the images of the test span during the test. However, the configuration of the test setup prevents the cameras from recording images for the whole test region; the camera lenses are not wide enough and therefore need to be a further distance from the specimen, which causes the steel columns to block part of the test span from the camera. Consequently, all test specimens were rotated 25-degrees to allow the cameras to view the whole test span, as can be seen in Figure 3-63 and Figure 3-64.

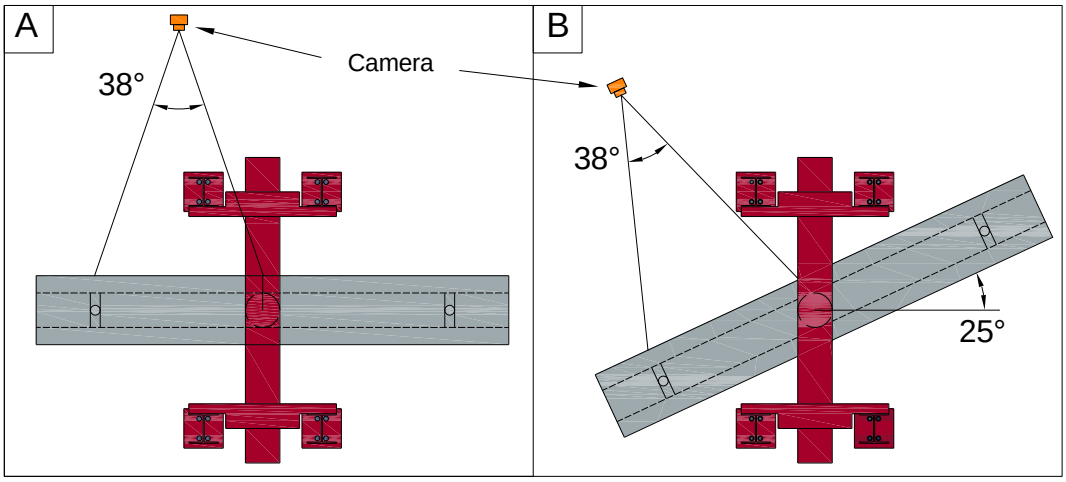

Figure 3-63: (A) regular position, (B) rotated 25-degrees.

Figure 3-64: As-built test setup with 25-degrees rotation

3.3.1 Loading and reaction

A 1000-kips. capacity load cell was attached to the hydraulic ram to monitor the load applied to the specimen. A 2 ½-in. thick steel plate was placed between the load cell and the flange of the specimen to uniformly distribute the applied load, as seen in Figure 3-65. Hydrostone was used to create a smooth surface between thick steel plate and the top surface of the specimen; therefore, a lighter plate was preferable to ease the process of placing the hydrostone. Additionally, a 1-in. thick steel plate was placed between the thick plate and the top surface of the specimen. A spherical head was placed on top of the load cell to insure proper alignment between the load cell and the hydraulic ram. Figure 3-65 shows the loading system.

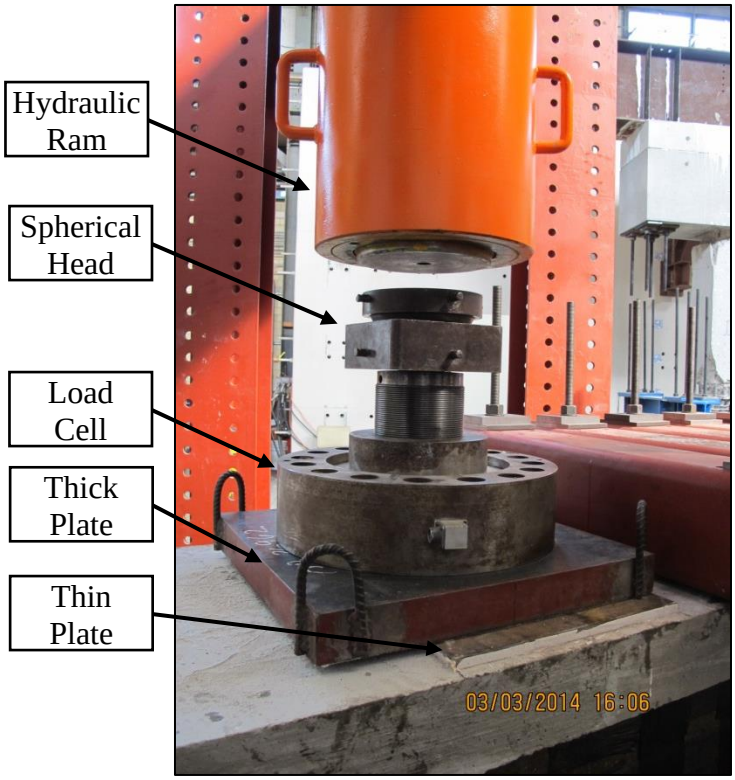

Figure 3-65: Loading system

Each one of the two reactions points consisted of the following: 1) a 21x18-in. concrete block, 2) a 2-in. diameter steel roller welded on top of a 6x2-in. steel plate, and 3) a 12x1-in steel plate used as a bearing plate as shown in Figure 3-66.

Hydrostone was used to provide an even surface for load transfer from the loading system to the specimen and from the specimen to the reactions. Hydrostone was used in different locations: 1) to attach the roller to the concrete block and form a pin support, 2) to attach the steel bearing plate to the bottom of the specimen, 3) to attach the plate under the load cell to the top surface of the flange and top, and 4) to attach plates under the hollow steel sections (HSS) to the top surface of the flange.

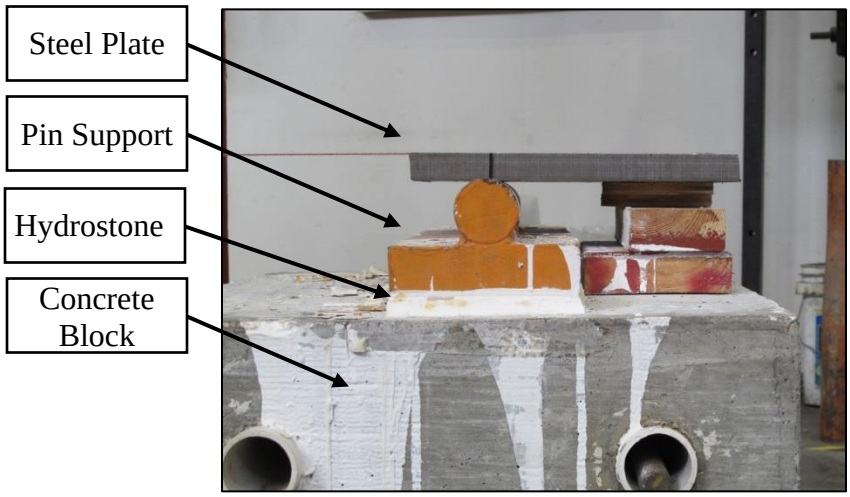

Figure 3-66: Components of a typical reaction

3.3.2 External clamps

For the test setup shown above, the load was applied between the two reactions resulting in a large shear force in a shorter span (test span) and a smaller shear force in the longer span. However, this shear force was large enough to cause failure in the untested span. Therefore, in order to perform two tests from each specimen with the given test setup, some sort of strengthening must be provided to the untested region. Pre-stressed external clamps were used to increase the shear capacity of that region as shown in Figure 3-67. For specimens with a/d of 3, five hollow steel sections (HSS)

were used for external pre-stressing, whereas three HSS were used for specimens with a/d of 1.5.

Figure 3-67: External clamps for specimens of a/d =3

These pre-stressed clamps consisted of two HSS 8x8x1/2-in. tubes placed on the top of the flange and under the web of the specimen. To protect the bottom face of the web from local crushing, 3-in. thick bearing pads were placed between the web and the bottom HSS as shown in Figure 3-68. Each pair of HSS tubes were connected by two high strength 1-in. diameter all-thread steel rods. These steel rods were pre-stressed by applying a 30-35 kips of tension force to each rod resulting in 60-70 kips compression from each pair. The pre-stressing force was applied by two small hydraulic rams, as seen in Figure 3-69.

Figure 3-68: 3-in bearing pads to protect the web of the specimen

Figure 3-69: Two hydraulic rams pre-stressing not tested region

The external clamping system was not only used in the untested span to prevent shear failures, but it was also used in strengthening the previously tested span to prevent it from failing before the second test was completed. Therefore, when testing the right span of the specimen, the left span was clamped. Then, after the specimen was rotated 180 degrees, the previously tested span was clamped before testing the undamaged span. A detailed description of the pre-stressed clamping system is shown in Figure 3-70.

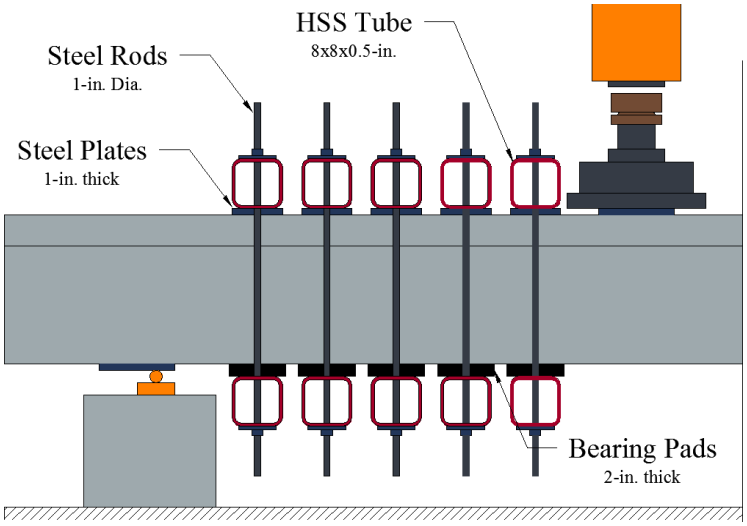

Figure 3-70: External pre-stressing system

3.4 INSTRUMENTATION

This section details all measurement devices used to monitor data during the tests in the experimental program. The instruments include: steel reinforcement strain gauges, CFRP strain gauges, Linear Variable Differential Transformation (LVDTs), and Vision System.

3.4.1 Steel strain gauges

Special epoxy-coated strain gauges were used to monitor strain variations in the transverse and longitudinal steel reinforcement. Most strain gauges were placed on transverse reinforcement to determine the contribution of the stirrups to the shear capacity. To avoid flexural yielding of longitudinal reinforcement and to assure the shear failure of the test specimen, additional strain gauges were placed on the longitudinal reinforcement to monitor the flexural response of the beams.

The surface of the reinforcement where the strain gauge was placed was lightly sanded by a die grinder. Precise sanding is necessary to avoid excessive reduction in the bar area. After sanding the rebar, the smooth surface was cleaned with acetone to ensure a strong bond between the bar and the strain gauge. The strain gauge was then attached to the bar using CN adhesive and covered with a wax coating and electrical tape. Then the strain gauge was wrapped with aluminum tape to ensure that the strain gauge was not damaged when the concrete was placed. Figure 3-71 shows a protected strain gauge on both transverse and longitudinal bar.

(1) (2)

Figure 3-71: Protected strain gauge: (1) in transverse reinforcement, (2) in longitudinal reinforcement

Since the transverse reinforcement detail of specimens with a/d of 1.5 is different than the detail with a/d of 3, a systematic grid was developed for each type to determine the exact location of strain gauges. The grids of deep specimen and slender specimens are shown in Figure 3-72 and Figure 3-73, respectively. Strain gauges were applied primarily to one side of the steel cage, with a few additional strain gauges placed on the other side of the cage to provide redundant readings for the critical section.

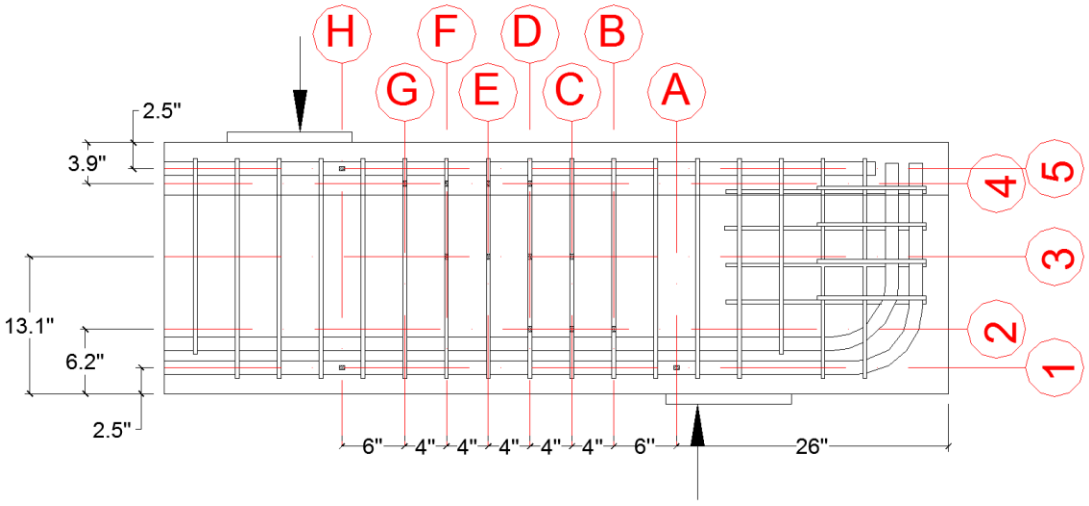

Figure 3-72: Steel strain gauges grid system for specimens with an a/d of 1.5 (deep)

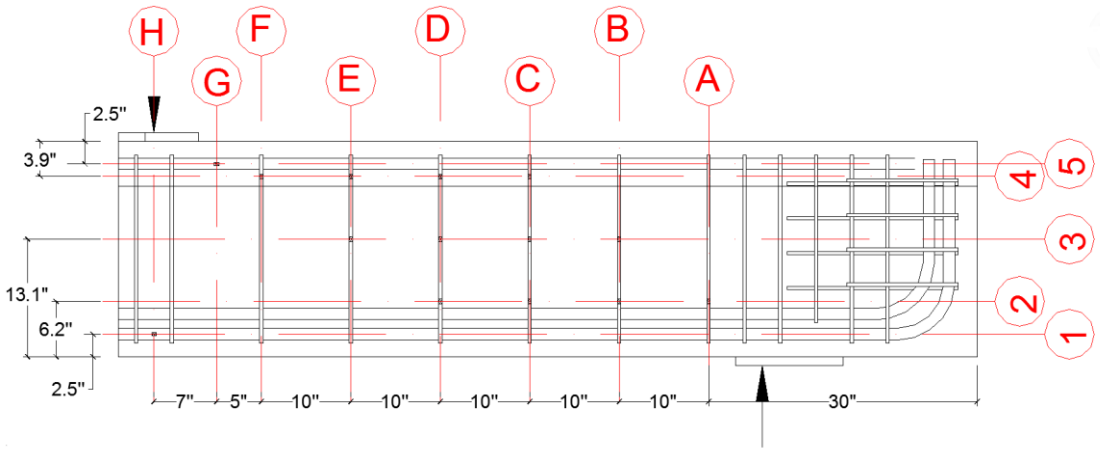

Figure 3-73: Steel strain gauges grid system for specimens with a/d of 3 (slender)

A notation system was developed in order to organize the data obtained from the different steel strain gauges. Strain gauges were named according to their location in the grid system. Figure 3-74 displays the nomenclature system for steel strain gauges.

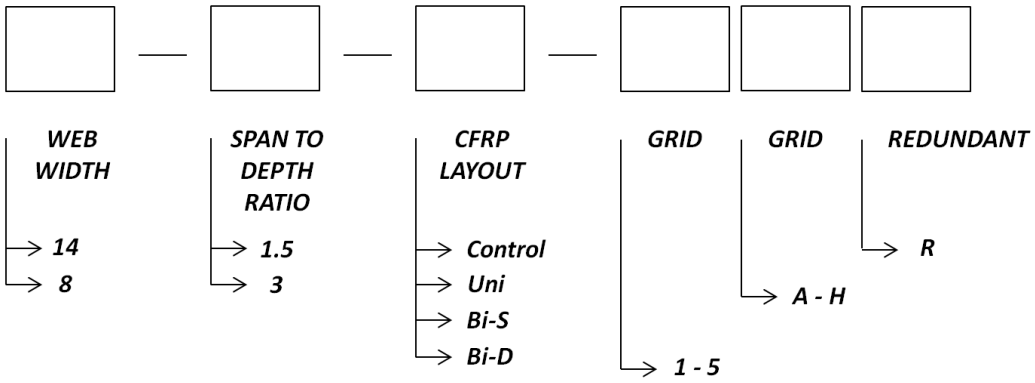

Figure 3-74: Notation for steel strain gauges

3.4.2 CFRP strain gauges

Special strain gauges for composite material were employed to monitor strains in the CFRP laminates during the test. The 5-mm. strain gauges were applied to both horizontal and vertical CFRP strips. A typical gauge is shown in Figure 3-75.

Figure 3-75: Typical strain gauge for composite material

The process of installing CFRP strain gauges is different than the one used in installing steel strain gauges. To create the desired smooth surface, a two component adhesive was applied to the surface of the CFRP strip. To allow the strain gauge to record more accurate strains during testing, a very small amount of the adhesive material was applied to give the minimal thickness possible. Figure 3-76 shows the two components of the PS adhesive.

Figure 3-76: The two components adhesive used to provide smooth surface

Then a small plastic sheet was placed and fixed on top of the adhesive. After five hours curing, the plastic sheet was removed, and a smooth surface was attained.

Then the strain gauge was placed on the smooth surface, the gauge wires were separated, and the entire strain gauge was covered by electrical tape. Figure 3-77 presents the process of installing the CFRP stain gauge.

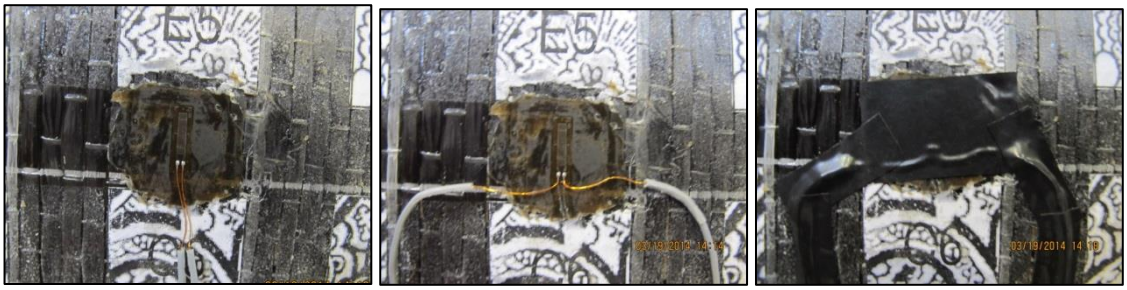

(1) (2) (3)

Figure 3-77: Process of installing CFRP stain gauges: (1) apply the gauges (2) separate the wires (3) cover it with electrical tape

Another grid system was developed to ensure the exact location of CFRP strain gauges in each test. The grid systems for deep specimen and slender specimen are shown in Figure 3-78 and Figure 3-79, respectively.

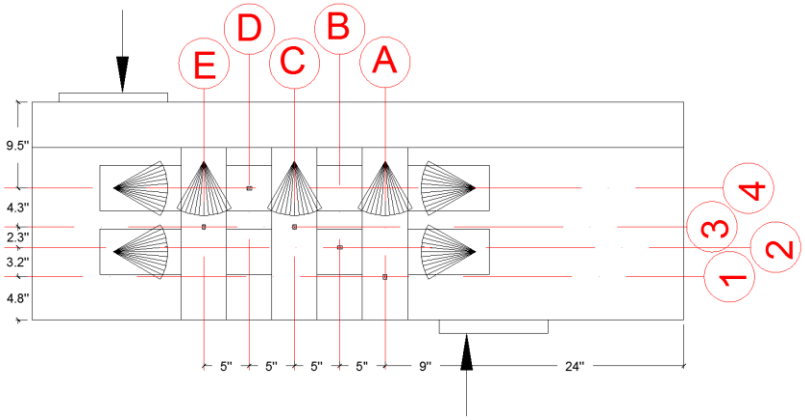

Figure 3-78: CFRP strain gauges grid system for specimens with a/d of 1.5

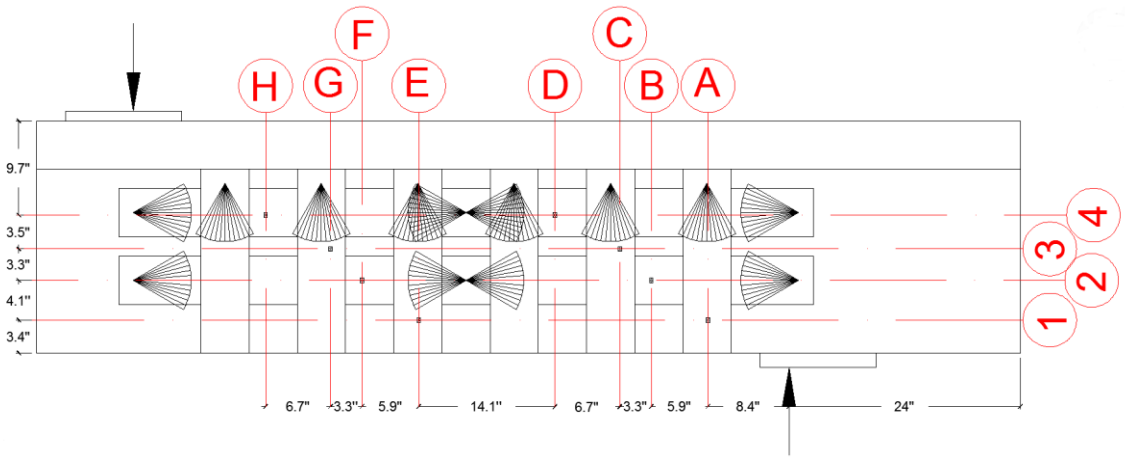

Figure 3-79: CFRP strain gauges grid system for specimens with a/d of 3

Another notation system was developed in order to organize the data obtained from the CFRP strain gauges. Strain gauges were named according to their location in the grid system. Figure 3-80 displays the nomenclature system for the CFRP strain gauges.

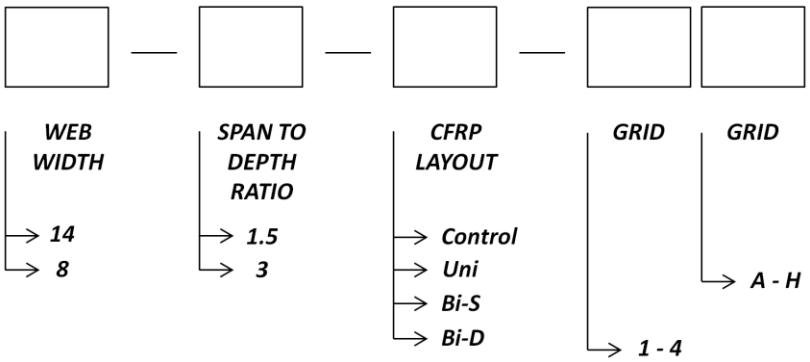

Figure 3-80: Notation for CFRP strain gauges

3.4.3 Linear Variable Differential Transformers (LVDTs)

Two Linear Voltage Displacement Transducers (LVDTs) were utilized in each test to measure the displacement of the specimen throughout the test. Twisting of the specimen was not a concern in this test setup since each test specimen was supported by a 1-in. thick steel plate with a rigid pin on each side. This rigid support condition also eliminated the possibility of rigid body displacement in addition to the actual displacement (shear and flexural deformation).

Consequently, only two 4-in. LVDTs were employed in each test. The two LVDTs were placed at mid-span on each side of the specimen (east and west) to measure the mid-span displacement. As can be seen in Figure 3-81, each LVDT was supported by a steel hanger, and the plunger was pointed upward resting directly against the bottom face of the web.

Figure 3-81: LVDT's to measure mid-span displacement

3.5 UT VISION SYSTEM

The use of optical measurement techniques has been proven to be a valuable technique in measuring deformations. The limitations of the conventional measurement techniques, such as strain gauges, increase the interest in employing the digital image correlation techniques (DIC) in structural engineering experimental work. This technique, unlike the conventional techniques, provides full-field deformation data. It is also a contact-free measurement that allows the specimen to be monitored even if large deformations occur.

In this experimental program, the UT Vision System, developed at the Ferguson Laboratory of the University of Texas at Austin and consisting of computer programs and optical instruments, was used to measure deformation of the test specimen. The system consists of two high-resolution cameras, two computers connected through a network that record image data and synchronize image acquisition, a software package utilizing the Matlab Image Processing Toolbox and the NI Vision Development Module (National Instruments), paper targets, and lights.

3.5.1 Setup of the UT Vision System

The setup of the UTVS was started by identifying the test area that needed to be tracked by the vision system, as shown in Figure 3-82.

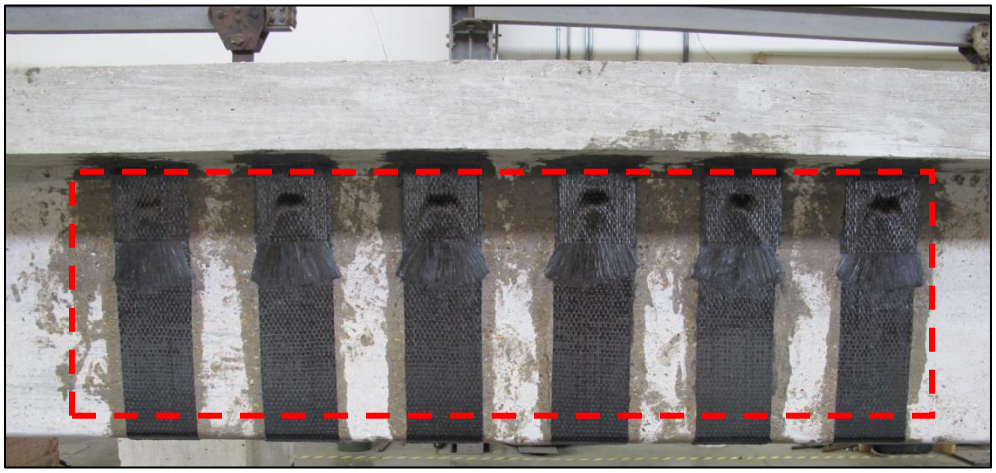

Figure 3-82: Identifying the test span

The larger the target size, the higher the resolution with which the UTVS can track its movements. A target size of 100x100 pixels was selected in this project. The size of the paper targets can be calculated using Equation 3-1.

$$\text{Target size} = \frac{100}{4872} \times w \qquad \textit{Equation 3-1}$$

Where, 4872 is the number of pixels in the long direction of the camera sensor (for a 16Megapixel sensor) and w = width of the field view

Once the size of the paper targets was determined and the targets were cut, a grid was drawn on the surface of the test specimen to create a mesh. The marked grid assisted in placing targets consistently in the desired locations. Figure 3-83 shows the grid drawn on the specimen.

Figure 3-83: Grid lines drawn on the test span

After drawing the grid, the specimen surface was cleaned with air pressure to remove all debris. Subsequently, the paper targets were attached to the surface using a spray adhesive, as can be seen in Figure 3-84.

Figure 3-84: Placing paper targets in their location using spray adhesive

The grid was designed such that no target would be placed over the boundaries between different components (concrete, CFRP strip, or CFRP anchor), where discontinuities in strains can occur. Figure 3-85 shows the distribution of the targets on the grid.

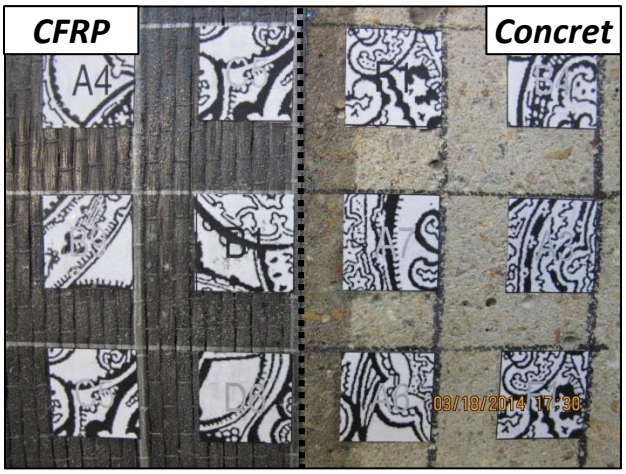

Figure 3-85: No target was located over the boundaries between different material

Two high-resolution cameras with 50-mm lenses were used to record the images of the targets on the test specimen. The two cameras were placed on a horizontal mounting bar that stands on a tripod, as shown in Figure 3-86.

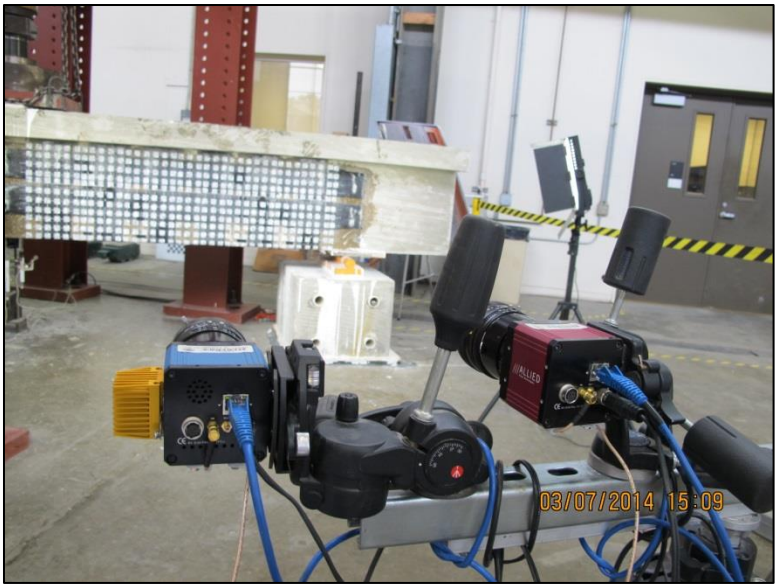

Figure 3-86: Two high resolution cameras stand on tripod

The location of the camera relative to the specimen can be calculated using Equation 3-2. The distance between the two cameras can be calculated using Equation 3-3. As can be seen in Figure 3-87, one camera was mounted perpendicular to the specimen's surface while the other camera was rotated inward 5 degrees (toward the first camera).

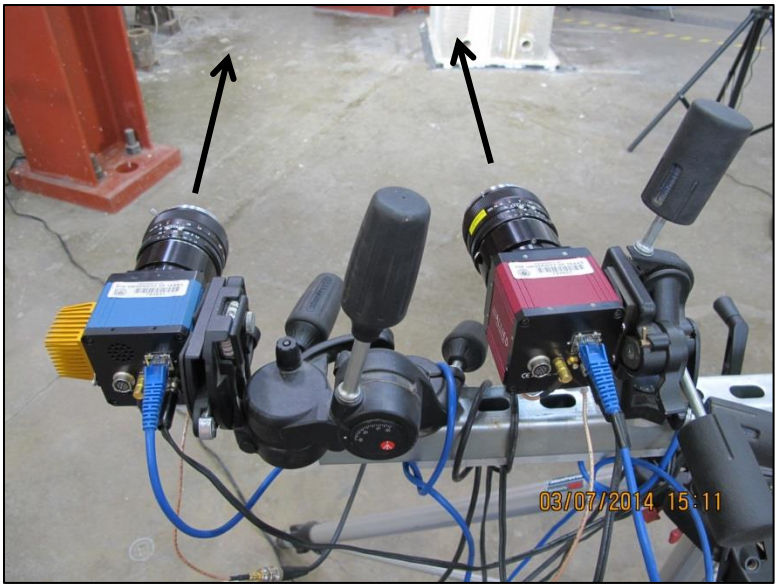

Figure 3-87: Left camera (master) straight, right (slave) rotated

$$\textit{Camera distance from specimen (D)} = \frac{W}{2} \times \frac{1}{\tan(HVA/2)} \times 1.1 \qquad \textbf{Equation 3-2}$$

Where W = width of the field view
HVA = horizontal viewing angle (38.4° for 50-mm lenses)

$$\textit{Distance between cameras} = D \times \tan 5° \qquad \textbf{Equation 3-3}$$

Two computers running the vision measurement software were connected to each other through a network and to the cameras. The master computer triggered frame grabbing for all cameras in synchronization through the network. The two computers were also connected to a third computer that controls the DAQ system (load cells, LVDT's, strain gauges). The master UTVS computer delivered the image frame number to the DAQ such that the UTVS data and data from other instruments could be synchronized (Figure 3-88).

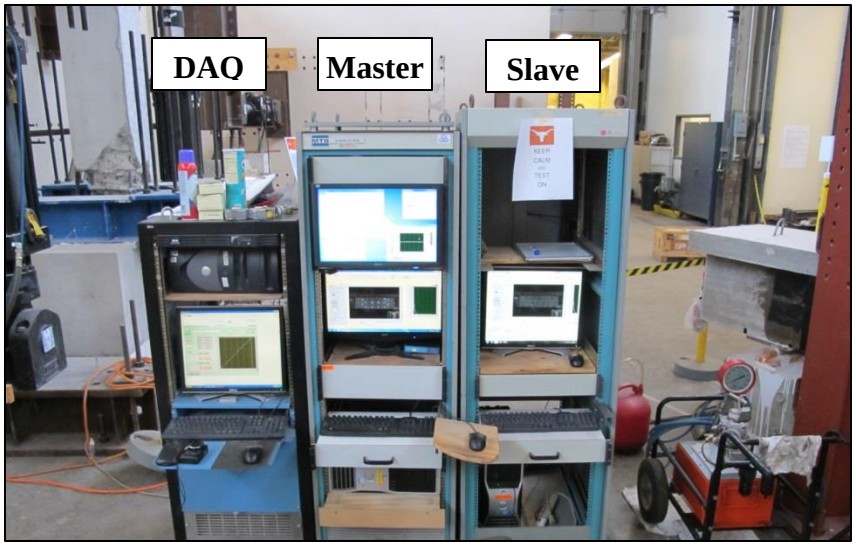

Figure 3-88: Computer system associated with the Vision System

Two LED lights were used as a light source to improve the imaging quality of the cameras. The lights were placed in a way that minimized glare from the images, as shown in Figure 3-89

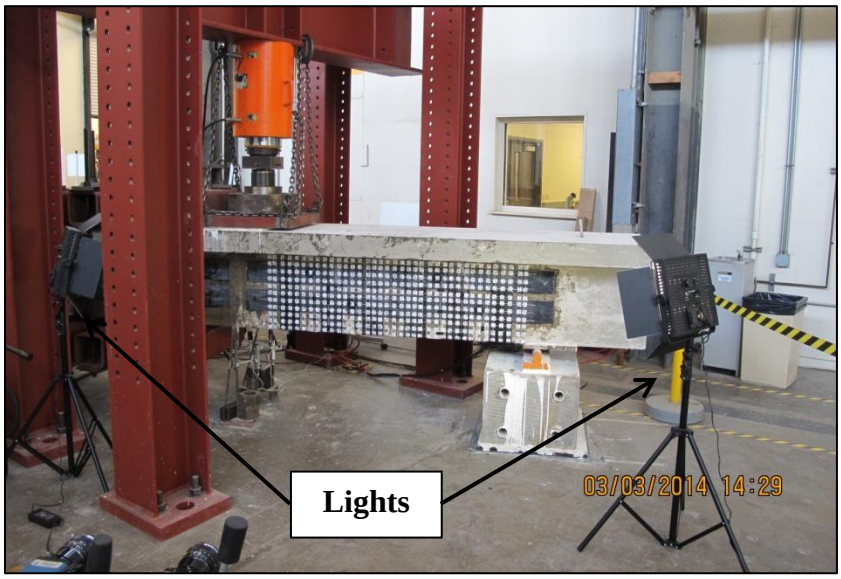

Figure 3-89: Lights for better images

3.5.2 Monitoring Shear Deformation

Conventional instrumentation such as LVDT's can be used to monitor the shear deformation. However, LVDT's must be instrumented on the critical section, which will only be known after failure. Therefore, if the installed LVDT's did not cover the failure section, shear deformation data will not be useful.

In this experimental program, the UTVS was used to monitor the shear deformation during the test. Using UTVS in measuring shear deformation is advantageous as strain data can be measured for the entire section. Therefore, no matter where the critical crack crosses a specimen, shear deformations can be calculated using targets that cover the critical section. For calculating shear strains, three targets were selected to form a triangular shape as shown in Figure 3-90 and Figure 3-91. To get the shear deformation response of the beam, only targets that are located on the concrete surface (not on the CFRP) were selected. The shear deformation response of specimens with a/d of 3 is presented in Chapter 4.

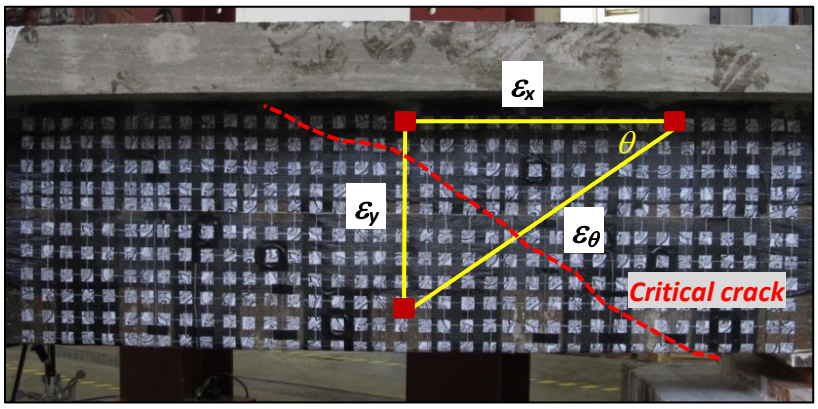

Figure 3-90: Shear deformation triangular

Shear strains (γ_{xy}) between selected targets can calculated from Equation 3-4.

$$\gamma_{xy} = \frac{\varepsilon_\theta - (\varepsilon_x cos^2\theta + \varepsilon_y sin^2\theta)}{cos\theta\ sin\theta} \qquad \textit{Equation 3-4}$$

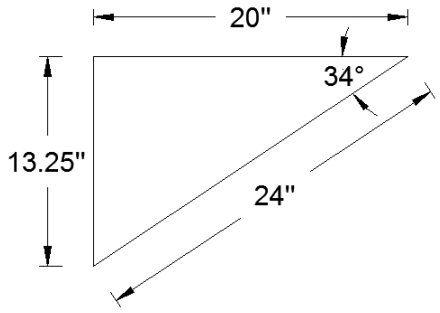

Figure 3-91: Dimensions of shear deformation triangle

3.5.3 Monitoring CFRP Strains

In addition to conventional strain gauges, the UTVS was used to monitor strains in CFRP strips during tests. To measure the axial strains in the vertical CFRP strips using the UTVS, two targets located at the straight vertical gridline were selected. Targets located on the patch that covered the anchor fan, or on the boundaries between the vertical strip and the anchor fan were avoided there strains are not representative of the strip strains. This limited the number of targets that could be used to measure the axial strain of the vertical strip (Figure 3-92). The red area represents all targets located either on the patch or on the boundaries, and the green area represents all targets that can be used in analyzing the axial strain of the vertical strips.

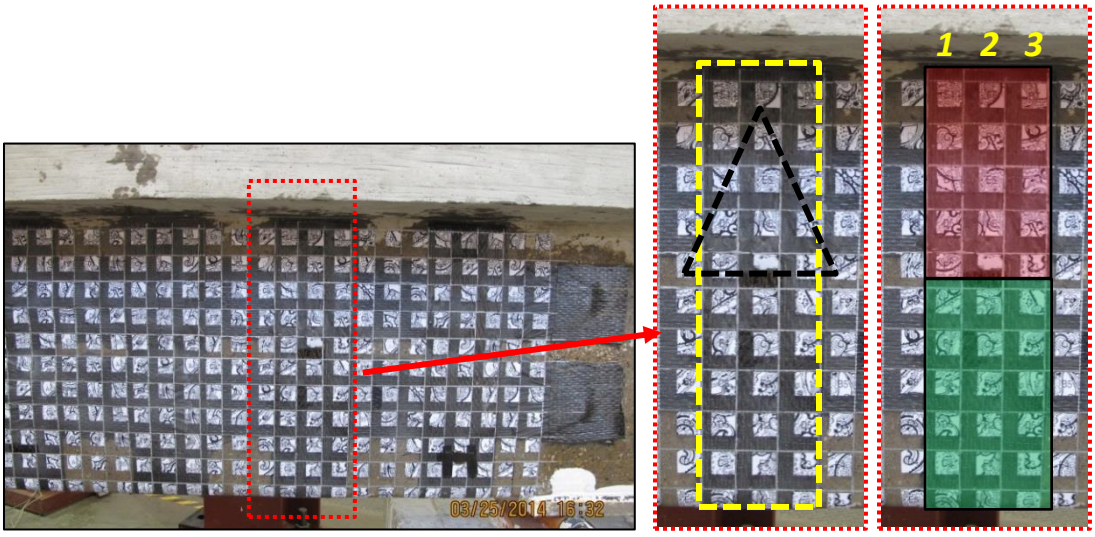

Figure 3-92: Vertical strips in bi-directional with targets associated with UTVS

As can be seen in Figure 3-92, there are three vertical gridlines on each vertical strip (three targets per width of the vertical strip). Targets at the centerline of the strip can be assumed to represent the average strain cross the width of the strip. However, for more accurate strain data, the average of strains from three pairs of targets were used to measure vertical strip strains, as shown in Figure 3-93. Strains from the left, middle, and right targets were measured and averaged as shown in Figure 3-94.

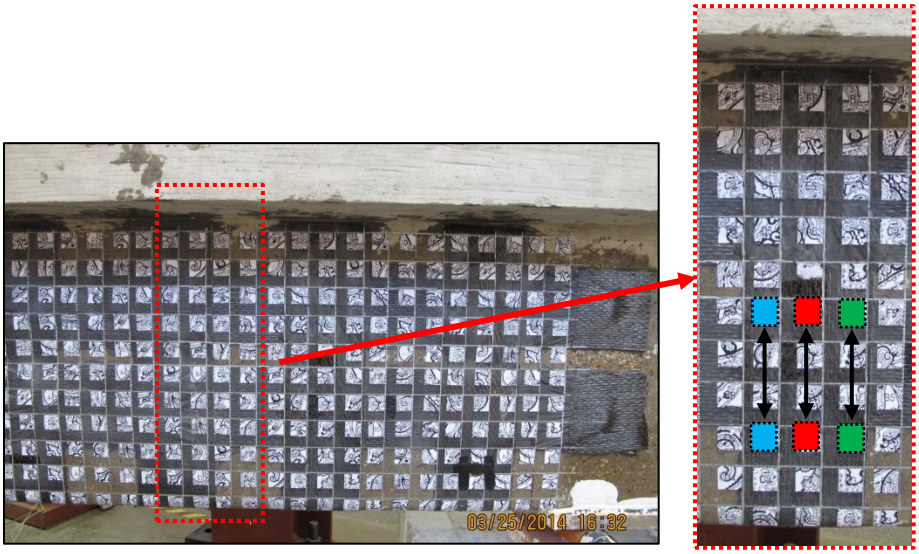

Figure 3-93: Three targets selected across the width to measure strains CFRP strips

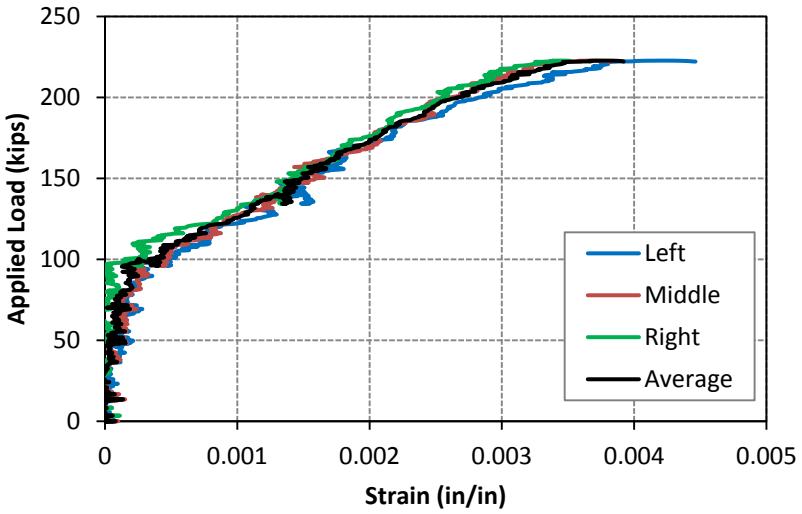

Figure 3-94: Strains across the width of a vertical strip

This graph confirms that the strain measured in the middle of a strip can to some extent accurately represents the average strain across the width of a vertical CFRP strip. Based on the aforementioned procedure, strains in the vertical strips were monitored during testing each specimen.

CHAPTER 4
Experimental Results

4.1 OVERVIEW

The overall response and behavior of eight shear tests conducted on four T-beam specimens are presented in this chapter. The effects of three parameters on the shear behavior of the 24-in. deep reinforced concrete T-beams strengthened with Carbon Fiber Reinforced Polymer (CFRP) strips and CFRP anchors were investigated. The parameters studied were 1) web width (14-in. and 8-in.), 2) the shear span-to-depth-ratio (a/d) (1.5 and 3), and 3) the amount of CFRP material (single and double layers). Results will be presented in this chapter according to the specimens' classification. Therefore, the results of the deep specimen (a/d of 1.5) will be presented first, and the results of the sectional specimens (a/d of 3) will be presented last. A detailed discussion of the test results will be presented in Chapter 5.

4.2 TEST SPECIMEN DETAILS

A simple notation system was established to designate each test. Each test label consists of three identifiers. Figure 4-1 illustrates the notation system used. Key parameters of each test are given in Table 4-1.

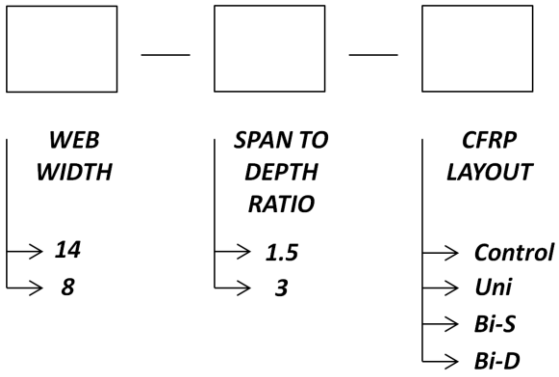

Figure 4-1: Test specimen notation

Table 4-1: Test matrix for 24-in deep T-beams

Specimen No.	*Test No.*	*Web Width*	*Shear span-to-depth ratio*	*CFRP application*	*No. of CFRP layers*	*Test Name*
1	1	14	1.5	Bi-directional	Single	14-1.5-Bi-S
	2	14	1.5	Bi-directional	Double	14-1.5-Bi-D
2	3	14	3	Bi-directional	Single	14-3-Bi-S
	4	14	3	Bi-directional	Double	14-3-Bi-D
3	5	8	3	None	None	8-3-Control
	6	8	3	Uni-directional	Single	8-3-Uni
4	7	8	3	Bi-directional	Single	8-3-Bi-S
	8	8	3	Bi-directional	Double	8-3-Bi-S

As shown in Table 4-1, for the first two specimens (with 14-in. web), neither a control specimen nor a uni-directionally strengthened specimen were tested. This is because the control specimen and uni-directionally strengthened specimen were tested in Tx-DOT Project 0-6306 and will be compared with test results from this study.

4.3 SHEAR CONTRIBUTION OF STEEL, CFRP, AND CONCRETE

The shear capacity of strengthened test specimens was evaluated by calculating the contribution of transverse reinforcement (V_s) vertical CFRP strips (V_f), and concrete (V_c) to the shear resistance. The contributions of transverse steel and CFRP strips were estimated by using strain data obtained from the instrumentation. The applied load was measured by the load cell, and strains in the steel stirrups and CFRP strips were measured using strain gauges and the UTVS. These data were recorded during each test by the data acquisition (DAQ) system.

A simple free-body diagram based on a critical shear crack was used to estimate the shear forces carried by steel stirrups and vertical CFRP strips. To satisfy equilibrium for the system, internal shear forces carried by concrete, stirrups, and CFRP should be equal to the external applied shear force. Only steel stirrups and CFRP strips that cross the critical shear crack were assumed to contribute to the internal shear resistance (Figure 4-2.)

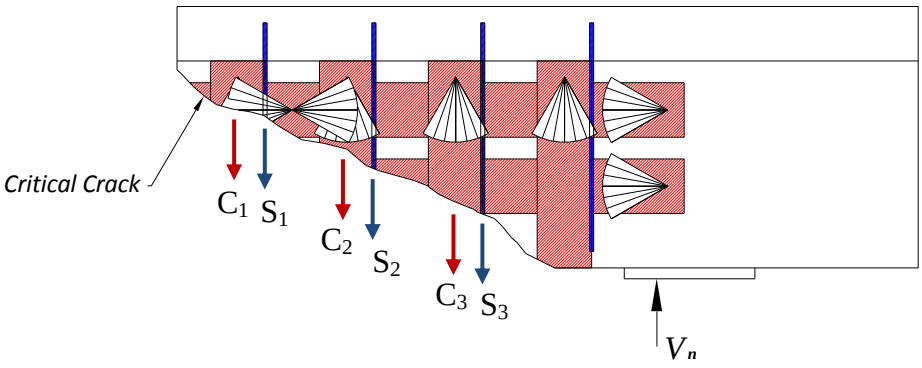

Figure 4-2: Internal forces in a cracked strengthened beam

For transverse steel, strain gauges were attached to all stirrups within the test region. The strain value at a certain point on a stirrup will depend on the distance between this point and the critical crack. The closer the point to the critical crack, the higher the strain value will be recorded. For this reason, several strain gauges were installed along the length of the stirrups located in the middle of the test region where the critical crack would most likely occur. A typical bi-linear stress-strain relationship with a yielding plateau was assumed to estimate the force in a steel stirrup (Equation 4-1). The shear contribution of the stirrups can be evaluated by summing the forces of the stirrups that cross the critical shear crack (Equation 4-2).

$$F_{s,i} = A_s \times E_s \times \varepsilon_{s,i} \quad : \varepsilon_{s,i} < \varepsilon_y \qquad \textit{Equation 4-1}$$
$$= A_s \times E_s \times \varepsilon_y \quad : \varepsilon_{s,i} \geq \varepsilon_y$$

$$F_s = \sum_{i=1}^{n} F_{s,i} \qquad \textit{Equation 4-2}$$

Although the bi-directional application involves horizontal strips as well as vertical strips, only vertical strips will contribute directly to the shear equilibrium across a crack. CFRP materials are brittle materials that do not experience a yielding plateau; therefore, a linear stress-strain relationship was assumed to estimate the force in a vertical strip (Equation 4-3). The shear contribution of the CFRP strips can be evaluated by summing the forces of the strips that cross the critical shear crack (Equation 4-4).

$$F_{f,i} = w_f \times t_f \times E_f \times \varepsilon_{f,i} \qquad \textit{Equation 4-3}$$

$$F_f = \sum_{i=1}^{n} F_{f,i} \qquad \textit{Equation 4-4}$$

The shear capacity of a reinforced concrete member strengthened with CFRP material can be computed by summing the shear contributions of the concrete, the stirrups, and the CFRP strips (Equation 4-5).

$$V_n = V_c + V_s + V_f \qquad \textit{Equation 4-5}$$

Since it is difficult to quantify the concrete contribution to the shear strength of a reinforced concrete member experimentally, it can be determined using the equilibrium equation given that the shear contribution of the steel stirrups, the shear contribution of the CFRP strips, and the external applied shear are all known (Equation 4-6), so that

$$V_c = V_n - V_s - V_f \qquad \textit{Equation 4-6}$$

4.4 TEST RESULTS

Results obtained from the eight tests are presented in this section. These results are divided into three groups based on 1) web width of 14-in. or 8-in. and 2) shear span to depth ratio of 1.5 or 3 (deep beam or sectional beam). Therefore, the test results are presented as follows:

- Results of 14-in. web specimens with a/d of 1.5 (deep beam)
- Results of 14-in. web specimens with a/d of 3 (sectional beam)
- Results of 8-in. web specimens with a/d of 3 (sectional beam)

The CFRP layout for bi-directional application on the deep beam series (a/d of 1.5) consisted of three 5-in. wide vertical CFRP strips spaced at 10-in. on center in addition to two 5-in. wide horizontal CFRP strips spaced at 10-in. on center. For the shallow beams (a/d of 3), the CFRP layout consisted of six 5-in. wide vertical CFRP strips spaced at 10-in. on center, in addition to two 5-in. wide horizontal CFRP strips spaced at 10-in. on center. Both vertical and horizontal CFRP strips were anchored by CFRP anchors. Vertical strips were anchored with CFRP anchors at the ends only, whereas horizontal CFRP strips were anchored with middle-anchors as well as end-anchors.

The discussion of the test results will include some of the following information:

- Images of the specimens during the failure
- Load vs displacement curves
- Shear deformation curves
- Figures of the cracking pattern
- Observations on the failure of the test specimens
- Shear at first yielding of steel stirrups
- Strains in steel stirrups and CFRP strips

- Strains in longitudinal reinforcement
- Estimated shear contribution of each material

The reported shear force was calculated from the applied load using statics as shown in Figure 4-3. The shear force equals to 0.604 of the applied load for beams with a/d of 1.5 and equals to 0.528 of the applied load for beams with a/d of 3.

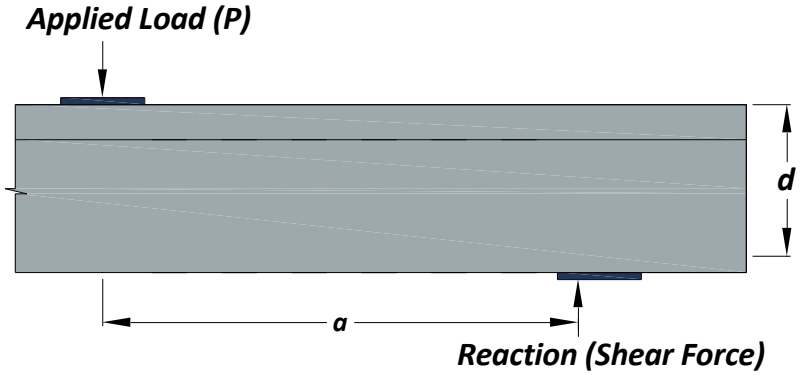

Figure 4-3: Applied load and shear force

4.4.1 Results of 14-in. web specimen with a/d of 1.5

Two tests were conducted on which the only difference between the tests was the amount of CFRP material. Neither control nor uni-directionally strengthened specimens were tested in this series because they were tested in Tx-DOT Project 0-6306 and will be linked to current results in Chapter 5.

4.4.1.1 14–1.5–Bi–S (Bi-directional with single layer of CFRP)

This test was conducted to evaluate the effect of the bi-directional application of CFRP strips and CFRP anchors on the shear capacity of a reinforced concrete T-beam with 14-in. web and a/d of 1.5 (deep beam). The test specimen was strengthened vertically and horizontally with a single layer of CFRP strips as an external strengthening

reinforcement to form the bi-directional configuration. Both vertical and horizontal strips were anchored with single end-anchors. The CFRP layout for this test specimen is shown in Figure 4-4.

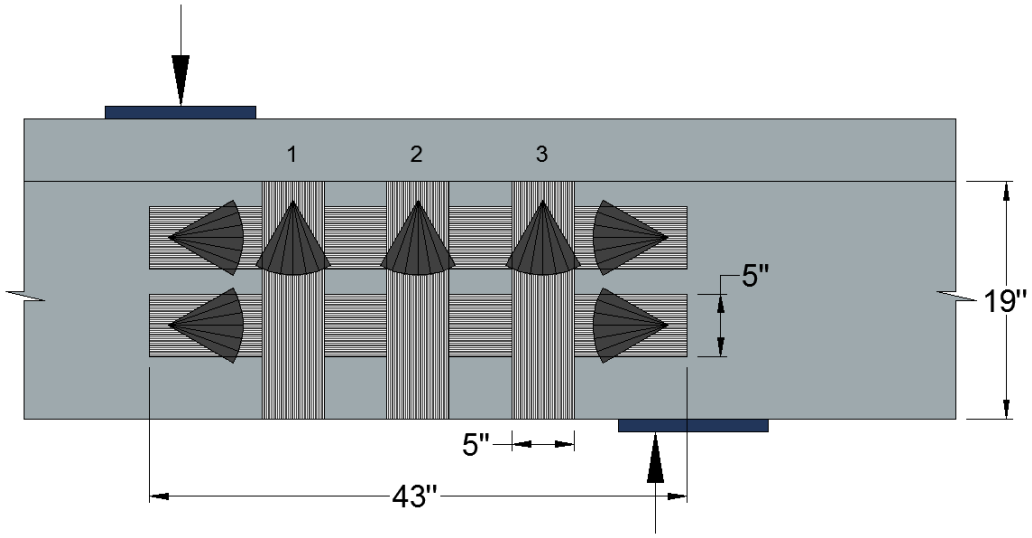

Figure 4-4: CFRP configuration of 14-1.5-Bi-S

Shear failure occurred at a shear force of 259-kips (applied load of 429-kips). Photos of the test specimen before and after shear failure can be seen in Figure 4-5.

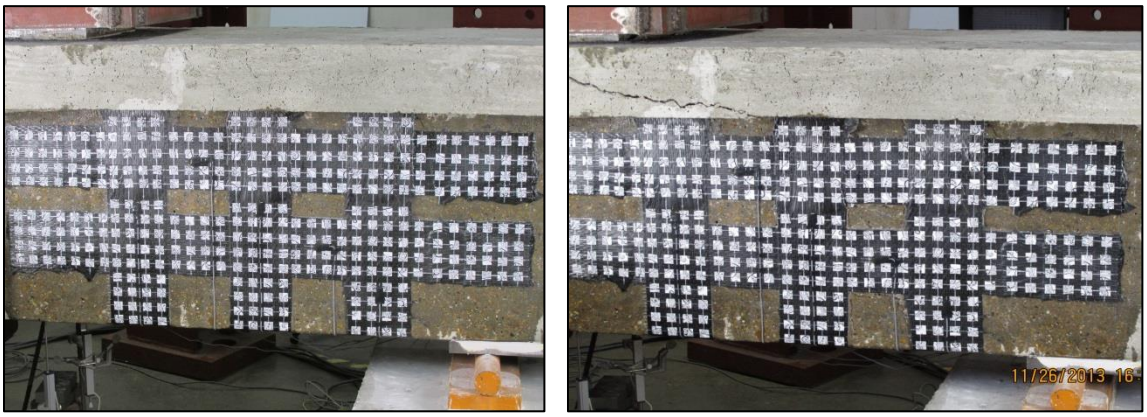

Figure 4-5: left (before) and right (after) loading of 14-1.5-Bi-S

The vertical displacement under the applied load was measured by two LVDTs. The applied load versus displacement curve for *14-1.5-Bi-S* observed during testing is plotted in Figure 4-6. Mid-span displacement corresponding to the maximum applied load was 0.29-in.

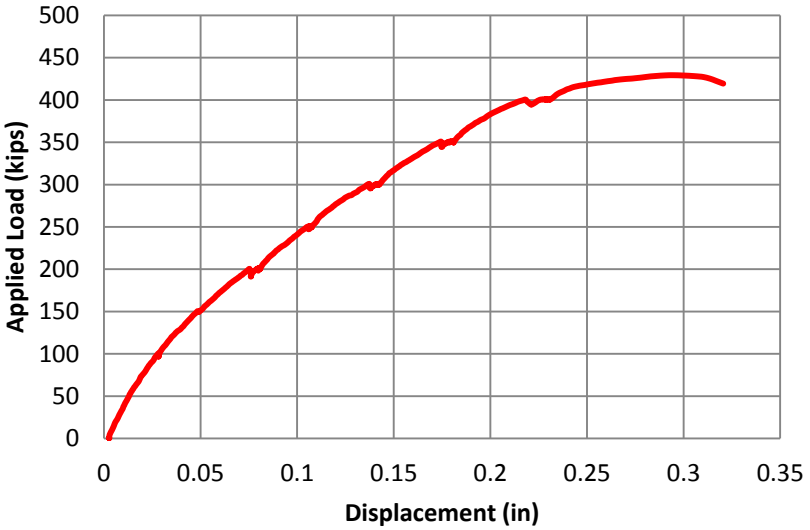

Figure 4-6: Load-displacement curve of 14-1.5-Bi-S

Concrete cracking was marked during the course of testing. A sketch of the cracking pattern can be seen in Figure 4-7. Although the crack pattern could not be traced beneath the CFRP strips, the general direction of cracking can be projected.

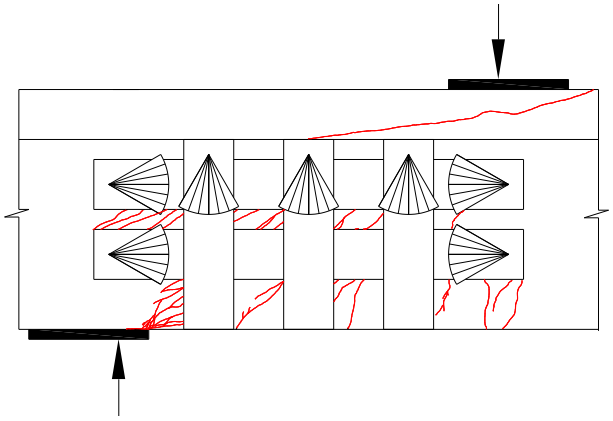

Figure 4-7: Cracking pattern of west face 14-1.5-Bi-S

Shear cracks started to initiate on the web of the specimen after reaching an applied load of approximately 150-kips. As the applied load increased, additional shear cracks continued to form between the point load and the reaction. The failure was a combination of concrete crushing at the face of the node next to the support and the crushing of concrete strut that formed between the point of applied load and the support as shown in Figure 4-8.

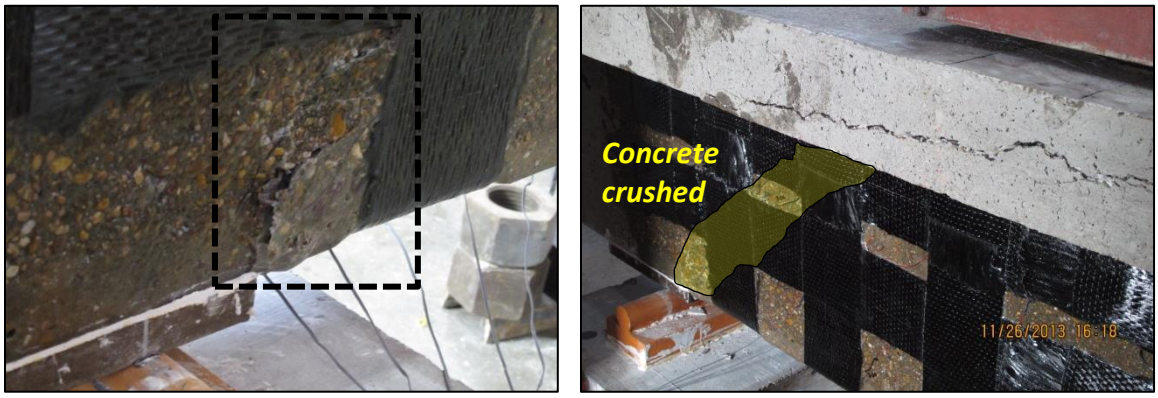

Figure 4-8: crushing of concrete at nodal zone (left) and crushing of strut (right)

CFRP anchors prevented the complete debonding of CFRP strips. No strip rupture or anchor fracture was observed in this test. However, a number of minor cracks were observed at the edges of the CFRP strips (Figure 4-9). These cracks caused different parts

of the strips to delaminate from the concrete surface. The extent of delamination could be determined by tapping on the CFRP strip.

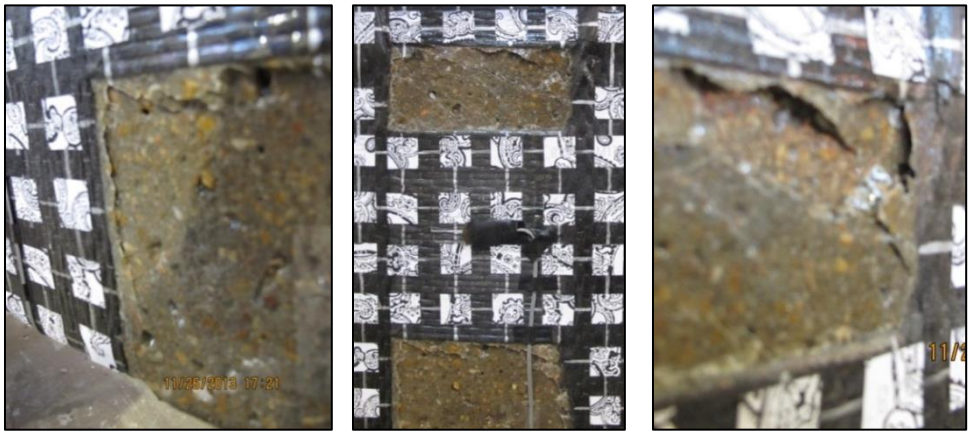

Figure 4-9: Cracks at the edges of the strips

The maximum strain recorded in vertical CFRP strips was 0.007 in the middle vertical strip (strip #2), while the maximum strain recorded in the horizontal CFRP strip was 0.004 in the upper strip. Both of these strains were reported at 93% of the maximum applied load. The strains in vertical CFRP strips at different loading stages were recorded by several strain gauges. The UT Vision System (UTVS) was not used to measure strains in CFRP strips for specimens with a/d of 1.5.

The locations of the strain gauges that recorded the strain in the vertical strips and the strain variations during the loading of *14-1.5-Bi-S* are presented in Figure 4-10. The strain drop in strip #2 and the strain rise in strip #1 at a 429-kips applied load occurred during the time of marking the cracking pattern at a 400-kips applied load and was likely the result of debonding along the strip that permitted the strains to decrease since a longer length of the strip debonded.

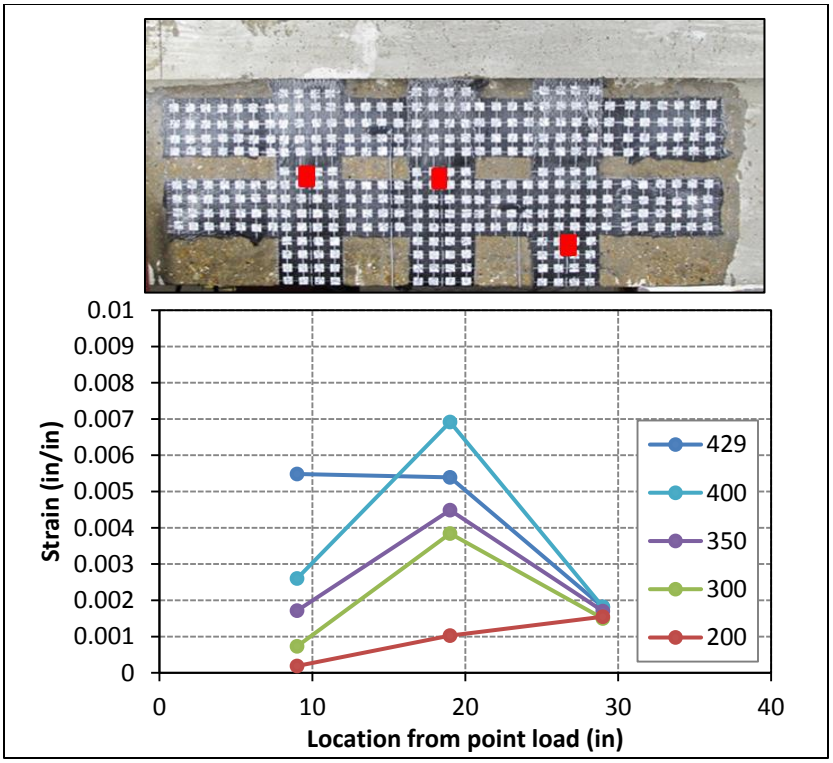

Figure 4-10: Strains in vertical strips at different loading stages of 14-1.5-Bi-S

Strains in steel stirrups were also measured by strain gauges. The strains in the steel stirrups located within the test region were recorded during testing and are shown in Figure 4-11. The steel stirrups started yielding at a shear force of 201-kips (an applied load of 333-kips). All measured strains within the test region were above yield except at the gauge on the stirrup closest to the point load (G4). Strains in steel stirrups during loading are reported in Figure 4-12.

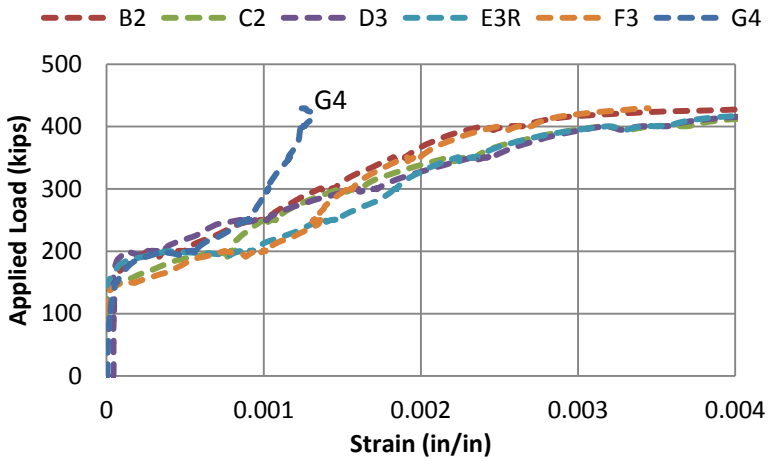

Figure 4-11: Load versus maximum recorded strain in steel stirrups (14-1.5-Bi-S)

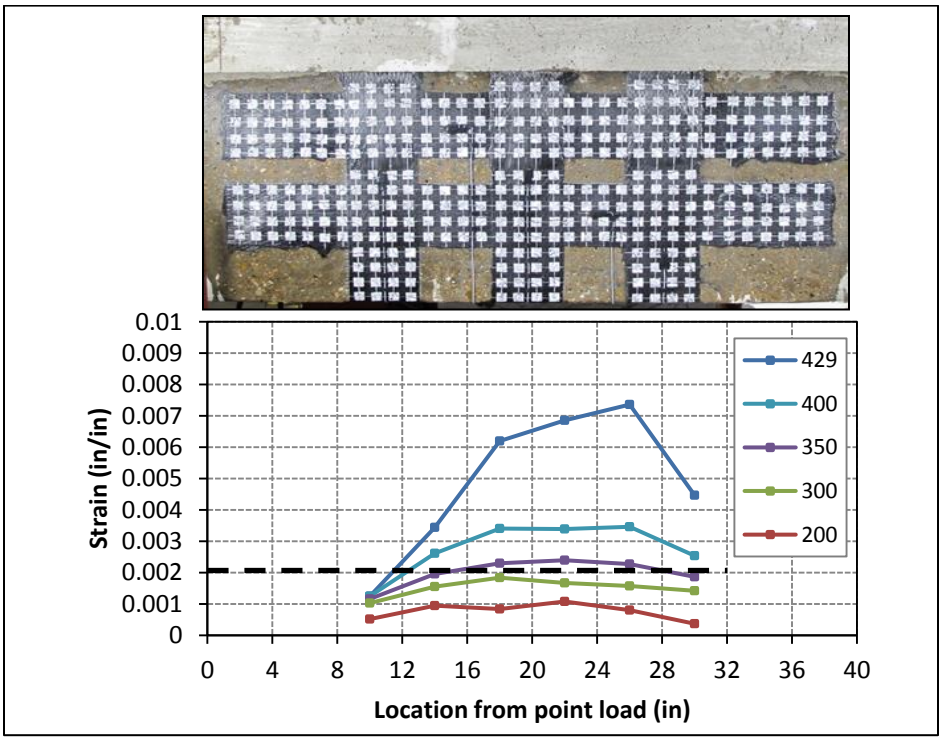

Figure 4-12: Strains in steel stirrups at different loading stages of 14-3-Bi-S

Strains in the stirrups and the vertical CFRP strips at various levels of applied load are shown in Figure 4-13. The x-axis represents location from point load in inches.

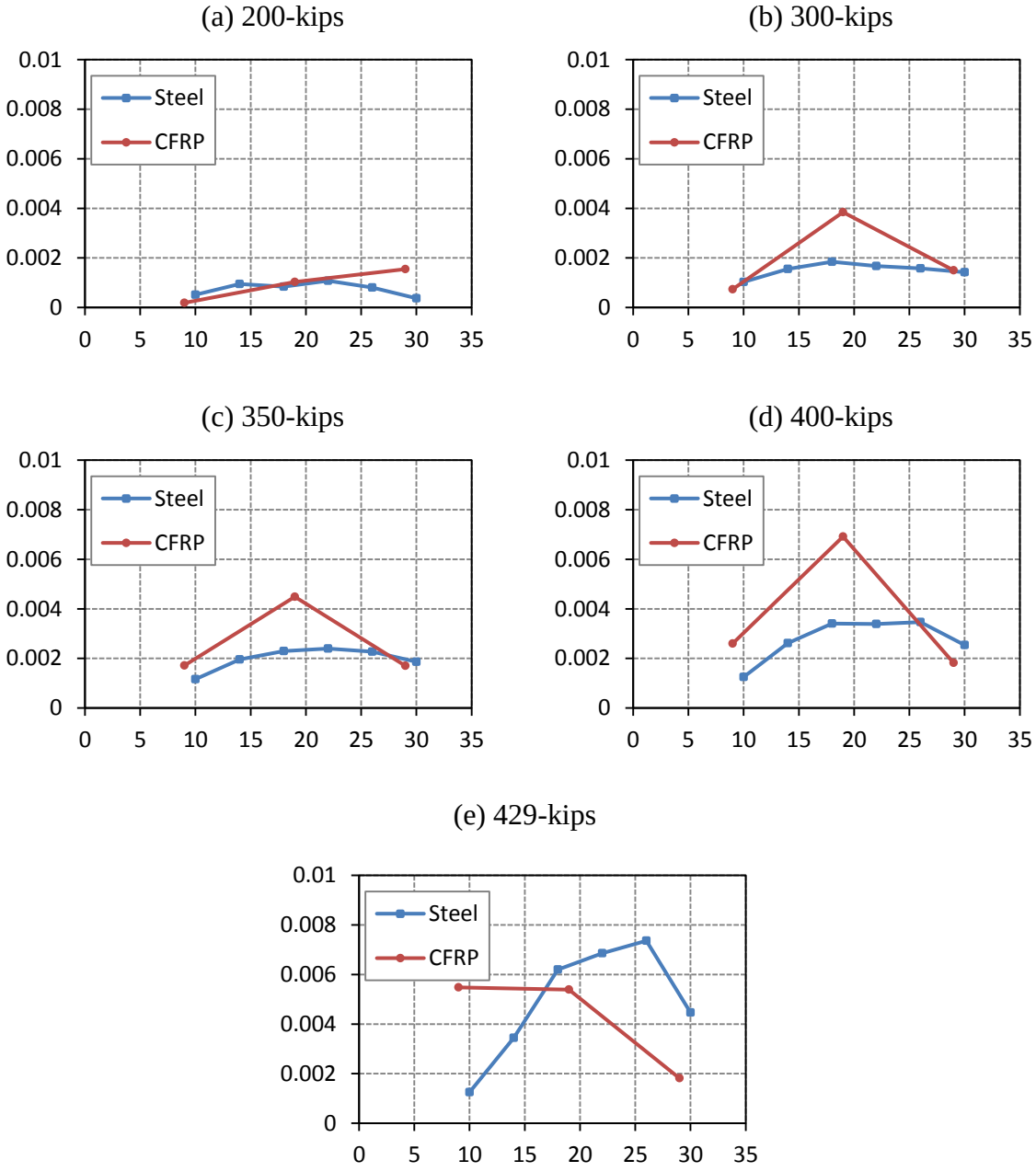

Figure 4-13: Strains in steel stirrups and CFRP strips during loading of 14-1.5-Bi-S

As expected, none of longitudinal reinforcement yielded during the test. The maximum strain recorded in the longitudinal reinforcement was 0.0016 for the bottom layer of tension reinforcement.

4.4.1.2 14–1.5–Bi–D (Bi-directional with single layer of CFRP)

This test was conducted to examine the effect of the amount of CFRP material on the shear strength of a bi-directionally strengthened reinforced concrete T-beam with 14-in. web and a/d of 1.5 (deep beam). The specimen was strengthened vertically and horizontally with two layers of CFRP strips acting as an external strengthening reinforcement to form the bi-directional configuration. The CFRP layout for this test specimen is shown in Figure 4-14.

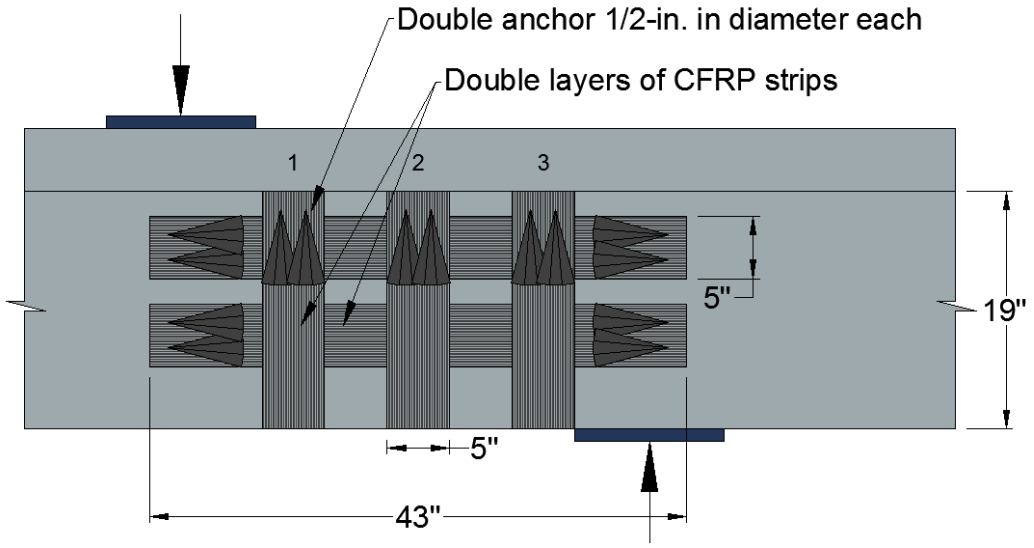

Figure 4-14: CFRP configuration of 14-1.5-Bi-D

Increasing the amount of CFRP material may lead to stress concentrations at the anchor bend, which may result in a reduction of the tensile capacity of the CFRP anchor.

In order to avoid this reduction, (Orton, Jirsa et al. 2008) recommended using a CFRP anchor with a cross-sectional area that is equal to or greater than twice the CFRP strip cross-sectional area. Therefore, since the cross-sectional area of the CFRP strip was doubled, two CFRP anchors were used at each end instead of one CFRP anchor to balance the increase in the area of the CFRP strips. Figure 4-14 shows the difference in the number of CFRP anchors implemented in this test in comparison to the previous test.

Shear failure occurred at a shear force of 255-kips (applied load of 422-kips). Photos of the test specimen before and after shear failure can be seen in Figure 4-15.

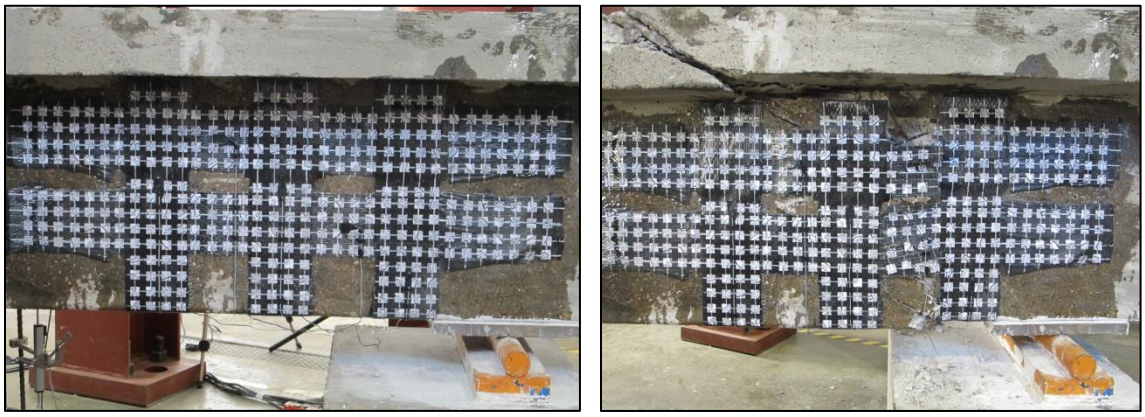

Figure 4-15: left (before) and right (after) loading of 14-1.5-Bi-D

The applied load versus the displacement curve is plotted in Figure 4-16. The mid-span displacement corresponding to the maximum applied load was 0.35-in.

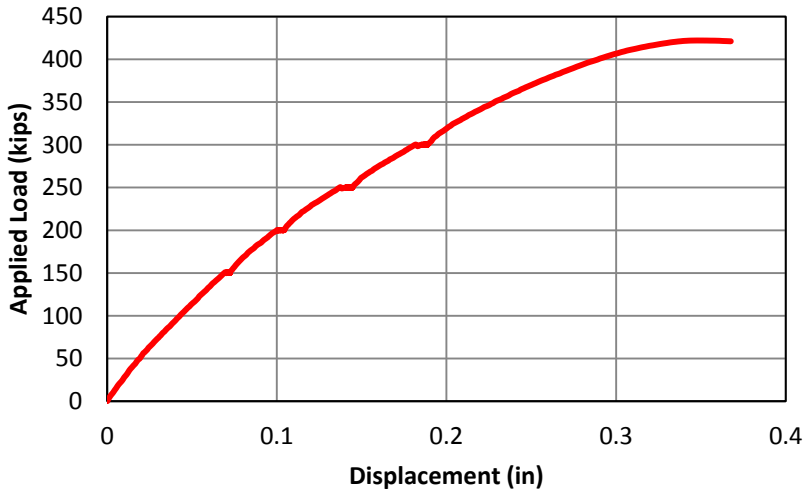

Figure 4-16: Load-displacement curve of 14-1.5-Bi-D

Concrete cracking during the course of testing was marked. A sketch of the cracking pattern is shown in Figure 4-17.

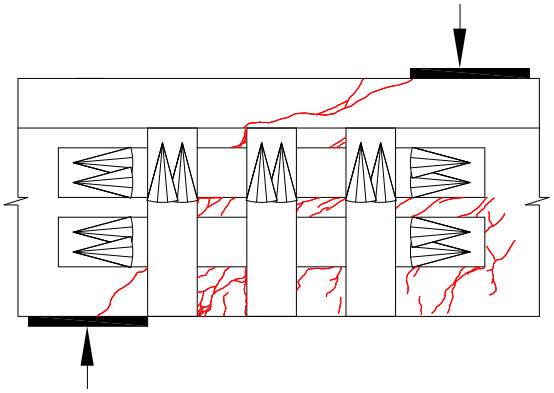

Figure 4-17: Cracking pattern of west face 14-3-Bi-D

Shear cracks initiated on the web of the specimen after reaching an applied load of approximately 150-kips. As the applied load continued to increase, additional shear cracks formed between the point load and the reaction. The failure was a combination of concrete crushing at the face of the node next to the support and crushing of the concrete strut that formed between the point of applied load and the support as seen in Figure 4-18

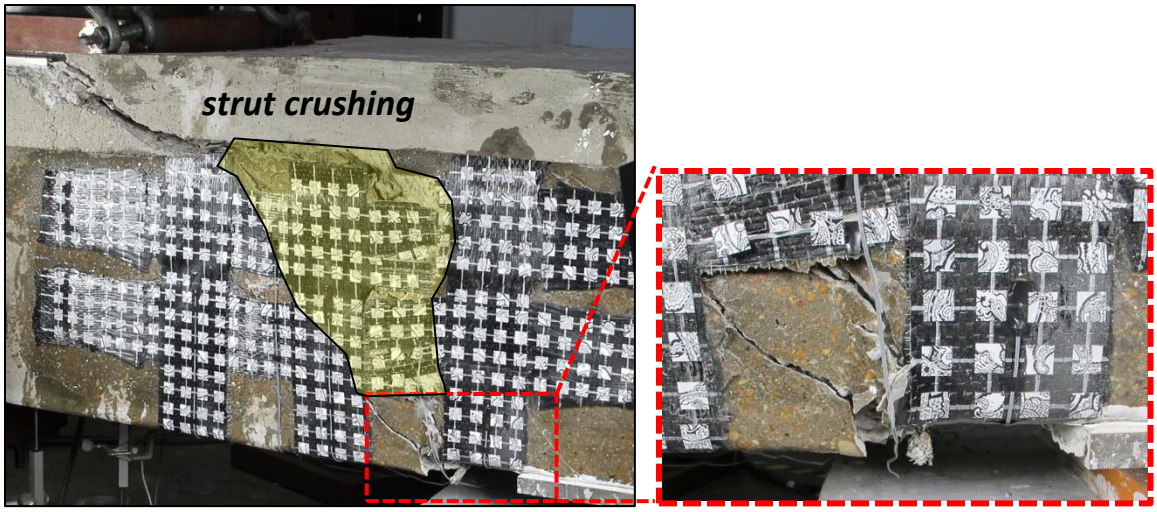

Figure 4-18: Crushing of concrete strut and node

CFRP anchors prevented the complete debonding of CFRP strips. No strip rupture or anchor fracture was observed in this test. However, due to crushing of the concrete strut, one of the CFRP anchors detached from the core of the web, and affected the entire strengthening system (Figure 4-19).

Figure 4-19: Separation of CFRP strip and anchor as one unit

The maximum strain recorded in the vertical CFRP strips was 0.004 in the vertical strip next to the support (strip #3); the maximum strain reported in the horizontal CFRP

strip was 0.0027 in the lower strip. Both of these strains were recorded at the maximum applied load. Strains in the vertical CFRP strips at different loading stages were recorded by several strain gauges as indicated in Figure 4-20.

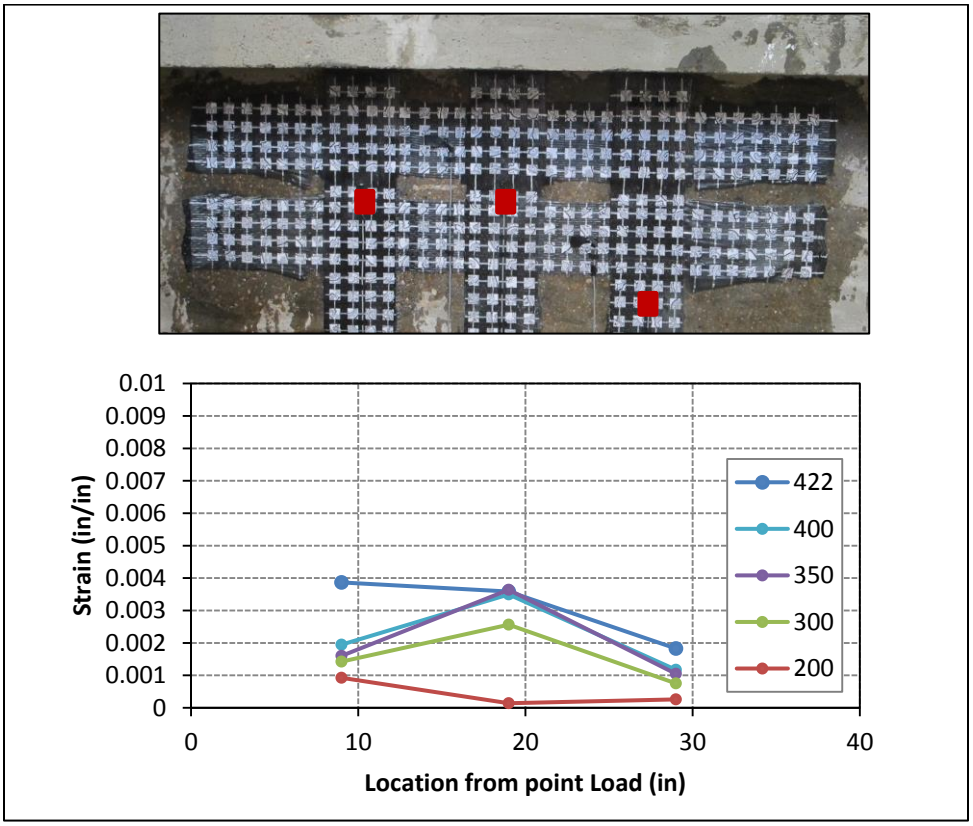

Figure 4-20: Strains in vertical strips at different loading stages of 14-1.5-Bi-D

The strains in the steel stirrups during testing are shown in Figure 4-21 and Figure 4-22. First yielding of steel stirrups occurred at an applied shear load of 180-kips (applied load of 299-kips.). All measured strains within the test region were above yield except at the gauge on the stirrup closest to the point load (G4).

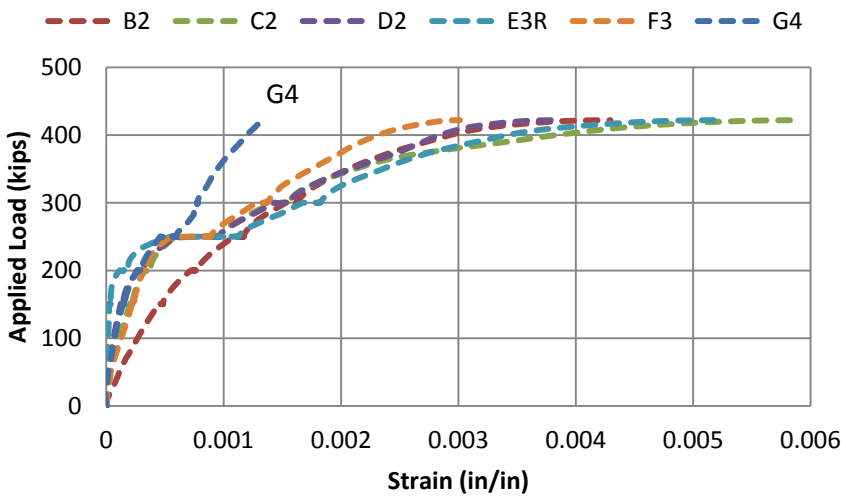

Figure 4-21: Load versus maximum measured strain in stirrups for 14-1.5-Bi-D

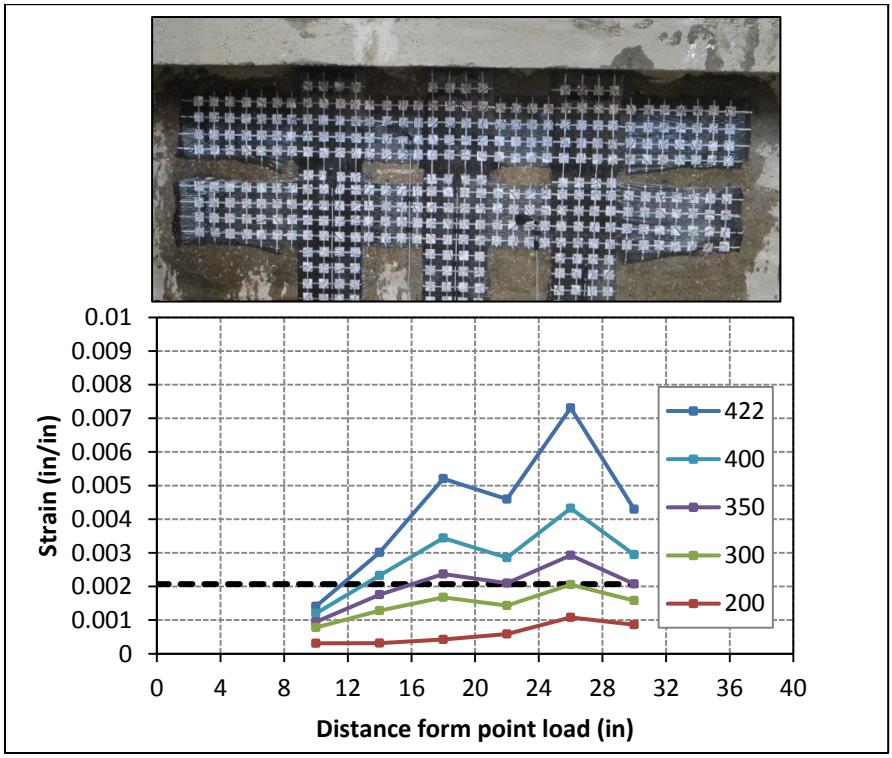

Figure 4-22: Strains in steel stirrups at different loading stages of 14-1.5-Bi-D

Strains in the stirrups and the vertical CFRP strips at various levels of applied load are shown in Figure 4-23. The x-axis represents location from point load in inches.

(a) 200-kips

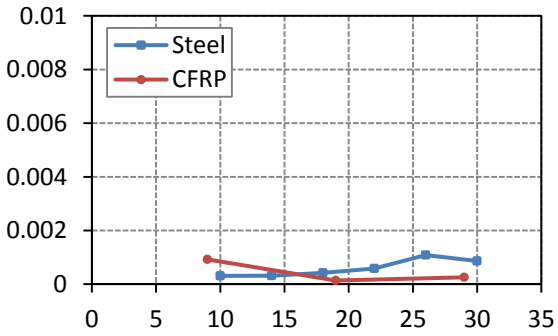

(b) 300-kips

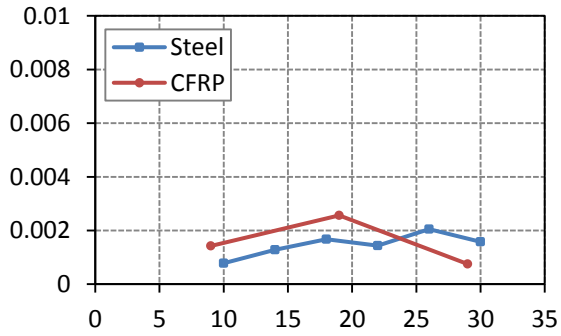

(c) 350-kips

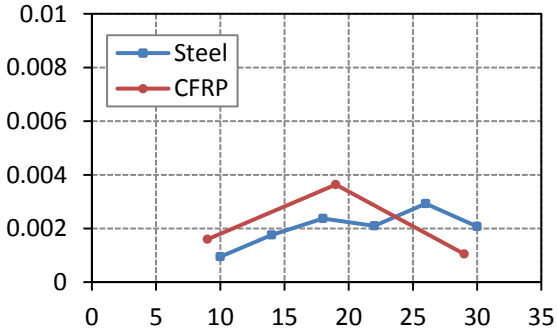

(d) 400-kips

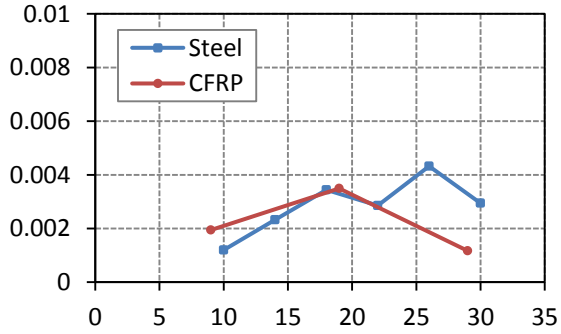

(e) 422-kips

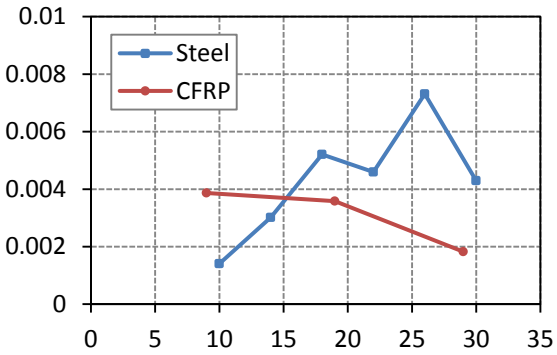

Figure 4-23: Strains in steel stirrups and CFRP strips during loading of 14-1.5-Bi-D

Longitudinal reinforcement did not yield during the test. The maximum strain reported in longitudinal reinforcement was 0.0017 for the bottom layer of tension reinforcement.

4.4.2 Results of 14-in. web specimens with a/d of 3

Two tests were conducted under this series. The only difference between these tests was the amount of CFRP material used in order to evaluate its effect on the shear capacity of a bi-directionally strengthened beam. Neither control nor uni-directionally strengthened specimens were tested in this series because they were tested in Tx-DOT Project 0-6306 and will be linked to current results in Chapter 5.

4.4.2.1 14–3–Bi–S (Bi-directional with single layer of CFRP)

The test specimen was strengthened with a single layer of CFRP strips bi-directionally. CFRP anchors were used to provide sufficient anchorage and to prevent the premature debonding of CFRP strips, and therefore, develop the maximum tensile capacity of the CFRP material. Since a single layer of CFRP strips were applied as external reinforcement, a single CFRP anchor per anchorage location was sufficient to provide necessary anchorage. The CFRP layout for this test is shown in Figure 4-24.

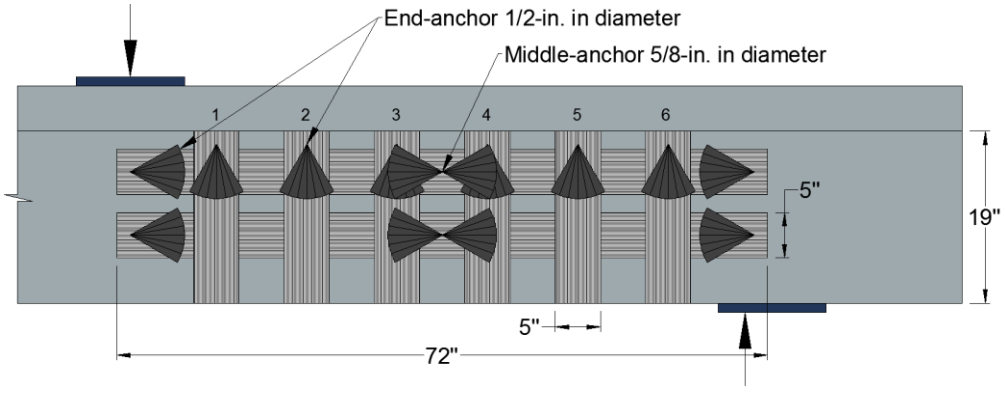

Figure 4-24: CFRP configuration of 14-3-Bi-S

Shear failure occurred at a shear force of 156-kips (applied load of 295-kips). Photos of the test specimen before and after shear failure can be seen in Figure 4-25. The presence of horizontal CFRP strips in addition to the paper targets for vision system made it difficult to see the cracks in the photos.

Figure 4-25: left (before), right (after) loading of 14-3-Bi-S

The applied load versus displacement curve is plotted in Figure 4-26. The shear force versus shear strain is provided in Figure 4-27.

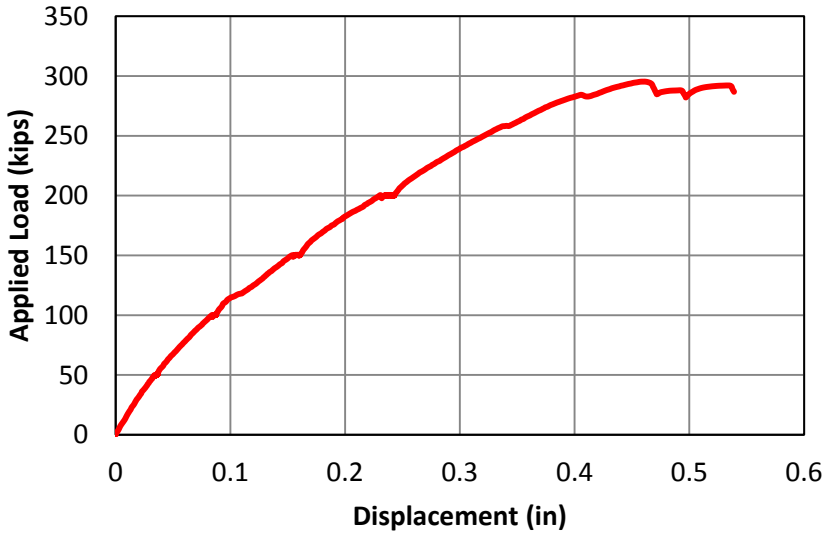

Figure 4-26: Load-displacement curve of 14-3-Bi-S

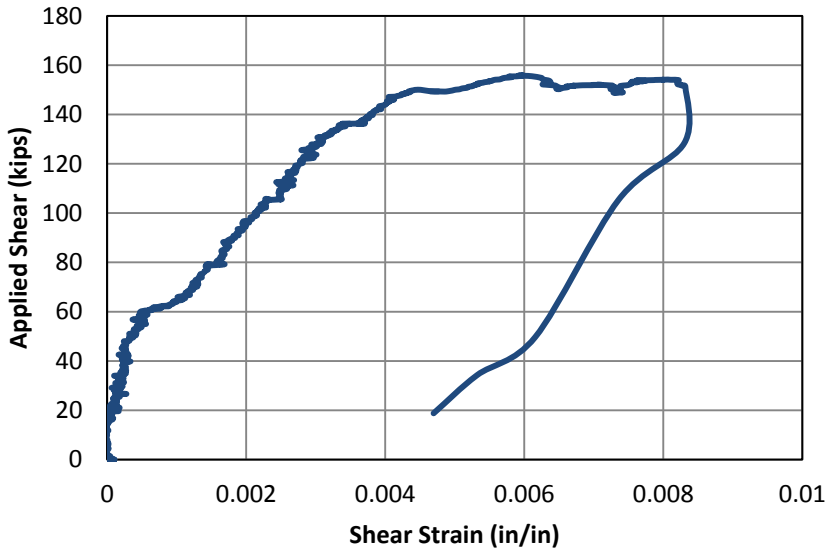

Figure 4-27: Shear deformation curve of 14-3-Bi-S

Concrete cracking was marked during the course of testing. A sketch of the cracking pattern of *14-3-Bi-S* can be seen in Figure 4-28 and Figure 4-29.

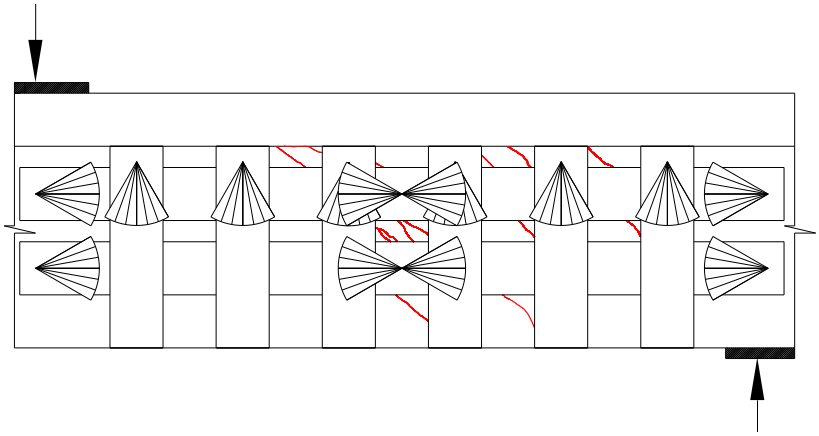

Figure 4-28: Cracking pattern of east face of 14-3-Bi-S

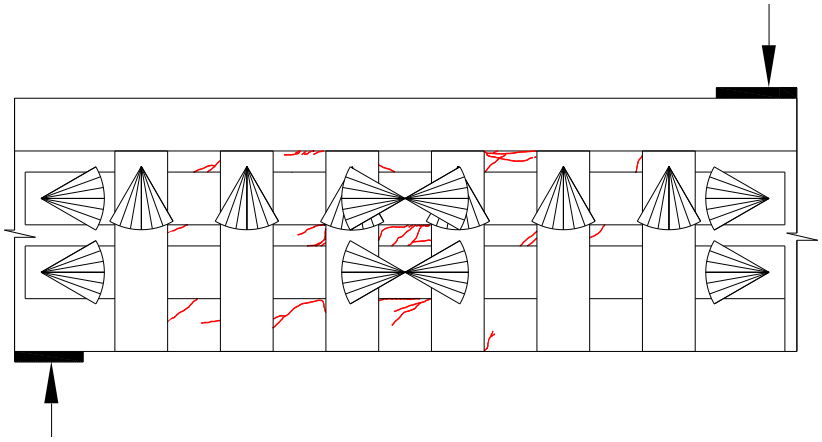

Figure 4-29: Cracking pattern of west face of 14-3-Bi-S

Fine shear cracks initiated in the web of the specimen after reaching an applied load of approximately 150-kips. As the applied load increased, additional minor cracks developed, especially at the edges of the CFRP strips as seen in Figure 4-30. The failure was initiated by large cracks at the web-flange interface, as shown in Figure 4-31

Figure 4-30: Cracking at the boundaries between concrete and CFRP

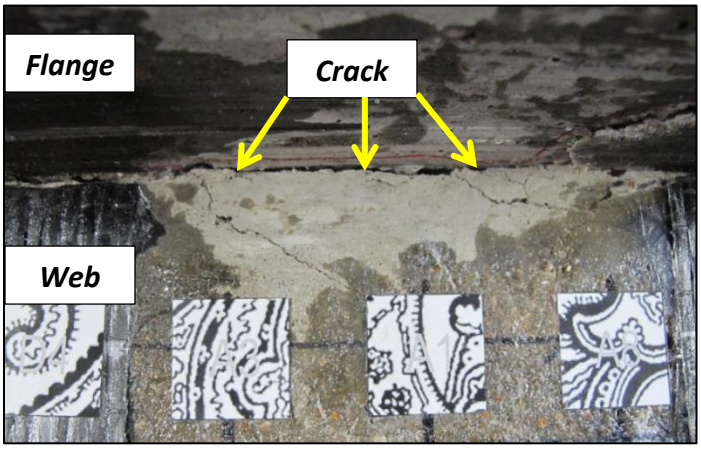

Figure 4-31: Critical crack at web-flange interface

CFRP anchors prevented the complete deonding of CFRP strips. No strip rupture, or anchor fracture was observed in this test. Nevertheless, both the minor cracks around CFRP strips and the major crack at the web-flange interface led to a failure in the core of the web directly behind the CFRP anchor. The maximum strain recorded in vertical CFRP strips was 0.006 in vertical strip #2 (second vertical strip from the reaction),

whereas the maximum strain recorded in the horizontal CFRP strip was 0.0015 in the lower strip. Both of these strains were reported at the maximum applied load.

Strains in the vertical CFRP strips at different loading stages were recorded using data from the UTVS (refer to 3.5.3). The location of targets selected to measure the strain in the vertical strips and the strain variations during the loading are presented in Figure 4-32.

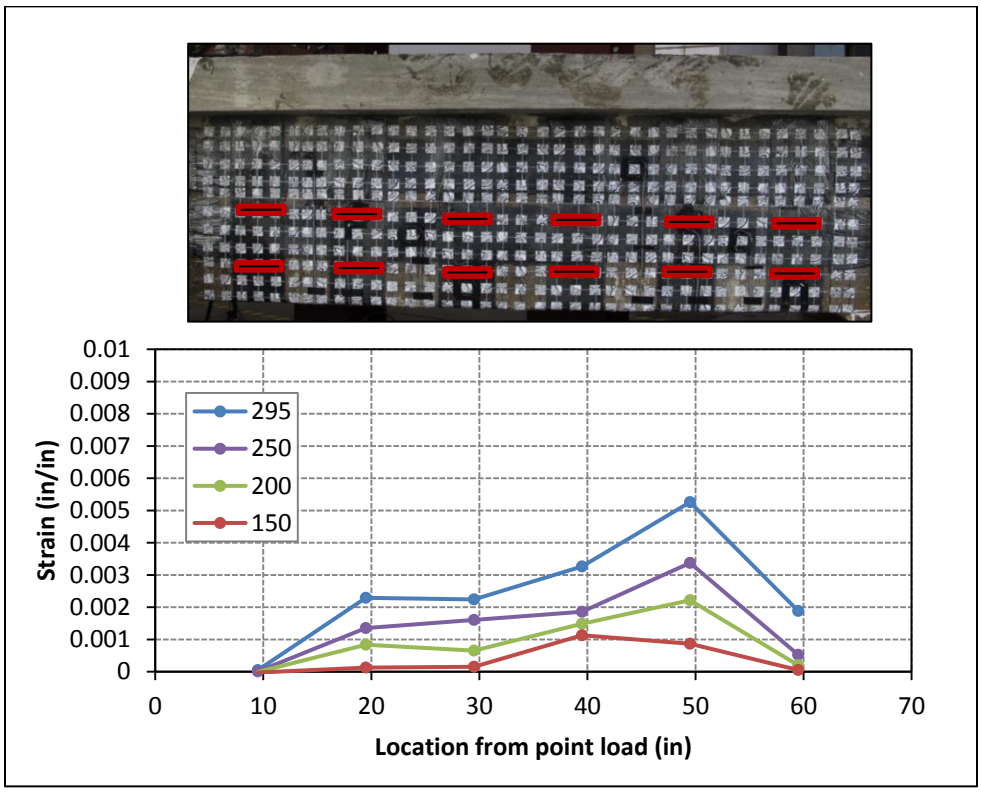

Figure 4-32: Strains in vertical strips at different loading stages of 14-3-Bi-S

Strains in the steel stirrups and the CFRP strips were measured by strain gauges. The strains recorded in the steel stirrups at different loading stages are shown in Figure 4-33. The transverse reinforcement started yielding at a shear force of 79-kips

(applied load of 150-kips). All measured strains within the test region were above yield except at the gauges on the stirrups closest to the point load (G4) and the support (A2). The strains in the stirrups during the loading are reported in Figure 4-34.

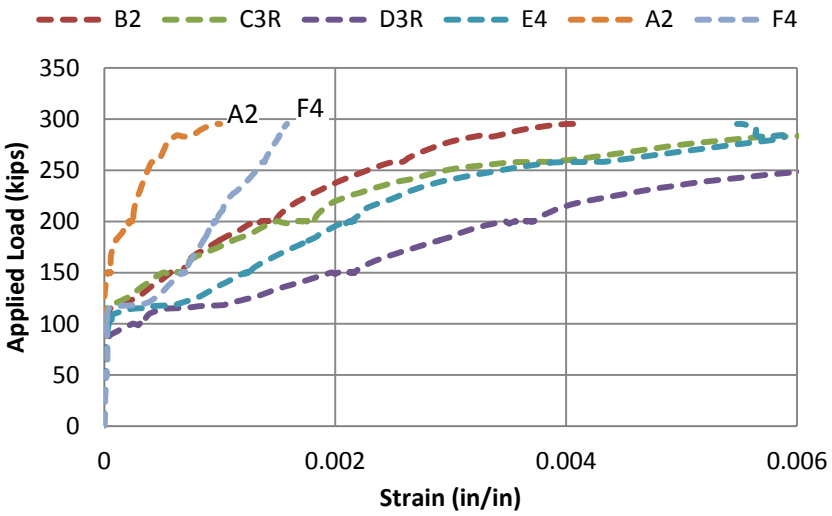

Figure 4-33: Load versus maximum measured strain in stirrups for 14-3-Bi-S

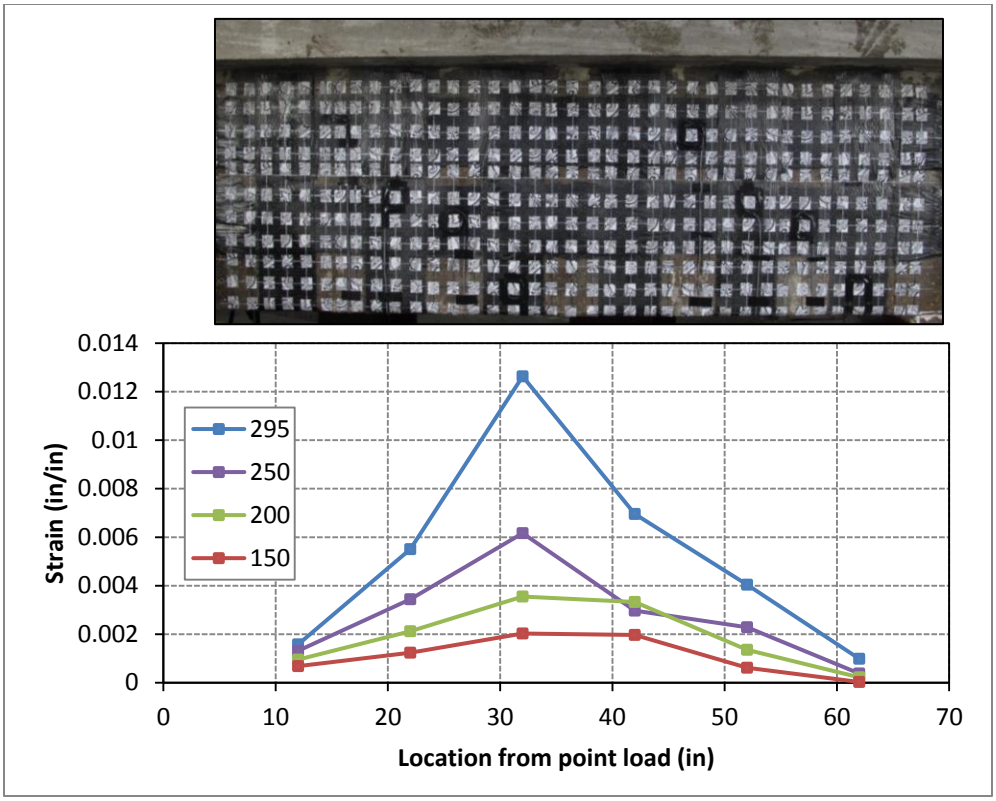

Figure 4-34: Strains in steel stirrups at different loading stages of 14-3-Bi-S

Strains in the stirrups and the vertical CFRP strips at various levels of applied load are shown in Figure 4-35. The x-axis represents location from point load in inches.

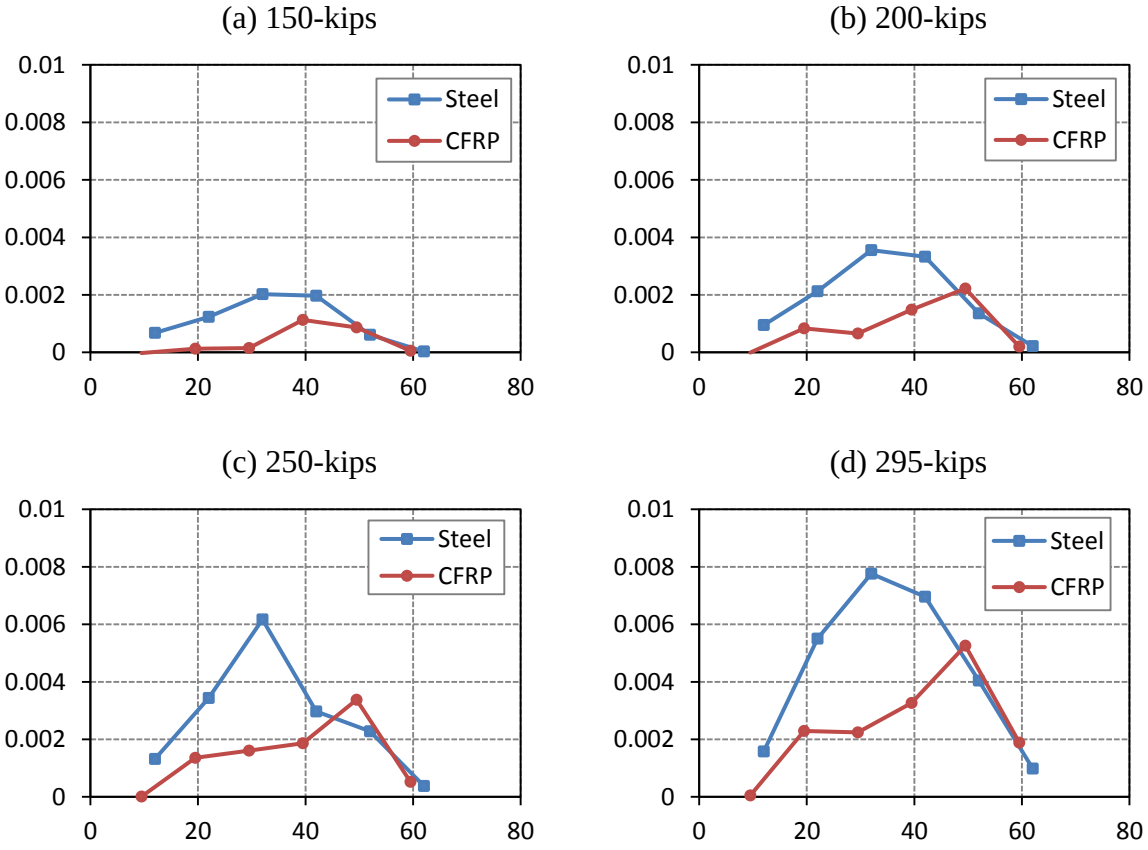

Figure 4-35: Strains in steel stirrups and CFRP strips during loading of 14-3-Bi-S

As expected, none of longitudinal reinforcement yielded during the test. The maximum strain reported in the longitudinal reinforcement was 0.0015 for the bottom layer of tension reinforcement.

Each component's (concrete, steel, and CFRP) contribution to the shear resistance of *14-3-Bi-S* was estimated (Figure 4-36). The x-axis represents the applied shear force, and the y-axis represents the shear contribution of each material.

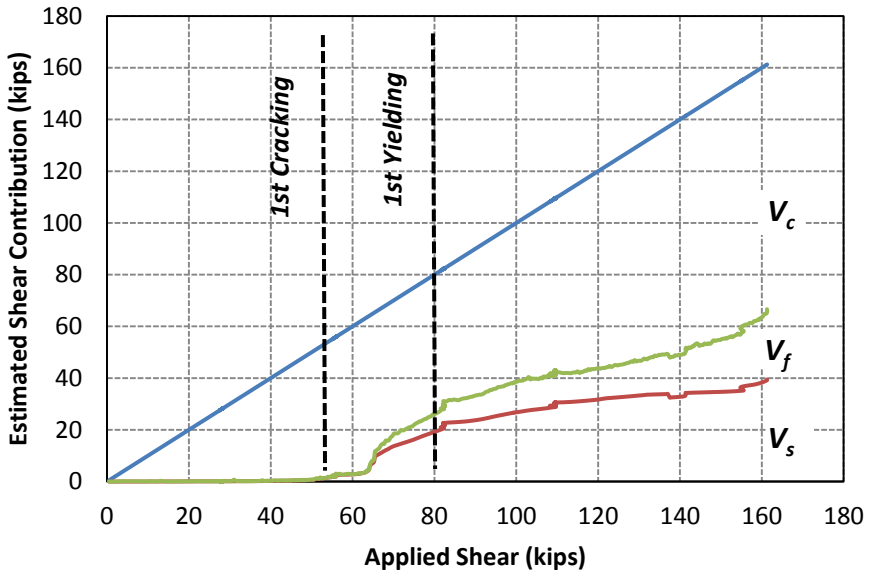

Figure 4-36: Estimated shear contribution of concrete, steel, and CFRP (14-3-Bi-S)

4.4.2.2 14–3–Bi–D (Bi-directional with double layer of CFRP)

This test was conducted to examine the effect of the amount of CFRP material on the shear strength of a strengthened specimen. The specimen was strengthened vertically and horizontally with two layers of CFRP strips. The CFRP layout for this test is shown in Figure 4-37.

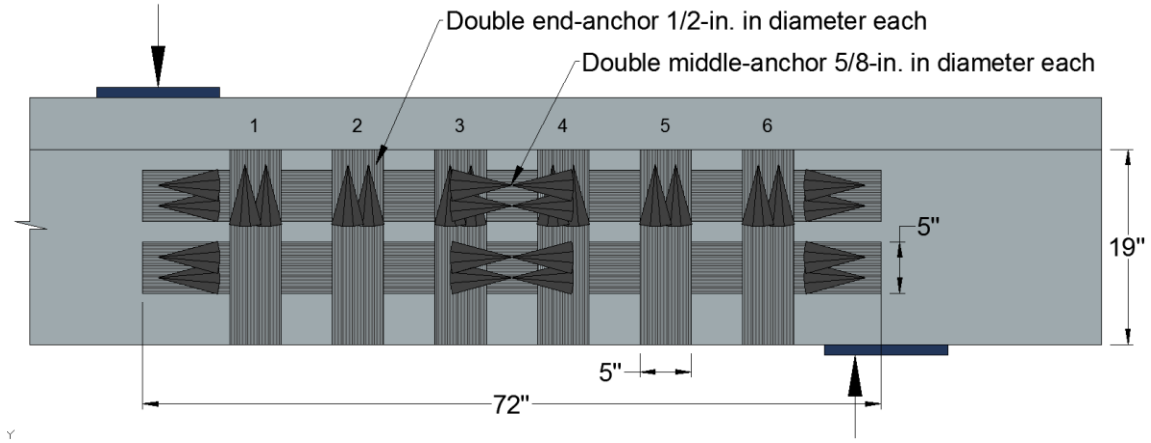

Figure 4-37: CFRP configuration of 14-3-Bi-D

Shear failure occurred at a shear force of 167-kips (applied load of 316 kips). Photos of the test specimen before and after shear failure can be seen in Figure 4-38.

Figure 4-38: left (before), right (after) loading of 14-3-Bi-D

The applied load versus displacement curve is plotted in Figure 4-39. Mid-span displacement corresponding to the maximum applied load was 0.58-in. The applied shear force versus shear strain curve is provided in Figure 4-40.

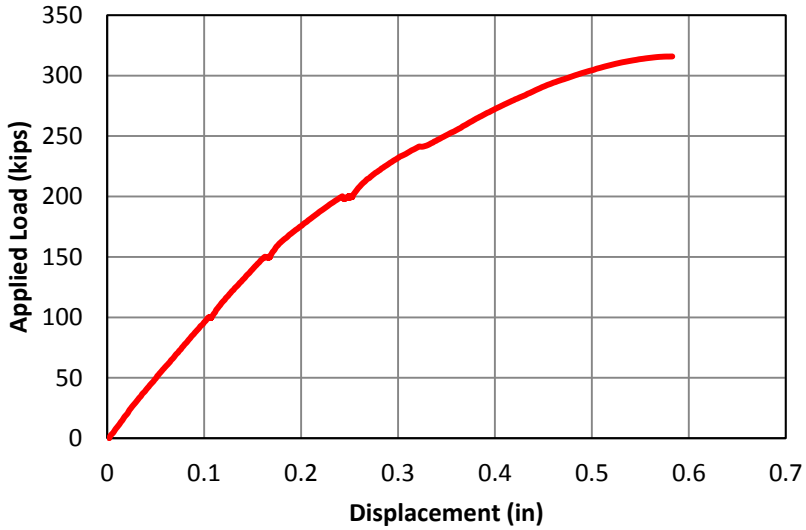

Figure 4-39: Load-displacement curve of 14-3-Bi-D

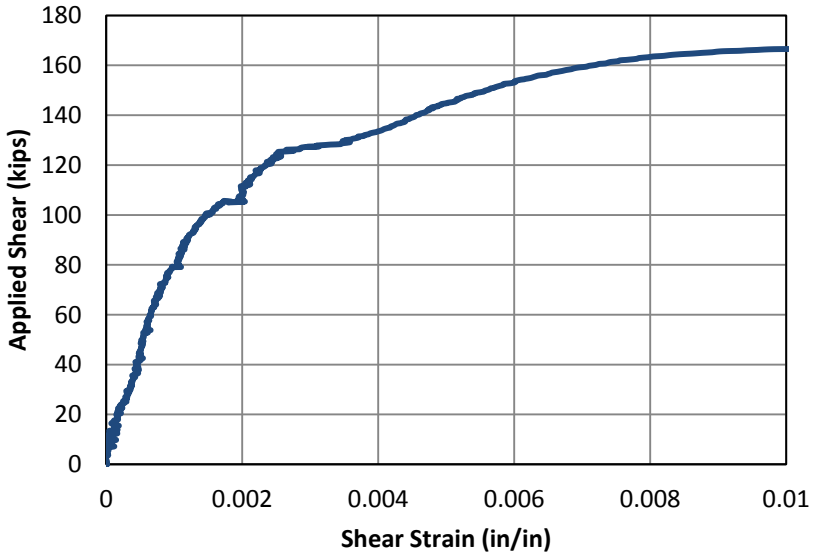

Figure 4-40: Shear deformation curve of 14-3-Bi-D

The cracking pattern can be seen in Figure 4-41 and Figure 4-42.

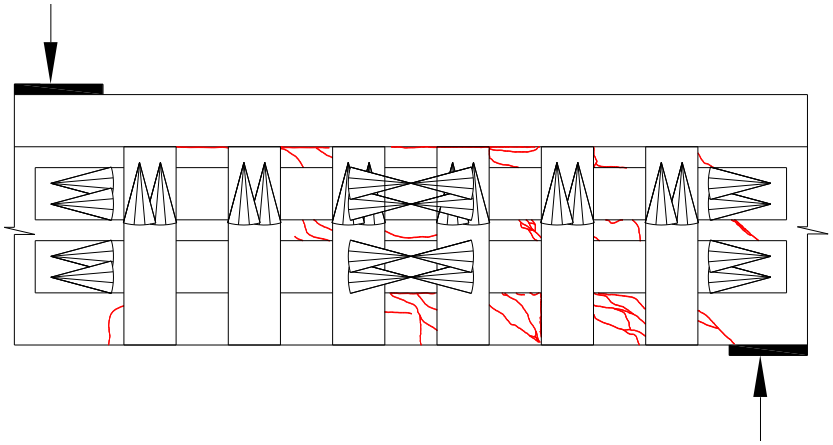

Figure 4-41: Cracking pattern of east face of 14-3-Bi-D

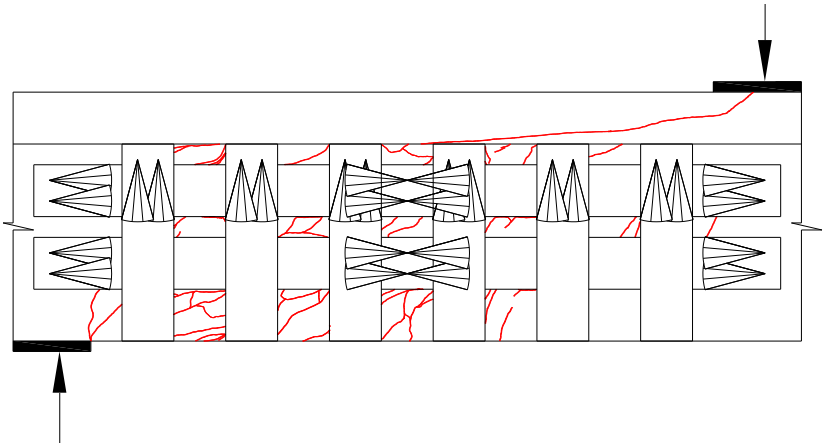

Figure 4-42: Cracking pattern of west face of 14-3-Bi-D

Fine shear cracks initiated in the web of the specimen after reaching an applied load of approximately 150-kips. As the applied load increased, additional minor cracks developed especially at the edges of the CFRP strips, as seen in Figure 4-43. As the applied load was increasing, these minor cracks developed and concrete spalling was observed at ultimate loads as shown in Figure 4-43.

Figure 4-43: Development of cracks at CFRP edges for 14-3-Bi-D

The failure was initiated as a large flat crack propagating from the point load to the flange-web interface, as can be seen in Figure 4-44. This crack progressed to the support reaction after passing above the first five vertical strips. This resulted in some debonding in the upper portions of the vertical CFRP strips, as shown in Figure 4-45.

Figure 4-44: Critical crack in 14-3-Bi-D: left (east), right (west)

Figure 4-45: Separation of CFRP strips

Neither CFRP strip rupture nor anchor rupture was observed in this test. Nevertheless, both the minor debonding of CFRP strips and the major crack at the web-flange interface led to a failure in the core of the web directly behind the CFRP anchor. The failure pattern confirmed the efficacy of the strengthening system.

Based on CFRP strain gauges, the maximum strain recorded in the vertical CFRP strip was 0.002 in strip #3, whereas the maximum strain recorded in the horizontal CFRP strip was 0.003 in the upper strip. Strains in vertical CFRP strips at different loading stages were recorded using data from the UTVS (refer to 3.5.3). The location of targets selected to determine the strain in the vertical strips and the strain variations are presented in Figure 4-46.

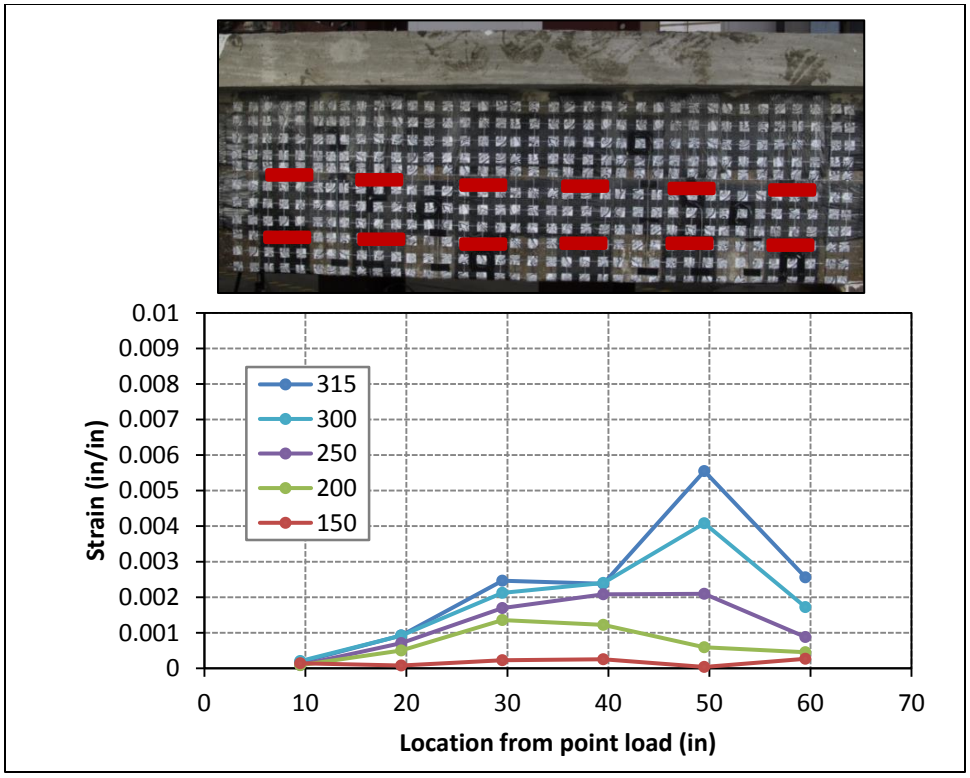

Figure 4-46: Strains in vertical strips at different loading stages of 14-3-Bi-D

Several strain gauges monitored the strains in the steel stirrups and the CFRP strips. The maximum strain reported in the steel stirrups different loading stages is shown in Figure 4-47. The internal transverse reinforcement started yielding at a shear force of 111-kips (an applied load of 240-kips). All measured strains within the test region were above yield except at the gauge on the stirrup closest to the support (A2). Strains in the steel stirrups during the loading of *14-3 -Bi-D* are reported in Figure 4-48.

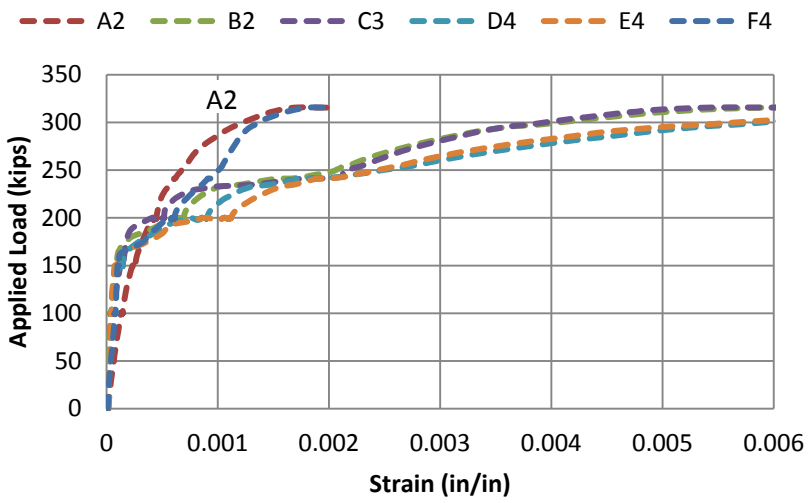

Figure 4-47: Load versus maximum measured strain in stirrups for 14-3-Bi-D

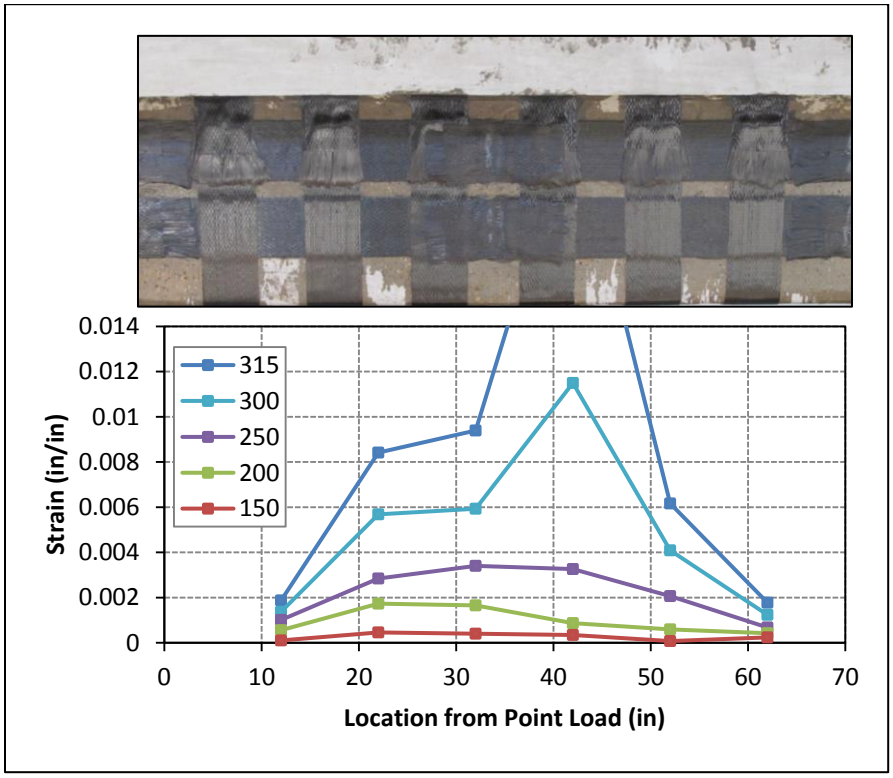

Figure 4-48: Strains in steel stirrups at different loading stages of 14-3-Bi-D

Strains in the stirrups and the vertical CFRP strips at various levels of applied load are shown in Figure 4-49. The x-axis represents location from point load in inches.

(a) 150-kips

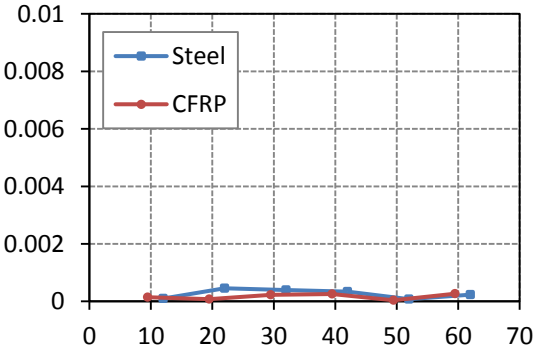

(b) 200-kips

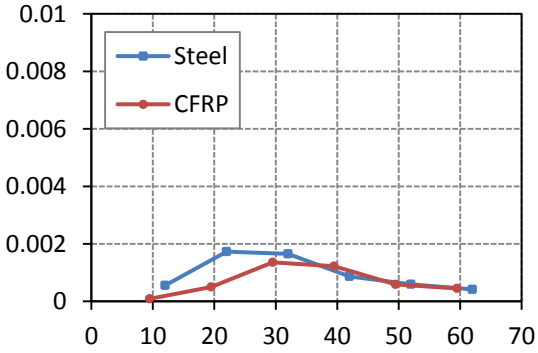

(c) 250-kips

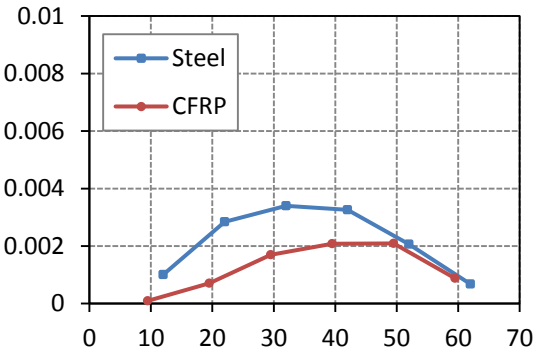

(d) 300-kips

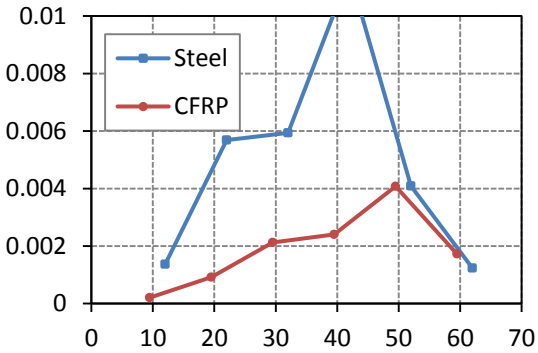

(e) 315-kips

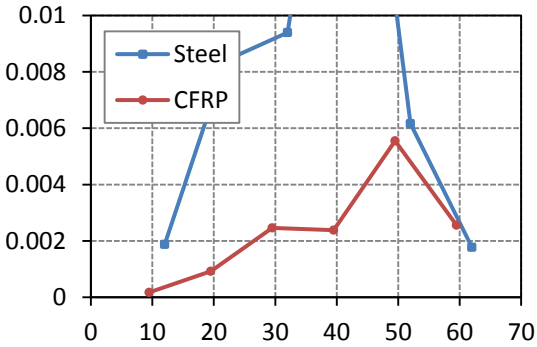

Figure 4-49: Strains in steel stirrups and CFRP strips during loading of 14-3-Bi-D

Longitudinal reinforcement did not yield during the test. The maximum strain recorded in the longitudinal reinforcement was 0.0017 for the bottom layer of tension reinforcement.

Each component's (concrete, steel, and CFRP) contribution to the shear resistance of *14-3-Bi-D* was estimated (Figure 4-50).

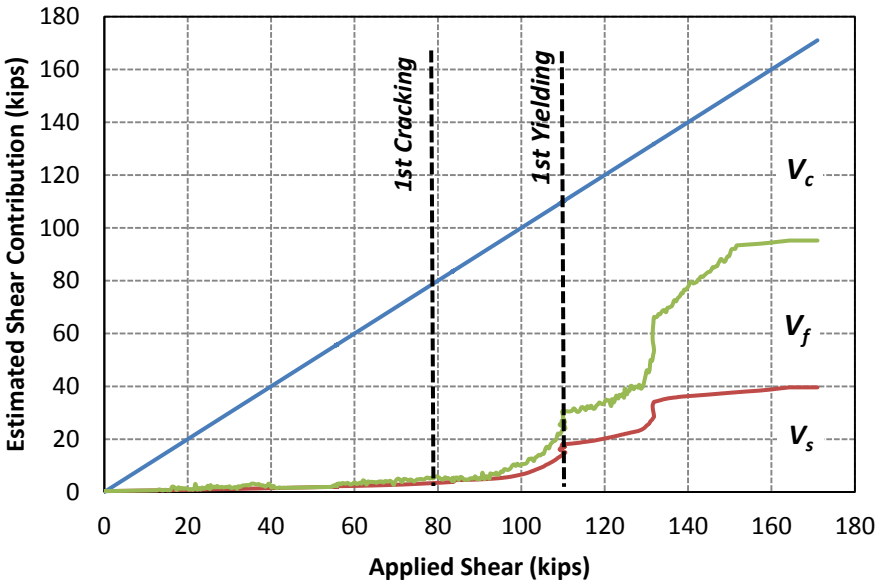

Figure 4-50: Estimated shear contribution of concrete, steel, and CFRP (14-3-Bi-D)

4.4.3 Results of 8-in. web specimens with a/d of 3

In the third series of testing, four tests were conducted on specimens with an 8-in. web width. All the tests in this series were performed with a/d of 3. The behavior of specimens strengthened with single and double layers of bi-directional application of CFRP was compared to the control specimen and to the specimen with uni-directional application of CFRP.

The typical cross-section of an 8-in. web specimen tested under this series is shown in Figure 4-51.

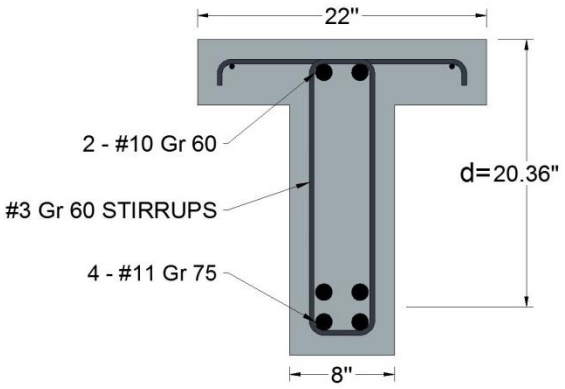

Figure 4-51: Typical cross-section of 8-in. web specimen

4.4.3.1 8–3–Control

This test was conducted on a non-strengthened 8-in. web specimen (Figure 4-52) to determine its base shear strength with a/d of 3.

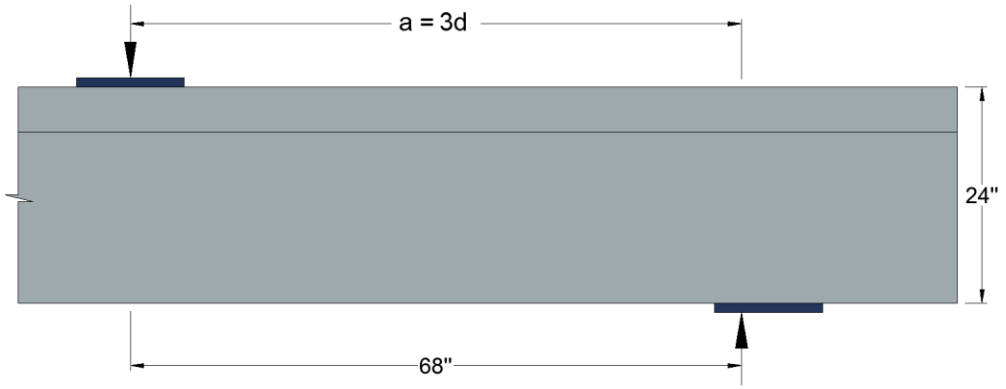

Figure 4-52: Test 8-3-Control (non-strengthened specimen)

Shear failure occurred at a shear force of 76-kips (applied load of 144 kips). Photos of the test specimen before and after shear failure can be seen in Figure 4-53.

Figure 4-53: left (before), right (after) loading of 8-3-Control

The applied load versus displacement curve for *8-3-Control* is plotted in Figure 4-54. Mid-span displacement corresponding to the maximum applied load was 0.49-in. The applied shear force versus shear strain is plotted in Figure 4-55.

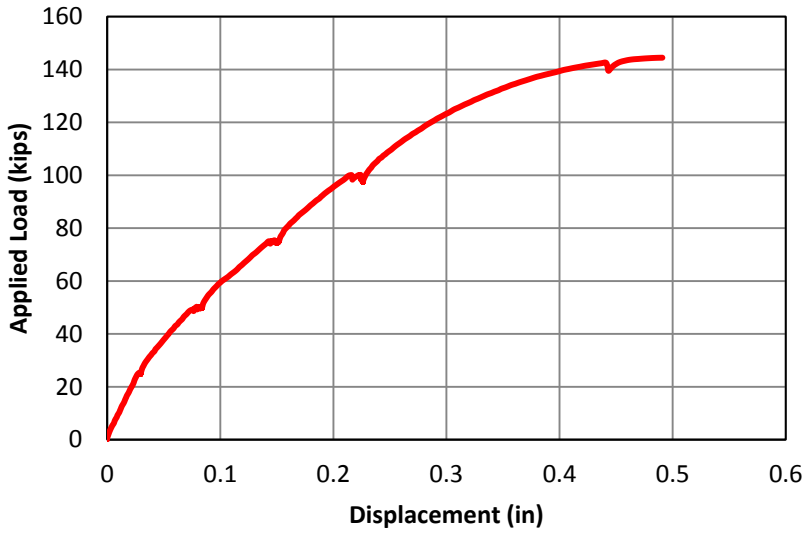

Figure 4-54: Load-displacement curve of 8-3-Control

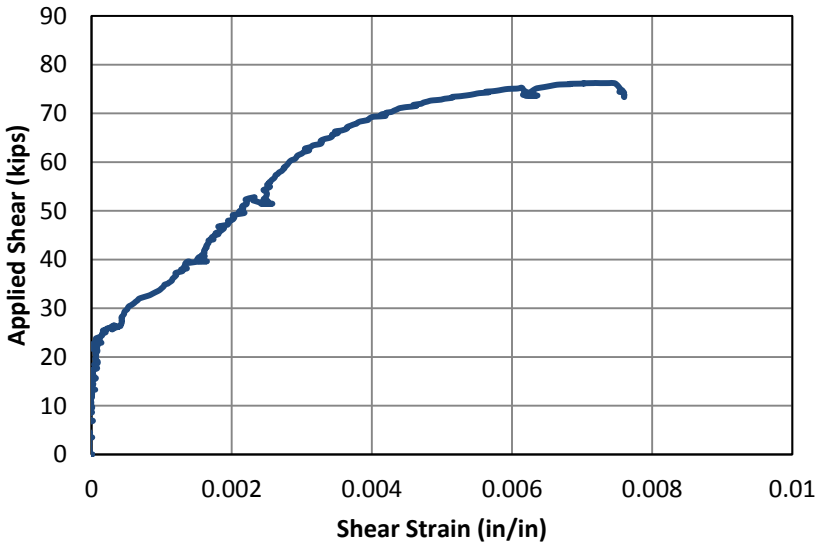

Figure 4-55: Shear deformation curve of 14-8-Control

Concrete cracking was marked during the course of testing. A sketch of the crack pattern of specimen *8-3-Control* can be seen in Figure 4-56 and Figure 4-57.

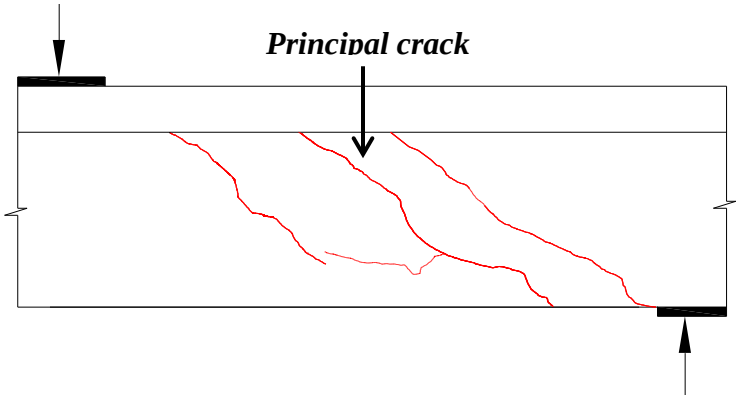

Figure 4-56: Cracking pattern of east face 8-3-Control

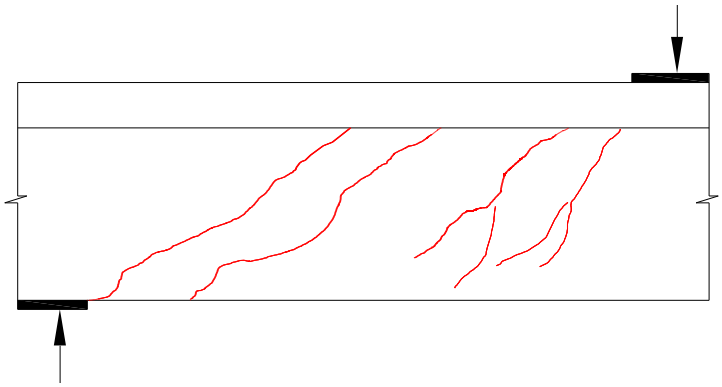

Figure 4-57: Cracking pattern of west face 8-3-Control

Diagonal shear cracking initiated on the middle of the web of the specimen after reaching an applied load of approximately 50-kips (Figure 4-58). As the applied load continued to increase, a principal crack started to form at an angle of 35° and propagated simultaneously toward the support and the flange, as seen in Figure 4-59.

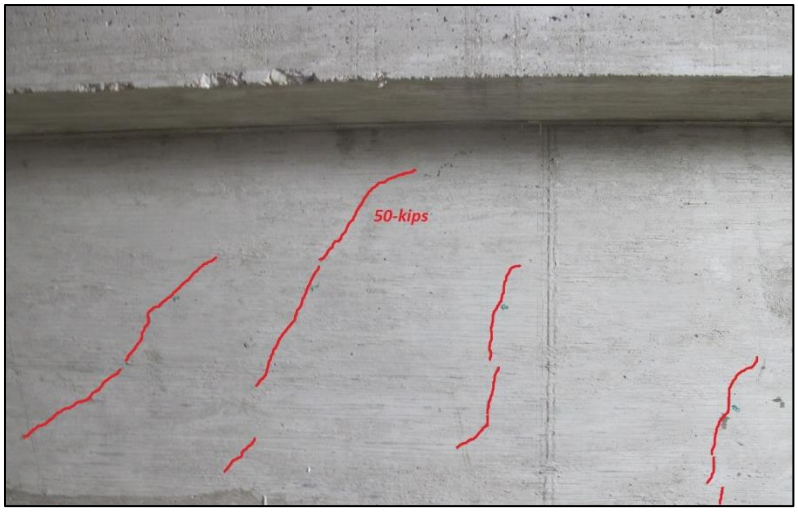

Figure 4-58: Diagonal cracks at 50-kips applied load

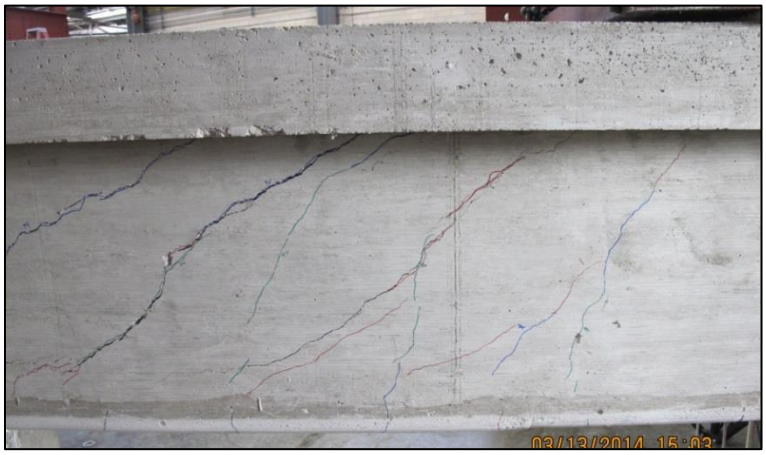

Figure 4-59: Cracking pattern at applied load of 144-kips.

The maximum strain reported in the steel stirrups at different loading stages is shown in Figure 4-60. This figure shows the consistency between the onset of diagonal cracks in the middle of the test region and the progress of strains in the steel stirrups (B,C, and D) at an applied load of 50-kips. The internal transverse reinforcement started yielding at a shear force of approximately 49-kips (applied load of 94-kips). All measured strains within the test region were above yield except at the gauge on the stirrup closest to

the support (A2). Strains in the stirrups during the loading of *8-3 -Control* are reported in Figure 4-61.

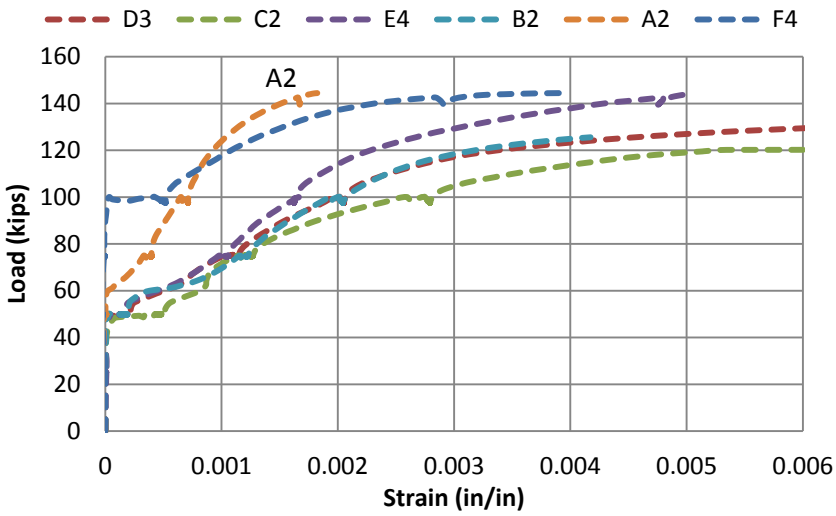

Figure 4-60: Applied load vs strain in stirrups of 8-3-Control

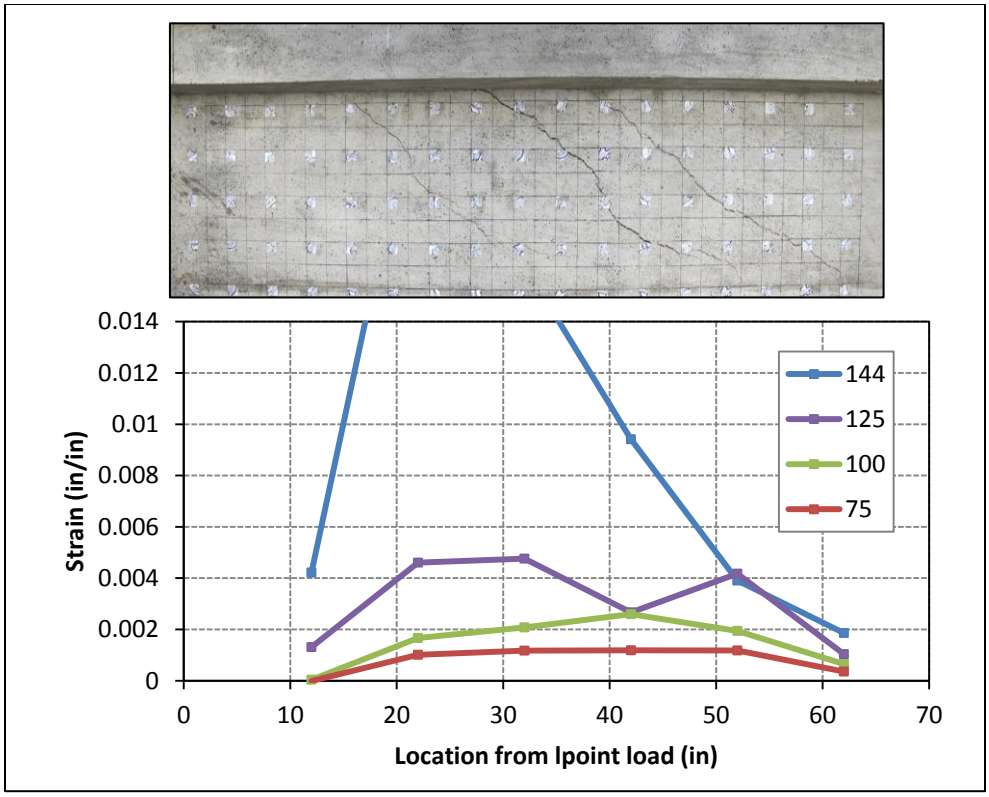

Figure 4-61: Strains in steel stirrups at different applied loading stages of 8-3-Control

Longitudinal reinforcement did not yield during the test. The maximum strain recorded in the longitudinal reinforcement was 0.0017 for the bottom layer of tension reinforcement.

The contribution of each component (concrete, steel, and CFRP) to the shear resistance of *8-3-Control* was estimated (Figure 4-62).

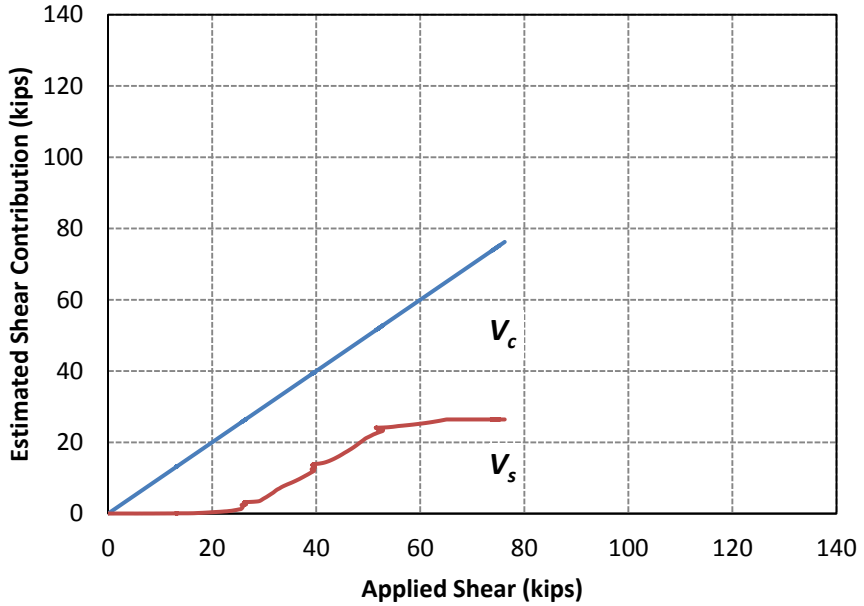

Figure 4-62: Estimated shear contribution of concrete and steel (8-3-Control)

4.4.3.2 8–3–Uni (Unidirectional with single layer of CFRP)

This test was conducted to evaluate the effect of the uni-directional application of CFRP strips and CFRP anchors on the shear capacity of a specimen with an 8-in. web. This test also provides the basis for comparing the effect of the uni-directional application to the bi-directional application of CFRP on the shear resistance of an 8-in. web specimen. The test specimen was strengthened with six 5-in. wide vertical strips as an external strengthening reinforcement to form the uni-directional configuration. A single anchor per strip was used to provide anchorage against premature debonding. The CFRP layout for this test specimen is shown in Figure 4-63.

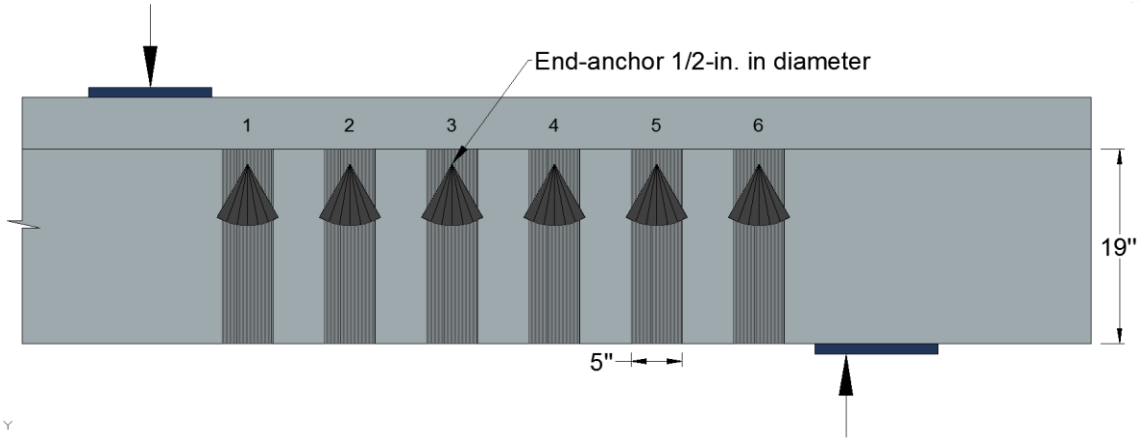

Figure 4-63: CFRP configuration of 8-3-Uni

Shear failure occurred at a shear force of 99-kips (applied load of 188 kips). Photos of the test specimen before and after shear failure can be seen in Figure 4-64

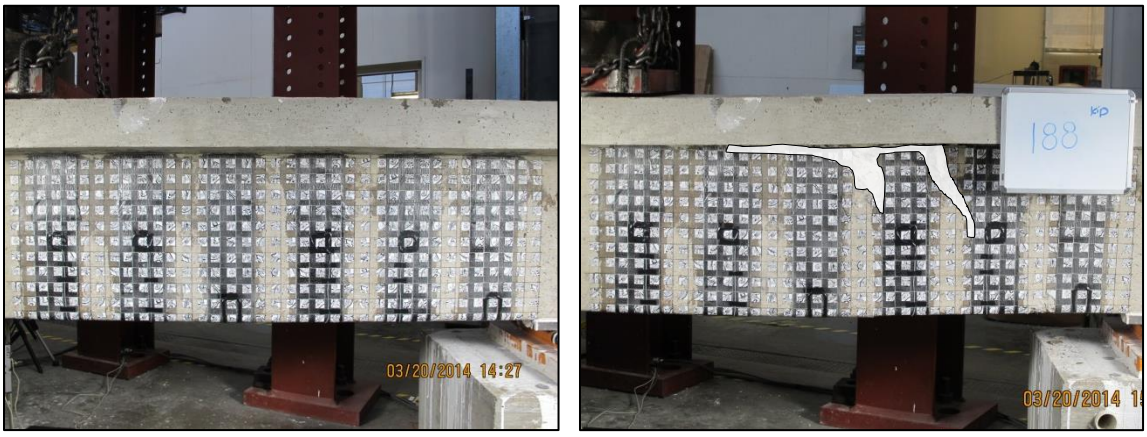

Figure 4-64: left (before), right (after) loading of 8-3-Uni

The applied load versus displacement curve for *8-3-Uni* is plotted in Figure 4-65. Mid-span displacement corresponding to the maximum applied load was 0.58-in. The applied shear force versus shear strain is provided in Figure 4-66.

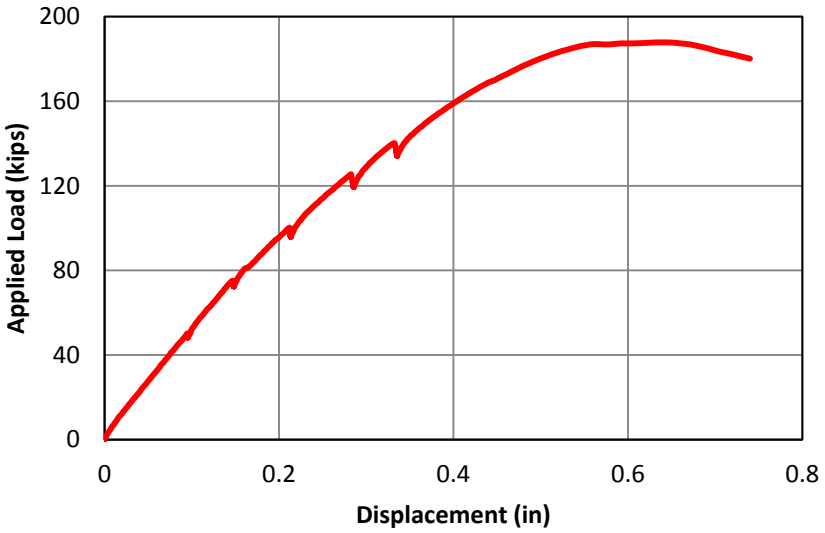

Figure 4-65: Load-displacement curve of 8-3-Uni

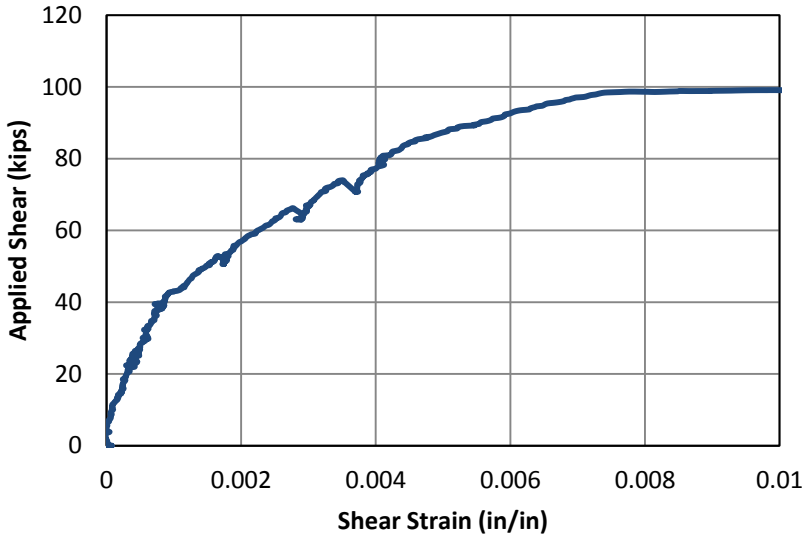

Figure 4-66: Shear deformation curve of 8-3-Uni

Concrete cracking was marked during the course of testing. A sketch of the cracking pattern of specimen *8-3-Uni* can be seen in Figure 4-67 and Figure 4-68.

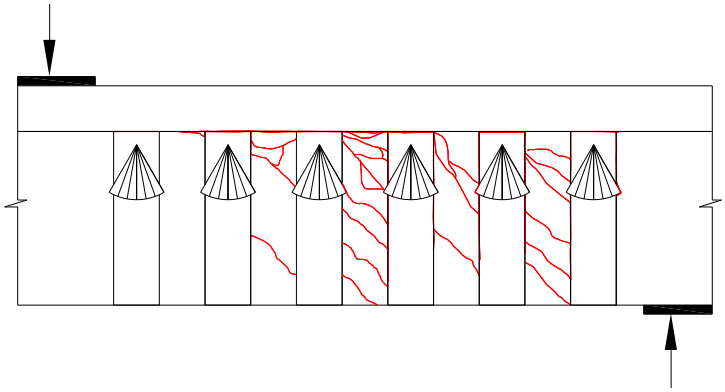

Figure 4-67: Cracking pattern of east face 8-3-Uni

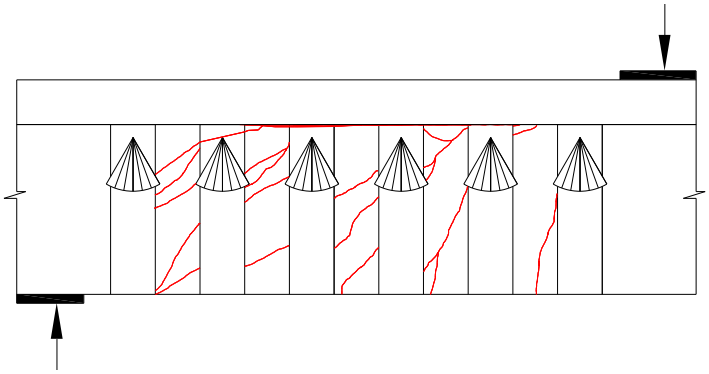

Figure 4-68: Cracking pattern of west face 8-3-Uni

During the initial loading, small flexural-shear cracks initiated on the lower end of the web after reaching an applied load of approximately 50-kips. As the load increased, these cracks propagated vertically until they reached the middle of the web at an applied load of 75-lips. At applied load of 100-kips, diagonal shear cracks were observed on the middle of the web. More diagonal cracks were observed at applied loads of 125-kips and 140-kips. As the applied load continued to increase, a principal crack formed at an angle of 44° and propagated simultaneously toward the support and the flange, resulting in the web crushing. Figure 4-69 shows the development of the cracking prior to failure. The principal crack that caused the web to crush is presented in Figure 4-70.

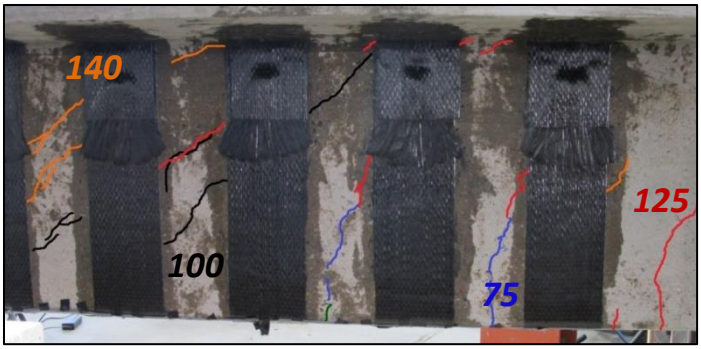

Figure 4-69: Cracking at different load stages of 8-3-Uni

Figure 4-70: failure mode of 8-3-Uni

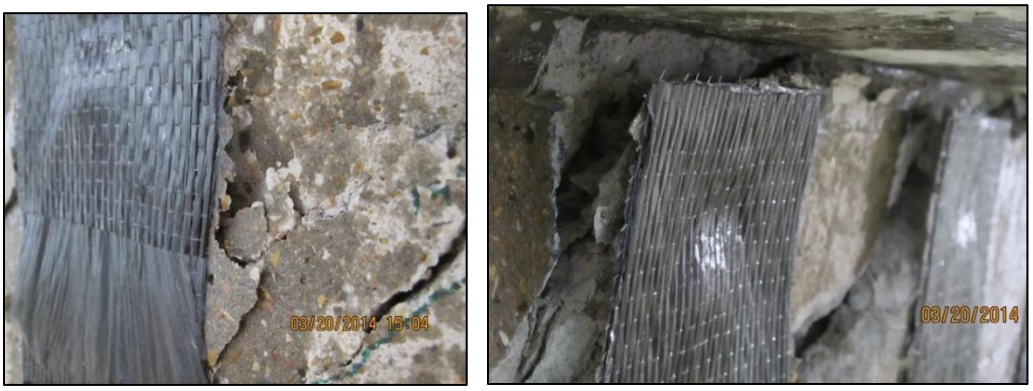

Figure 4-71: Failure of web behind CFRP anchor

As in previous tests, neither CFRP strip rupture nor anchor rupture was observed in this test. However, both the cracks around the CFRP strips and the major crack at the web-flange interface led to a failure in the core of the web directly behind the CFRP anchor (Figure 4-71).

Several strain gauges monitored the strains in the steel stirrups and the CFRP strips. The maximum strain recorded in the vertical CFRP strips was 0.0047 in vertical strip #5 (second vertical strip from the reaction). This strain was recorded before the maximum applied load was reached. Strains in the vertical CFRP strips at different loading stages were recorded using data from UTVS (refer to 3.5.3). The location of targets selected to measure the strain in the vertical strips and the strain variations during the loading are presented in Figure 4-72.

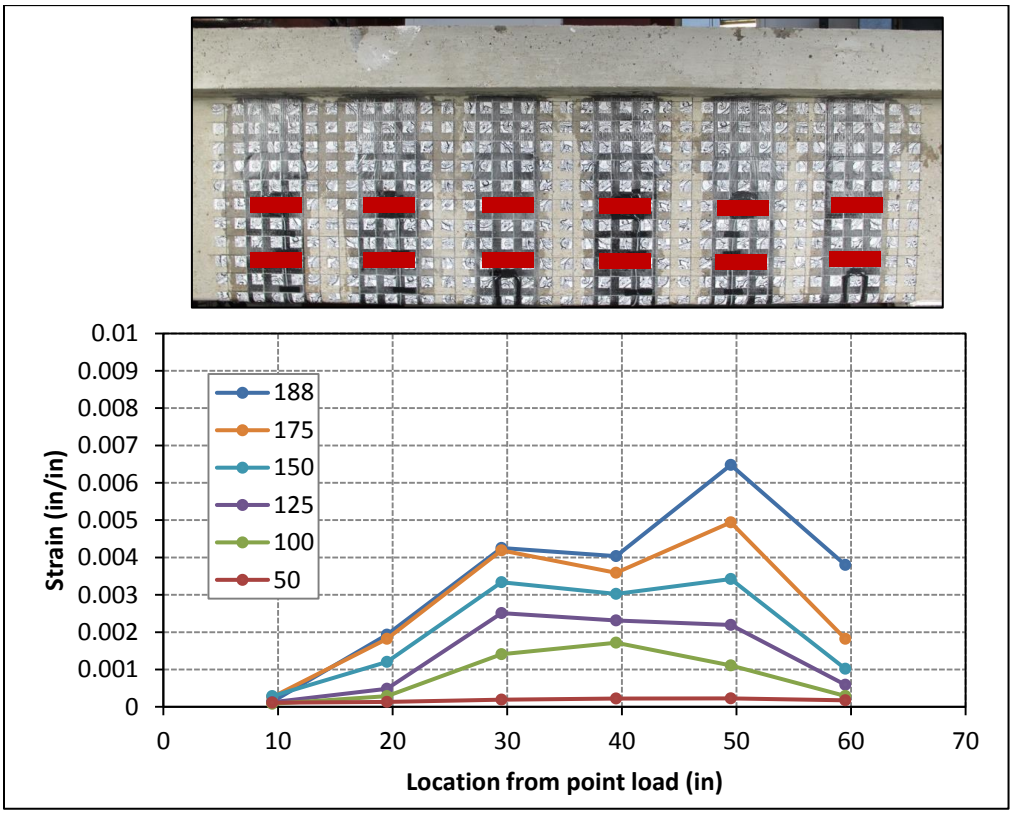

Figure 4-72: Strains in vertical strips at different loading stages of 8-3-Uni

The maximum strain reported in the steel stirrups at different loading stages is shown in Figure 4-73. The internal transverse reinforcement started yielding at a shear force of 60-kips (applied load of 114-kips). All stirrups within the test region yielded in this test. Strains in the steel stirrups were recorded and are plotted in Figure 4-74.

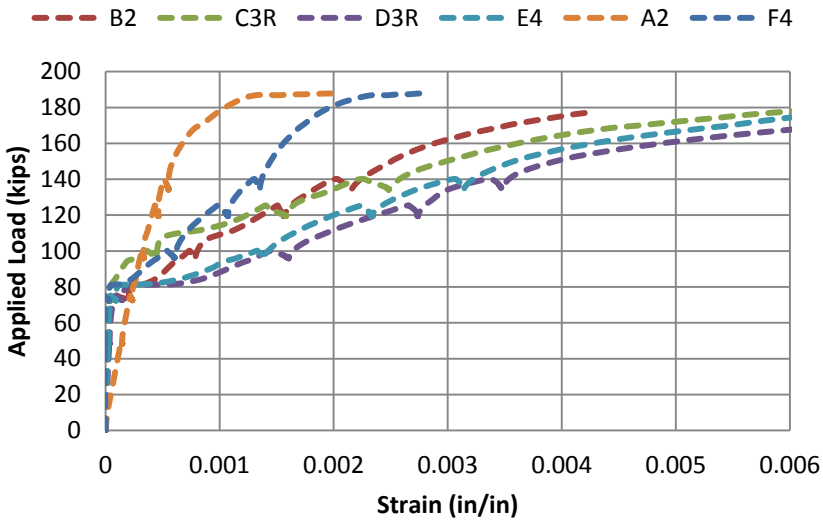

Figure 4-73: Applied load versus maximum measured strain in stirrups for 8-3-Uni

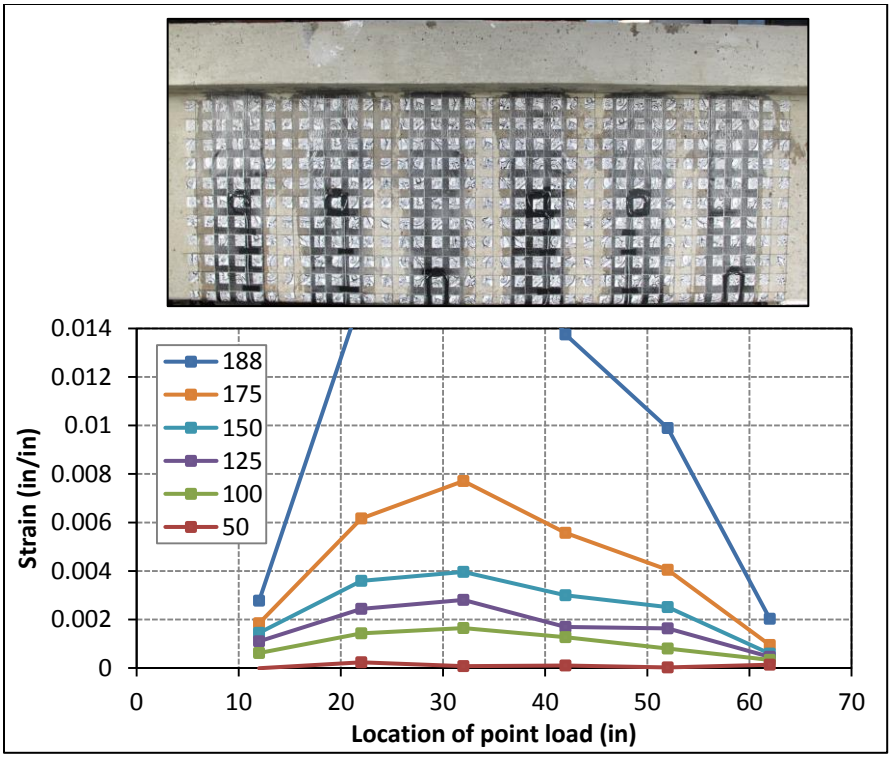

Figure 4-74: Strains in steel stirrups at different loading stages of 8-3-Uni

Strains in the stirrups and the vertical CFRP strips at various levels of applied load are shown in Figure 4-75. The x-axis represents location from point load in inches.

(a) 50-kips.

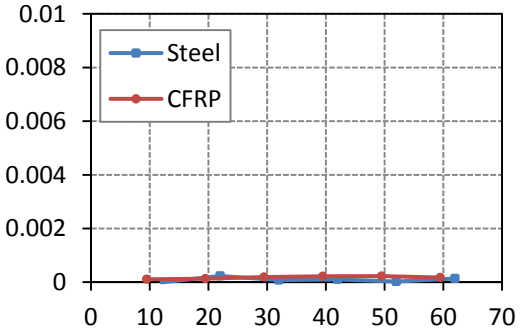

(b) 100-kips.

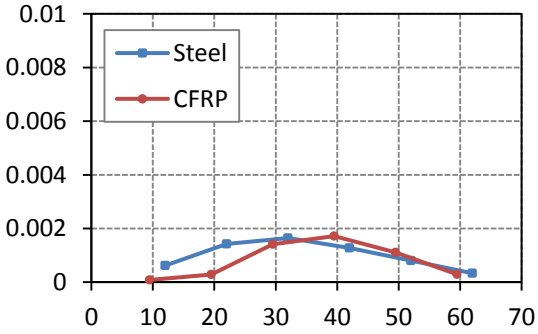

(c) 125-kips.

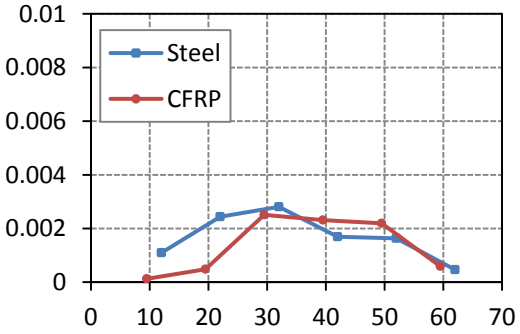

(d) 150-kips.

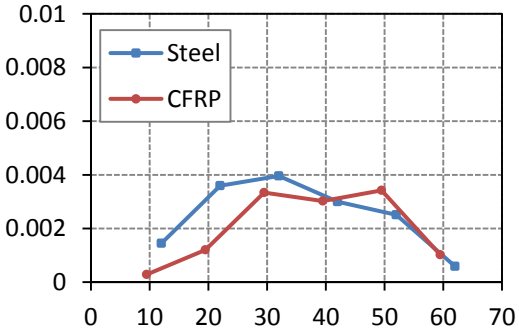

(e) 175-kips.

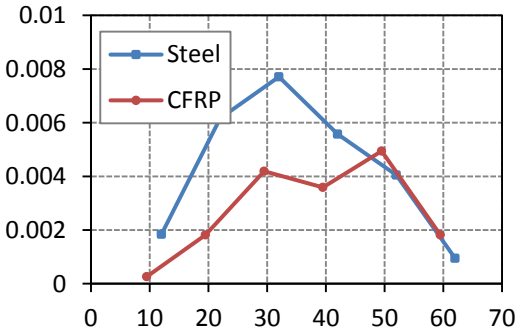

(f) 188-kips.

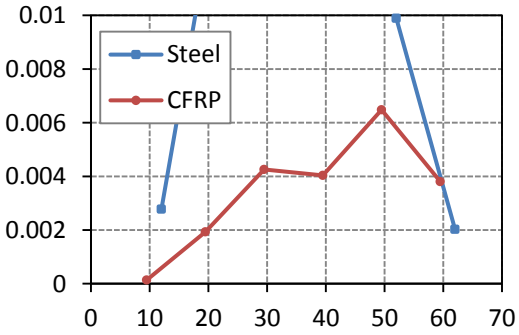

Figure 4-75: Strains in steel stirrups and CFRP strips during loading of 8-3-Uni

Longitudinal reinforcement did not yield during the test. The maximum strain recorded in the longitudinal reinforcement was 0.0021 for the bottom layer of tension reinforcement.

The contribution of each component (concrete, steel, and CFRP) to the shear resistance of *8-3-Uni* was estimated (Figure 4-76).

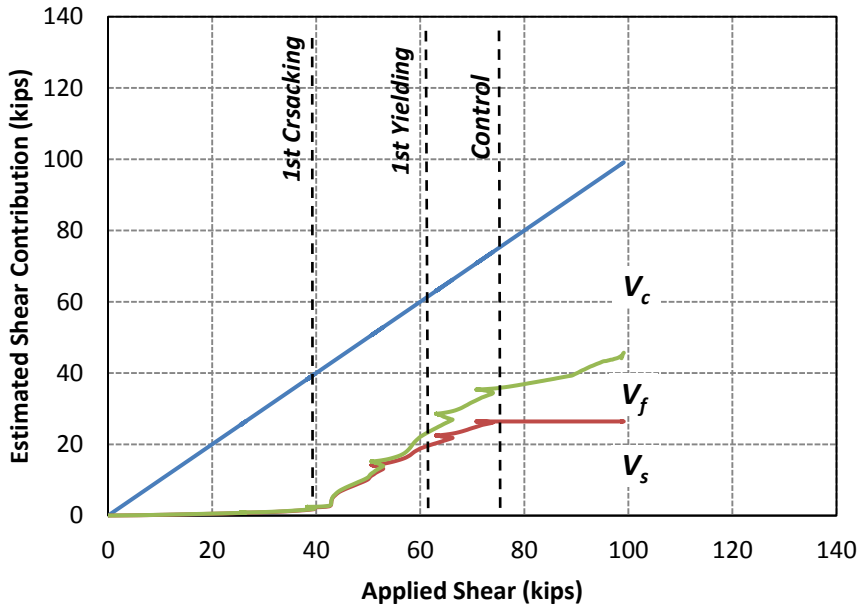

Figure 4-76: Estimated shear contribution of concrete, steel and CFRP (8-3-Uni)

4.4.3.3 8–3–B–S (Bi-directional with single layer of CFRP)

This test was conducted to evaluate the effect of the bi-directional application of CFRP strips and CFRP anchors on the shear capacity of a thin-web specimen (8-in. web). Results from this test can be directly compared to test 8-3-Control and 8-3-Uni to understand the role of the bi-directional application of CFRP.

The test specimen was strengthened with six vertical strips and two horizontal strips as an external strengthening reinforcement to form the bi-directional CFRP configuration. Both end-anchorage and middle-anchorage consist of a single CFRP anchor. Vertical strips were anchored with single end-anchors, while horizontal strips were anchored with single end and single middle-anchors. The CFRP layout for this test specimen is shown in Figure 4-77.

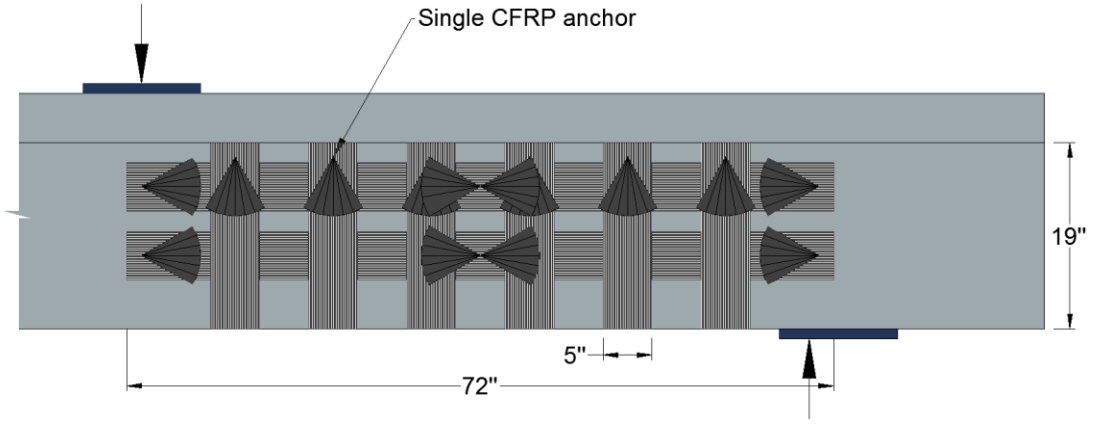

Figure 4-77: CFRP configuration of 8-3-Bi-S

Shear failure occurred at a shear force of 115-kips (applied load of 218 kips). Photos of the test specimen before and after shear failure can be seen in Figure 4-78.

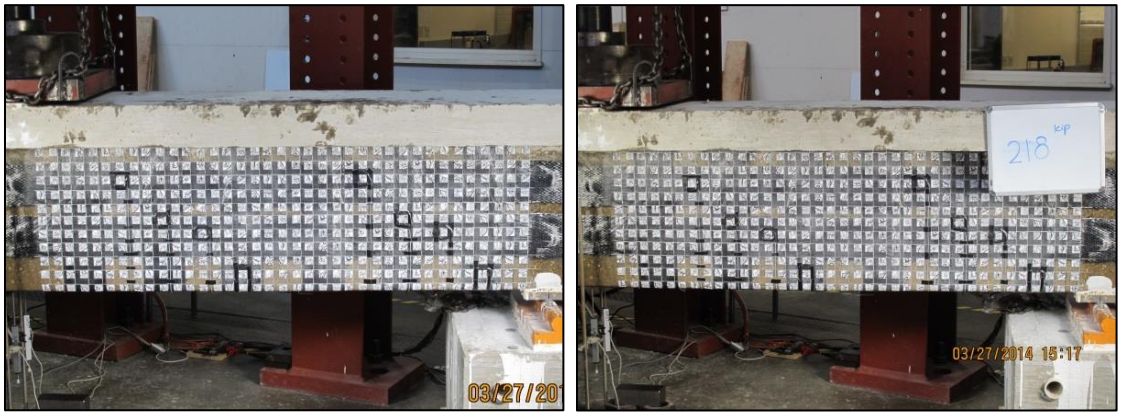

Figure 4-78: left (before), right (after) loading of 8-3-Bi-S

The applied load versus displacement curve for *8-3-Bi-S* is plotted in Figure 4-79. The mid-span displacement corresponding to the maximum applied load was 0.58-in. The applied shear force versus shear strain is provided in Figure 4-80.

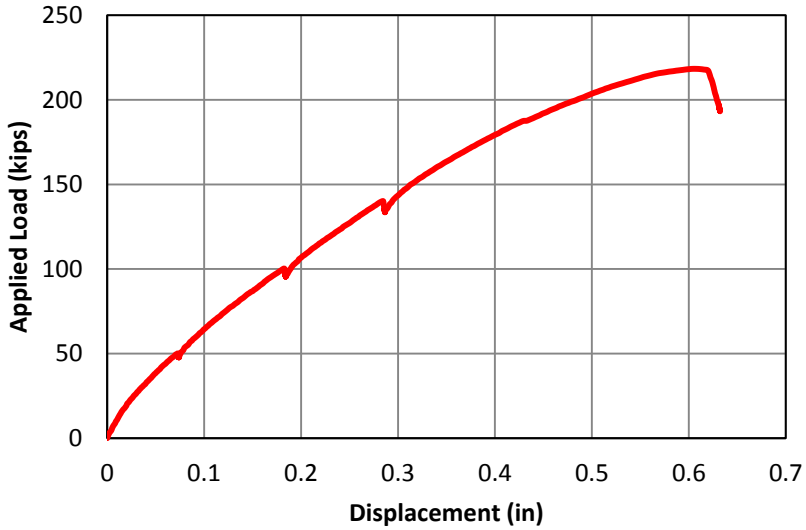

Figure 4-79: Load-displacement curve of 8-3-Bi-S

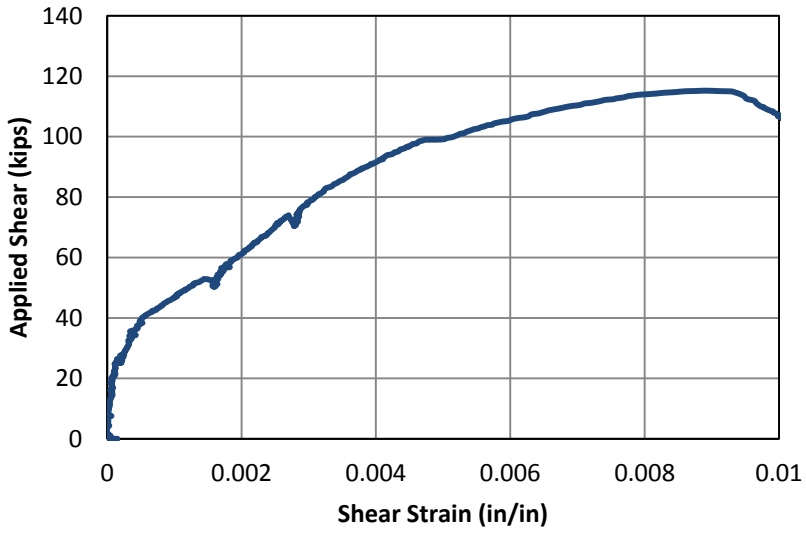

Figure 4-80: Shear deformation cure of 8-3-Bi-S

Concrete cracking was marked during the course of testing. A sketch of the cracking pattern of *8-3-Bi-S* can be seen in Figure 4-81 and Figure 4-82.

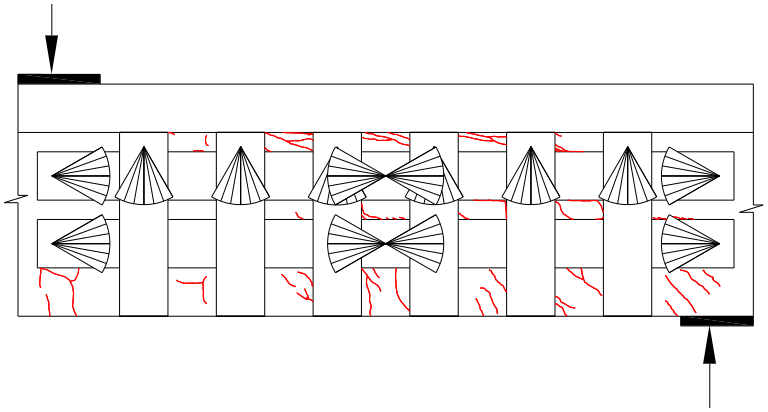

Figure 4-81: Cracking pattern of east face 8-3-Bi-S

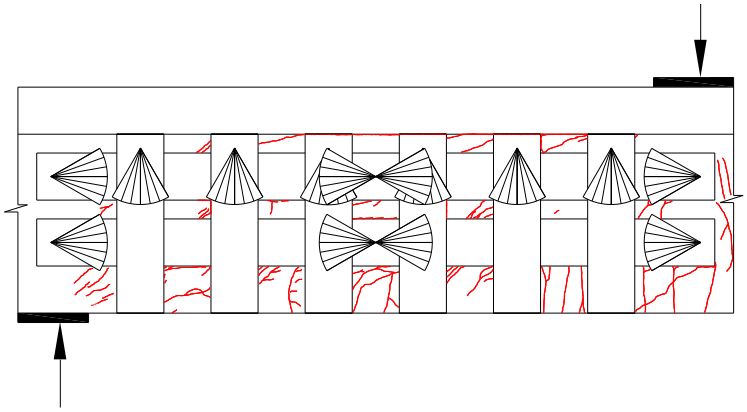

Figure 4-82: Cracking pattern of west face 8-3-Bi-S

At the initial loading, small vertical flexural-shear cracks initiated on the lower side of the web after reaching an applied load of approximately 50-kips (Figure 4-83(a)). At an applied load of approximately 100-kips, diagonal shear cracks were observed on the middle portion of the web (Figure 4-83(b)). More diagonal cracks were observed at an applied load of 140-kips (Figure 4-83(c)). As the applied load increased, shear cracks

continued propagating toward the web-flange interface. This resulted in a principal crack that crossed the web-flange interface.

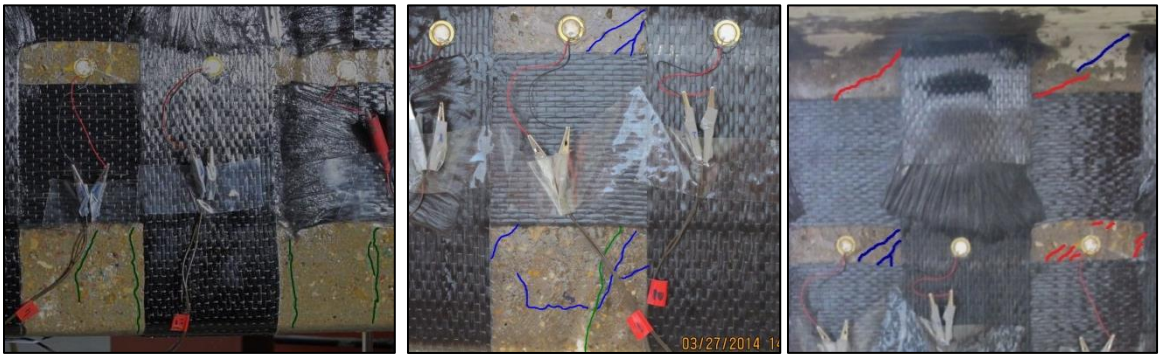

(a) 50-kips (green) ***(b) 100-kips (blue)*** ***(c) 140-kips (red)***

Figure 4-83: Development of cracks in 8-3-Bi-S

Neither CFRP strip rupture nor anchor rupture was observed in this test. However, both the minor cracks around CFRP strips and the major crack at the web-flange interface led to a failure of the web directly behind the CFRP anchor Figure 4-84.

Figure 4-84: Failure mode of 8-3-Bi-S

Several strain gauges monitored the strains in the steel stirrups and the CFRP strips. . Based on the CFRP strain gauges, the maximum strain recorded in the vertical CFRP strips was 0.009 in vertical strip #5 (second vertical strip from the reaction). This strain was reported at the maximum applied load. As can be seen in Figure 4-85, the

vertical strips started carrying load when the diagonal shear cracking started to form between 50-kips and 100-kips.

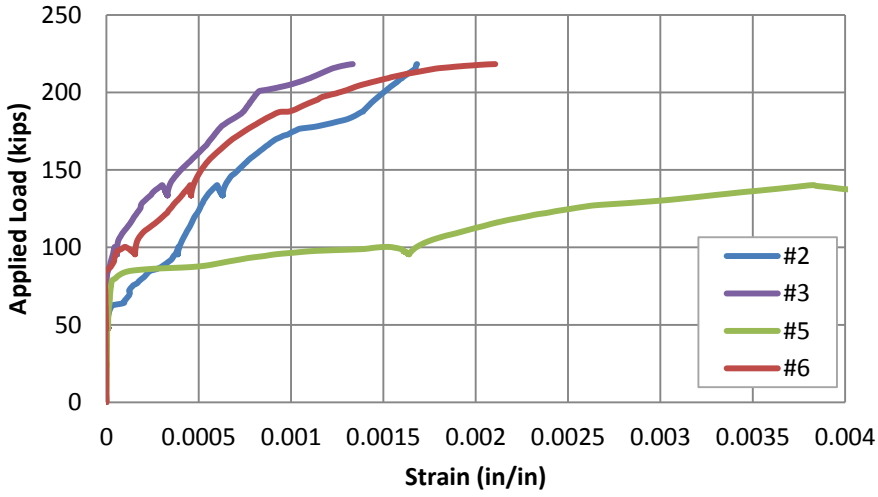

Figure 4-85: Applied load vs maximum strain in vertical strips for 8-3-Bi-S

In addition to the aforementioned conventional strain gauges, strains in the vertical CFRP strips at different loading stages were recorded using data from the UTVS (refer to 3.5.3). The location of the targets selected to measure the strain in the vertical strips and the strain variations during the loading are presented in Figure 4-86.

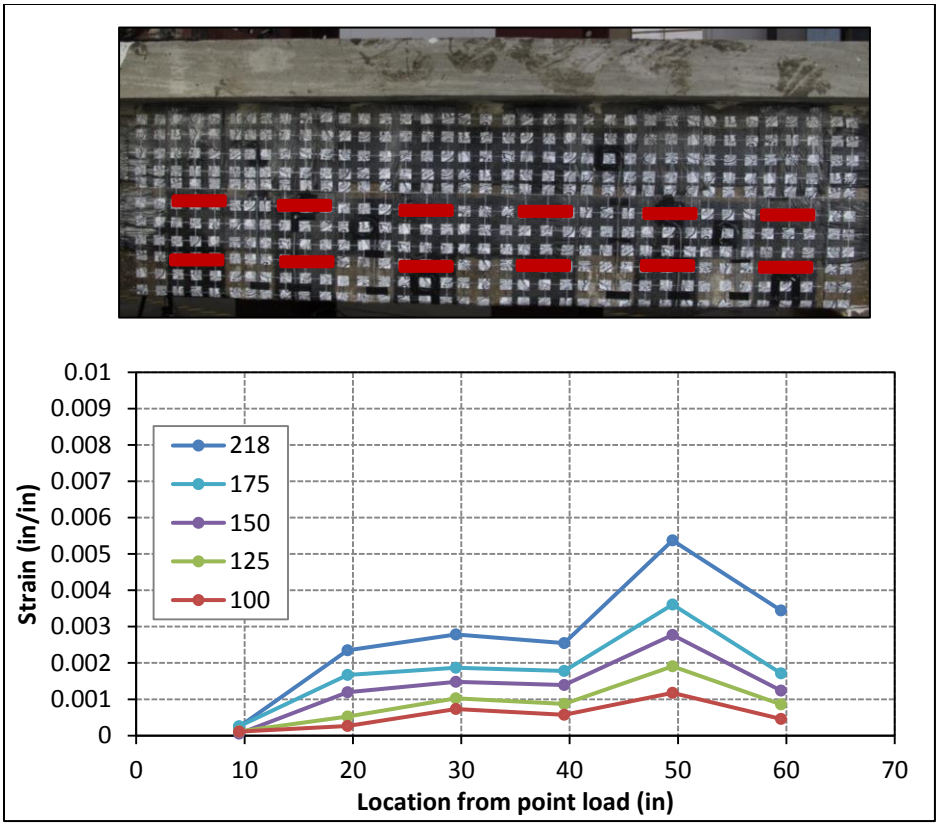

Figure 4-86: Strains in vertical strips at different loading stages of 8-3-Bi-S

The strain reported in the steel stirrups during testing is shown in Figure 4-87. The transverse reinforcement started yielding at a shear force of 73-kips (applied load of 138-kips). All measured strains within the test region were above yield except at the gauge on the stirrup closest to the support (A2)

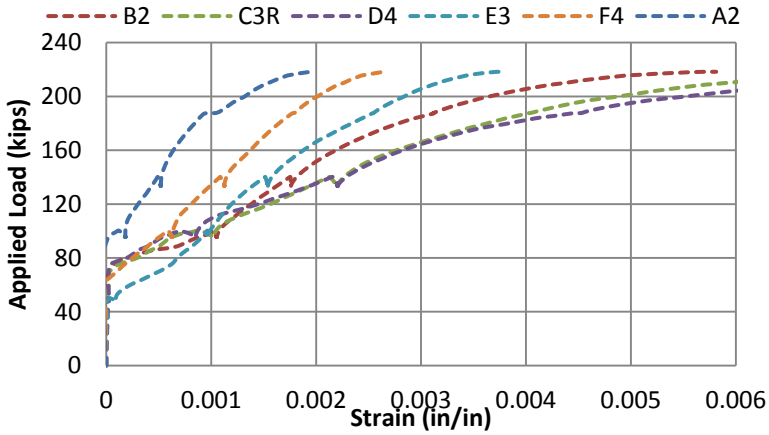

Figure 4-87: Applied load versus maximum strain in stirrups for 8-3-Bi-S

Strains in the steel stirrups during the loading of *8-3-Bi-S* are shown in Figure 4-88.

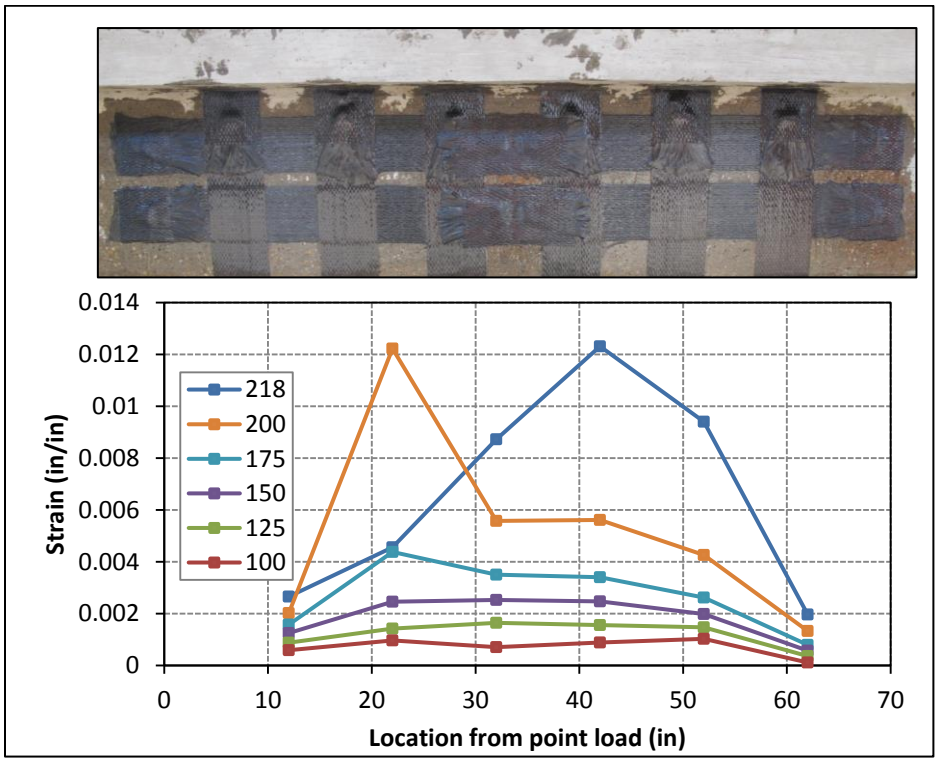

Figure 4-88: Strains in steel stirrups at different loading stages of 8-3-Bi-S

Strains in the stirrups and the vertical CFRP strips at various levels of applied load are reported in Figure 4-89. The x-axis represents location from point load in inches.

(a) 100-kips.

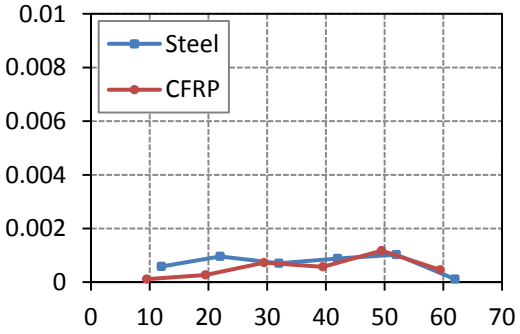

(b) 125-kips.

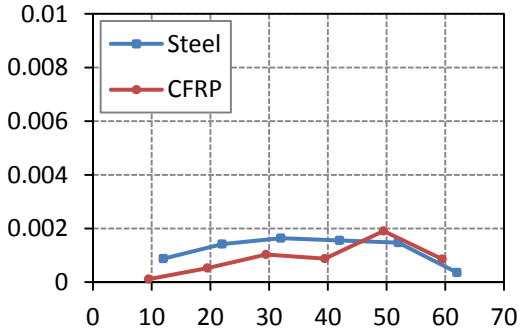

(c) 150-kips.

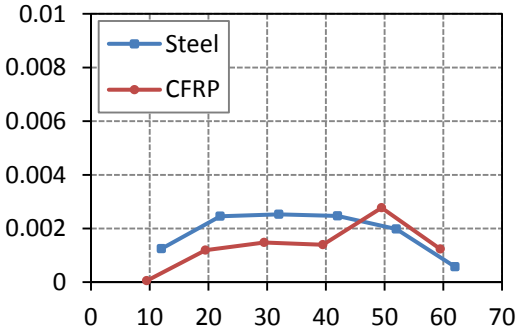

(d) 175-kips.

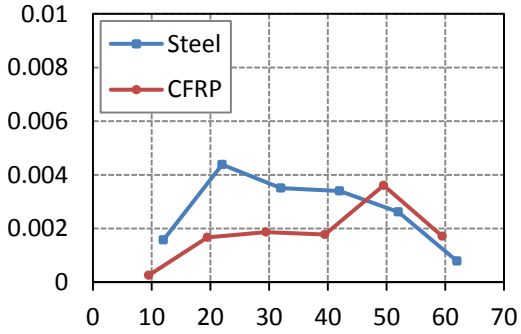

(e) 200-kips.

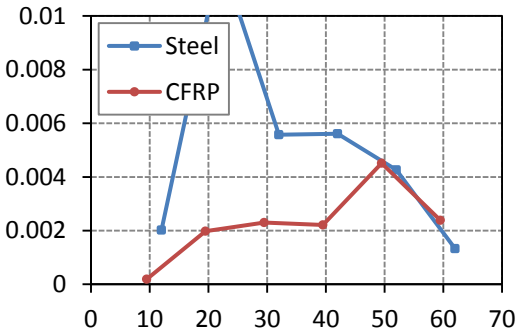

(f) 225-kips.

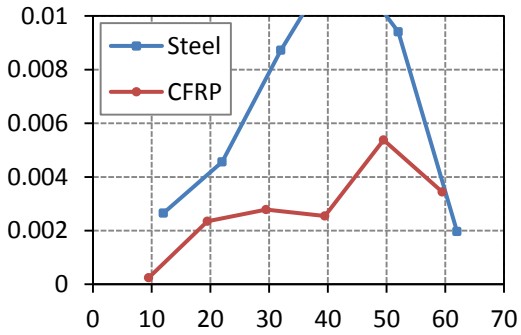

Figure 4-89: Strains in steel stirrups and CFRP strips during loading of 8-3-Bi-S

Longitudinal reinforcement did not yield during the test. The maximum strain recorded in longitudinal reinforcement was 0.0023 for the bottom layer of tension reinforcement.

Each component's (concrete, steel, and CFRP) contribution to the shear resistance of *8-3-Bi-S* was estimated (Figure 4-90).

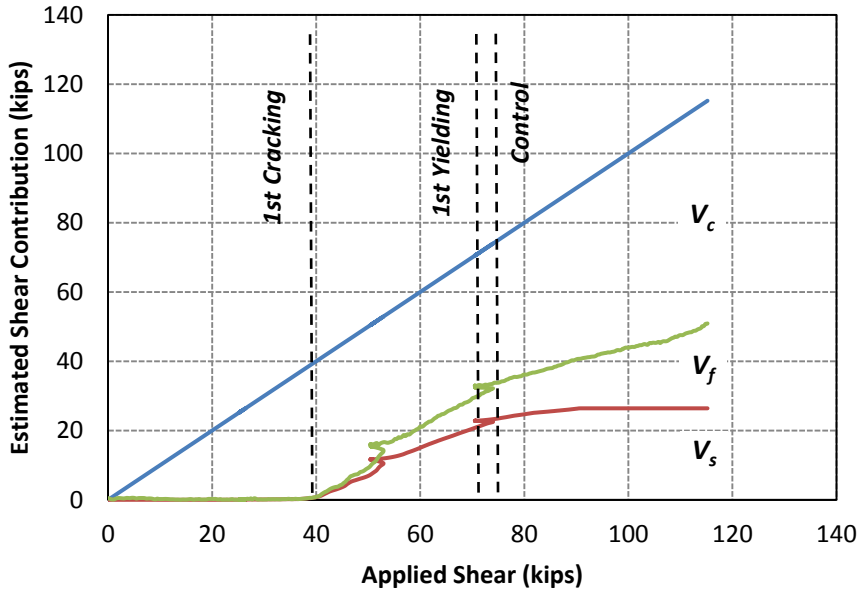

Figure 4-90: Estimated Contribution of concrete, steel, and CFRP (8-3-Bi-S)

4.4.3.4 8–3–Bi–D (Bi-directional with double layer of CFRP)

This test was conducted to examine the effect of the amount of CFRP material on the shear capacity of a thin-web specimen (8-in. web) that has been strengthened bi-directionally with CFRP strips and CFRP anchors. The specimen was strengthened vertically and horizontally with two layers of CFRP strips. The CFRP layout of this

specimen consisted of six vertical strips and two horizontal strips as an external strengthening reinforcement to form the bi-directional CFRP configuration. Both end-anchorage and middle-anchorage consists of double CFRP anchors. Vertical strips were anchored with double end-anchors, while horizontal strips were anchored with double end- and double middle-anchors. The CFRP layout for this test specimen is shown in Figure 4-91.

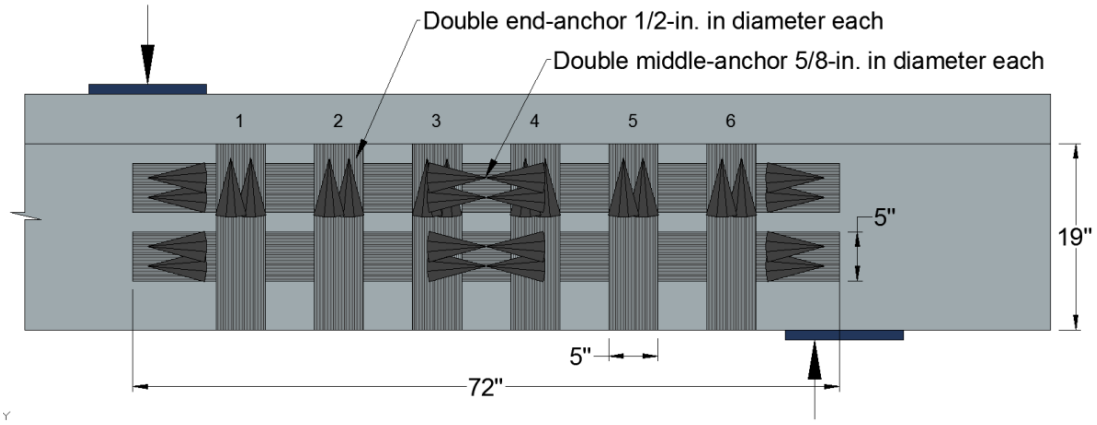

Figure 4-91: CFRP configuration of 8-3-Bi-D

Shear failure occurred at a shear force of 118-kips (applied load of 223 kips). Photos of the test specimen before and after shear failure can be seen in Figure 4-92.

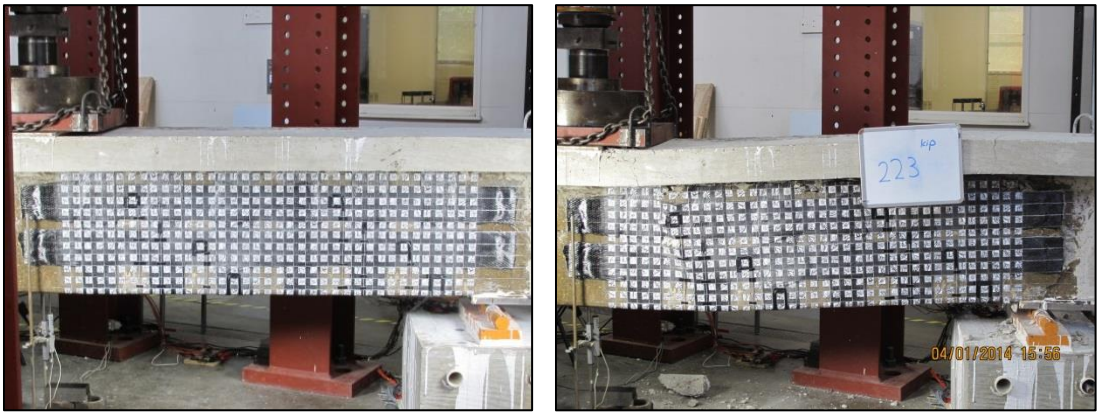

Figure 4-92: left (before), right (after) loading of 8-3-Bi-D

The large deformation of *8-3-Bi-D, as* shown in Figure 4-92 (right), is due to excessive loading and does not correspond to 223-kips (maximum applied load). The applied load versus displacement curve for *8-3-Bi-D* is plotted in Figure 4-93. Mid-span displacement corresponding to the maximum applied load was 0.6-in. The applied shear force versus shear strain is provided in Figure 4-94.

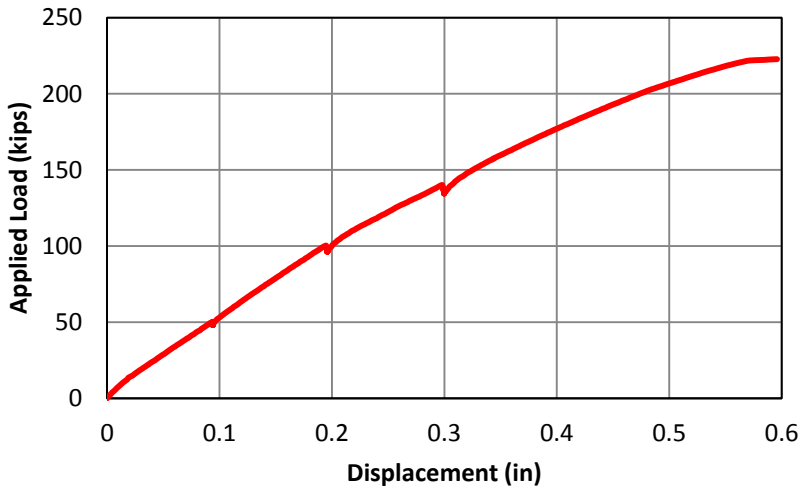

Figure 4-93: Load-displacement curve of 8-3-Bi-D

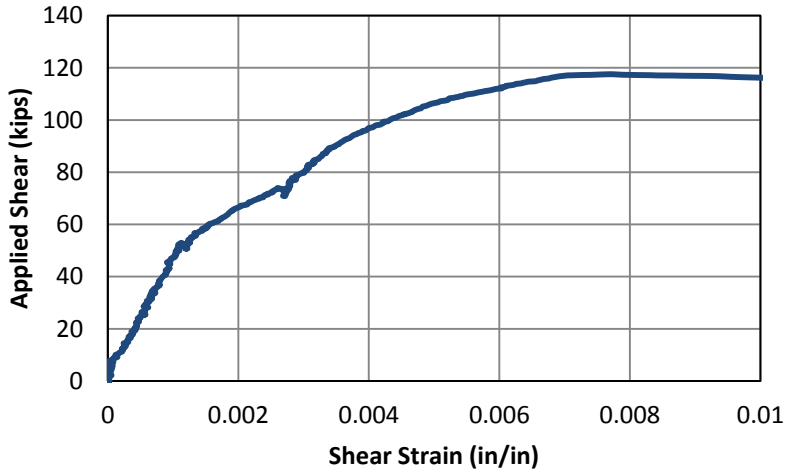

Figure 4-94: Shear deformation of 8-3-Bi-D

Concrete cracking during the course of testing was marked. Sketches of the cracking pattern during the testing of specimen *8-3-Bi-D* can be seen in Figure 4-95 and Figure 4-96.

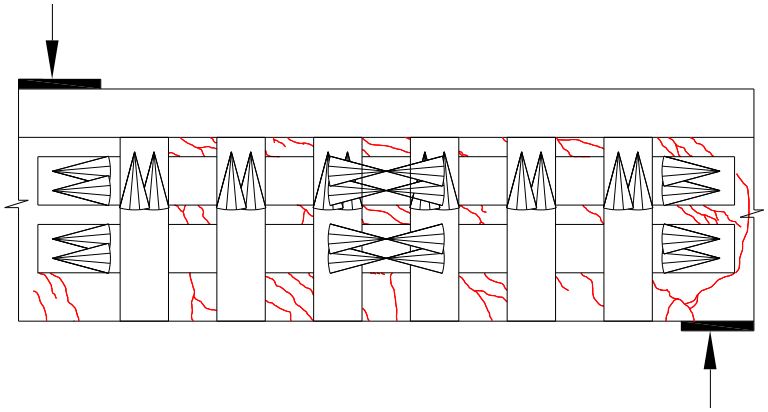

Figure 4-95: Cracking pattern of east face of 8-3-Bi-D

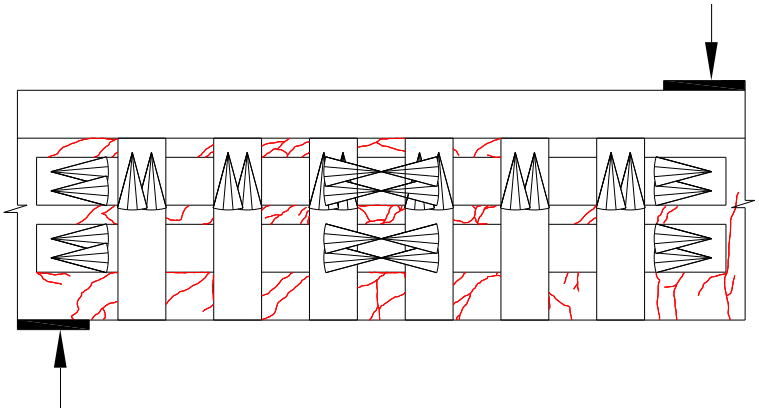

Figure 4-96: Cracking pattern of west face of 8-3-Bi-D

At initial loading, small vertical flexural-shear cracks initiated on the lower side of the web after reaching an applied load of approximately 50-kips. As the load was increasing, the small vertical flexural cracks extended at an incline, forming diagonal cracks. At an applied load of approximately 100-kips, little diagonal shear cracks were observed on the web (Figure 4-97). More diagonal cracks were observed at the upper

portion of the web (mainly towards the flange-web interface) at an applied load of 140-kips. As the applied load continued to increase, shear cracks propogated toward the web-flange interface.

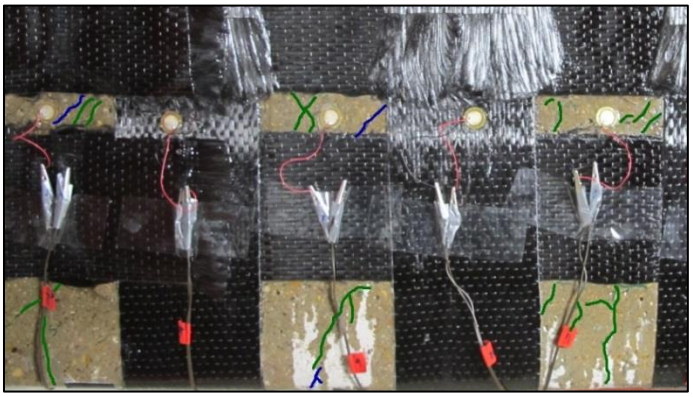

Figure 4-97: Cracking at initial loading (up to100-kips.) of 8-3-Bi-D

As in prior tests, neither CFRP strip rupture nor anchor rupture was observed. However, both the minor cracks around the CFRP strips and the major crack at the web-flange interface led to a failure of the web directly behind the CFRP anchor. Figure 4-98 shows the failure mode of *8-3-Bi-D*, which was due to loading the specimen well beyond its capacity.

Figure 4-98: Failure mode of 8-3-Bi-D due to extreme loading

Several strain gauges monitored the strains in the steel stirrups and the CFRP strips. The maximum strain recorded in the vertical CFRP strips was 0.006 in vertical strip #5 (second vertical strip from the reaction). This strain was reported at the maximum applied load. As can be seen in Figure 4-99, vertical strips started carrying the load when the diagonal shear cracking started to form between 100-kips and 140-kips.

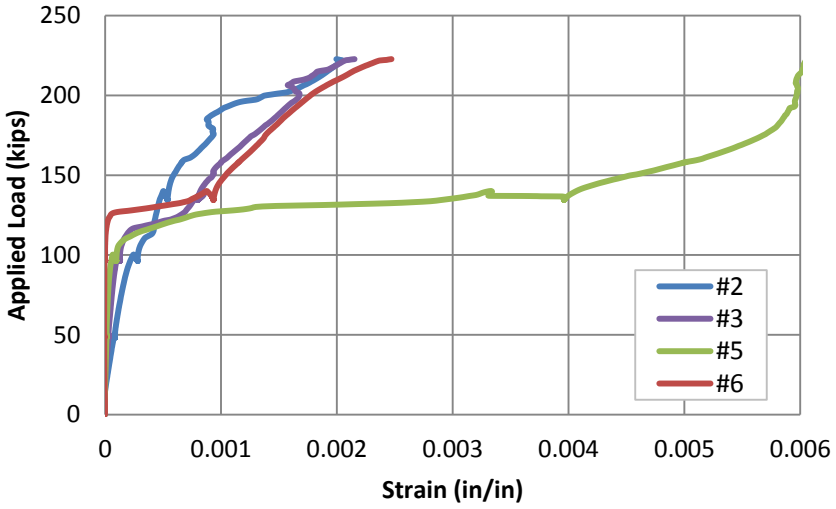

Figure 4-99: Applied load versus maximum strain in vertical strips of 8-3-Bi-D

Strains in the vertical CFRP strips at different loading stages were recorded using data from UTVS (refer to 3.5.3). The location of the targets selected to measure the strain in the vertical strips and the strain variations during the loading of *8-3-Bi-D* are presented in Figure 4-100. The strains in the steel stirrups during the loading of *8-3-Bi-D* were recorded (Figure 4-102).

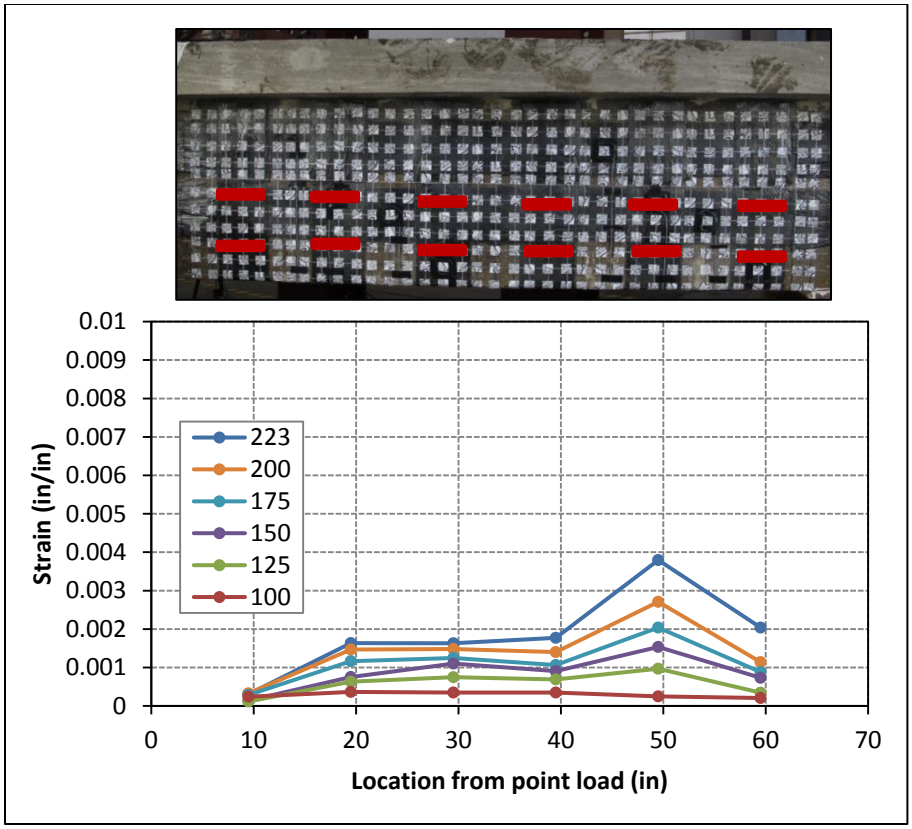

Figure 4-100: Strains in vertical strips at different loading stages of 8-3-Bi-S

The maximum strain recorded in the steel stirrups at different loading stages is shown in Figure 4-101. The internal transverse reinforcement started yielding at a shear force of 76-kips (applied load of 144-kips). All measured strains within the test region were above yield except at the gauge on the stirrup closest to the support (A2)

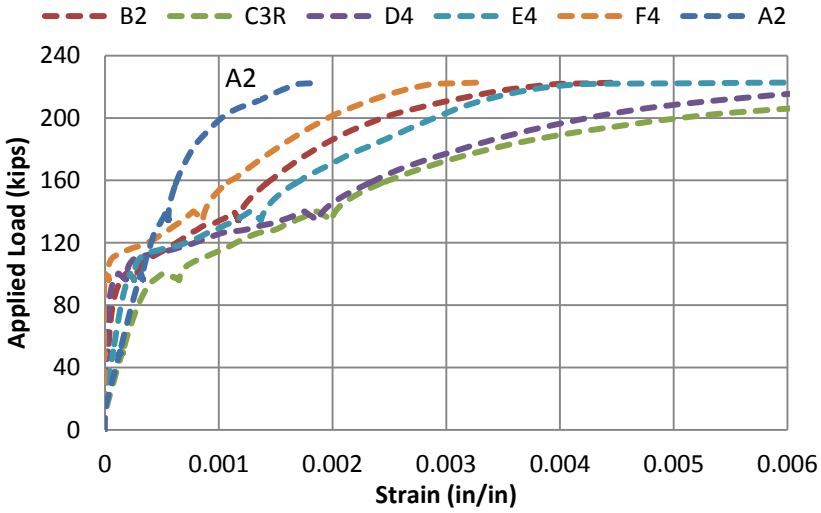

Figure 4-101: Applied load versus maximum measured strain in stirrups for 8-3-Bi-D

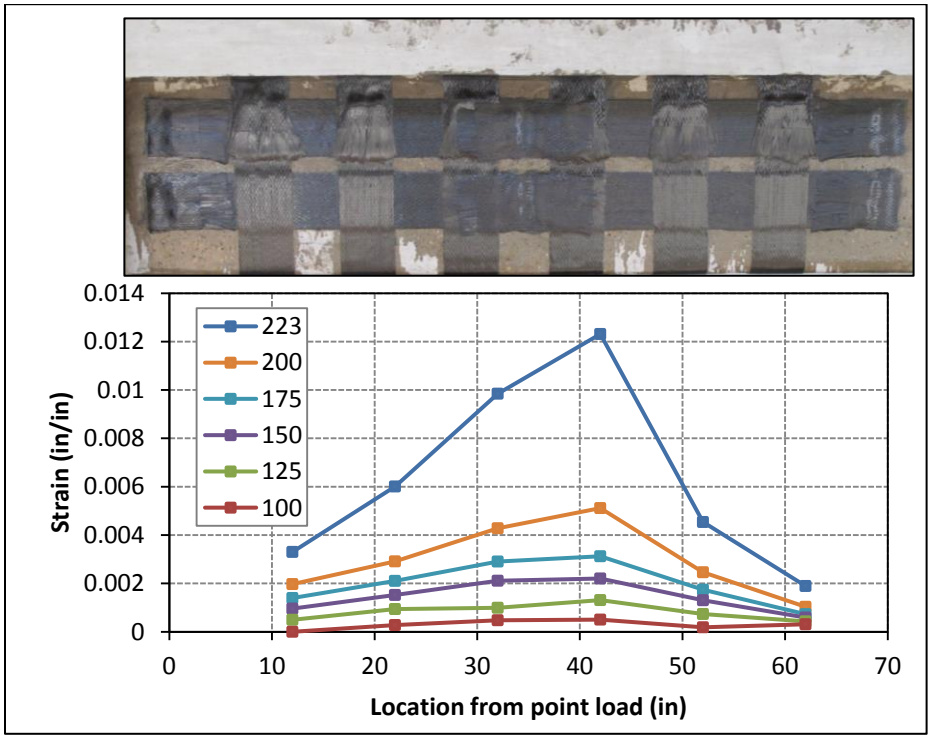

Figure 4-102: Strains in steel stirrups at different loading stages of 8-3-Bi-D

Strains in the steel stirrups and the vertical CFRP strips at various levels of applied load are reported in Figure 4-103. The x-axis represents location from point load in inches.

(a) 100-kips.

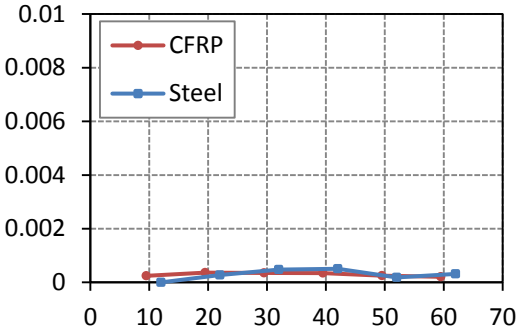

(b) 125-kips.

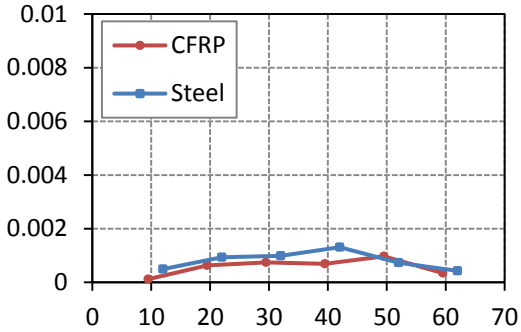

(c) 150-kips.

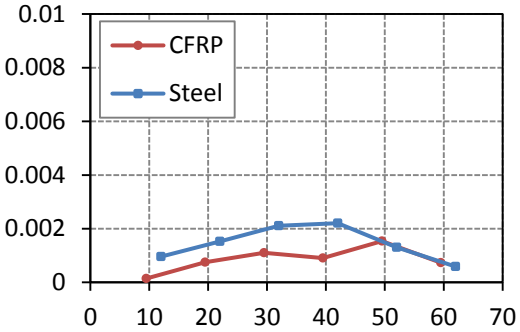

(d) 175-kips.

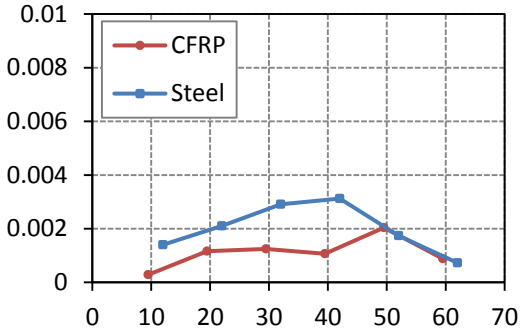

(e) 200-kips.

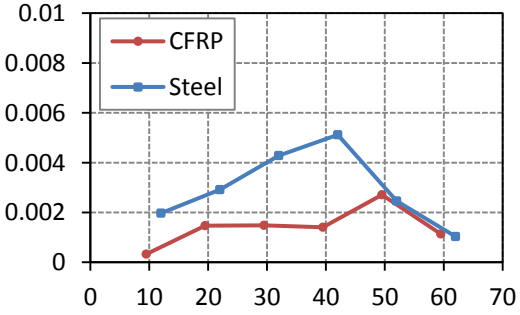

(f) 223-kips.

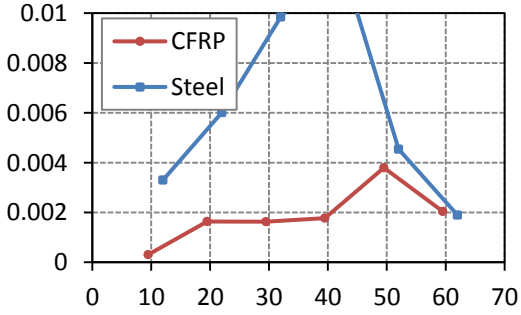

Figure 4-103: Strains in steel stirrups and CFRP strips during loading of 8-3-Bi-D

Longitudinal reinforcement did not yield during the test. The maximum strain recorded in longitudinal reinforcement was 0.0024 for the bottom layer of tension reinforcement.

The contribution of each component (concrete, steel, and CFRP) to the shear resistance of *8-3-Bi-D* was estimated (Figure 4-104).

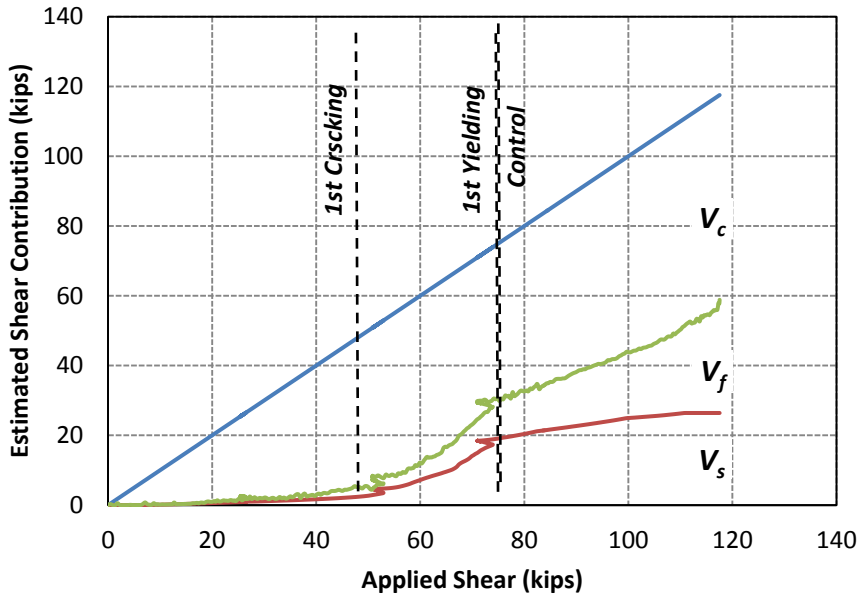

Figure 4-104: Estimated Contribution of concrete, steel, and CFRP (8-3-Bi-D)

CHAPTER 5
Analysis of Results

5.1 OVERVIEW

A detailed analysis of the test results presented in Chapter 4 is presented. As the test matrix of this research is tied to the results obtained from Tx-DOT Project 0-6306, the results from Tx-DOT Project 0-6306 were linked to the results from the current research.

Table 5-1: Test Matrix for T-beams

Beam	*Test No.*	*Web Width*	*Shear span-to-depth ratio*	*CFRP application*	*No. of CFRP layers*	*Test Name*
A	1	14	1.5	Bi-directional	Single	14-1.5-Bi-S
	2				Double	14-1.5-Bi-D
B	3		3	Bi-directional	Single	14-3-Bi-S
	4				Double	14-3-Bi-D
C	5	8	3	None	None	8-3-Control
	6			Uni-directional	Single	8-3-Uni
D	7			Bi-directional	Single	8-3-Bi-S
	8				Double	8-3-Bi-S

As shown in Table 5-1, for the first two beams (14-in. web) where beam (A) with a shear span-to-depth ratio (a/d) of 1.5 and beam (B) with a/d of 3, neither a control specimen nor a uni-directionally strengthened specimen were tested. However, these specimens were tested under Tx-DOT Project 0-6306 and are included in Table 5-2.

As can be seen in Table 5-2, the results from twelve tests will be analyzed and discussed in this chapter to explain the effect of the bi-directional application of CFRP strips with CFRP anchors on the shear behavior of reinforced concrete T-beams.

These twelve tests were divided into three categories according to the test parameters: 1) specimens with 14-in. webs and a/d of 1.5 (deep beam), 2) specimens with 14-in. webs and a/d of 3 (sectional beam), and 3) specimens with 8-in. webs and a/d of 3 (sectional beam). Test results from Project 0-6306 are comparable to tests conducted in this experimental program; however, specimens tested in Project 0-6306 were strengthened with CFRP material that has a thickness of 0.011-in. That particular material is not available anymore by the manufacturer and CFRP material with 0.02-in. thickness was used in current tests.

Table 5-2: Relation between current program and project 0-6306

Category	*Beam*	*Test No.*	*Concrete Compressive strength, fc' (psi)*	*Test Name*
1	***Previous 0-6306***		3300	14-1.5-Control
				14-1.5-Uni
	A	1	3200	14-1.5-Bi-S
		2		14-1.5-Bi-D
2	***Previous 0-6306***		3600	14-3-Control
				14-3-Uni
	B	3	3200	14-3-Bi-S
		4		14-3-Bi-D
3	**C**	5	2500	8-3-Control
		6		8-3-Uni
	D	7	3400	8-3-Bi-S
		8		8-3-Bi-S

5.2 SHEAR FORCE-DISPLACEMENT RELATIONSHIPS

In each category, the response of the bi-directionally strengthened specimens is compared with the uni-directionally strengthened specimens and the non-strengthened (control) specimen. Displacements were measured by averaging the displacements measured on both sides of the beams at mid-span.

Since the shear strength of a strengthened reinforced concrete member is equal to the summation of the contributions of concrete, steel and CFRP, variations in concrete compressive strength (f_c') between test specimens will directly affect the concrete contribution to the shear strength of these specimens. The variation in the test specimens' concrete compressive strength is provided in Table 5-2.

Therefore, to make a reasonable comparison between different tests in each category, variations in concrete compressive strength should be eliminated by normalizing the shear strength with respect to the concrete strength.

5.2.1 Specimens with 14-in. webs and a/d of 1.5 (deep beams)

Specimens in the first category are classified as deep beams. The shear failure mechanism of a deep beam is usually controlled by the crushing of the concrete strut that forms between the point load and the support. As a result, normalizing the shear strength of these specimens with respect to the compressive strength of the concrete (f_c') is more appropriate for the shear failure mechanism. Since the variation in concrete compressive strength between test specimens in this category is negligible (100-psi.), normalizing the shear capacity by the compressive strength of the concrete (f_c') or the tensile strength of the concrete ($\sqrt{f_c'}$) led to similar trends, even though normalizing by the compressive strength is more appropriate than normalizing by the tensile strength of concrete. The normalized shear capacities of specimens in the first category are presented in Table 5-3.

Table 5-3: Test results of 14-in. web specimens with a/d of 1.5

Test No.	Test Name	Shear Capacity V_{max} (kips)	Maximum Normalized Shear $\frac{V_{max}}{f_c'.b_w.d}$ (kips)	Shear Strength Gain based on f_c'	Maximum Normalized Shear $\frac{V_{max}}{\sqrt{f_c'}.b_w.d}$ (kips)	Shear Strength Gain based on $\sqrt{f_c'}$	Displacement at peak capacity (in)
Previous 0-6306	14-1.5-Control	233	0.246	0%	14.1	0%	0.27
	14-1.5-Uni	264	0.279	13%	16.0	13%	0.48
1	14-1.5-Bi-S	259	0.284	15%	16.1	14%	0.31
2	14-1.5-Bi-D	255	0.280	14%	15.8	12%	0.36

The normalized shear strength versus the displacement under the point load for the control and the strengthened specimens in Category 1 are presented in Figure 5-1.

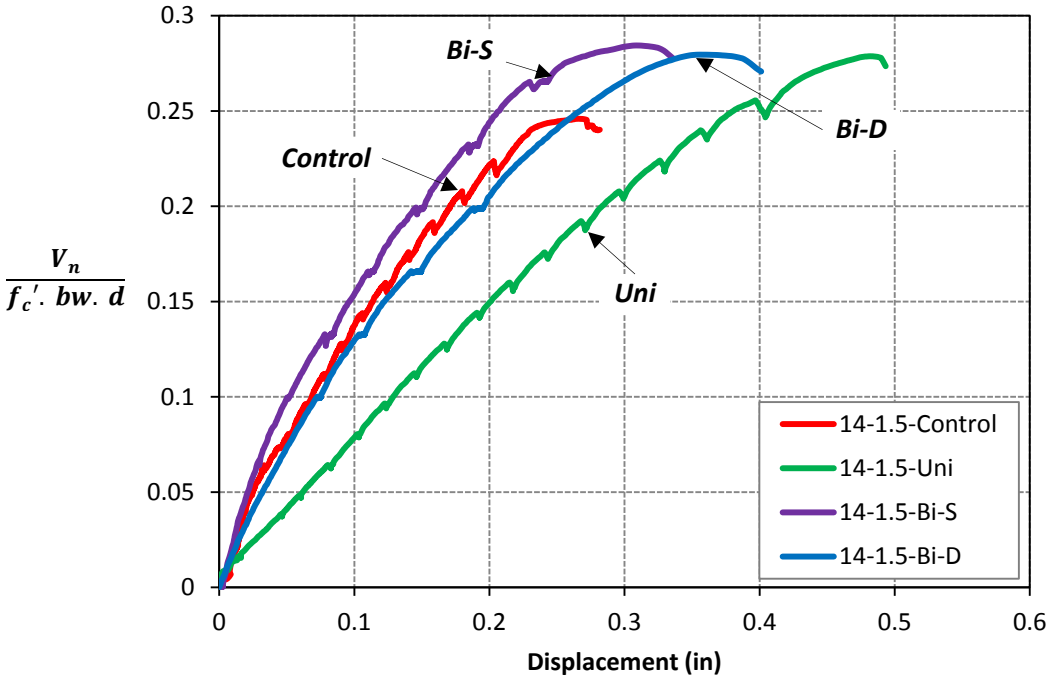

Figure 5-1: Normalized shear versus displacement curve for 14-in. web beams with a/d of 1.5

The initial stiffness of all test specimens is almost identical except for specimen *14-1.5-Uni*. The low stiffness of that specimen is attributed to the fact that this span experienced some cracking while testing the other shear span of the beam as test *14-1.5-control*. It is also important to note that *14-1.5-Uni* was strengthened with CFRP strips and anchors after *14-1.5-Control* was tested. The CFRP strengthening system has a negligible effect on the stiffness of deep reinforced concrete members. It is also shown that all strengthened specimens had slightly higher strength and deformation at peak load than the control specimen. Nevertheless, the increase is minimal overall.

With a shear span-to-depth ratio of 1.5, the forces are directly transferred from the load point to the closest reaction through a compression strut. Therefore, the shear failure mechanism is controlled by crushing of concrete in the strut or node close to the loading or reaction points. The failure mechanism of the two tests conducted in this series was a combination of crushing of concrete on the strut and at the face of the node, as shown in Figure 5-2.

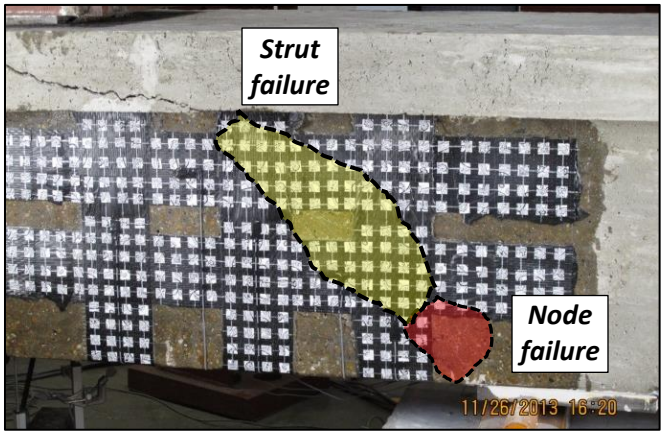

Figure 5-2: Failure of 14-1.5-Bi-S

After the node failure on *14-1.5-Bi-S*, the steel plate was moved closer to the vertical strip closer to the support to allow the CFRP strip to provide additional confinement to the nodal zone in *14-1.5-Bi-D*. As a result, crushing failure of the strut was observed just before the vertical strip, as illustrated in Figure 5-3.

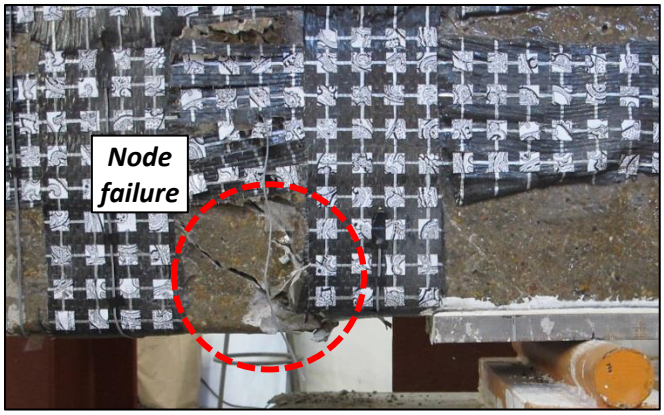

Figure 5-3: Failure of 14-1.5-Bi-D

Since the shear capacities of the deep members depend primarily on the concrete compressive strength and not on the transverse reinforcement, the amount of internal reinforcement (stirrups) or external reinforcement (CFRP) will have a small effect on the shear capacities of these specimens.

All specimens in this category were provided with steel stirrups spaced at 4-in. This closely spaced transverse reinforcement provided sufficient confinement for the test specimens and enhanced the shear strength of the control specimen to $14\sqrt{f_c'}.b_w.d$ (Figure 5-4). The ACI Code 318-11 limit for the shear strength of deep beams is $10\sqrt{f_c'}.b_w.d$. With such a high strength of the original specimen, it is unlikely that the CFRP will increase the shear capacity significantly.

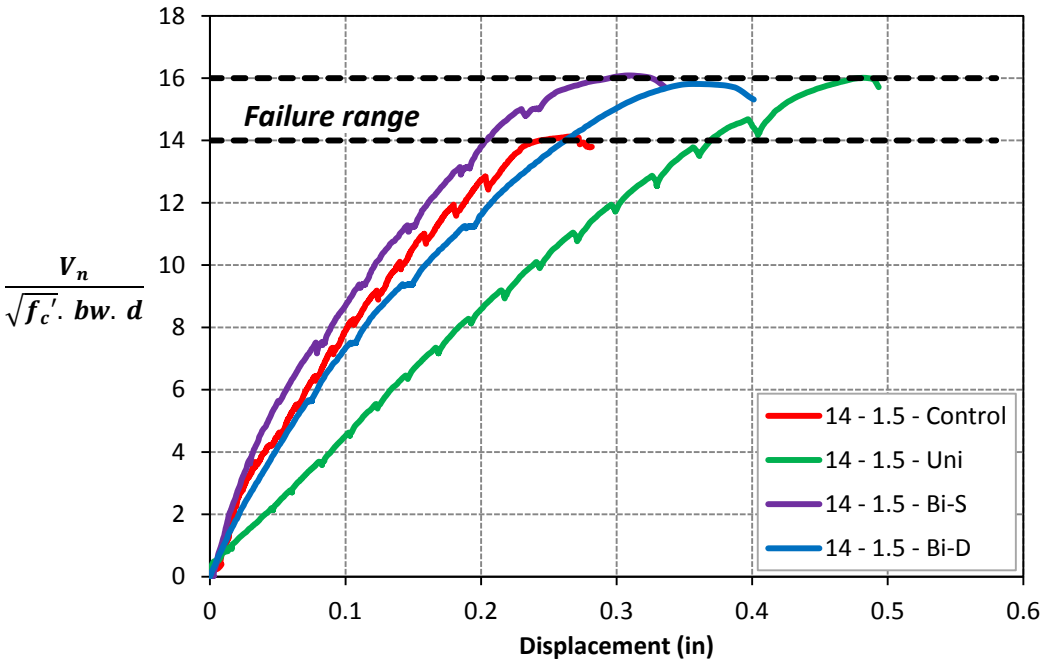

Figure 5-4: Normalized shear versus displacement curve for 14-in. web beams with a/d of 1.5

5.2.2 Specimens with 14-in. webs and a/d of 3

Specimens in the second category had 14-in. webs and were loaded with a shear span-to-depth ratio of 3 (sectional beam). Test results of this category normalized by the square root of the compressive strength of concrete $\sqrt{f_c'}$ as the shear failure mechanism is controlled by the tensile strength of concrete. The normalized shear capacities of specimens in the second category are presented in Table 5-4.

Table 5-4: Test results of 14-in. web specimens with a/d of 3

Test No.	***Test Name***	***Shear Capacity V_{max} (kips)***	***Concrete strength fc' (psi)***	***Maximum Normalized Shear $\frac{V_{max}}{\sqrt{f_c'}\cdot b_w\cdot d}$ (kips)***	***Shear Strength Gain***	***Displacement at peak capacity (in)***
Previous 0-6306	14-3-Control	105	3600	6.1	0%	0.47
	14-3-Uni	151	3600	8.8	44%	0.54
3	14-3-Bi-S	156	3200	9.7	59%	0.46
4	14-3-Bi-D	167	3200	10.4	70%	0.59

It is important to mention that specimen *14-1.5-Uni* tested in Tx-DOT Project 0-6306 failed due to the combination of CFRP strip rupture and CFRP anchor fracture. This type of failure means that the full capacity of the strengthening system was utilized. However, neither CFRP strip rupture nor CFRP anchor fracture was observed in any of the specimens strengthened bi-directionally. This might suggest that the full capacity of the strengthening system was not developed, and the shear capacity was limited by other failure states. The normalized shear strength versus the displacement under the point load for the control and the strengthened specimens in this category is presented in Figure 5-5.

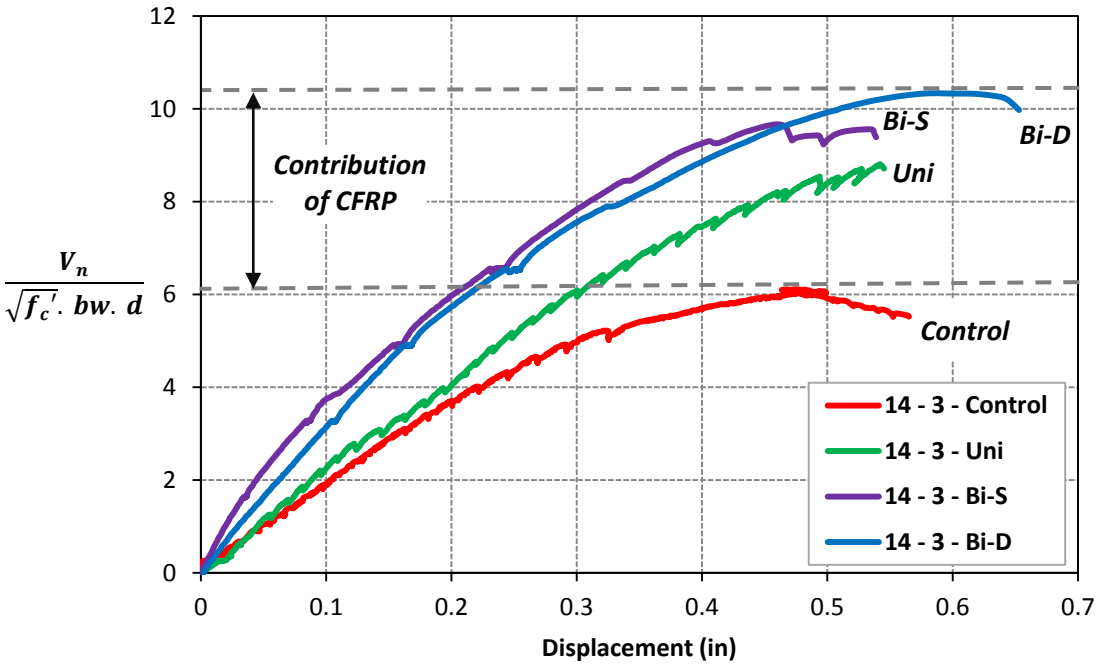

Figure 5-5: Normalized shear versus displacement curve for 14-in. web beams with a/d of 3

The shear force-displacement curves reflect typical behavior of a reinforced concrete beam failing in shear. A reduction in the slopes of the curve (stiffness) is a sign of crack propagation. As can be seen from Figure 5-5, the CFRP strengthening system has little effect on the deformation at failure of the members. In fact, the strengthened and control specimens had similar displacements.

Overall, the strengthened specimens showed higher strength and stiffness than the control test. It was observed that bi-directionally strengthened specimens had higher strength than the uni-directionally strengthened specimen. It was also observed that the bi-directionally strengthened specimens exhibited greater initial stiffness than the uni-directionally strengthened specimen. This may be attributed to the ability of bi-directional application of CFRP to restrain the crack propagation and opening of cracks.

A substantial shear strength gain was observed in the bi-directionally strengthened specimens in comparison to the control specimen. The shear strength increase in *14-3-Bi-S* and *14-3-Bi-D* was 59% and 70%, respectively. The shear capacity of *14-3-control* was $6.1\sqrt{f_c'}.b_{w.}d$, while *14-3-Bi-D* had a shear capacity of $10.4\sqrt{f_c'}.b_{w.}d$. The base shear strength of *14-3-control* was equivalent to about 50% of ACI-318 limit on the shear strength which is the sum of $3.5\sqrt{f_c'}.b_{w.}d$ for the concrete contribution and $8\sqrt{f_c'}.b_{w.}d$ for the steel contribution.

Results of the tests in this category show that a significant increase in the shear capacity of a reinforced concrete T-beam was achieved (up to 70% for *14-3-Bi-D*) when CFRP strips were applied bi-directionally. The results also indicate that CFRP shear strengthening system had a marginal effect on the deformation of a reinforced concrete T-beam.

5.2.3 Specimens with 8-in. webs and a/d of 3

Specimens in the third category had 8-in. webs and were loaded with a shear span-to-depth ratio of 3 (sectional beam). Test results of this category were also normalized by the tensile strength of concrete$\sqrt{f_c'}$. The normalized shear capacities of specimens in the second category are presented in Table 5-5.

Table 5-5: Test results of 8-in. web specimens with a/d of 3

Test No.	*Test Name*	*Shear Capacity V_{max} (kips)*	*Concrete strength fc' (psi)*	*Maximum Normalized Shear $\frac{V_{max}}{\sqrt{f_c'}.b_w.d}$ (kips)*	*Shear Strength Gain*	*Displacement at peak capacity (in)*
5	8-3-Control	76	2500	9.4	0%	0.49
6	8-3-Uni	99	2500	12.2	30%	0.64
7	8-3-Bi-S	115	3400	12.3	31%	0.60
8	8-3-Bi-D	118	3400	12.6	35%	0.60

In this category, the control and the uni-directionally strengthened specimens failed in diagonal tension. The failure of the bi-directionally strengthened specimens was due to the failure of the concrete in the web behind the CFRP anchor. The normalized shear strength versus the displacement under the point load for the control and the strengthened specimens of this category is presented in Figure 5-6.

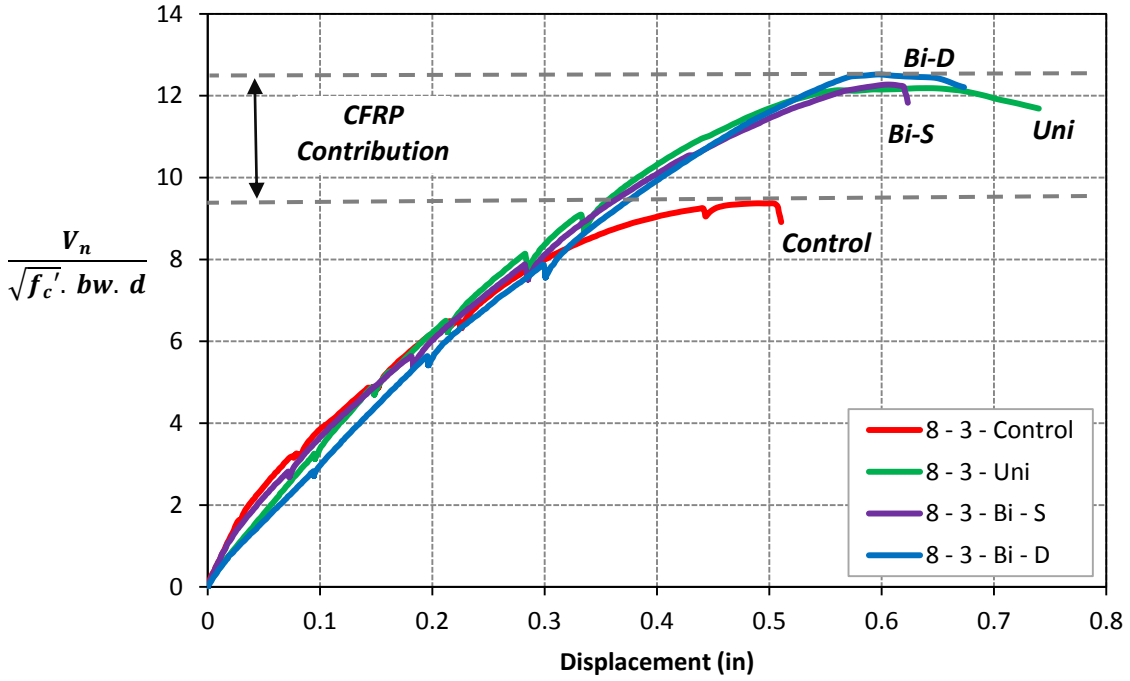

Figure 5-6: Normalized shear versus displacement curve for 8-in. web beams with a/d of 3

As can be seen from Figure 5-6, the CFRP strengthening system has a marginal effect on the deformation of the members. The difference in the mid-span displacement between the strengthened and control specimens was 0.1-in.

Overall strengthened specimens showed higher strength than the control test. In this series, both the control and the strengthened specimens exhibit similar initial stiffness. It was observed that the bi-directionally strengthened specimens did not exhibit a higher strength than the uni-directionally strengthened specimen, as in the second category (14-in. webs).

The highest shear strength gain in the 8-in. webs was 35%, as observed in *8-3-Bi-D*. It is essential to mention that even though the shear capacity gain for this category is equivalent to half the shear capacity gain observed in the 14-in. webs, this gain is considered to be significant in comparison to tests reported in the literature with the same transverse reinforcement ratio (refer to section 2.5). The lower strength gain of specimens in the third category in comparison to the second category may be attributed to the large shear strength of *8-3-Control* which is $9.4\sqrt{f_c'}.b_{w.}d$. This results in a base shear strength that is equivalent to 80% of the ACI-318 limit on the shear strength of sectional reinforced concrete members. Consequently, the increment of strength related to CFRP strengthening is smaller than with 14-in. webs.

5.3 STRAIN ANALYSIS IN BI-DIRECTIONAL APPLICATIONS

Strains in the transverse steel reinforcement during testing were recorded by several strain gauges, whereas strains in the CFRP strips were recorded by strain gauges and UT Vision System (UTVS). Data obtained from these measurements were used to evaluate the effect of the bi-directional CFRP strengthening system on the strains of the transverse steel. One of the observations of Tx-DOT Project 0-6306 was the delayed yielding of transverse steel in the presence of CFRP (uni-directional application).

5.3.1 Strains in transverse steel for bi-directional application of CFRP

For this research project, strain data from steel stirrups and CFRP strips with a bi-directional application of CFRP are available, it is important to examine the effect of the bi-directional application of CFRP on the strains in the steel and CFRP. It is also important to compare those strains with the ones generated in the uni-directional application of CFRP.

To achieve the aforementioned objective, the strains in the transverse steel of strengthened and non-strengthened specimens were compared. Figure 5-7 shows strain

variations in transverse steel between *14-3-Uni* and *14-3-Bi-S*. It is important to note that the recorded strains in transverse steel might not be the actual maximum strains developed in the steel depending on how far the strain gauge is located from the critical crack. Nevertheless, in most cases measured strains are reported from the strain gauges that are close to the critical crack. In all strain data, figures are presented such that the x-axis represents the distance from the applied load to where the strain was measured.

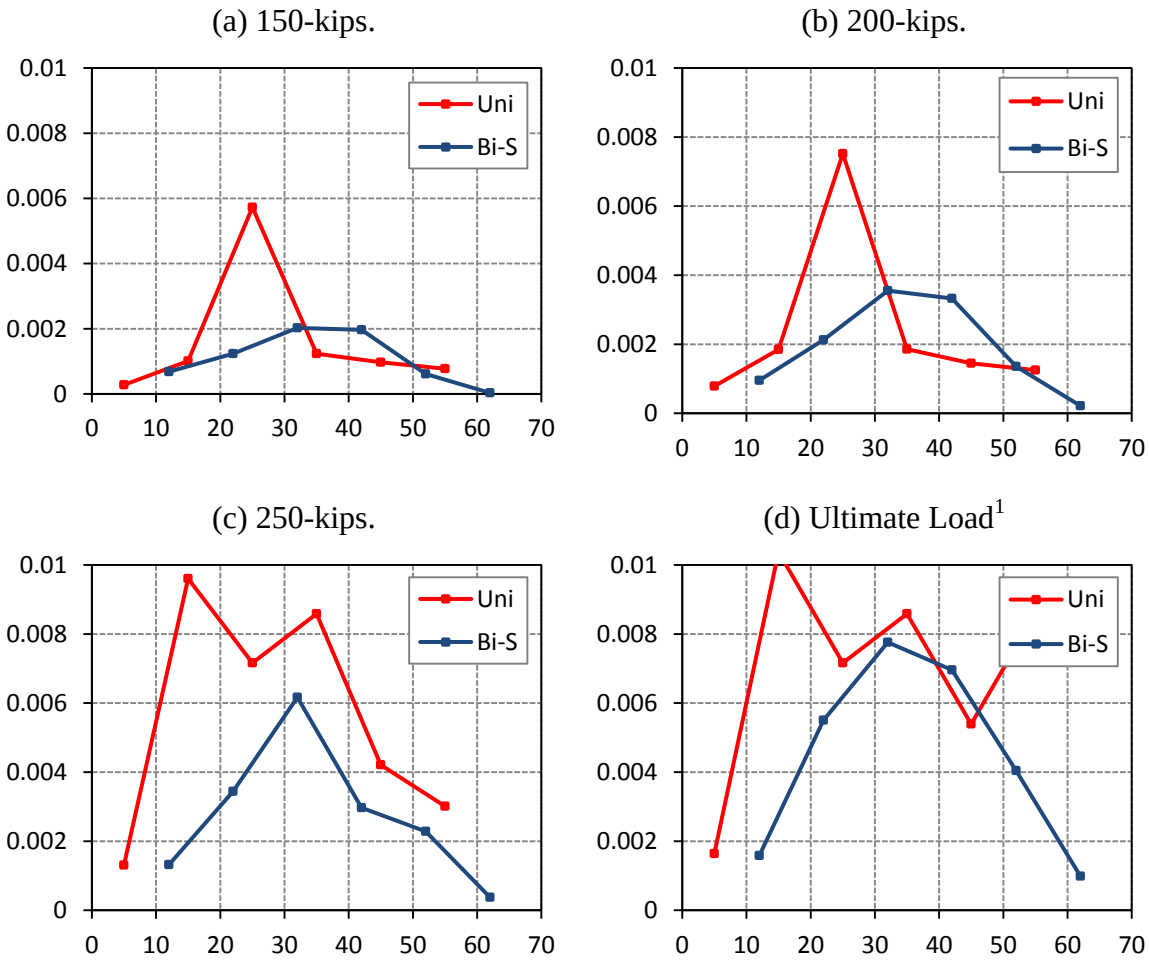

Figure 5-7: Strain variations in steel stirrups between 14-3-Uni and 14-3-Bi-S

[1] Ultimate load of *14-3-Uni* and *14-3-Bi-S* are 287-kips. and 295-kips, respectively.

Figure 5-8 shows strain variations in the transverse steel of *8-3-Control*, *8-3-Uni*, and *8-3-Bi-S*. The x-axis represents the distance from the point load in inches.

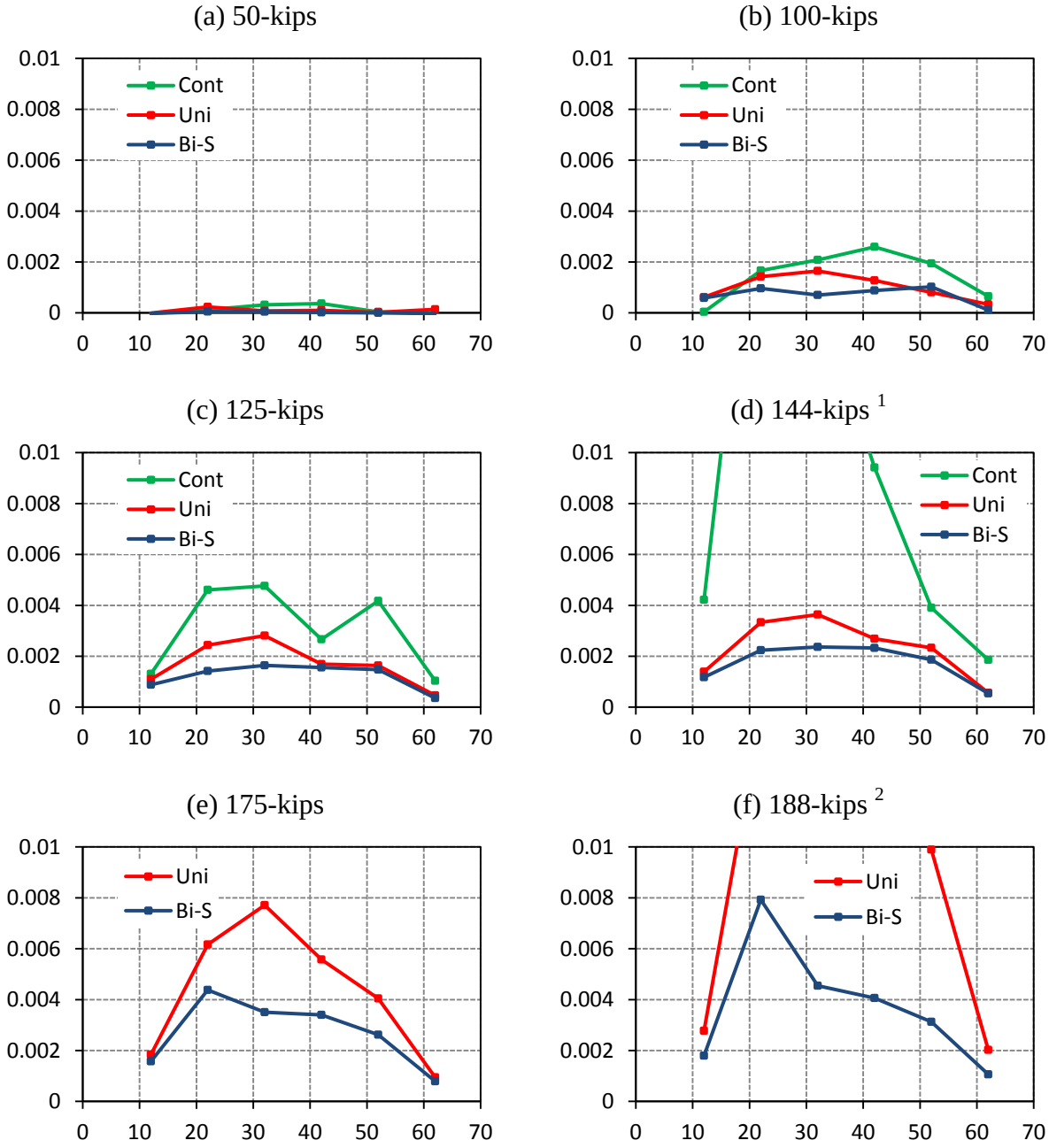

Figure 5-8: Strain variations in transverse steel of 8-3-Control, 8-3-Uni, and 8-3-Bi-S

[1]Ultimate load of 8-3-Control

[2] Ultimate load of 8-3-Uni

A reduction in the transverse steel strains was observed in bi-directionally strengthened specimens in comparison to uni-directionally specimens under the same applied load. From tests conducted on bi-directionally strengthened specimens, it was observed that most of the transverse steel within the test region and all transverse steel crossing the critical crack yielded before the ultimate load was reached. This is in agreement with assumptions made by design guidelines and code provisions. Figure 5-8 shows that yielding of transverse steel was further delayed when a bi-directional application is employed.

In order to compare the effect of the amount of CFRP material on the strains in the transverse steel, the strains in the transverse steel of specimen strengthened with a single layer of CFRP were compared to those in a specimen strengthened with double layers of CFRP. The x-axis represents the distance from the point load in inches.

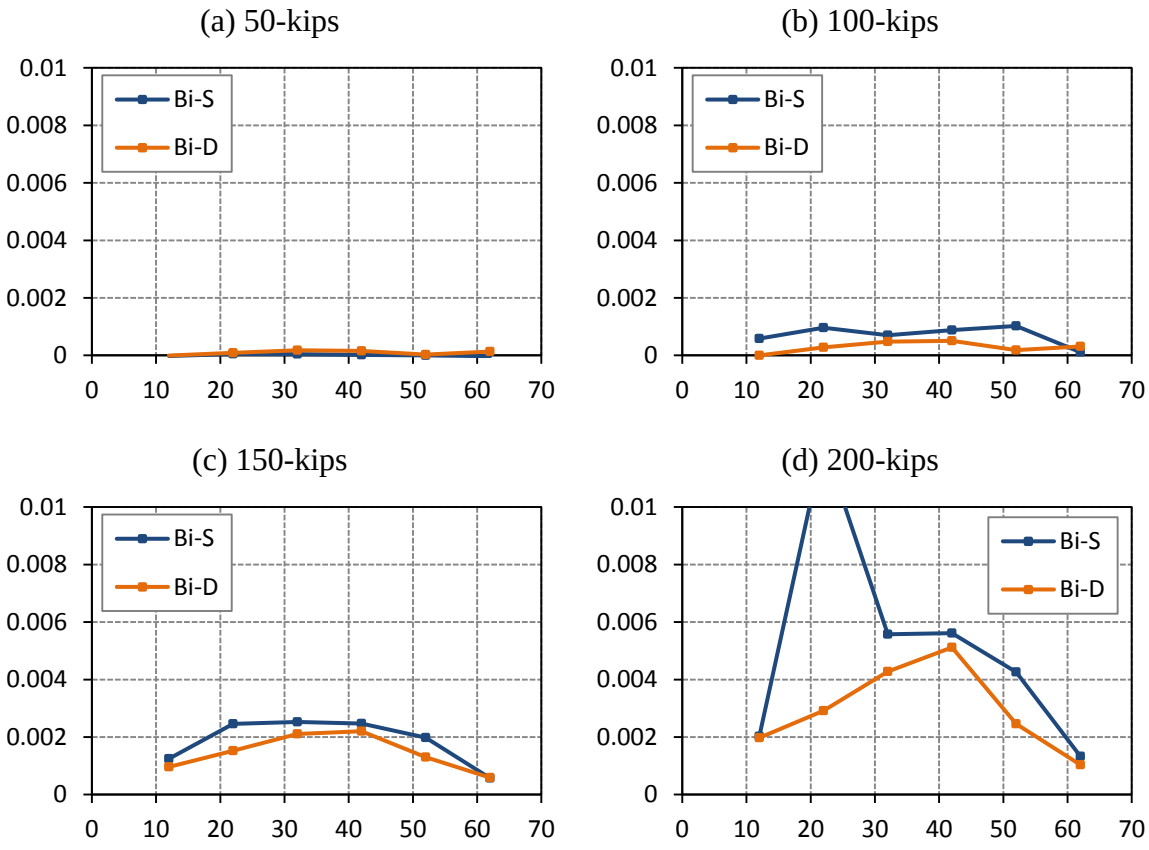

Figure 5-9: Strain variations in transverse steel of 8-3-Bi-S, and 8-3-Bi-D

Figure 5-9 indicates that increasing the amount of CFRP material in the bi-directional application of CFRP has a lesser effect on the strains in the transverse steel. It also shows that the transverse steel contribution to the shear resistance starts at the onset of diagonal cracking, as reported in Chapter 4.

5.3.2 Strains in vertical CFRP strips for bi-directional application

As discussed earlier (refer to 3.5.3), strains in CFRP strips were monitored during testing by the UTVS along with several strain gauges. To measure the axial strains in the vertical CFRP strips using UTVS, two targets located at the straight vertical gridline were selected. Targets located on the patch that covered the anchor fan, or on the boundaries between the vertical strip and the anchor fan were avoided.

Targets on the middle of the strip can be selected and assumed to represent the average strain cross the width of the specimen. However, for more accurate strain data, three pairs of targets were chosen to measure the strains between each pair, as shown in Figure 5-10.

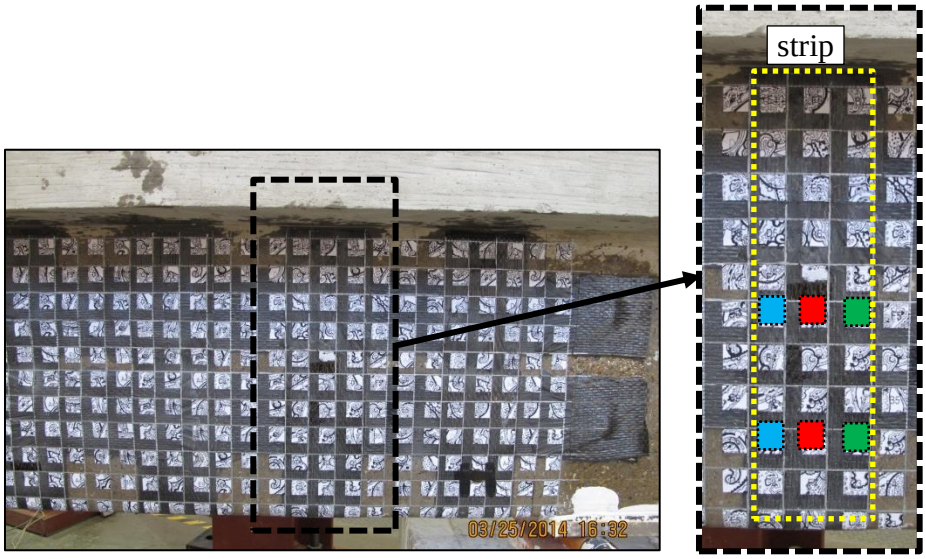

Figure 5-10: Three targets selected across the width to measure strains in vertical CFRP strips

Based on the aforementioned procedure, strains in the vertical strips were monitored during testing each specimen. Strains in the vertical strips of uni-directionally strengthened specimens were compared to those developed in the vertical strips of bi-directionally strengthened specimens. Comparing these strains provide a better understanding of the role of the horizontal strips associated with the bi-directional application of CFRP on the strains of the vertical strips. In Figure 5-11, strain variations in vertical CFRP strips of *14-3-Uni*, and *14-3-Bi-S* are compared.

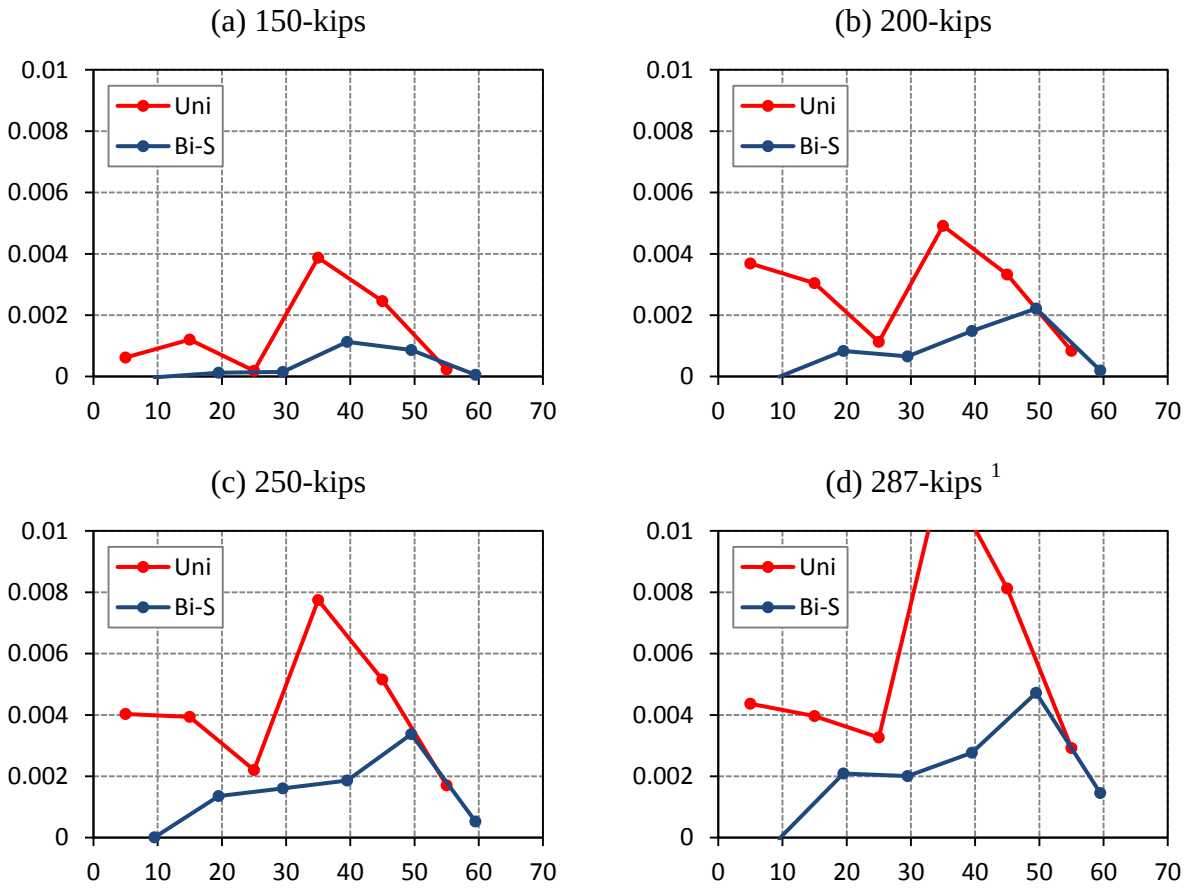

Figure 5-11: Strain variations in vertical strips of 14-3-Uni and 14-3-Bi-S

[1] Ultimate load of *14-3-Uni*
Horizontal axis represents the distance from the point load in inches.

Figure 5-12 shows strain variations in the CFRP strips of *8-3-Uni*, and *8-3-Bi-S*.

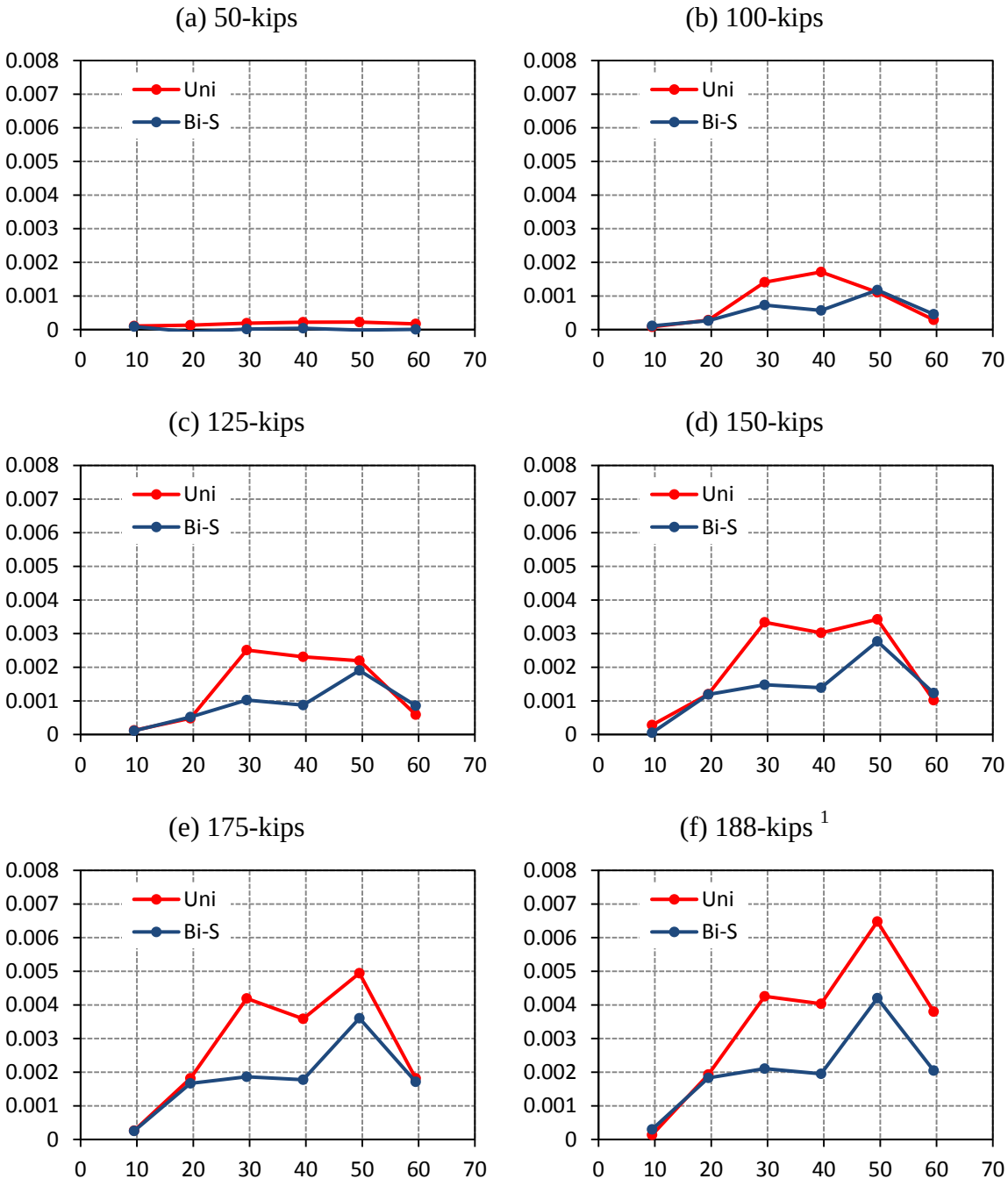

Figure 5-12: Strain variations in vertical strips of 8-3-Uni and 8-3-Bi-S

[1] Ultimate load of *8-3-Uni*

Horizontal axis represents the distance from the point load in inches.

From the strain data presented, several observations can be made concerning the effect of the horizontal CFRP strips. The strains in vertical strips of *14-3-Bi-S* are found to be lower than the strain in *14-3-Uni*. A comparison of the strains in the vertical strips of the 8-in. web test specimens shows that the vertical strips in the bi-directionally strengthened specimen experienced lower strains than in the uni-directionally strengthened specimens.

In order to compare the effect of the amount of CFRP material on the strains in the vertical strips, strains in the vertical strips of bi-directionally strengthened specimen with a single layer of CFRP were compared to the strains in a specimen strengthened with double layers of CFRP, as shown in Figure 5-13.

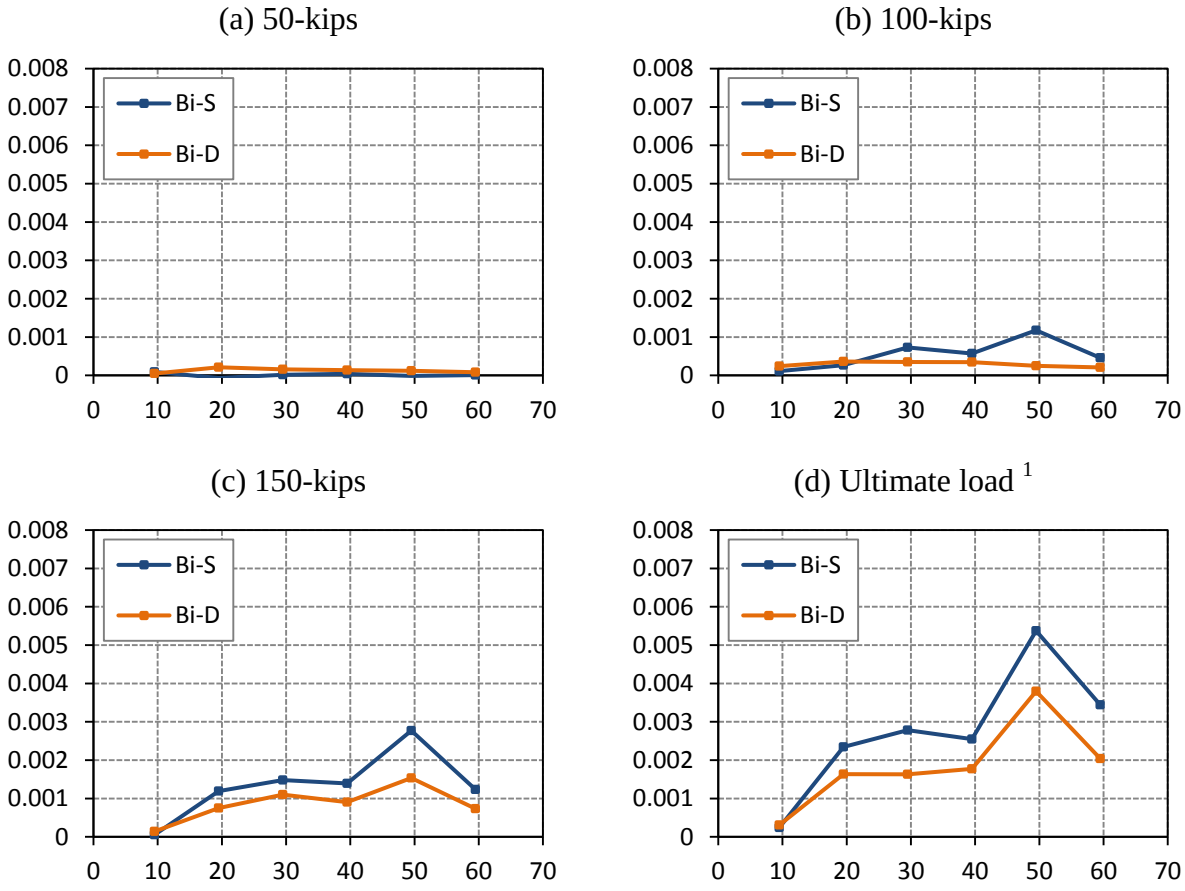

Figure 5-13: Strain variations in vertical strips of 8-3-Bi-S and 8-3-Bi-D

[1] Ultimate load for 8-3-Bi-S and 8-3-Bi-D are 218-kips. and 223-kips., respectively

Figure 5-13 shows that doubling the amount of CFRP material in the bi-directional application of CFRP resulted in a further reduction in strains experienced by vertical strips.

The interaction between the transverse steel and the vertical CFRP strips can be evaluated from data monitored during the test. Figure 5-14 shows a comparison between strains exhibited by the transverse steel and the vertical CFRP strips in the uni-directionally and bi-directionally strengthened specimen. The addition of the horizontal strips in the bi-directional application was found to reduce the strain level in the transverse steel and the CFRP. This can be attributed to the fact that horizontal strips contributed to reducing the crack width and delayed its propagation.

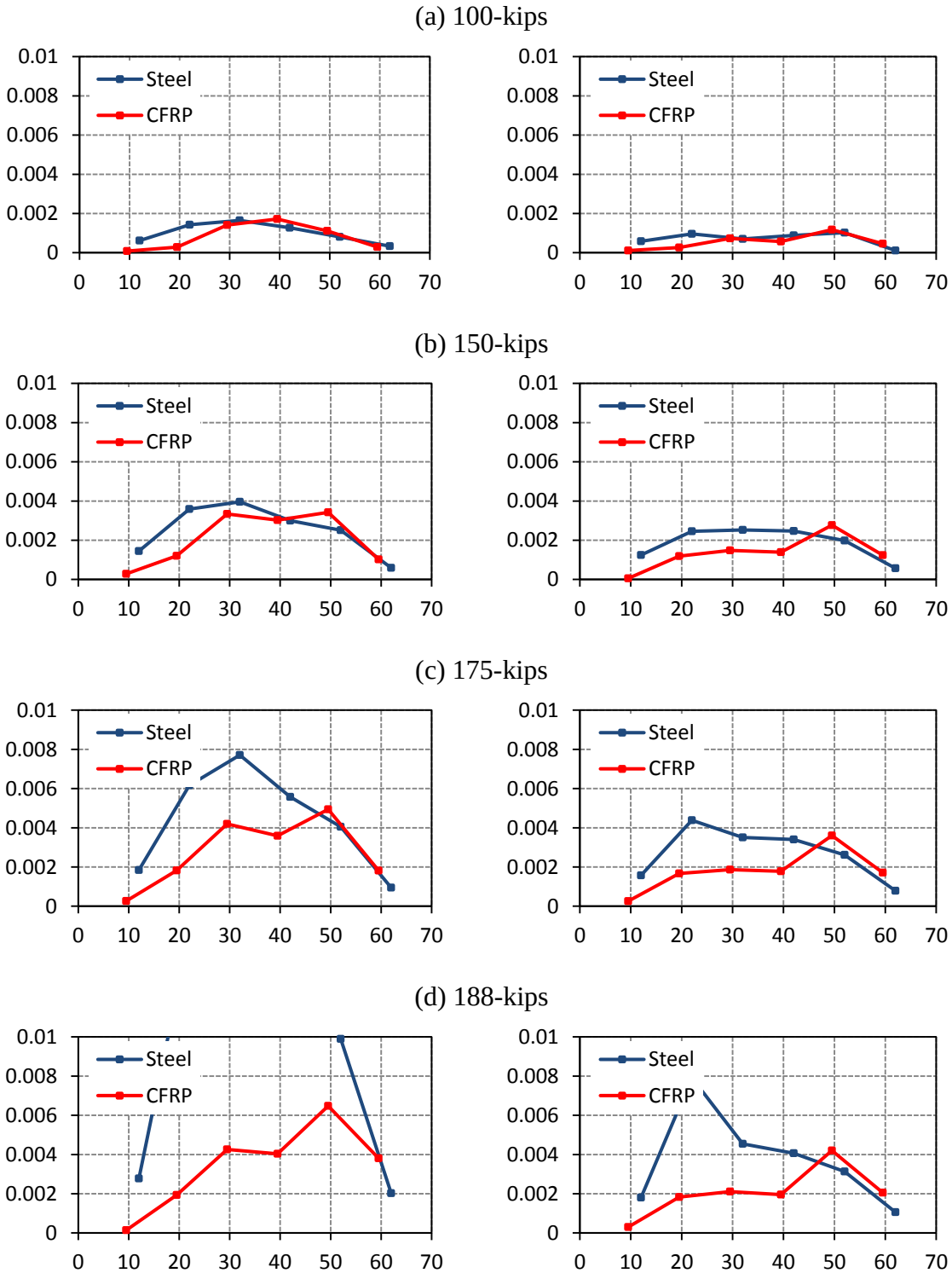

Figure 5-14: Strain in steel and CFRP of 8-3-Uni (left) and 8-3-Bi-S (right)

5.4 SHEAR CONTRIBUTION ANALYSIS OF CONCRETE, STEEL, AND CFRP

To better understand the shear contribution mechanism of the bi-directional application of CFRP, the shear contribution of each component (concrete, steel, and CFRP) was estimated and compared for all tests with a/d = 3.

To eliminate the effect of concrete compressive strength variation, the concrete contribution to the shear strength was normalized by the concrete strength of the control specimen. A normalized shear capacity was then achieved by adding the normalized concrete contribution to the steel and CFRP contributions, as shown in Equation 5-1.

$$V_{normalized} = V_c \times \frac{\sqrt{f_{c'\ control}}}{\sqrt{f_{c'\ test}}} + V_s + V_f \qquad \textit{Equation 5-1}$$

The shear contributions of transverse steel and CFRP strips were estimated based on the measured strains, while the concrete contribution was assumed as the difference between the shear strength of the beam and the steel and CFRP components. Based on this approach, the gain in the shear capacity is calculated as the difference in the shear capacity between the strengthened specimen and the control specimen.

5.4.1 Components of shear for 14-in. webs specimens with a/d of 3

The shear contribution of each component with the shear strength gain due to CFRP strengthening for 14-in. web specimens is presented in Table 5-6. Each component contribution to the shear resistance for specimens in the first category are shown in Figure 5-17.

Table 5-6: Shear contributions and strength gain for 14-in. web specimens

Specimen	*Normalized Shear Capacity*	*Steel Contribution*	*CFRP Contribution*	*Normalized Concrete Contribution*	*Shear Gain*
14-3-Control	105.3	42.4	-	62.8	0%
14-3-Uni	152.7	43.5	29.0	80.2	45%
14-3-Bi-S	161.3	39.5	27.2	94.6	53%
14-3-Bi-D	170.9	39.6	57.3	74.0	62%

A substantial gain in the shear capacity (up to 62%) was achieved in test specimen *14-3-Bi-D*. This gain is higher when compared to test results reported in the literature for specimens with the same transverse reinforcement ratio (refer to section 2.5). Most of the significant shear strength gains reported in the literature are for specimens with no or little transverse reinforcement. A comparison in the contribution of each component to the shear capacity is presented in Figure 5-15.

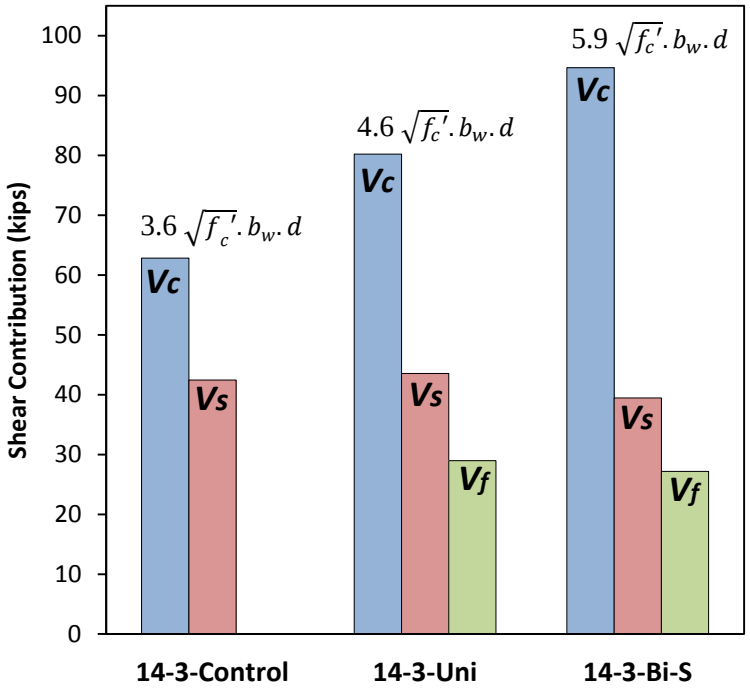

Figure 5-15: Shear contribution of each component in 14-in. web specimens

The increase in the concrete contribution observed in *14-3-Uni* and *14-3-Bi-S* is attributed to the fact that (V_c) of the control specimen was only $3.6\sqrt{f_c'}.b_w.d$ and V_n= $6.1\sqrt{f_c'}.b_w.d$, which is well below code limits. For *14-3-Uni* and *14-3-Bi-S*, the steel contribution was nearly the same but with the addition of the CFRP, the concrete contribution increased considerably and V_n= $8.9\sqrt{f_c'}.b_w.d$ and $10\sqrt{f_c'}.b_w.d$; values that approach code limits. This is in agreement with design guidelines and code provisions where shear resisted by steel (V_s) for strengthened beams is assumed to be same as for

non-strengthened beams. The shear resisted by vertical CFRP strips (V_f) in *14-3-Uni* and *14-3-Bi-S* was found to be similar. However, when double layers of CFRP are used as external strengthening, the CFRP contribution almost doubled, as can be seen in Figure 5-16.

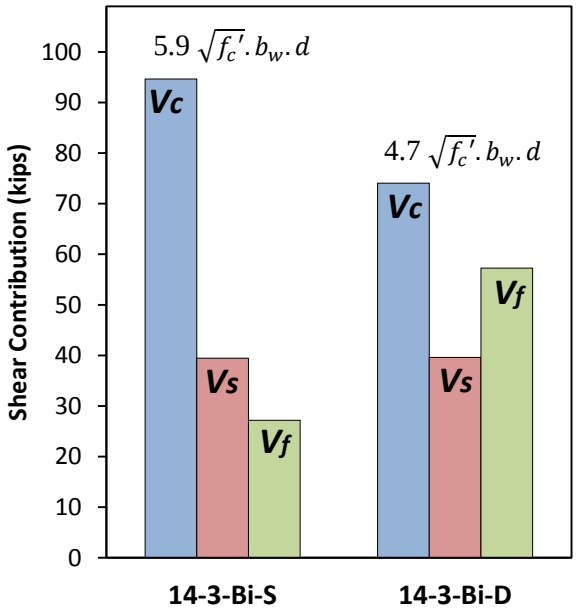

Figure 5-16: Shear contribution component of 14-3-Bi-S and 14-3-Bi-D

The additional resistance provided by the additional CFRP material led to a reduction in the concrete contribution to the shear strength. This indicates that some of the shear that was resisted by the concrete in *14-3-Bi-S* is resisted by the additional CFRP in *14-3-Bi-D*.

Figure 5-17 shows the estimated shear contribution of each material for specimens with 14-in.webs. The cracking load of *14-3-Control* and *14-3-Uni* is not well defined because these tests were conducted in 0-6306 on a single beam by loading one span until yielding of transverse steel (pre-cracked) before conducting the control test on the other span. As expected, both steel stirrups and CFRP strips start to take load, after the initiation of diagonal cracks.

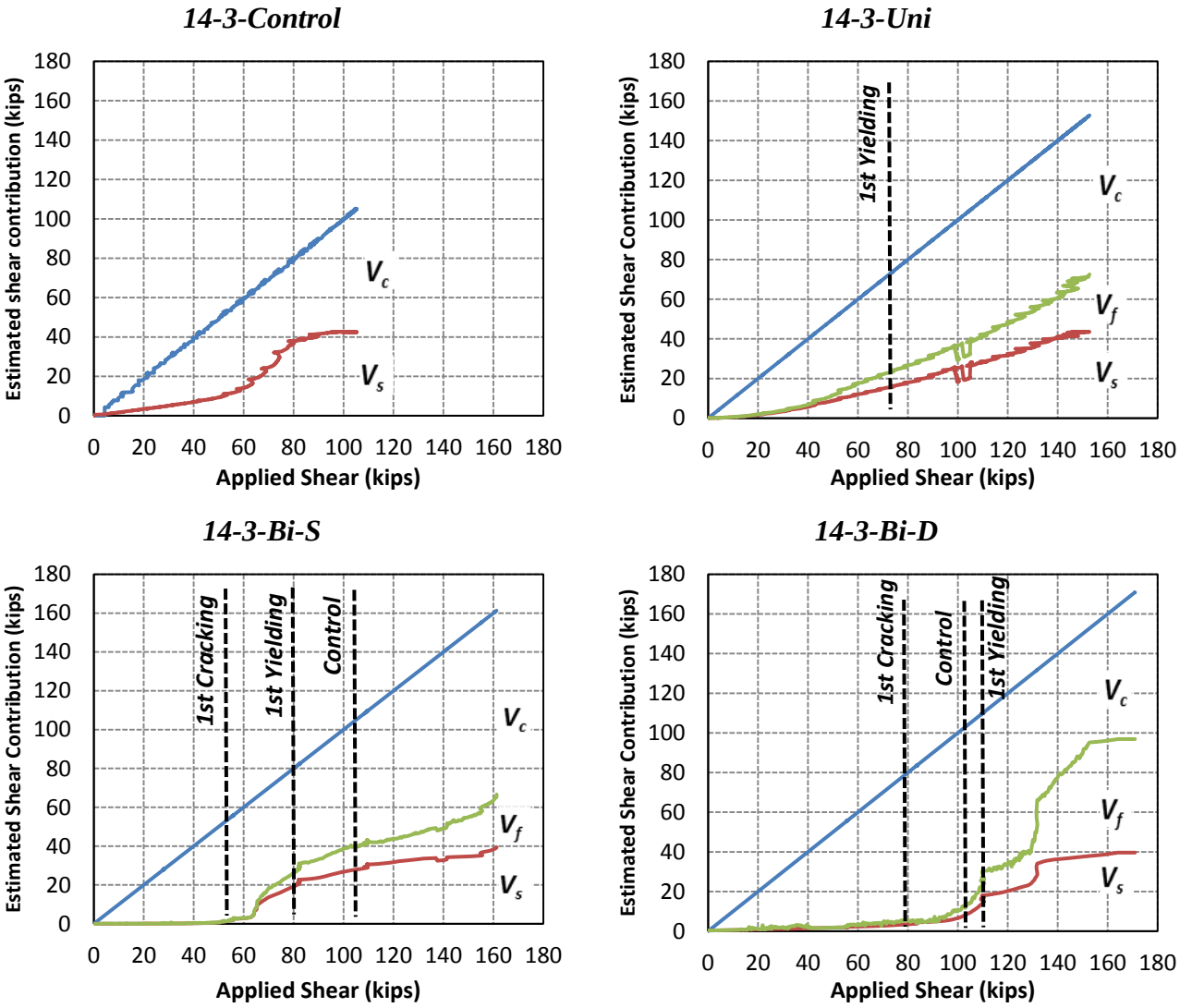

Figure 5-17: Estimated shear contributions for specimens with 14-in. webs

The yielding of transverse steel in *14-3-Bi-S* was more delayed than in *14-3-Uni*. The addition of CFRP material in *14-3-Bi-D* delayed the initiation of diagonal cracks and the yielding of transverse steel relative to *14-3-Bi-S*.

5.4.2 Components of shear for 8-in. web specimen with a/d of 3

The results of normalized shear capacity and gain in the shear strength of test specimens with 8-in. webs are presented in Table 5-7.

Table 5-7: Shear contributions and strength gain for 8-in. web specimens

Specimen	*Normalized Shear Capacity*	*Steel Contribution*	*CFRP Contribution*	*Normalized Shear Contribution*	*Shear Gain*
8-3-Control	76.2	26.4	-	49.8	0%
8-3-Uni	99.1	26.4	19.3	53.4	30%
8-3-Bi-S	106.1	26.4	24.5	55.1	39%
8-3-Bi-D	109.2	26.4	32.4	50.3	43%

A considerable gain in the shear capacity (up to 43%) was achieved in test specimen *8-3-Bi-D*. This gain is a large gain when compared to test results in the literature for specimens with the same transverse reinforcement ratio. A comparison of the contribution of each component to the shear capacity is presented in Figure 5-18.

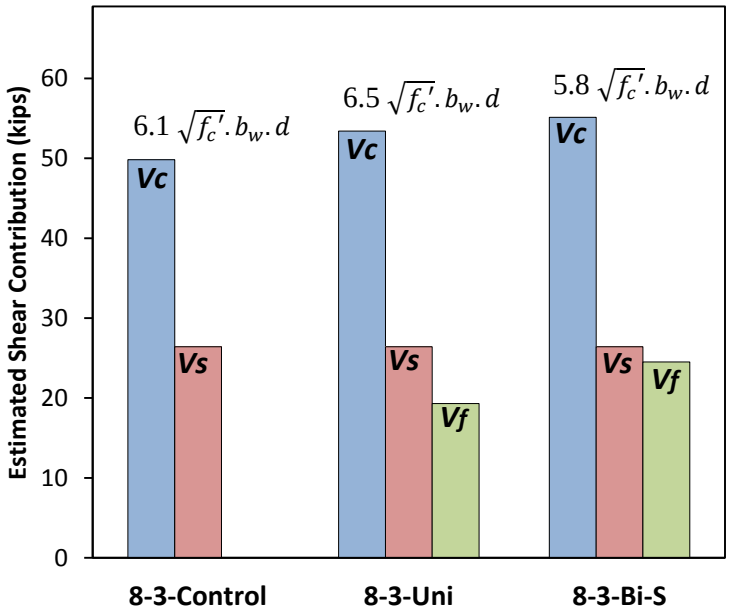

Figure 5-18: Shear contribution of each component in 8-in. web specimens

As for the 14-in. web tests, the transverse steel contribution was not be affected by the external strengthening system. This agrees with the assumption that the steel resistance to the shear is the same for strengthened and non-strengthened reinforced concrete beams as long as steel stirrups yield before failure. A small increase was

observed in the concrete contribution due to the addition of the horizontal strips for this series. This can be attributed to the fact that the concrete contribution of *8-3-Control* was 6.1 $\sqrt{f_c'}.b_w.d$, which is approximately twice the concrete contribution of *14-3-Control*. Additional shear contribution from the concrete should not be expected since the maximum concrete contribution reported in the 14-in. webs specimens was 95-kips, which is equivalent to $5.6\sqrt{f_c'}.b_w.d$. Therefore, the addition of the horizontal strips increases the concrete contribution to from 53.4-kips ($6.5\sqrt{f_c'}.b_w.d.$) for test *8-3-Uni* to 55.1-kip ($5.8\sqrt{f_c'}.b_w.d.$) for test *8-3-Bi-S*. The reduction in $\sqrt{f_c'}.b_w.d$ term is due the variation in f_c' term between the two tests. It may be important to mention here that ACI 318-11 code provisions limit the concrete contribution to the shear strength of conventional reinforced concrete members to $3.5\sqrt{f_c'}.b_w.d$.

In general, the bi-directional application of CFRP improved the shear performance relative to the uni-directional application. The effect of increasing the amount of CFRP material on the shear capacity of bi-directionally strengthened specimens with 8-in. webs can be seen in Figure 5-19.

The effect of increasing the CFRP material on the shear contribution mechanism of specimens with 8-in. webs is found to be identical, but to a lesser extent, to its effect on the specimens with 14-in. webs. This can be observed from several aspects: 1) the steel contribution was not affected by increasing the amount of CFRP material, 2) the CFRP contribution was increased due to increasing the amount of CFRP material, and 3) the increase in the CFRP contribution was combined with a decrease in the concrete contribution. This indicates that some of the shear that was resisted by the concrete in *8-3-Bi-S* is resisted by the additional CFRP material in *8-3-Bi-D*.

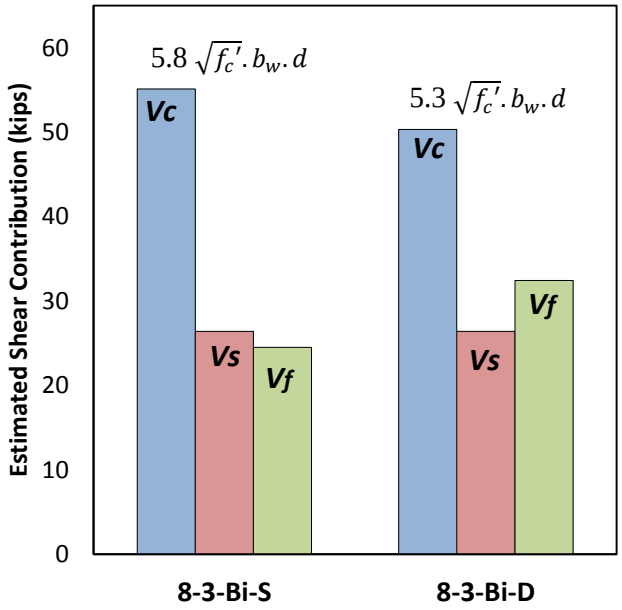

Figure 5-19: Shear contribution component of 8-3-Bi-S and 8-3-Bi-D

Figure 5-20 shows the estimated shear contribution of each material for specimens with 8-in.webs. Cracking occurred at the same shear load for *8-3-Uni* and *8-3-Bi-S*, while *8-3-Bi-D* exhibited a delayed first cracking. The yielding plateau observed in all test specimens indicates yielding of transverse steel well before reaching the ultimate load, as observed in section 5.3.1 in this Chapter.

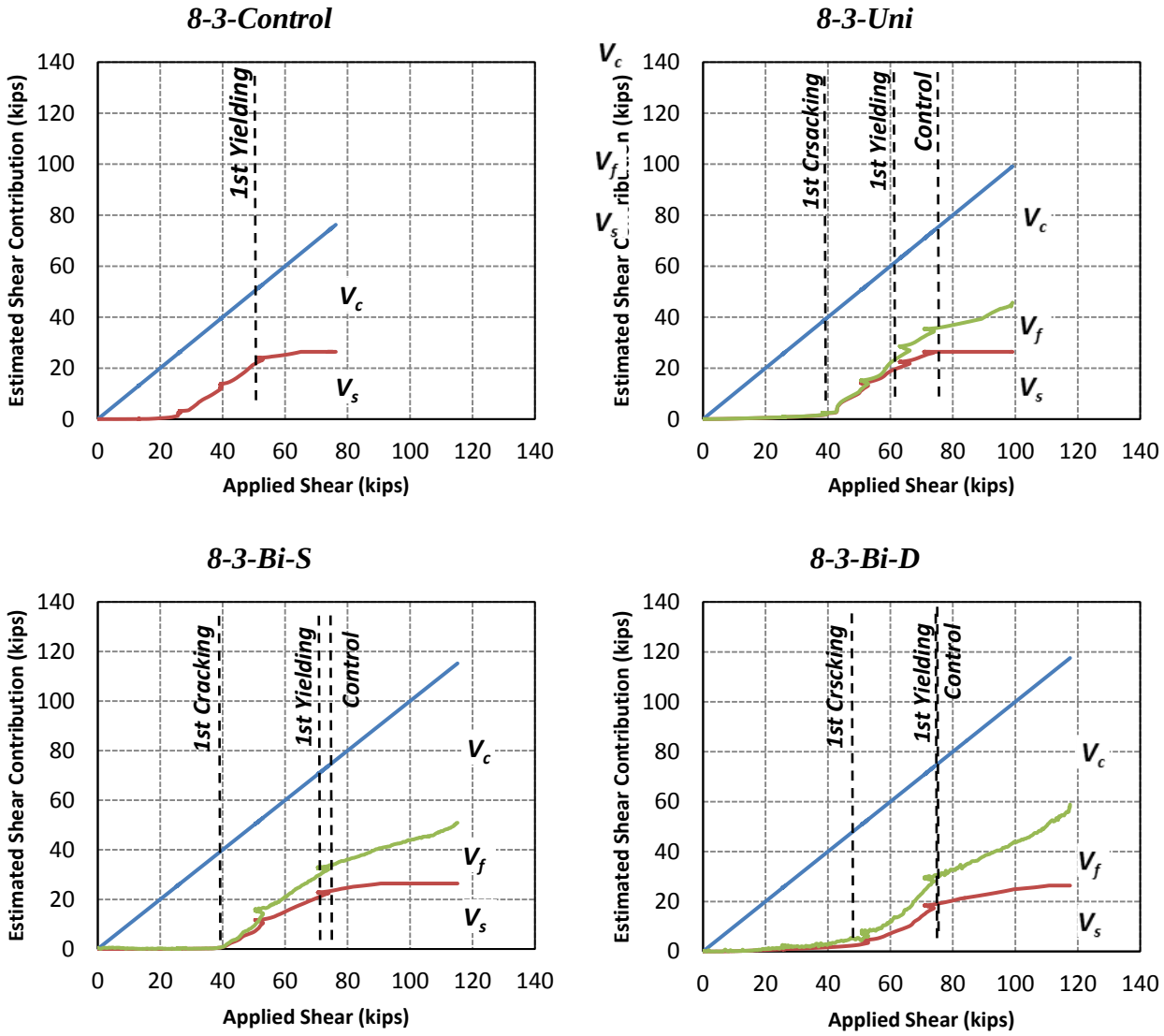

Figure 5-20: Estimated shear contributions for specimens with 8-in. webs

Test results confirm that the steel contribution to shear capacity was not affected by the external application of CFRP material (uni-directionally or bi-directionally); as long as steel stirrups yield prior to failure. However, the steel contribution to the shear resistance is found to be delayed by the external application of CFRP material. As shown in Figure 5-21, in all test specimens the steel contribution to the shear capacity is the same; however, this contribution is found to be delayed in *8-3-Bi-D* more than in *8-3-Bi-S* and *8-3-Uni*.

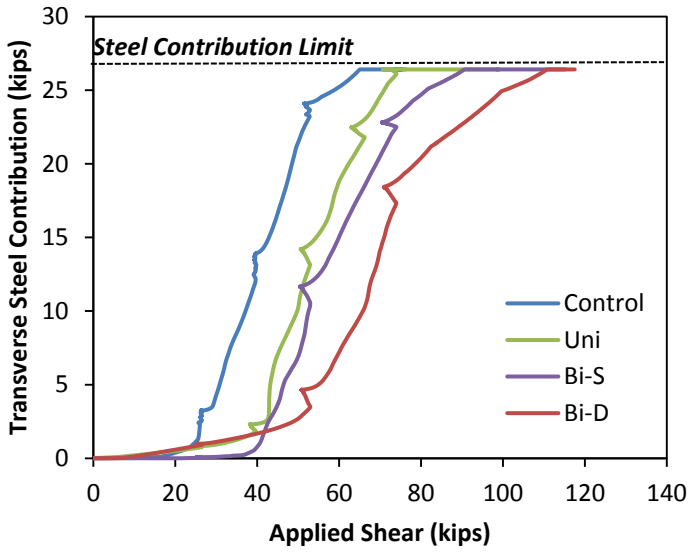

Figure 5-21: Transverse steel contribution in 8-in. web specimens

From the shear contribution analysis, the bi-directional application of CFRP exhibited better performance in comparison with the uni-directional application. A summary of test results is presented in Table 5-8.

Table 5-8: Summary of test results

Test	*Normalized Shear Capacity*	*Steel Contribution*	*Steel Contribution %*	*CFRP Contribution*	*CFRP Contribution %*	*Normalized Concrete contribution*	*Concrete Contribution %*	*Gain due CFRP*	*Shear Gain %*
14-3-Cont	105.3	42.4	40.3%	-	-	62.8	59.7%	0	0%
14-3-Uni	152.7	43.5	28.5%	29.0	19.0%	80.2	52.5%	47.5	45.1%
14-3-Bi-S	161.3	39.5	24.5%	27.2	16.9%	94.6	58.7%	56	53.2%
14-3-Bi-D	170.9	39.6	23.2%	57.3	33.5%	74.0	43.3%	65.7	62.4%
8-3-Cont	76.2	26.4	34.6%	-	-	49.8	65.4%	0	0%
8-3-Uni	99.1	26.4	26.6%	19.3	19.5%	53.4	53.9%	22.9	30.0%
8-3-Bi-S	106.1	26.4	24.9%	24.5	23.1%	55.1	52.0%	29.8	39.1%
8-3-Bi-D	109.2	26.4	24.2%	32.4	29.7%	50.3	46.1%	32.9	43.2%

5.5 OBSERVATIONS OF THE CRACKING PATTERNS

All test specimens failed in shear. The failure was always caused by a critical shear crack that passed through the web of the beam. In several cases, when a specimen was strengthened bi-directionally, the principal crack was found to develop along the flange-web interface before it propagated to the support. To evaluate the effect of the strengthening system on the cracking pattern of a reinforced concrete beam, the vertical and horizontal CFRP strips were removed after testing each specimen.

The difference between the cracking pattern of strengthened and non-strengthened specimens with 8-in. webs can be seen in Figure 5-22. Specimen *8-3-Control* failed by a typical shear tension failure where the failure was caused by a principal shear crack with two minor cracks in parallel to the major crack. The angle with respect to beam longitudinal axis of the principal shear crack that caused the failure of *8-3-Control* was in the range of 30° to 35°.

(a) *8-3-Control*

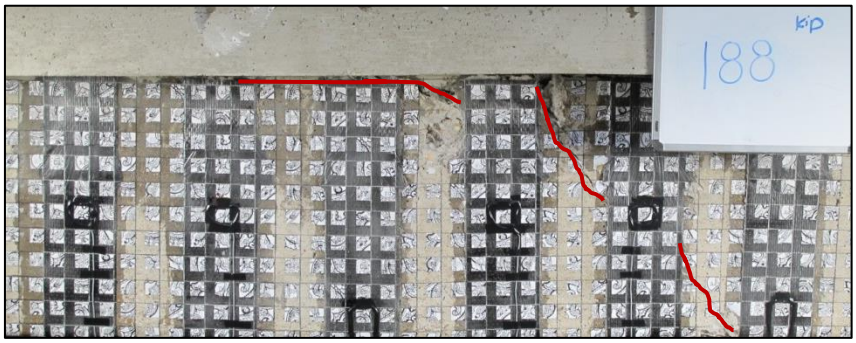

(b) *8-3-Uni*

Figure 5-22: Cracking of control and uni-directionally strengthened

Specimen *8-3-Uni* failed by a major crack, as shown in Figure 5-23. This crack was observed to start horizontally, and then it inclined to 45° before the last vertical strip. It was observed that cracking after the removal of the CFRP was well-distributed (Figure 5-24)

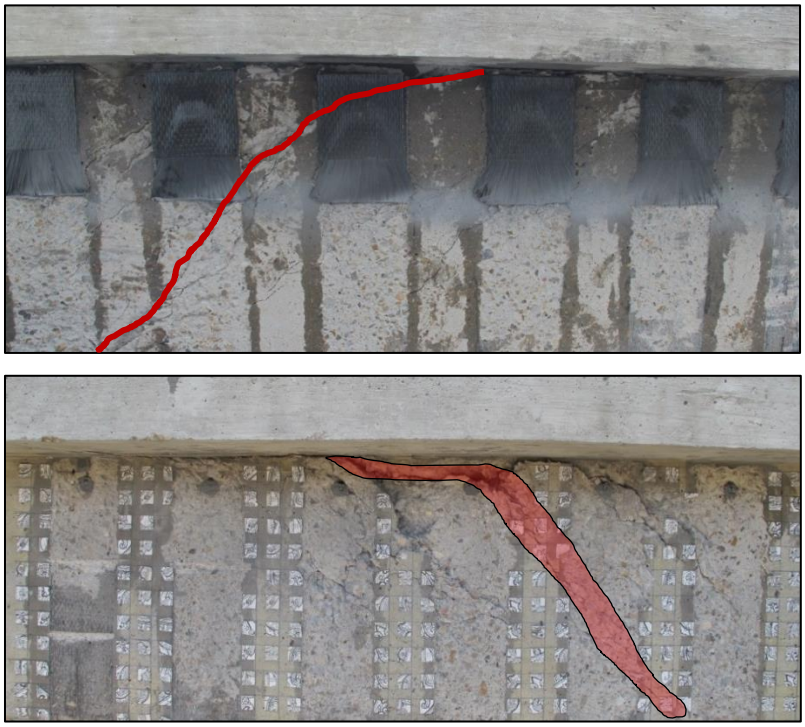

Figure 5-23: Principal crack of 8-3-Uni: west face (top), east face (bottom)

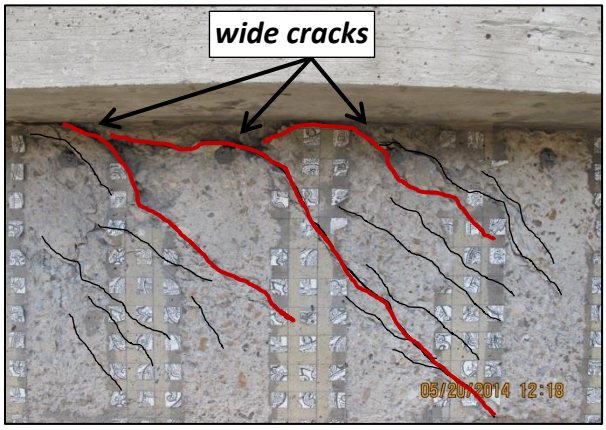

Figure 5-24: Distribution of cracks in 8-3-Uni

Specimen *8-3-Bi-S* exhibited a cracking pattern (Figure 5-25) that is different than the pattern seen in *8-3-Uni*.

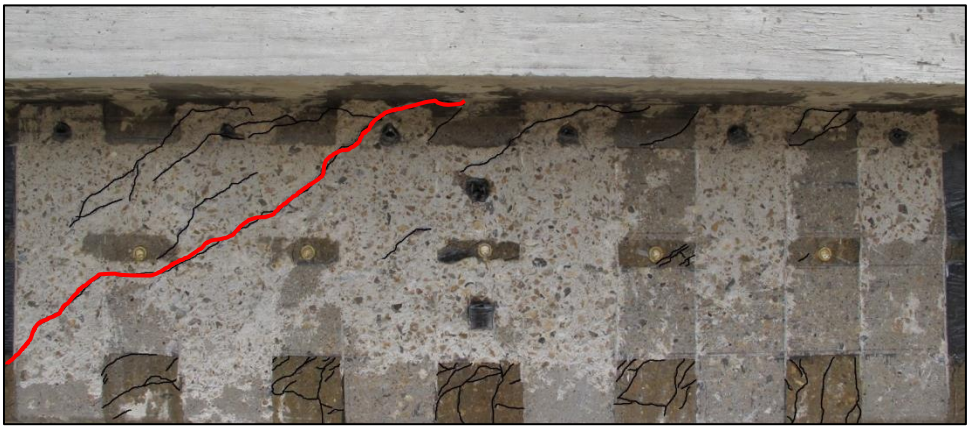

Figure 5-25: Cracking pattern of 8-3-Bi-S (west face)

The cracks were more distributed than in *8-3-Uni*; however, no wide cracks were observed in *8-3-Bi-S*.

A similar cracking trend was observed in the 14-in. web specimens. *14-3-Control* failed by two major shear cracks. Specimen *14-3-Uni* failed by a principal shear crack with distributed minor cracks. In the bi-directionally strengthened specimens, the cracking pattern at failure consisted of very distributed minor cracks. The cracks' width was narrow when compared to the *14-3-Uni*. Figure 5-26 shows the cracking pattern of 14-in. web specimens.

(1) 14-3-Control

(2) 14-3-Uni

(3) 14-3-Bi-S

Figure 5-26: Cracking pattern of 14-in. web specimens

CHAPTER 6
Summary and Conclusions

6.1 SUMMARY

Eight tests were conducted to investigate the performance of bi-directional external application of Carbon Fiber Reinforced Polymer (CFRP) strips and CFRP anchors for strengthening reinforced concrete (RC) members in shear. Test specimens consisted of 24-in. deep T-beams with shear span-to-depth ratios *(a/d)* of 1.5 and 3. Test specimen cross-sections consisted of 1) a 14-in wide web with 28-in. wide flange, and 2) an 8-in. wide web with 22-in. wide flange. The flange thickness was 5-in. in all specimens.

The experimental testing program was designed to evaluate the effect of three parameters on the shear behavior of a RC beam strengthened with bi-directional application of CFRP strips and CFRP anchors: 1) shear span-to-depth ratio (a/d), 2) number of CFRP layers applied to strengthen the beam, and 3) web width of the beam.

Two tests were conducted on a specimen with *a/d* of 1.5 and a web width of 14-in. to evaluate the performance of the bi-directional application of CFRP in shear strengthening deep beams. Six tests were conducted on specimens with *a/d* of 3 to evaluate the performance of the bi-directional application of CFRP in shear strengthening slender beams. Two tests were conducted with a 14-in. web width while the rest were conducted on specimens with an 8-in. web width.

In general, the bi-directional application of CFRP strips and CFRP anchors had little effect on the performance of specimens with *a/d* of 1.5. However, the bi-directional application of CFRP strips and CFRP anchors significantly increased the shear capacity of specimens with *a/d* of 3. No CFRP strips rupture or CFRP anchor fracture were observed in any test.

6.2 CONCLUSIONS

The performance of reinforced concrete T-beams strengthened with the bi-directionally applied CFRP strips and CFRP anchors was evaluated through experimental testing. Findings from the eight test specimens performed in this investigation are summarized below:

1. Effect of bi-directional application on shear resistance

   - The bi-directional application of CFRP had a negligible effect on the shear capacity of reinforced concrete beams with a/d of 1.5 (deep beam). The use of CFRP material in shear strengthening RC deep beams is not recommended.
   - The bi-directional application of CFRP had a substantial effect on the shear capacity of a slender reinforced concrete beams. A shear strength gain up to 62% was achieved when compared to the non-strengthened beams with 14-in. webs, and (up to 43%) for beams with 8-in.webs.
   - There was an interaction between the concrete shear contribution V_c and the CFRP shear contribution V_f.
   - In ACI 318, the maximum shear strength of a conventional reinforced concrete beam is typically limited to ($11.5\sqrt{f_c'}.b_w.d$). This comes from limiting the concrete contribution to the onset of diagonal cracks ($3.5\sqrt{f_c'}.b_w.d$) and limiting the steel contribution to ($8\sqrt{f_c'}.b_w.d$) to protect against crushing of the web. The difference in strength gain observed between 14-in. webs and8-in. webs can be attributed to their base shear capacity (shear contribution of concrete and steel only). The shear capacity of test *14-3-Control* was $6\sqrt{f_c'}.b_w.d$ (52% of the ACI limit) where the shear capacity of test *8-3-Control* was $9.4\sqrt{f_c'}.b_w.d$ (82% of ACI limit) which resulted in a higher CFRP contribution for 14-in. webs than for 8-in. webs.

- The contribution of transverse steel to the shear capacity in strengthened beams (uni- or bi-directionally) was found to be identical to its contribution in non-strengthened beams (control). This is because all steel stirrups crossing the critical inclined crack yielded in all tests. The steel contribution to the shear capacity was not affected by the type of external application of CFRP (uni-directional or bi-directional). However, the steel contribution was reached at higher loads in bi-directional than in uni-directional applications.

2. Performance of CFRP strips and steel stirrups

- Although most of transverse steel within test region and all transverse steel crossing the critical crack yielded before the ultimate load was reached, the use of a bi-directional layout resulted in a considerable reduction in transverse steel strains at loads close to ultimate. The reduction can be attributed to better crack control with a bi-directional layout.
- Vertical CFRP strips in bi-directional application experienced lower strains than in uni-directional application. A maximum strain of 0.005-in/in was observed in vertical strips of bi-directionally strengthened beams. ACI 440.2R-08 limits effective strain to 0.004-in/in to control crack opening and avoid loss of aggregate interlock at the crack.
- There was a substantial reduction in strains in the steel stirrups and the CFRP strips in bi-directional in comparison with uni-directional applications.
- The cracking pattern of a bi-directionally strengthened beam was different than a uni-directionally strengthened beam. The use of bi-directional application resulted in a more distributed cracking pattern with smaller crack widths compared with uni-directional application.

3. Anchor performance and installation of CFRP

   - The CFRP anchors used in this experimental program, worked well. No CFRP anchor failure was observed in any test.
   - The performance of lap splicing vertical CFRP strips under the web was comparable to the performance of wrapping a single vertical CFRP strip around the web. Therefore, the difficulty of wrapping vertical CFRP strips around the web of reinforced concrete girders in the filed can be eliminated by lap splicing the vertical strips under the web of the girder.

Refrences

AASHTO (2007), AASHTO LRFD Bridge Design Specifications, 4th edition, Washington, DC, USA.

ACI Committee 318 (2008). Building Code Requirements for Structural Concrete (ACI 318-08), American Concrete Institute, Farmington Hills, Michigan, USA

ACI Committee 440 (2008). Guide for the Design and Construction of Externally Bonded FRP Systems for Strengthening Concrete Structures (ACI 440.2R-08), American Concrete Institute, Farmington Hills, Michigan, USA

Adhikary, B. B., & Mutsuyoshi, H. (2004). Behavior of concrete beams strengthened in shear with carbon-fiber sheets. *Journal of Composites for Construction, 8*(3), 258-264. doi: 10.1061/(asce)1090-0268(2004)8:3(258)

Al-Sulaimani, G. J., Sharif, A., Basunbul, I. A., Baluch, M. H., & Ghaleb, B. N. (1994). Shear repair for reinforced concrete by fiberglass plate bonding. *ACI Structural Journal, 91*(4).

Belarbi, A., Bae, S. W., & Brancaccio, A. (2012). Behavior of full-scale RC T-beams strengthened in shear with externally bonded FRP sheets. *Construction and Building Materials, 32*, 27-40.

Bousselham, A., & Chaallal, O. (2006a). Behavior of reinforced concrete T-beams strengthened in shear with carbon fiber-reinforced polymer - An experimental study. *Aci Structural Journal, 103*(3), 339-347.

Bousselham, A., & Chaallal, O. (2006b). Effect of transverse steel and shear span on the performance of RC beams strengthened in shear with CFRP. *Composites Part B-Engineering, 37*(1), 37-46.

Bousselham, A., & Chaallal, O. (2008). Mechanisms of shear resistance of concrete beams strengthened in shear with externally bonded FRP. *Journal of Composites for Construction, 12*(5), 499-512.

Bousselham, A., & Chaallal, O. (2009). Maximum shear strength of RC beams retrofitted in shear with FRP composites. *Journal of Composites for Construction, 13*(4), 302-314.

Cao, S., Chen, J., Teng, J., Hao, Z., & Chen, J. (2005). Debonding in RC beams shear strengthened with complete FRP wraps. *Journal of Composites for Construction, 9*(5), 417-428.

Carolin, A., & Täljsten, B. (2005). Experimental study of strengthening for increased shear bearing capacity. *Journal of Composites for Construction, 9*(6), 488-496.

Chaallal, O., Shahawy, M., & Hassan, M. (2002). Performance of reinforced concrete T-girders strengthened in shear with carbon fiber-reinforced polymer fabric. *ACI Structural Journal, 99*(3).

Chajes, M. J., Januszka, T. F., Mertz, D. R., Thomson Jr, T. A., & Finch Jr, W. W. (1995). Shear strengthening of reinforced concrete beams using externally applied composite fabrics. *ACI Structural Journal, 92*(3).

Chen, G. M., Teng, J. G., Chen, J. F., & Rosenboom, O. A. (2010). Interaction between Steel Stirrups and Shear-Strengthening FRP Strips in RC Beams. *Journal of Composites for Construction, 14*(5), 498-509.

Chen, J., & Teng, J. (2003). Shear capacity of fiber-reinforced polymer-strengthened reinforced concrete beams: Fiber reinforced polymer rupture. *Journal of Structural Engineering, 129*(5), 615-625.

Chen, J. F., & Teng, J. G. (2003). Shear capacity of FRP-strengthened RC beams: FRP debonding. *Construction and Building Materials, 17*(1), 27-41.

De Lorenzis, L., Miller, B., & Nanni, A. (2001). Bond of fiber-reinforced polymer laminates to concrete. *ACI Materials Journal, 98*(3).

Deifalla, A., & Ghobarah, A. (2010). Strengthening RC T-beams subjected to combined torsion and shear using FRP fabrics: Experimental study. *Journal of Composites for Construction, 14*(3), 301-311.

Deniaud, C., & Cheng, J. J. R. (2001). Sheer behavior of reinforced concrete T-beams with externally bonded fiber-reinforced polymer sheets. *Aci Structural Journal, 98*(3), 386-394.

Deniaud, C., & Cheng, J. J. R. (2003). Reinforced concrete T-beams strengthened in shear with fiber reinforced polymer sheets. *Journal of Composites for Construction, 7*(4), 302-310.

Dirar, S., Lees, J., & Morley, C. (2012). Precracked Reinforced Concrete T-Beams Repaired in Shear with Bonded Carbon Fiber-Reinforced Polymer Sheets. *ACI Structural Journal, 109*(2).

Eshwar, N., Nanni, A., & Ibell, T. J. (2008). Performance of two anchor systems of externally bonded fiber-reinforced polymer laminates. *ACI Materials Journal, 105*(1).

Grande, E., Imbimbo, M., & Rasulo, A. (2009). Effect of Transverse Steel on the Response of RC Beams Strengthened in Shear by FRP: Experimental Study. *Journal of Composites for Construction, 13*(5), 405-414.

Higgins, C., Williams, G. T., Mitchell, M. M., Dawson, M. R., & Howell, D. (2012). Shear Strength of Reinforced Concrete Girders with Carbon Fiber-Reinforced Polymer: Experimental Results. *ACI Structural Journal, 109*(6), 805-814.

Hoult, N. A., & Lees, J. M. (2009). Efficient CFRP strap configurations for the shear strengthening of reinforced concrete T-beams. *Journal of composites for construction, 13*(1), 45-52.

Hsu, C.-T., Punurai, W., & Zhang, Z. (2003). Flexural and Shear Strengthenings of RC Beams Using Carbon Fiber Reinforced Polymer Laminates. *ACI Special Publication, 211*.

Hutchinson, R., & Rizkalla, S. (1999). Shear strengthening of AASHTO bridge girders using carbon fiber reinforced polymer sheets. *ACI Special Publication, 188*(November 1999), pp. 945-958.

Kalfat, R., Al-Mahaidi, R., & Smith, S. T. (2013). Anchorage Devices Used to Improve the Performance of Reinforced Concrete Beams Retrofitted with FRP Composites: State-of-the-Art Review. *Journal of Composites for Construction, 17*(1), 14-33.

Khalifa, A., Gold, W. J., Nanni, A., & MI, A. A. (1998). Contribution of externally bonded FRP to shear capacity of RC flexural members. *Journal of Composites for Construction, 2*(4), 195-202.

Khalifa, A., & Nanni, A. (2000). Improving shear capacity of existing RC T-section beams using CFRP composites. *Cement & Concrete Composites, 22*(3), 165-174.

Khalifa, A., Tumialan, G., Nanni, A., & Belarbi, A. (1999). Shear strengthening of continuous reinforced concrete beams using externally bonded carbon fiber reinforced polymer sheets. *ACI Special Publication, 188*.

Kim, I., Jirsa, J. O., & Bayrak, O. (2011). Use of carbon fiber-reinforced polymer anchors to repair and strengthen lap splices of reinforced concrete columns. *ACI Structural Journal, 108*(5).

Kim, I., Jirsa, J. O., & Bayrak, O. (2013). Anchorage of Carbon Fiber-Reinforced Polymer on Side Faces of Reinforced Concrete Beams to Provide Continuity. *ACI Structural Journal, 110*(06).

Kim, I. S. (2008). *Use of CFRP to provide continuity in existing reinforced concrete members subjected to extreme loads.* (Ph.D. Dissertation), The University of Texas at Austin, Austin, Texas.

Kim, S. J., & Smith, S. T. (2009). Behaviour of Handmade FRP Anchors under Tensile Load in Uncracked Concrete. *Advances in Structural Engineering, 12*(6), 845-865.

Kim, Y., Quinn, K. T., Satrom, C. N., Ghannoum, W. M., & Jirsa, J. O. (2011). Shear strengthening RC T-beams using CFRP laminates and anchors. *ACI Special Publication, 275*.

Kim, Y. G. (2011). *Shear behavior of reinforced concrete T-beams strengthened with carbon fiber reinforced polymer (CFRP) sheets and CFRP anchors.* (Ph.D. Dissertation), The University of Texas at Austin, Austin, TX

Kim, Y. G., Quinn, K., Satrom, N., Garcia, J., Sun, W., Ghannoum, W., & James, O. J. (2012). Shear Strengthening of Reinforced and Prestressed Concrete Beams Using Carbon Fiber Reinforced Polymer (CFRP) Sheets and Anchors (R. a. T. I. Office, Trans.). Austin, Texas, Texas Department of Transportation.

Mofidi, A., & Chaallal, O. (2011). Shear strengthening of RC beams with EB FRP: Influencing factors and conceptual debonding model. *Journal of Composites for Construction, 15*(1), 62-74.

Mofidi, A., & Chaallal, O. (2014). Effect of Steel Stirrups on Shear Resistance Gain Due to Externally Bonded Fiber-Reinforced Polymer Strips and Sheets. *ACI Structural Journal, 111*(1-6).

Monti, G., Renzelli, M., & Luciani, P. (2003). *FRP adhesion in uncracked and cracked concrete zones.* Paper presented at the Proceedings of the Sixth International Symposium on FRP Reinforcement for Concrete Structures (FRPRCS-6).

Nakaba, K., Kanakubo, T., Furuta, T., & Yoshizawa, H. (2001). Bond behavior between fiber-reinforced polymer laminates and concrete. *ACI Structural Journal, 98*(3).

Orton, S., Jirsa, J. O., & Bayrak, O. (2009). Carbon fiber-reinforced polymer for continuity in existing reinforced concrete buildings vulnerable to collapse. *ACI Structural Journal, 106*(5).

Orton, S. L. (2007). *Development of a CFRP system to provide continuity in existing reinforced concrete building vulnerable to progressive collapse.* (Ph.D. Dessertation), The University of Texas at Austin, Austin, Texas

Orton, S. L., Jirsa, J. O., & Bayrak, O. (2008). Design Considerations of Carbon Fiber Anchors. *Journal of Composites for Construction, 12*(6), 608-616.

Ozbakkaloglu, T., & Saatcioglu, M. (2009). Tensile Behavior of FRP Anchors in Concrete. *Journal of Composites for Construction, 13*(2), 82-92.

Pellegrino, C., & Modena, C. (2002). Fiber reinforced polymer shear strengthening of reinforced concrete beams with transverse steel reinforcement. *Journal of Composites for Construction, 6*(2), 104-111.

Pellegrino, C., & Modena, C. (2006). Fiber-reinforced polymer shear strengthening of reinforced concrete beams: Experimental study and analytical modeling. *Aci Structural Journal, 103*(5), 720-728.

Pham, L. T. (2009). *Development of a Quality Control Test for Carbon Fiber Reinforced Polymer Anchors* (Maset of Science Thesis), The University of Texas at Austin, Austin, Texas

Quinn, K. T. (2009). *Shear Strengthening of Reinforced Concrete Beams with Carbon Fiber Reinforced Polymer (CFRP) and Improved Anchor Details.* (Master of Science), The University of Texas at Austin, Austin, Texas.

Sato, Y., Ueda, T., Kakuta, Y., & Tanaka, T. (1996). *Shear reinforcing effect of carbon fiber sheet attached to side of reinforced concrete beams.* Paper presented at the Proceedings of the 2nd International Confrence on Advanced Composite Materials in Bridges and Structures, Monterial 1996.

Triantafillou, T. C. (1998). Shear strengthening of reinforced concrete beams using epoxy-bonded FRP composites. *Aci Structural Journal, 95*(2), 107-115.

Triantafillou, T. C., & Antonopoulos, C. P. (2000). Design of concrete flexral members strengthened im shear with FRP. *Journal of Composites for Construction, 4*(4), 198-205.

Zhang, Z., Hsu, C.-T. T., & Moren, J. (2004). Shear strengthening of reinforced concrete deep beams using carbon fiber reinforced polymer laminates. *Journal of Composites for Construction, 8*(5), 403-414.

Zhang, Z. C., & Hsu, C. T. T. (2005). Shear strengthening of reinforced concrete beams using carbon-fiber-reinforced polymer laminates. *Journal of Composites for Construction*, *9*(2), 158-169.

VITA

Nawaf Khaled Alotaibi was born in Khaitan, Kuwait. He attended Abdullatif Thunayan Alghanim High School in Alardiyah, Kuwait. Upon successful completion of his work in 2003, Nawaf enrolled at Kuwait University and received a Bachelor of Science in Civil Engineering with Class Honors in June 2008. In August 2012, Nawaf enrolled in a graduate program in Structural Engineering at the University of Texas at Austin. He graduated with a Master of Science in Engineering in August 2014 and will continue to work towards a Doctor of Philosophy at the University of Texas at Austin.

Permanent e-mail: Alotaibi@utexas.edu

This thesis was typed by the author.